ANNUAL REPORT 2003

COLUMBIA UNIVERSITY

College of Physicians and Surgeons

Center for Radiological Research – 630 W. 168th St., New York, NY 10032 – http://crr-cu.org

ANNUAL REPORT 2003

Eric J. Hall
Director

Howard B. Lieberman
Editor

Mary T. Coady
Moshe Y. Friedman
Assistant Editors

COLUMBIA UNIVERSITY

College of Physicians and Surgeons

Table of Contents

Collaborating Departments and Institutions

Individuals from the following departments and institutions (listed alphabetically) collaborated with Center for Radiological Research staff in the above research abstracts (for individual attributions see specific reports):

Collaborating Columbia University Departments:

- **Department of Dermatology**
- **Department of Environmental Health Sciences, Joseph Mailman School of Public Health**
- **Department of Genetics & Development**
- **Department Obstetrics and Gynecology**
- **Department of Neurology**
- **Department of Radiology**
- **Institute for Human Nutrition**

Collaborating Institutions:

- **Harvard School of Public Health, Boston, MA**
- **Johns Hopkins, Dept. of Epidemiology, Upton, NY**
- **IATIA Ltd., Victoria, Australia**
- **Medical Research Council, Radiation and Genome Stability Unit, Harwell, UK**
- **Memorial Sloan-Kettering Cancer Center, NY, NY**
- **National University of Singapore, Singapore**
- **New York University School of Medicine, Developmental Genetics Program, Skirball Institute of Biomedical Medicine and Howard Hughes Medical Institute, New York, NY**
- **Radcliffe Infirmary, Oxford, UK**
- **Radiation Effects Research Foundation, Hiroshima, Japan**
- **Southern Urals Biophysics Institute, Ozyorsk, Russia**
- **University of California, Department of Mathematics, Berkeley, CA**
- **University of Leicester, UK**
- **University of Tarapaca, Arica, Chile**
- **US Department of Health and Human Services**
  - **National Institutes of Health**
    - **National Cancer Institute**
      - **Biostatistics Branch, Bethesda, MD**
      - **Division of Basic Science, Bethesda, MD**
      - **Radiation Epidemiology Branch, Bethesda, MD**
    - **National Human Genome Research Institute, Bethesda, MD**
  - **Center for Disease Control and Prevention**
    - **National Institute for Occupational Safety and Health, Cincinnati, OH**
- **US Environmental Protection Agency**
  - **Environmental Carcinogenesis Division, Research Triangle Park, NC**
  - **Office of Radiation and Indoor Air, Washington, DC** ■

Columbia Colloquium and Laboratory Seminars

At approximately one month intervals during the academic year the Center for Radiological Research is pleased to welcome accomplished specialists from around the world to present formal seminars and/or spend time discussing ongoing research. The seminars are attended by Center and RARAF professional staff, senior technical staff and graduate students, as well as doctors and scientists from other departments of the College of Physicians & Surgeons interested in collaborative research. Attention has focused on recent findings and future plans, with special emphasis on the interdisciplinary nature of our research effort.

The 2003 sessions, which were organized and scheduled by Dr. Yuxin Yin, included the following guest speakers (listed alphabetically):

- Dr. Rajamanickam Baskar, University of Iowa, "Tumor Suppressor Genes in Carincogenesis." Dr. Baskar has since joined the Center staff.
- Dr. Amato Giaccia, Stanford University, "Epigenetic Regulation of Tumor Resistance."
- Dr. Corinne Leloup, Weizmann Institute of Sciences, Rehovot, Israel, "Radiation Damage to DNA: Measurement of the Effect of Ionization Density." Dr. Leloup has since joined the Center staff.
- Dr. Chunyan Liu, National Institute of Mental Health, NIH, "Repair of Topoisomerase I Damage to DNA in Eukaryotes."
- Dr. Alexandra Miller, Armed Forces Radiobiology Research Institute, "The Biological Hazards of Depleted Uranium."
- Dr. Takehiko Nohmi, Section Chief, Div. of Genetics & Mutagenesis, National institute of Health sciences, Tokyo, Japan, "Molecular Nature of Genome Rearrangements Induced by Crosslinker Mitomycin C In Vivo."
- Dr. Charles Waldren, Chief of Research, Radiation Effects Research Foundation, Hiroshima, Japan, "Biological Significance of Long Lived Organic Radicals."

Seminars were also conducted by several Center for Radiological Research staff members:

- Dr. Alan Bigelow, "Update on the Laser Ion Source for the Columbia University Microbeam."
- Dr. Lubomir Smilenov, "Haploinsufficiency for ATM Confers Radiosensitivity."
- Dr. Yuxin Yin, "A New Prospect for Regulation of p53-Target Genes." ■

Acknowledgment of Support

In 2003 the Center for Radiological Research was supported by competitively awarded grants from the following agencies:

Federal:

- **Department of Energy**
  - **Office of Energy Research**
  - **Office of Environment, Safety and Health**
  - **Office of Health Programs**
- **Department of Health and Human Services**
  - **Health Resources and Services Administration**
  - **National Institutes of Health:**
    - **National Cancer Institute [Program Project (PO1) & Individual Research Grants (RO1s)]**
    - **National Institutes of Environmental Health and Safety (RO1s)**
    - **National Institute of General Medical Sciences (RO1)**
    - **National Institute of Bioimaging and Bioengineering (P41)**
    - **National Center for Research Resources (S10)**
- **National Aeronautics and Space Administration**

Private:

- **Avon**
- **Herbert Irving Comprehensive Cancer Center of Columbia University**
- **Lance Armstrong Foundation**
- **Radiological Society of North America**
- **Ruth Estrin Goldberg Memorial for Cancer Research** ■

Web Sites

- **Center for Radiological Research** ..... **http://crr-cu.org**
- **CRR Annual Reports** *(1998-present; any corrections will be posted here)* .....**http://crr-cu.org/reports.htm**
- **Radiological Research Accelerator Facility**.....**http://www.raraf.org**
- **Web-Rad-Train**..... **http://www.web-rad-train.org**
- **Department of Radiation Oncology**.....**http://cpmcnet.columbia.edu/dept/radoncology**
- **Radiation Safety Office** ..... **http://cpmcnet.columbia.edu/dept/radsafety**

Introduction

The *raison d'etre* of the Center for Radiological Research of Columbia University is to foster a multi disciplinary approach towards understanding the biological consequences of ionizing radiation exposures. The Center's staff includes professionals from fields as diverse as molecular biology, cell biology, radiation physics, computational physics, engineering and radiation oncology.

This report summarizes the principal research initiatives and academic activities during the past year.

The Center has signed on as a member of the International Consortium for the Promotion of Radiation Life Sciences organized by the Graduate School of Biomedical Sciences of Nagasaki University, Japan (see picture to the right). The Center now joins eight other international institutions with the aim of promoting international collaboration in radiation research and education.

Sponsored by a grant from NASA, we were able to show that mice haploinsufficient for the *atm* gene were more susceptible to ocular cataracts induced by heavy Fe ions than their wild-type counterparts.

The tumor suppressor function of the Betaig-h3 gene, originally established in human lung cancer samples, has now been extended to two other major tumor types including prostate and breast. These findings provide a potential diagnostic and therapeutic target in the management of these cancers.

Based on mechanistic findings that arsenic-induced genetic damages are mediated by reactive oxygen species (PNAS: 1998 and 2001), clinical trails to ascertain the chemo-preventive effects of selenium and vitamin A in the management of arsenic induced keratosis have been initiated by Columbia investigators in collaboration with WHO in Bangladesh.

The observation that short term, low doses of sodium arsenite treatment can induce a high frequency of apoptosis in metastatic melanoma that are non-responsive to radiotherapy and chemotherapy provides a new ray of hope for patients. The finding is being highlighted in the Dean's 2003 annual report.

(L-r): Dr. Masao Tomonaga of Nagasaki University, Dr. Edgar Housepian, Special Advisor to the Dean for International Affairs, Dr. Masami Watanabe of Nagasaki University, Dr. Joanna Rubinstein, Associate Dean for International Affairs, with Dr. Tom Hei, Dr. Eric J. Hall and Dr. Yong-Liang Zhao.

The Columbia microbeam continues to be a major research resource for the Center. Recent findings include the detection of reactive oxygen and nitrogen species in targeted cytoplasmic irradiation, which mediate the genotoxic response in the nucleus of the irradiated cells, the ability of cytoplasmic irradiation in the induction of a bystander response, and the identification of specific genes that are associated with bystander mutagenic signaling.

The productivity of the Center continues at a high level, as evidenced by a steady stream of scientific papers in peer-reviewed journals, including several in high profile journals. Members of the staff are frequently invited to participate in national and international meetings, and are frequently called upon to serve as consultants, reviewers or site visitors by government agencies.

The teaching activities of the Center include the teaching of radiation biology and radiation physics to undergraduates, medical students, and graduate students in the School of Public Health, and to residents in both Radiology and Radiation Oncology, as well as a City-wide course for residents in Radiology. ■

Dr. Gerhard Randers-Pehrson (l) and Dr. Charles R Geard.

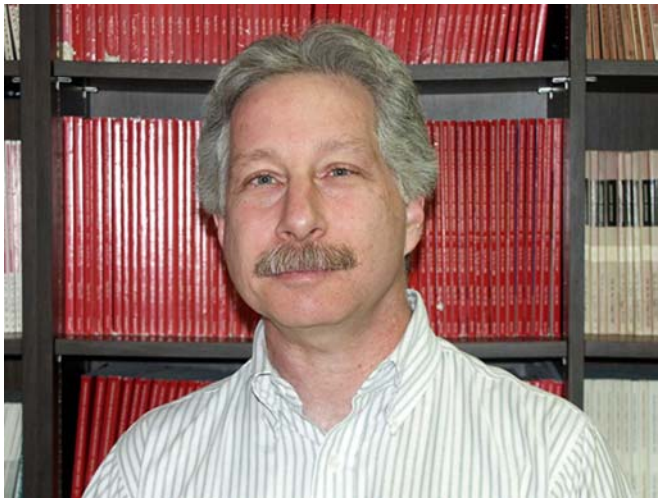

Dr. Howard B. Lieberman, editor of this year's report.

Faculty and Staff

FACULTY

ERIC J. HALL, D.Phil., D.Sc., FACR, FRCR, Higgins Professor of Radiation Biophysics, Professor of Radiology and Radiation Oncology, Chairman of Joint Radiation Safety Committee – ***Director***

CHARLES R. GEARD, Ph.D., Professor of Clinical Radiation Oncology – ***Associate Director***

DAVID J. BRENNER, Ph.D., D.Sc., Professor of Radiation Oncology and Public Health (Environmental Health Science) – ***RARAF Director***

TOM K. HEI, Ph.D., Professor of Radiation Oncology and Professor of Environmental Health Sciences

HOWARD B. LIEBERMAN, Ph.D., Professor of Radiation Oncology

SALLY A. AMUNDSON, Ph.D., Associate Professor of Radiation Oncology

HAIYING HANG, Ph.D., Assistant Professor of Radiation Oncology

LUBOMIR SMILENOV, Ph.D., Assistant Professor of Radiation Oncology

YUXIN YIN, M.D., Ph.D., Assistant Professor of Radiation Oncology

YONG-LIANG ZHAO, Ph.D., Assistant Professor of Radiation Oncology

RESEARCH STAFF

GERHARD RANDERS-PEHRSON, Ph.D., Research Scientist

ADAYABALAM BALAJEE, Ph.D., Associate Research Scientist

ALAN BIGELOW, Ph.D., Associate Research Scientist

GLORIA CALAF, Ph.D., Associate Research Scientist

VLADMIR IVANOV, Ph.D., Associate Research Scientist

BRIAN PONNAIYA, Ph.D., Associate Research Scientist

HONGNING ZHOU, M.D., Associate Research Scientist

KEVIN HOPKINS, M.S., Senior Staff Associate

STEPHEN A. MARINO, M.S., Senior Staff Associate

CHANG-QING PIAO, M.D., Senior Staff Associate

CARL ELLISTON, M.S., Staff Associate

SU-XIAN LIU, M.D., Staff Associate

AIPING ZHU, M.D., Staff Associate

GREGORY ROSS, M.S., Programmer Analyst

POST-DOCTORAL FELLOWS

RAJAMANICKAM BASKAR, Ph.D., Post-Doctoral Research Scientist

GUY GARTY, Ph.D., Post-Doctoral Research Scientist

PENG HE, Ph.D., Post-Doctoral Research Scientist

CORINNE LELOUP, Ph.D., Post-Doctoral Research Scientist

CATHERINE R. MITCHELL, Ph.D., Post-Doctoral Research Scientist

STEPHEN A. MITCHELL, Ph.D., Post-Doctoral Research Scientist

RUDRANATH (Ravi) PERSAUD, Ph.D., Post-Doctoral Research Scientist

JIANLI WANG, Ph.D., Post-Doctoral Research Scientist

FU-RU ZHAN, Ph.D., Post-Doctoral Research Scientist

PRE-DOCTORAL FELLOWS

MARNI HALL, M.S., Staff Associate

DESIGN AND INSTRUMENT SHOP

GARY W. JOHNSON, A.A.S., Senior Staff Associate – ***Design & Instrument Shop Director***

DAVID CUNIBERTI, B.A., Instrument Maker

ROBERT ARCHIGIAN, Instrument Maker

TECHNICAL STAFF

GLORIA JENKINS-BAKER, B.A., Research Worker

XIAOJIAN WANG, M.S., Research Worker

RONALD BAKER, B.S., Senior Technician

CUI-XIA KUAN, Technical Assistant

ADMINISTRATIVE AND SECRETARIAL STAFF

MONIQUE REY, B.A., Center Administrator

MARY COADY, Administrative Coordinator

MOSHE FRIEDMAN, B.A., Administrative Assistant

DIANA MORRISON, Administrative Assistant

HEIDY HERNANDEZ, Jr. Accountant

ANNERYS RODRIGUEZ, Clerk Typist

ANGELA LUGO, Clerk Typist ■

Faculty and Staff

Front row (*l-r*): Dr. Tom Hei, Dr. Charles Geard, Ms. Monique Rey, Dr. Eric Hall, Ms. Mary Coady, Dr. David Brenner, Dr. Howard Lieberman, Dr. Sally Amundson.

2nd row: Ms. Josephine Tsakok, Mr. Gary Johnson, Dr. Yuxin Yin, Mrs. Cui-Xia Kuan, Dr. Peng He, Ms. Jessica Berenguer, Dr. Corrine Leloup, Dr. Catherine Mitchell, Dr. Su-Xian Liu, Ms. Diana Morrison, Ms. Heidy Hernandez, Mr. Ronald Baker.

3rd row: Dr. Brian Ponnaiya, Dr. Jaime Rubin, Ms. Xiaojian Wang, Dr. Aiping Zhu, Ms. Sarah Baker, Dr. Alan Bigelow, Dr. Stephen Mitchell, Dr. Vladmir Ivanov, Dr. Yong-Liang Zhao, Ms. Gloria Jenkins-Baker.

4th row: Dr. Rajamanickam Baskar, Dr. Adayabalam Balajee, Dr. Haiying Hang, Mr. Robert Archigian, Dr. Lubomir Smilenov, Mr. David Cuniberti, Dr. Jianli Wang, Dr. Chang-Qing Piao.

Back row: Mr. Moshe Friedman, Dr. Fu-ru Zhan, Dr. Hongning Zhou, Mr. Joseph Gillespie, Dr. Rudranath Persaud, Mr. Carl Elliston, Dr. Gerhard Randers-Pehrson, Mr. Gregory Ross, Mr. Stephen Marino, Dr. Guy Garty, Mr. Kevin Hopkins.

Not pictured: Dr. Gloria Calaf, Ms. Marni Hall, Ms. Annerys Rodriguez, Ms. Angela Lugo.

Staff News

Dr. Eric Hall concluded his term as President of the International Association of Radiation Research at the International Congress in Brisbane, Australia. He was awarded the Henry S. Kaplan Distinguished Scientist Award, and delivered the eponymous lecture. Dr. Hall continues to serve as Senior Biology Editor of the *International Journal of Radiation Oncology, Biology, Physics*.

Drs. Hall and Brenner are both Councilors of the National Council on Radiological Protection. Dr. Brenner serves on NCRP Committee 12, on the use of ionizing radiations to combat terrorism.

Dr. Howard B. Lieberman is currently a member of the Basic and Preclinical Subcommittee C of the National Cancer Institute Initial Review Group. In addition, he is a member of the Scientific Advisory Board for the Israel Cancer Research Foundation, a private organization that supports biomedical research related to cancer.

Dr. Howard B. Lieberman edited a book entitled "*Cell Cycle Checkpoint Control Protocols*," published by Humana Press, Totowa, NJ.

Dr. Tom K. Hei continues to serve as an ad hoc member of the NCI Cancer Etiology Study Section and as chairman of several special emphasis panels.

Dr. Tom Hei has been appointed by the Dean as faculty advisor to Chinese exchanged medical students to Columbia's College of Physicians & Surgeons. Three students from Fudan University spent three months performing clinical rotations in the medical center.

Research findings of Dr. Tom Hei and his team on radiation induced bystander genetic changes have been featured in the November issue of the *Forbes* magazine as well as in the *P&S In Vivo* magazine.

Dr. Tom K. Hei has been elected to be a panel member in the Division of Cancer Biology of NCI to evaluate the status of chemical carcinogenesis research.

A major event in the past year was the recruitment of Sally A. Amundson, Ph.D., from the National Cancer Institute, NIH, Bethesda, MD. Dr. Amundson joins the Center faculty as Associate Professor of Radiation Oncology. She brings expertise involving the analysis of gene expression profiles and signal transduction pathways altered in response to ionizing radiation exposure.

Dr. Eric J. Hall and Dr. Sally A. Amundson.

Many of our personnel participated in the 6th International Workshop on Microbeam Probes of Cellular Radiation Response, held at Oxford, UK, March 29-31, 2003. Those participating and delivering talks and extended abstracts included Drs. Eric J. Hall, Charles R. Geard, David J. Brenner, Gerhard Randers-Pehrson, Stephen Marino, Alan Bigelow, Stephen Mitchell, Brian Ponnaiya and Hongning Zhou.

The International Association for Radiation Research held the 13th International Congress on Radiation Research, in Brisbane, Australia, August 2003, was attended by a number of our staff. Aside from Dr. Hall's award and lecture (mentioned above), other participants from the Center included Drs. David Brenner, Charles Geard, Tom Hei and Hongning Zhou.

For several years now there has been a successful collaboration between the Center and the Southern Urals Biophysics Institute (SUBI) in Ozyorsk, Russia. In December 2003, Drs. David Brenner, Charles Geard and Catherine Mitchell, accompanied by Nathalie Latham (a photographer interested in recording details of the study) travelled to SUBI to discuss future research and to demonstrate mFISH and mBAND hybridizations and analysis. The trip proved fruitful and interesting both from a work perspective and also because it allowed us a rare opportunity to experience, albeit briefly, this fascinating city. A lively diary of the week-long trip is featured in the Cytogenetic Studies section (page 51).

Personnel changes at the Center, aside from the addition of Dr. Amundson, included the following:

- Dr. Lubomir Smilenov and Dr. Yong-Liang Zhao were promoted to Assistant Professors of Radiation Oncology.
- Dr. Oleg Belyakov and Dr. Debasish Roy, Post-Doctoral Research Scientists at the Center, left to assume new positions with the Radiation and Nuclear Safety Authority (STUK), Helsinki, Finland, and with Brookhaven National Laboratory, Upton, NY.
- Dr. Gloria Calaf, Associate Research Scientist, accepted a professorship at the University of Tarapaca in Chile and left in December, 2003.
- Vladmir Ivanov, Ph.D., joined the Center as an Associate Research Scientist.
- Gregory Ross, M.S., joined the Center as a Programmer Analyst.
- There are three new Post-Doctoral Research Scientists, Rajamanickam Baskar, from the University of Iowa, and Guy Garty and Corinne Leloup, both from the Weizmann Institute of Sciences, Rehovot, Israel.

As we began preparing the material for this year's annual report, Dr. Charles Geard, who has served for years as the editor of the report, had an unfortunate slip on the ice at the RARAF facility and suffered painful ankle fractures, putting him out of commission for a while. Dr. Howard Lieberman filled the vacancy and admirably performed the role of editor for this year's report. As we go to press Dr. Geard is recuperating and getting back to into his regular routine. ■

Update on the Laser Ion Source for the Columbia University Microbeam

Alan W. Bigelow, Gerhard Randers-Pehrson and David J. Brenner

The ion source that has been used on our Van de Graaff particle accelerator, a Duoplasmatron, ionizes atoms from the gas phase. This ion source has been suitable for experiments involving the irradiation of cells with protons, deuterons and alpha particles having linear energy transfers (LETs) from 10 to 200 keV/μm. To extend the upper LET range of our experiments, ions as heavy as iron are required with high enough energies to have usable particle ranges (≥20 μm). Because of the limited acceleration per charge by the new accelerator (5 MV), highly charged initial heavy ions are needed to obtain the required energetic particles. Laser ion sources, in which a high-power, pulsed light beam is focused to micron dimensions resulting in power densities on the order of 10^{12} W/cm^2, can produce high initial charge-states of heavy ions in sufficient fluxes for microbeam experiments.

Our laser ion source project development has been based on the laser-operated ion source (LOIS) used by Dr. Raymond Hughes' group at the University of Arkansas. Equipment from LOIS was acquired by Columbia University in 1999 and was used to build our prototype laser ion source, following specifications for the most recent version of LOIS (1). This prototype was used to demonstrate proof of principle. After initial testing of this source with its 1970's Holobeam Nd:YAG laser, we replaced it with our new Quanta-Ray LAB-190-100 Nd:YAG laser purchased from Spectra-Physics. This upgrade led to an approximately 30-times increase in laser power density at the ablation target and had a positive effect on the yield of high charge-state ions. To handle the added laser power, the slide cover glass that had protected the final focusing lens from ablation spatter was replaced by a more substantial lens protector – a 2 mm thick piece of BK7 glass with anti-reflection coating for the Nd:YAG fundamental wavelength.

High charge state yields increase with improved vacuum of the laser ion source. Since the component of the laser ion source that requires vacuum conditions will reside at the terminal end of the accelerator column, it will also experience an external environment of high pressure, the insulating gas within the accelerator tank. This is inconvenient for vacuum pumps that require an exhaust to atmospheric (or lower) pressure. Tests with a titanium sublimation pump (TSP) have shown it to be a viable choice of gettering pump. The inlet to a turbo pump on the laser ion source was constricted with a small aperture to simulate the pumping action on the laser ion source from the turbo pump at the exit end of the accelerator. The addition of the TSP brought the operating pressure down by an order of magnitude measured in torr. Testing with an aluminum target showed that the improved vacuum condition extended the high charge state threshold of detected charge states from Al^{+7} to Al^{+11} and possibly higher. Hence we are incurporating a TSP into the final design of our laser ion source.

Ions generated from the laser ablation process have a wide distribution in charge state and energy. To select and deliver the desired ions to the entrance of the accelerator, a 24-degree spherical electrostatic analyzer (ESA) was designed and then built in-house. This design is a double focusing element and is more suited to our application than the 180-degree cylindrical ESA used in the initial prototype. A picture of our spherical ESA is shown in Figure 1. The ESA is a self-contained module mounted on a six-inch flange. Special attention was also given to the type of electrical feed-throughs due to our unique environment of having a vacuum system reside inside a pressurized container.

Moving beyond our laser ion source prototype, the design for our new laser ion source has been finalized. A drawing of the new design is shown in Figure 2. This new source is being built within a mock section of our accelerator terminal frame to conserve the exact configuration it would have when installed on the particle accelerator.

Currently, all components that were purchased for the new ion source have arrived. The ESA is assembled and attached to its six-inch mounting flange with special pressure/vacuum electrical feedthroughs. The target and its vacuum-compatible stepping motor will attach to a similar flange. A differential drive for target manipulation was designed with an optimized choice of gears. This allows the target to rotate and advance at rates that maximize the

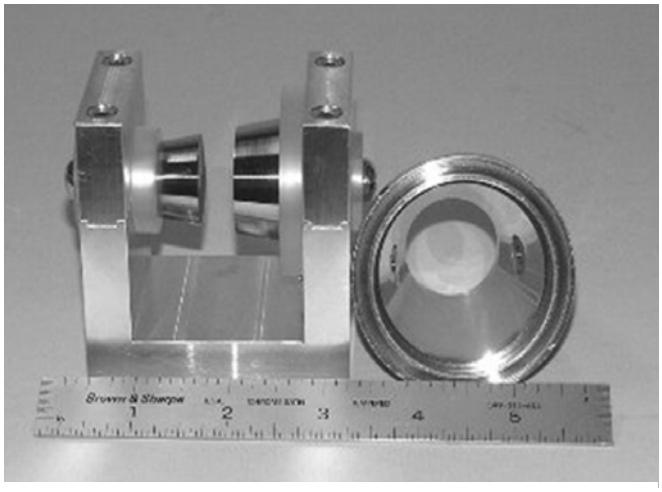

Fig. 1. This photograph of our Spherical ESA shows two electrodes and their insulating stand-offs mounted in a U-frame. On the right is a conical sheath that is placed around the electrodes and is a grounded surface that is used to shape the effective electric field boundary.

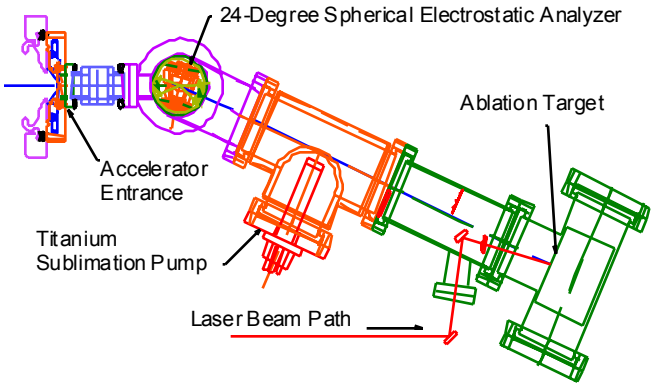

Fig. 2. Mechanical drawing of our new laser ion source.

target's usable lifetime. A final note is that this laser ion source configuration will fit within the terminal of our recently funded, new accelerator.

References

1. Miller RD, Wattuhewa G, Hughes RH, Pederson DO and Ye XM. Remnant charge of slow multicharged ions scattered from a gold surface. *Phys Rev B* **45**:12019-27, 1992. ■

Parylene, a Cell-Growth Substrate for Microbeam Applications

Alan W. Bigelow, Furu Zhan, Kurt A. Michel, Gerhard Randers-Pehrson and David J. Brenner

In the interest of improving the spatial properties of the microbeam, we have developed another substrate that will overcome the resolution uncertainties found with using polypropylene, our current substrate. There are often wrinkles that accumulate on the polypropylene substrate from the methods used to make a thin bottom dish. These wrinkles can degrade the optical resolution of cells grown on polypropylene because the corrugated effect leaves a variation in cell position with respect to the microscope's focal plane. To improve the substrate on which the cells are grown, we have developed a procedure that uses a polymer called parylene to make thin and optically flat films that can also withstand the harsh chemical treatments in a biology laboratory.

The framework for this project was to make a miniwell on a plastic microscope slide where the parylene film would form the bottom of the well. Parylene film growth occurs when its molecules in the gas phase condense on objects in a deposition chamber, leaving a conformal coating. A backing was needed for the parylene film to condense against to form the flat well bottom. For that reason, a glass slide coated with the water-soluble release agent, Victawet (applied by evaporation or by dipping), was sandwiched between two plastic slides with ¼" diameter holes cut into them. This assembly was then clamped together and tape was applied around the edges to serve as a mask for subsequent Victawet exposure to water. Several deposition trials of such assemblies were sent to Para Tech Coating, Inc. (Middletown, CT) for coating. After the assemblies were shipped back to us, the mask tape was removed and the sets of three slides were placed into a pan of water. After adequate time elapsed for the Victawet to dissolve, the slides with miniwells easily separated from the glass slide backing; thin parylene film was left intact, forming a flat bottom to the miniwells.

Para Tech Coating does not have an accurate method to monitor the parylene film thickness. We measured the parylene thickness by taking energy loss measurements of 6 MeV helium ions passing through the foil and discovered that for an initial deposition, film thickness was between 7 and 8 microns. A parylene film thickness of about 2.5 microns is preferred for our microbeam irradiation experiments and this is a thickness that can be realized by reducing the quantity of raw materials proportionately.

There were a few challenges to overcome for producing the parylene film slide dishes for cell culture. One was to keep the parylene film from separating or peeling away from the bottom edge of the miniwell. To correct this, the slides were held together firmly so that the parylene film would bridge across the bottom of a slide's miniwell. A top surface, parylene adhesion issue, visible in the photograph of a parylene cell dish shown in Figure 1, was solved by buffing the entire surface of the plastic slides with holes in them. An-

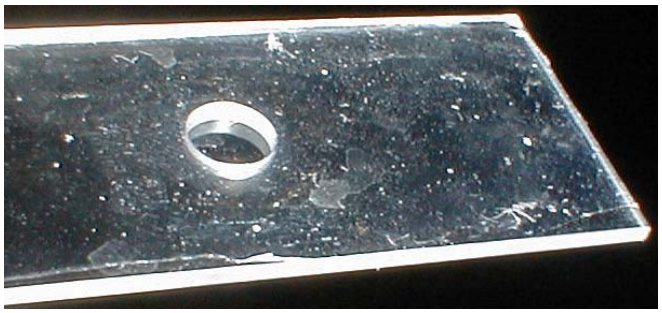

Fig. 1. Photograph of a parylene film across the bottom of a miniwell in a plastic slide. The film is noticeable with the reflections off the well walls and from the visible surface pattern that is due to growth defects in the parylene. Notice also how the parylene film is peeling away from the edges of the top slide surface; this problem has been solved by buffing the entire top surface of the slide.

other promising factor was that the parylene miniwell did withstand chemical treatments administered by the biologists during the cell growth cycles.

With the encouragement of the preliminary parylene deposition trials, we decided to move forward to purchase a parylene coater (Parylene Labcoter, Specialty Coating Systems, Indianapolis, IN). The system has been purchased and is installed in our facility. With the parylene coating system on hand, we have had some success with our first trials. With particle beam energy loss measurements, film thickness was validated to be acceptable for cell irradiation. Film quality is a concern because visible defects in the film can interfere with certain cell imaging and recognition routines; but using longer deposition times can reduce such defects. ■

Quantitative Phase Microscopy: Imaging Live Unstained Cells

Alan W. Bigelow, Charles R. Geard, Gloria Jenkins-Baker, Hongning Zhou, Brendan Allman,[1]
Gerhard Randers-Pehrson and David J. Brenner

Image recognition for locating cells and their nuclei is a crucial step in the process of microbeam irradiation. Our current protocols for microbeam irradiation of mammalian cell cultures use nuclear and cytoplasm stains to image and locate cells or cell nuclei. Even though we use very low stain concentrations (~50 nM), there is concern that these stains could alter cellular response to radiation. One of the most common requests both from users and from reviewers is to use an imaging system without stain.

Quantitative phase microscopy is a relatively new technique that can generate phase images and phase-amplitude images. In practice, to obtain a quantitative phase image one collects an in-focus image and very slightly positively and negatively defocused images, and uses these data to estimate the differential with respect to the defocus of the image. These images (a through-focal series) can be easily obtained in our system with our z-motion nano-positioner. The resulting data can be solved to yield the phase distribution by Fourier-transform methods. Results are obtained by essentially solving an optical transport equation. Significantly, the phase that is obtained does not have to be unwrapped, as is required for interferometry.

The Fourier transform-based software (QPm) for generating the phase images or the phase-amplitude images from the three microscope images is distributed by IATIA (Melbourne, Australia). In fact, because the methodology produces linear images of both amplitude and phase, it is possible to use the phase data to emulate other imaging modalities: differential interference contrast (DIC), Hoffman modulation contrast (HMC), Zernike phase contrast (ZPC), and simulated darkfield. The IATIA company has expressed enthusiasm to work with us to optimize our system for the QPm approach.

For initial QPm imaging trials, we chose two cell samples, normal human fibroblast cells plated on a glass slide and human-hamster hybrid (A_L) cells plated on polypropylene substrate, our current standard cell substrate for microbeam irradiation. Photographs of the live and unstained cells were taken with the cell-growth medium removed and according to the recommendations from IATIA using broadband Köhler illumination. Such images appear to be free of cells, as if they were not even there. In each case, a reference phase image was also acquired using DIC optics, a technique that requires transmission microscopy. With our microbeam application, we need to employ the imaging microscope in a reflection mode, a mode that is compatible with the QPm process. Nonetheless, in the reference phase images, it is possible to discern cell information that can be used as a comparison to the QPm results. To improve the signal-to-noise ratio, images were acquired using 100 frame averages. The through-focal series image sets were then sent off to IATIA in Australia for processing.

Reference phase images and QPm results are shown in the images in Figure 1 and in Figure 2 [printed at the top of the next page]. It is quite obvious that with false color applied to the QPm results, the location of the nucleus and the cell boundary is discernable. These boundary distinctions should suit the automated image recognition routine with the microbeam irradiation protocol. These preliminary trials lend optimism that if the QPm algorithm is incorporated into our microbeam irradiation protocol, targeting either the nucleus or the cytoplasm of live unstained cells will be allowed. ■

[1] *IATIA Ltd., Australia.*

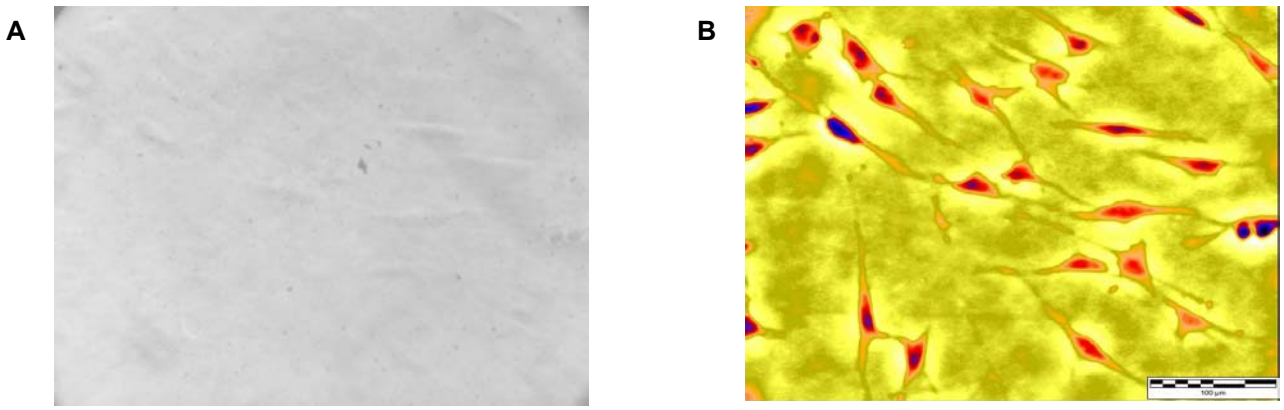

Fig. 1. Images taken with 20X magnification of live unstained normal human fibroblast cells plated on a glass slide; the reference phase image is in (a) and a false color applied to the QPm phase image is in (b).

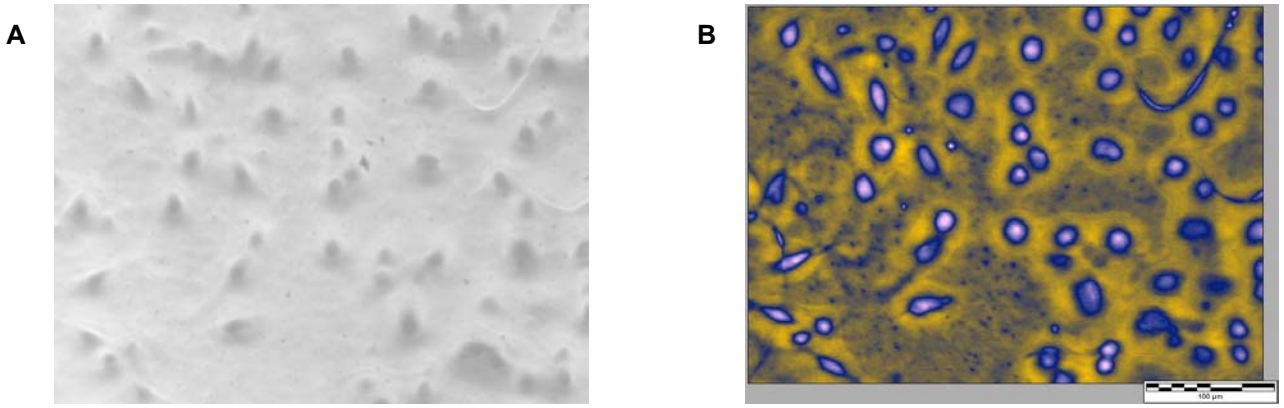

Fig. 2. Images taken with 20X magnification of live unstained human-hamster hybrid (AL) cells plated on polypropylene; the reference phase image is in (a) and a false color applied to the QPm phase image is in (b). The gold contour of these cells is possibly a combination of cell cytoplasm and residual cell-growth medium. The large arcs visible in these two images are artifacts of the polypropylene substrate. Such substrate artifacts can be an annoyance to automated image recognition routines.

Imaging Sub-Micron Particle Beams

Guy Y. Garty, Gerhard Randers-Pehrson and David J. Brenner

Ionizing radiation (IR) induces a wide spectrum of lesions including DNA single strand breaks (SSBs), double strand breaks (DSBs), base damage and DNA-protein cross links. Recent studies have indicated that the spectrum of lesions induced in the interphase nuclei largely depends both on the quality of radiation exposure and on the chromatin structure. Among IR induced DNA lesions, DSBs are considered to be very lethal as they lead to genomic instability and cell mortality if left unrepaired. Two major pathways exist in eukaryotic cells to repair DSBs in genomic DNA: (i) non-homologous end joining repair and (ii) recombinational repair. Both these repair pathways involve a number of proteins, which have dual roles in repair and DNA metabolic activities, interact with each other and sequentially assemble at the site of DNA lesions. Although substantial progress has been made in understanding the functional complexities of the various proteins in response to DNA damage, the precise participation of each of these proteins in the nuclear environment remains to be fully characterized. As compared to conventional gamma and x-ray irradiation, introduction of a minimum number of lesions at the defined sub-cellular compartments by microbeam irradiation would greatly enable us to understand the precise mode of action of the various protein complexes in DSB repair. Using such a facility developed at RARAF for microbeam α-particle irradiation, we have set out to examine the intra-nuclear dynamics of phosphorylated p53 protein in human cells in response to DNA strand breaks. P53 is a dynamic protein that is induced and

phosphorylated at several serine/threonine residues in response to DSBs. However, the role of phosphorylated p53 protein and its association with other DSB factors remain largely unknown. Knowledge on the intranuclear dynamics of phosphor-p53 protein in response to IR would enable us to better understand its role in DSB repair.

As we improve the spatial characteristics of the microbeam system, it becomes increasingly important to be able to assess the beam quality, in order to adjust the system to its optimum capabilities. For this purpose we are developing a secondary electron ion microscope (SEIM). This device would enable us to measure the beam profile and position, in real time, with sub-micron resolution.

The SEIM design was inspired by the common technique of photoelectron microscopy (PEM), used extensively in surface analysis (1). The SEIM design, shown in Figure 1, is based on conversion of incident projectiles using a secondary electron emitting film, generating one (or more) electrons per projectile. The ejected electrons are then imaged, using an electrostatic unipotential lens, forming a 500 times magnified image on an image intensified CCD.

The high magnification is required as the reasonably attainable resolution of an image intensified CCD is about 50 μm, 500 times larger than the required 100 nm resolution. In order to overcome the chromatic and spherical aberrations inherent in the electrostatic lens, the electrons are bent by a 45º angle, reflected by an electrostatic mirror and bent by an additional 45º before reaching the detector. This "folded" design of the SEIM is a novel one, developed at RARAF.

By using a specially designed, conical, electrostatic mirror (2) it is possible to exactly compensate for the aberrations induced by the lens. Furthermore, high energy electrons, which cannot be accurately focused, are sufficiently energetic to penetrate the mirror and are not reflected.

This is demonstrated in Figure 2, showing an example of 3 eV electrons, focused by the mirror and 15 eV electrons removed by the mirror. Figure 2b demonstrates the energy filtering of the mirror. The solid line is the theoretical energy spectrum of the electrons (3), the symbols are the energy spectrum of electrons which are reflected by the mirror. The mirror was seen to pass ~80% of all electrons below 5 eV and to filter out 80% of the electrons with energy above 5 eV. As energetic electrons are difficult to focus, we will obtain a better resolution by removing them. Using conventional electron optics techniques, energetic electrons are removed by placing an aperture in the focal plane of the mirror, resulting in a loss of more than 80% of the low energy electrons, and extremely poor efficiency.

We have performed extensive studies using SimIon (*Idaho National Engineering and Environmental Laboratory – INEEL*), in order to find the optimal mirror configuration for our geometry. By interfacing SimIon and Matlab (*The MathWorks, Inc., MA*), we have been able to implement a multidimensional search algorithm to automatically find the optimal SEIM operating parameters, for a given mirror geometry.

From these systematic studies we have found the "ideal" SEIM configuration, resulting in a resolution of 300 nm (Figure 3) and single electron detection efficiency of 75%. This figure was obtained by simulating electrons emitted with realistic energy and angular spectra. We expect that this

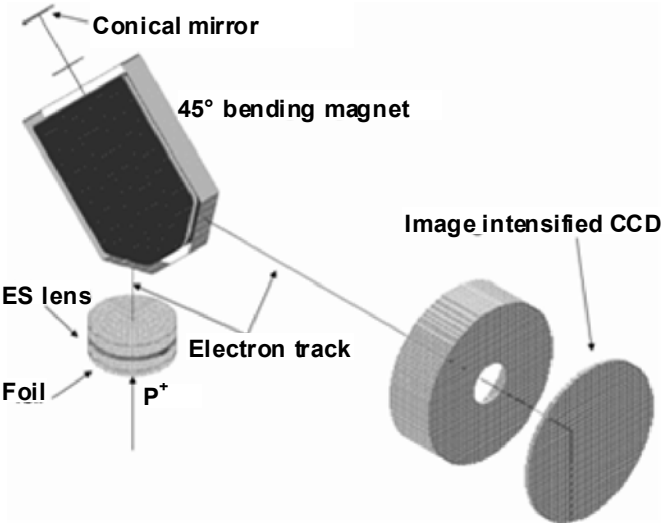

Fig. 1. Conceptual design of the secondary electron ion microscope. A typical electron trajectory is shown.

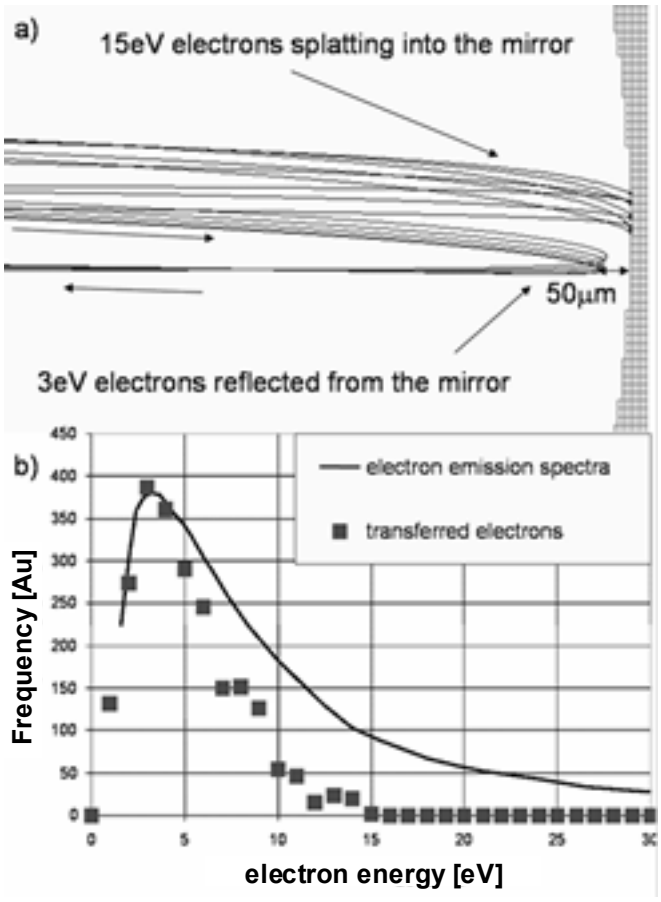

Fig. 2. (a) A SimIon simulation of the conical mirror. 3eV electrons are reflected whereas 15 eV electrons are absorbed. **(b)** The energy dependence of the mirror reflection. [The line represents the electron energy spectrum taken from (3)]. The symbols are the energy distribution of just those electrons which will be reflected from the mirror.

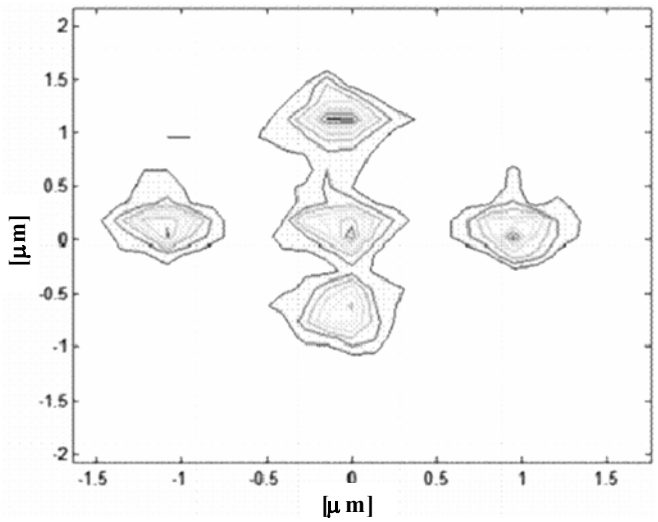

Fig. 3. The simulated image on the CCD camera, generated by five "zero-diameter" microbeams positioned 1 micron apart. The axes are scaled to the object plane. The resolution here is about 300 nm (FWHM).

resolution will improve as the square root of the electron yield which is expected to be higher than unity for heavy/energetic ions.

References

1. Günther S, Kaulich B, Gregoratti L and Kiskinova M. Photoelectron microscopy and applications in surface and materials science. *Prog Surf Sci* **70**:187-260, 2002.
2. Rempfer GF. A theoretical study of the hyperbolic electron mirror as a correcting element for spherical and chromatic aberration in electron optics. *J App Phys* **67**:6027-40, 1990.
3. ICRU report 55, Secondary electron spectra from charged particle interactions. International commission on radiation units and measurements, Washington, DC, 1996, pp 73 (figure 5.14). ■

Using Motion Predictive Control to Enhance Voice-Coil Stage Performance

Greg J. Ross, Gerhard Randers-Pehrson, Alan W. Bigelow and David J. Brenner

Central to the development of a submicron microbeam is the development of a comparably precise microscope stage. The custom designed Voice-Coil Stage (VCS), which we have built (Figure 1), uses thin coils in permanent magnetic fields to move the microscope stage, has been integrated into the new microbeam facilities and with Motion Predictive Control (MPC) algorithms has been shown to position the stage reliably under normal use to within ±0.4 μm, with a settling time of ~50 ms. Development is continuing to improve these numbers. Measurements of the commercial stage that we had previously used on the microbeam indicated that, for typical use, the error could be approximately 2 μm.

The VCS sample holder is attached to the frame by arms which are in turn attached to flexure mounts made from flat springs allowing motion in the two nearly orthogonal directions (x, y) while being very stiff in the z direction. The arms are also attached to voice coil winding holders positioned between permanent magnets so that when current is applied to windings, a force is produced. The displacement of the sample holder depends on the force on the coil (current) and the springs' restoring forces.

Although the movement of the sample holder in this system is in arcs rather than in straight lines, each x-y position on the dish corresponds to a single, calculable and reproducible set of coil currents. A digital-to-analog converter (DAC) in the computer provides the reference voltages for the current supplies for the two coils.

Drive Control System

The computer control system for the stage has evolved in three steps. First, an open-loop controller was used to move from selected position to position. Second, a standard closed-loop proportional-integral-differential (PID) system, based on a linear variable differential transformer (LVDT) sensor, was implemented to stabilize the position under disturbances such as air motion or vibration and errors due to differences in the relative level of the online and offline microscopes. Finally, a Model Predictive Control (MPC) system (1) was devised to allow driving the stage at speeds faster than its natural resonant frequency.

This MPC system is novel: We select a desired position vs. time profile from one half of a sine curve as shown in Figure 2. From this profile, we can directly calculate the desired velocity and acceleration. Modeling the system as a damped harmonic oscillator, we can then calculate the force needed to make the move along that profile. The calculated force is applied by directly feeding the appropriate signal to the driver stage of the closed-loop controller. Meanwhile, the expected position signal is fed to the normal control input of the controller so the error signal to be processed by

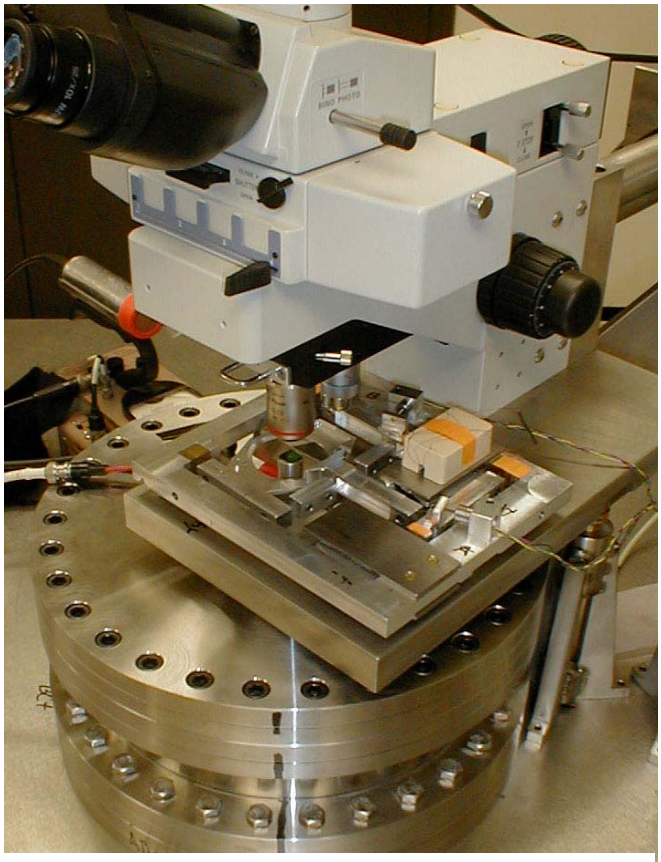

Fig. 1. Custom designed Voice-Coil Stage (VCS).

the PID stages of the controller contains only the stochastic errors. A fast four-channel Digital to Analog (D/A) computer card (General Standards 16AIO) is driven by a custom C++ program to provide the driving signals. The approach used in this particular MPC system works equally well for linear or non-linear systems.

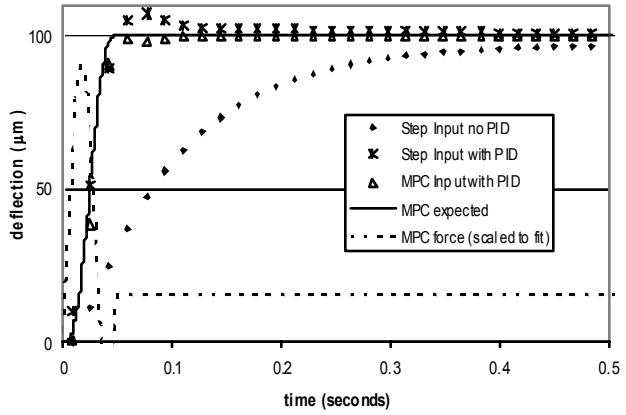

Fig. 3. The figure shows the improvement we get from using the PID circuit in closed–loop mode (◆ *vs* ∗), in terms of response to a step input change. The figure also shows an example (Δ) of the system response with the PID circuit in closed-loop mode and with a Model Predictive Control-based input. It can be seen that our typical settling time is 50 ms.

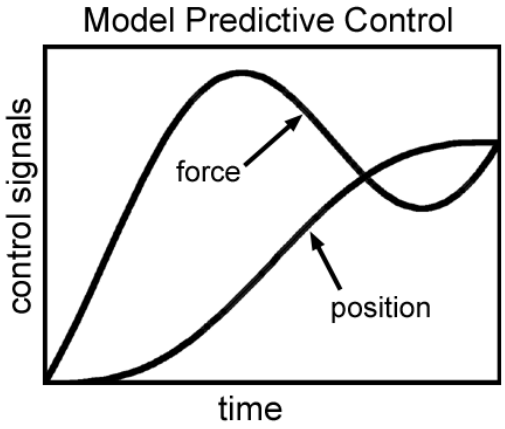

Fig. 2. Novel Model Predictive Control (MPC) system. We select a desired position vs. time profile from one half of a sine curve. From this profile, we can directly calculate the desired velocity and acceleration. Modeling the system as a damped harmonic oscillator, we can then calculate the force needed to make the move along that profile.

The Proportional-Integral-Differential (PID) Feedback System

In addition to the disturbances to position from external sources, the PID feedback using the LVDT position signal and fed into the controlling voltage negated the hysteresis effect in the springs. The PID fixed other smaller errors in the LVDT position caused by such disturbances as a small force from the lead wires going from the voice coils to the power supply and such as a small error (<1μm) in the LVDT's as a function of position (probably caused by inner winding structures).

Figure 3 shows the improvement we get from using the PID circuit in closed–loop mode (◆ *vs* ∗), in terms of response to a step input change. The Figure also shows an example (Δ) of the system response with the PID circuit in closed-loop mode and with a Model Predictive Control-based input. It can be seen that our typical settling time is 50 ms.

Thus, this closed-loop system demonstrates a submicron positional stability, as shown in Figure 4, with 99% of events (measurements) being within 0.4 μm over the course of 10 seconds (longer than the time spent in one 40x view of a sample during irradiation).

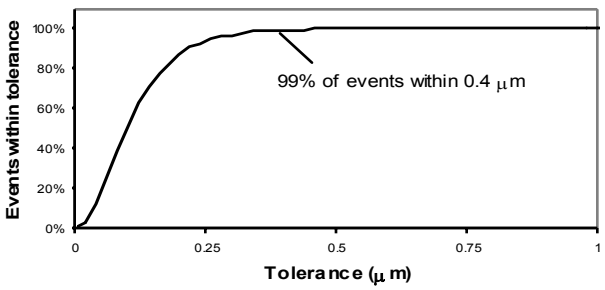

Fig. 4. This closed-loop system demonstrates a submicron positional stability, as shown in the figure, with 99% of events (measurements) being within 0.4 μm.

How Many Bystander Effects Are There?

Eric J. Hall and Stephen Mitchell

The "Bystander Effect" is not new. As early as the 1940s there were reports that the inactivation of biological entities may be brought about equally by ionizations produced within the entity or by the ionization of the surrounding medium (1-4). By 1947, Kotval and Gray (5) had shown that alpha particles which pass close to the chromatid thread, as well as those which pass through it, have a significant probability of producing chromatid and isochromatid breaks or chromatid exchanges.

The term used today to describe such phenomena is the "Bystander Effect," a name borrowed from the gene therapy field, where it usually refers to the killing of several types of tumor cells by targeting only one type of cell within a mixed population (6, for example).

In the radiation field, it has come to be loosely defined as the induction of biological effects in cells that are not directly traversed by a charged particle, but are in close proximity to cells that are.

Data now available concerning the bystander effect fall into two quite separate categories, and it is not certain that the two groups of experiments are addressing the same phenomenon. First, there are experiments involving the transfer of medium from irradiated cells, which results in a biological effect in unirradiated cells. Second, there is the use of sophisticated single particle microbeams, which allow specific cells to be irradiated and biological effects studied in their neighbors; in this case communication is by gap junction.

Medium transfer experiments have shown a bystander effect for cell lethality, chromosomal aberrations and cell cycle delay. The type of cell, epithelial versus fibroblast appears to be important, though data are conflicting. Experiments suggest that the effect is due to a molecule secreted by irradiated cells which is capable of transferring damage to distant cells. Use of a single particle microbeam has allowed the demonstration of a bystander effect for chromosomal aberrations, cell lethality, mutation and oncogenic transformation. When cells are in close contact, allowing gap junction communication, the bystander effect is a much larger magnitude than the phenomenon demonstrated in medium transfer experiments.

Evidence comes from experiments with V79 cells, where the endpoint observed was cell lethality. Lines of hygromycin and neomycin resistant V79 cells were produced. Before exposure the hygromycin resistant cells were stained with a low concentration of a vital nuclear dye. They were then plated in micro wells in the proportion nine neomycin-resistant for every one hygromycin resistant cell. The computer was programmed to irradiate only the 10% of cells stained with a nuclear dye with various numbers of alpha particles from 1 to 16, aimed at the centroid of the nucleus. The cells were then removed and cultured for survival in the appropriate growth media, which made it possible to obtain survival curves for hit and non-hit cells. The data are shown in Figure 1. There is a considerable degree of cell killing in the non-hit cells, implying a substantial bystander effect. The magnitude of the bystander effect in these studies is much greater than that reported by the Gray Institute for Cancer Research where only 5 to 10% lethality is seen in non-hit cells, using protons or soft-x-rays in a microbeam. The difference is probably accounted for by the cell density. In the Gray Institute studies, only about 200 cells were seeded in an area of 10 x 10 mm. The average distance between cells, therefore, was some hundreds of microns, so it is likely that communication via gap junction did not contribute to the effect observed (Barry Michael, Private Communication). By contrast, in the studies reported here, 1,000 to 1,200 cells were plated, in a mini-well of 6.3 mm diameter so that 50 to 60% were in contact, allowing gap junction communication that has been demonstrated to be of importance in mutation studies with the microbeam. Therefore, these data support the notion that communication via the medium and communication via gap junctions are separate phenomenon because the magnitude of the effect is so different.

A very large bystander effect was observed in studies of oncogenic transformation in C3H 10T1/2 cells, where, in

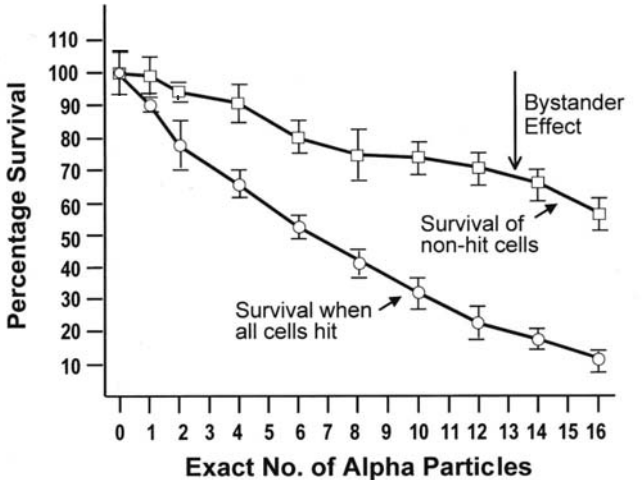

Fig. 1. The bystander effect for cell survival in V79 cells. Each data point (mean ± SE) on the line with circles refers to the survival of cells when all cell nuclei on each dish were exposed to the same exact numbers of alpha particle traversals using the microbeam system. The squares show survival for various numbers of alpha particles, from 1 to 16, traversing 10% of the cell population. The extent to which this falls below the 100% survival for the non-hit is an indication of the magnitude of the bystander effect. Each data point represents the mean ± SD of the clonogenic survivals from three culture plates. [Redrawn from Sawant et al. (7)].

order to have sufficient cells for this assay, cells were plated at high density and therefore were in gap-junction communication.

The data are shown in Figure 2 and illustrates that (a) more cells can be inactivated by alpha particles than were actually traversed by an alpha particle. (b) When 10% of the cells on a dish are exposed to two or more alpha particles, resulting frequency of induced oncogenic transformation is indistinguishable from that when all the cells on the dish are exposed to the same number of alpha particles. In these experiments mouse fibroblasts (C3H 10T1/2) cells were plated in a monolayer, and the computer was programmed to irradiate either every cell, or every tenth cell, selected at random with one to eight alpha particles directed at the centroid of the cell nucleus. The cells were subsequently removed by trypsinization, replated at low density, and transformed foci were identified 6 weeks later by their morphologic appearance.

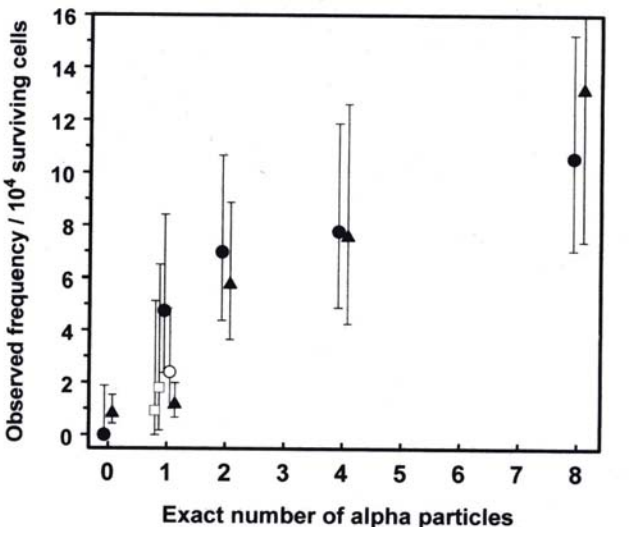

Fig. 2. Yield of oncogenically transformed cells per 10^4 surviving C3H 10T1/2 cells produced by nuclear traversals by 5.3 MeV α-particles. Triangles represent to exposure of all cell nuclei on each dish to exact numbers of α-particles, using the microbeam system. Solid circles represent exposure of 1 in 10 cell nuclei on each dish to exact numbers of α-particles. Open squares represent subsequent repeats of the experiment in which 1 in 10 cell nuclei were exposed to exactly one α-particle. Open circle represents combined data for all the experiments in which 1 in 10 cell nuclei were exposed to one α-particle including these repeat experiments (with caveats described in the text). Standard errors (± SD) were estimated assuming an underlying Poisson-distributed number of transformed cells. [Redrawn from the data of Sawant et al. (8).]

References

1. Dale WM. The effect of x-rays on enzymes. *Biochem J* 34:1367, 1940.
2. Dale WM. The effect of x-rays on the conjugated protein amino-acid oxidase. *Biochem J* **36**:80, 1942.
3. Dale WM. Effect of x-rays on aqueous solutions of biologically active compounds. *Brit J Radiol* **16**:171, 1943.
4. Lea DE, Smith KM, Holmes B and Markham R. Direct and indirect actions of radiation on viruses and enzymes. *Parasitology* **36**:110, 1944.
5. Kotval JP and Gray LH. Structural changes produced in microspores of Tradescantia by radiation. *J of Genetics* **48**:135-54, 1947.
6. Cheng TL, Wei SL, Chen BM, Chern JW, Wu MF, Liu PW and Roffler SR. Bystander killing of tumour cells by antibody-targeted enzymatic activation of a glucuronide prodrug. *Br J Cancer* **79**:1378-85, 1999.
7. Sawant SG, Zheng W, Hopkins KM, Randers-Pehrson G, Lieberman HB and Hall EJ. The radiation-induced bystander effect for clonogenic survival. *Radiat Res* **157**:361-4, 2002.
8. Sawant SG, Randers-Pehrson G, Geard CR, Brenner DJ and Hall EJ. The bystander effect in radiation oncogenesis: I. Transformation in C3H 10T1/2 cells in vitro can be initiated in the unirradiated neighbors of irradiated cells. *Radiat Res* **155**:397-401, 2001. ■

Identification of Signal Transduction Pathway(s) in High LET Radiation Induced Bystander Response by cDNA Microarray Analysis

Adayabalam S. Balajee, Brian Ponnaiya and Charles R. Geard

"Bystander effect" (BE) is the result of the ability of the cells directly affected by an agent to convey the manifestation of the damage to neighboring cells that are not directly targeted thereby eliciting a response similar to that of targeted cells. BE can be triggered either through direct contact with the damaged cells or through the growth factors released from the targeted cells (1). Although the signaling pathways responsible for bystander response are largely unknown at this moment, this multifaceted phenomenon is expected to have a significant impact on the radio- and che-

motherapy of tumors. A better understanding of molecular steps involved in BE is pivotal for modulation and evaluation of the protocols designed to improve the efficacy of the radio and chemotherapy treatments. In an attempt to understand the molecular basis for BE, we have undertaken a cDNA microarray approach to identify the components of diverse signal transduction pathways that mediate the response.

Primary fibroblast cells (normal human dermal fibroblasts, NHDF) were obtained from Clonetics. The cells were routinely maintained in fibroblast basal medium supplemented with 15% fetal bovine serum, vitamins, essential amino acids, non-essential amino acids and antibiotics (Gibco BRL). The cultures were maintained at 37°C in a humidified 5% CO_2 atmosphere. NHDF cells were seeded on double-sided Mylar dishes and the dishes were irradiated only on one side with different doses of track segment alpha particles (1 and 5 Gy). The protocol for preparation and irradiation of cells in double-sided Mylar dishes has been previously described (2). Total RNA was isolated from both irradiated (bottom) and non-irradiated (top) cells. cDNA synthesis was carried out using biotin-16-dUTP and the biotinylated cDNA samples were denatured and hybridized with cDNA signal transduction pathway finder array procured from Super Array, MD, USA. This array contains 96 marker genes associated with 18 different signal transduction pathways (Mitogenic pathway, Wnt pathway, Hedgehog pathway, TGF pathway, Survival pathway, p53 pathway, stress pathway, NFkB pathway, NFAT pathway, CREB pathway, Jak-Stat pathway, Estrogen Pathway, Androgen pathway, calcium and Protein kinase C pathway, phospholipase C pathway, insulin pathway, LDL pathway and Retinoic acid pathway). After hybridization, the signal was detected using streptavidin-alkaline phosphatase as per the instructions of the manufacturers. The membranes were used to expose Kodak BiomaX light films. Digital images were generated using the ScanAlyze2 programme (developed by Michael Eisen at Lawrence Berkeley National Laboratory). The analysis was done using GE array analyzer (Super Array). A representative example of hybridization patterns obtained for control direct hit and bystander cells is shown in Figure 1.

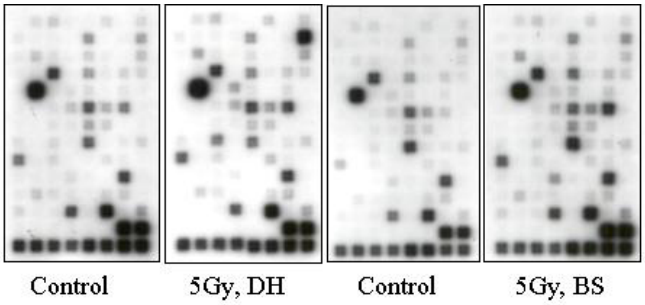

Fig. 1. cDNA expression profiling of genes associated with 18 signal transduction pathways in control, direct hit (DH) and bystander (BS) cells. Exponentially growing NHDF cells were irradiated with 5 Gy of α-particles. Total cellular RNA was isolated 3 hrs after irradiation and 1μg of the RNA was used for cDNA synthesis with biotin 16-dUTP for hybridization to super array filters.

The results of cDNA arrays indicated that 15 genes [Bcl-2, Bcl2L1 (Homo sapiens BCL-2 like protein 1), BIRC 1, BIRC2 (Homo sapiens baculovirus IAP repeat containing proteins), BRCA1, CD5 (T-cell surface glycoprotein), CDK2 (Cyclin dependent kinase 2), CDKNIA (p21), CDX1 (Homo sapiens caudal type homeo box transcription factor 1), CEBPB (Homo sapiens CCAAT/enhancer binding protein beta), FLJ12541 (Homo sapiens hypothetical protein FLJ12541 similar to mouse Stra6), GADD45A, HK2 (Homo sapiens hexokinase2, nuclear gene encoding mitochondrial protein), KLK2 (Prostrate kallikrein 2) and MDM2] out of a total of 96 belonging to p53, survival, TGF, androgen and Retinoic acid pathways showed a 2-4 fold increase in induction in direct hit NHDF cells as compared to unirradiated control cells. Of all, p21 showed the highest induction being 7.34 fold more than that of control cells. Distinct differences in the expression patterns were observed between direct hit and bystander cells. In contrast to direct hit cells, genes representing NF-kB, protein kinase C and p53 pathways were selectively induced in bystander cells. Out of 96 genes, 3 genes [IGFBP3 (insulin-like growth factor binding protein 3), NFKBIA (Nuclear factor of kappa light polypeptide gene enhancer in B-cells inhibitor alpha) and PRKCE (protein kinase C epsilon)] in bystander cells showed a 2 fold more induction than control cells. Both IGFBP3 and PRKCE showed a 2.8 fold more induction than the unirradiated cells. The unique expression patterns observed for direct hit and bystander cells indicate that the factors triggering the signal transduction pathways may differ between BE and radiation response.

We are presently doing cDNA experiments using RNA samples isolated at different post-irradiation times (30 min, 3 hrs, 6 hrs, 9 hrs and 24 hrs) to follow the differential expression of genes in both direct hit and bystander cells. Additionally, pathway specific arrays are being carried out to confirm the initial observations. Efforts are also underway to verify the cDNA array results by western blotting and RT-PCR. It would be interesting to know whether the signal transduction pathways that mediate the bystander response are defective in radiosensitive mutants. We plan to use several human mutant cells defective in important DSB repair genes to determine whether DSB repair efficiency contributes to bystander response. This project will be initiated by culture of wild type and AT cells in double-sided Mylar dishes to determine whether or not ATM kinase plays a role in radiation induced bystander response in human cells. This approach will be gradually extended to other double strand break repair defective cell lines with mutations in Nbs1 and DNA-PK gene products.

References

1. Iyer R and Lehnert BE. Effects of ionizing radiation in targeted and nontargeted cells. *Arch Biochem Biophys* **376**:14-25, 2000.
2. Geard CR, Jenkins-Baker G, Marino SA and Ponnaiya B. Novel approaches with track segment alpha particles and cell co-cultures in studies of bystander effects. *Radiat Prot Dosimet* **99**:233-6, 2002. ■

Involvement of Replication Protein A in Ionizing Radiation Induced Bystander Response in Human Cells

Adayabalam S. Balajee, Brian Ponnaiya and Charles R. Geard

"Bystander effect" (BE) is an interesting biological phenomenon where cells not directly affected by DNA damaging agents elicit a response similar to that of targeted cells. Increased levels of sister chromatid exchange, micronuclei, p21 and p53 proteins in bystander cells indicate that a complex DNA damage response pathway may mediate BE. Identification of the DNA repair and signal transduction proteins involved in BE may help in understanding the molecular cascade of events leading to this complex phenomenon. With this objective, we have studied the expression of replication protein A, which is involved in diverse DNA metabolic activities such as replication, repair and recombination.

RPA is induced in bystander cells

Using γ-rays as a DNA damaging agent, RPA expression was analyzed in both direct hit and bystander primary human fibroblast cells (MRC5 and WI38) by immunofluorescence and western blot techniques. Unirradiated control cells exhibited a punctuated pattern of RPA foci ranging from 30-40 in number per cell. The pattern of RPA distribution was essentially the same in cells treated for 30 min with irradiated-conditioned medium without cells. In contrast, intense numerous RPA foci were observed in cells treated with conditioned medium derived from irradiated MRC5 cells. The fluorescence intensity was 2-fold more than that of control cells. The pattern of RPA foci observed 30 min after treatment in bystander cells was different from cells that were directly irradiated with either 5 Gy or 10 Gy of γ-rays. The bystander cells were characterized by numerous intense RPA foci while the irradiated cells displayed large 30-40 distinct focal sites of RPA. Treatment of MRC5 cells with hydrogen peroxide (which predominantly induces single strand breaks and oxidative base lesions) also triggered numerous intense RPA foci 30 min after treatment similar to that observed in ionizing radiation (IR) induced bystander cells.

Western blot analysis was next carried out to determine whether the induced RPA was found either in the soluble fraction or in the chromatin bound fraction. For this purpose, total cellular proteins extracted using low (soluble) and high salt (insoluble) buffers were size fractionated on 4-20% SDS-PAGE and RPA was detected immunologically. Consistent with immunofluorescence data, RPA induction was observed in both soluble and chromatin bound protein fractions derived from bystander MRC5 cells. Bystander cells showed a 2-3 fold induction of RPA as compared to control cells and RPA induction was more pronounced in the chromatin bound fraction. In directly irradiated WI38 cells, RPA induction was hardly detectable in both soluble and insoluble protein fractions at 30 min after treatment. RPA induction was however observed at later times in WI38 cells yet the fold of induction was lower in the chromatin bound fractions during the first 2 hrs after irradiation. In bystander cells, RPA induction, which was rapid in the insoluble protein fractions at 30 min after treatment, showed a gradual decline at 4 hr with a subsequent increase at 6 hr after treatment. This biphasic kinetics of RPA induction observed in bystander cells was not detectable in direct hit cells. In addition to RPA, p53 induction was analyzed in both bystander and direct hit cells. Unlike RPA, p53 induction was noticed only in the insoluble protein fraction and the kinetics of induction was grossly similar in both bystander and direct hit cells reaching a peak at 4 hr after treatment. To clarify whether or not the increased level of RPA (observed by immunofluorescence and western blot analyses) is due to post-translational modifications, RT-PCR was carried out using the cDNA synthesized from total cellular RNA. RT-PCR analysis showed a 2-fold more induction of RPA in both direct hit and bystander cells as compared to untreated control cells, illustrating the transcriptional activation of RPA in response to DNA damage.

In order to verify whether or not the differences between the two-fibroblast cell lines (WI38 and MRC5) contribute to bystander effects, RPA induction was analyzed in bystander MRC5 cells treated with the transfer of medium derived from irradiated MRC5 cells. In corroboration with earlier results, RPA induction was observed both in the soluble and insoluble protein fractions of MRC5 bystander cells. RPA induction was detected at 30 min after treatment, which slowly declined to the level of control cells by 24 hr. To determine whether the induction of RPA in bystander cells was mainly due to the release of soluble factor(s) from the irradiated cells, RPA induction was analyzed in cells treated with complete medium that was irradiated without cells. RPA induction was not detectable in either of the protein fractions isolated from cells that were treated with irradiated medium alone (without cells) and the RPA level was approximately the same in both control and treated samples at different treatment times. This observation strongly suggests that the irradiated medium alone did not contribute to RPA induction but the signal elicited by the irradiated cells was chiefly responsible for increased RPA expression in bystander cells.

γ-H2AX, an indicator of DNA double strand breaks, is not elevated in radiation induced bystander cells

In order to determine the nature of DNA lesions leading to RPA induction, the expression of the phosphorylated form of histone H2AX (γ-H2AX) was analyzed in both direct hit and bystander cells. γ-H2AX has been shown to specifically bind to DNA double strand breaks induced by ionizing ra-

diation and radiomimetic chemicals. Western blot analysis indicated a 2.5 fold increase in the induction of γ-H2AX at 30 min after treatment, which gradually declined to the control level with increasing recovery times. On the contrary, bystander cells did not exhibit any increase in γ-H2AX level. The lack of γ-H2AX induction in bystander cells suggests that lesions other than DNA double strand breaks may be responsible for RPA induction in bystander cells.

In this study, we have shown that replication protein A, which is a key player in base excision repair (BER) pathway, is specifically induced in the bystander cells. The rapid induction of RPA and its subsequent decline with increasing recovery times suggest that the DNA lesions, which are substrates for BER pathway, are inflicted in the genomic DNA of bystander cells. ■

Gene Expression as a Window on Bystander Effects

Sally A. Amundson

Exposure of mammalian cells to ionizing radiation (IR) induces damage in multiple cellular compartments, resulting in complex biological responses, many of which are mediated through alterations in gene expression. While direct damage to DNA has long been considered the major initiator of cellular responses to IR, the more recent recognition of "non-targeted" effects of IR, such as radiation-induced bystander effects, is altering our understanding of radiation damage and response. Intra-cellular signaling from neighboring irradiated cells is thought to mediate bystander effects in cells not directly irradiated. Documented bystander effects include sister chromatid exchanges, reduced clonogenic survival, chromosome aberrations, apoptosis, micronucleation, oncogenic transformation, mutation induction, and changes of gene expression. Gene expression changes can represent effector responses, the mobilization of the molecular machinery that will execute the cellular endpoints observed, but they can also provide insight into the signal transduction pathways underlying bystander responses.

A functional genomics approach, such as microarray hybridization analysis (1), can survey expression changes in thousands of genes simultaneously. This will enable the identification of potential mediators of bystander signaling, including soluble factors, such as cytokines. This approach should also prove useful in determining the effects of bystander factors on gene expression in unirradiated cells, and suggesting key signaling pathways that might be engaged or blocked to mimic or prevent bystander responses.

Considering that cytokines, such as IL8 (2) and TGFß (3), are known to be released from irradiated cells and have been implicated in mediation of bystander effects in unirradiated cells, preliminary microarray studies examined whether additional cytokine-related genes showed IR-responsiveness and to determine if a soluble factor(s) from irradiated cells could affect gene expression in unirradiated (bystander) cells. As shown in Figure 1, expression of many cytokine-related and extracellular signaling genes increased at various times after IR in human myeloid ML-1 cells as well as after IR or UV radiation in the breast line MCF-7. We have also seen induction of cytokine mRNAs, including *IL1A, IL1B, IL6*, and *A4* in human peripheral blood lymphocytes (4) irradiated *ex vivo*. In addition, we have treated

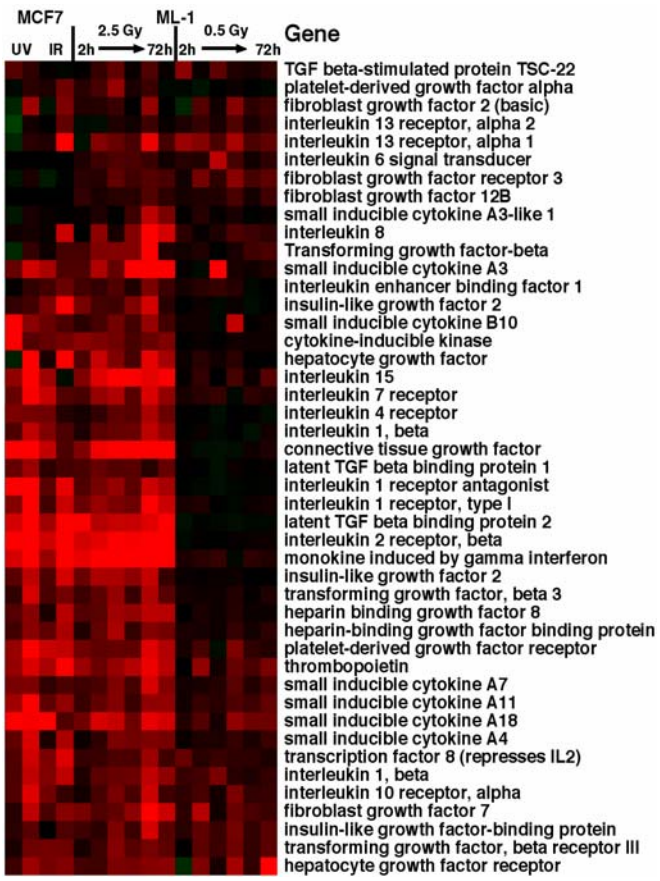

Fig. 1. Hierarchical clustering of radiation induced genes with roles in extracellular signaling (cytokines, interleukins and growth factors from a 6728 member microarray.) The experiments are (from left to right) MCF7 12 hours after 125 J/m2 UVB, 6 hours after 4 J/m2 UVC, 4 hours after 2.5 Gy α-particles, 24 hours after 2.5 Gy α-particles. These are followed by results for ML-1 2, 4, 8, 24, 48 and 72 hours after 2.5 Gy γ-rays, then at the same times following 0.5 Gy γ-rays.

Table I.

Bystander gene induction in TK6 cells.

HCT116		MCF7	
4 h	24h	4h	Gene
2.9	7.1	4.0	ESTs
2.8	7.4	4.2	SIAT8
2.8	6.4	2.3	CYP1B1
2.7	8.6	4.5	THBS2
2.6	5.9	2.0	LYZ
2.6	6.1	4.4	ESTs
2.5	7.1	2.9	PAI2
2.5	6.0	2.7	CCL11
2.5	6.2	3.4	UNG2
2.5	6.7	2.5	CEACAM1
2.4	6.5	3.6	CTGF
2.4	6.1	2.8	TGM3
2.3	5.9	3.3	TXN
2.3	7.0	3.8	CNGA1
2.3	4.9	2.8	MNDA
2.3	7.2	2.8	ESTs
2.3	9.5	2.4	MGC11271
2.3	5.9	2.9	AMPH
2.2	4.6	2.4	CTSG
2.2	4.9	3.3	ADH4
2.2	4.5	3.1	ESTs
2.2	4.9	3.2	FOXO1A
2.2	5.9	3.3	CDH11
2.2	6.1	3.3	VDR
2.2	6.0	2.8	BRAF
2.1	6.3	2.7	GSTA2
2.1	8.1	3.7	PYGL
2.1	5.8	3.1	CD8A
2.1	5.9	2.6	PPBP
2.1	5.6	2.9	PCYOX1
2.1	5.2	2.8	ESTs
2.1	5.8	3.3	FGA
2.1	4.5	2.2	TNA
2.0	7.2	3.4	LTBP2
2.0	6.9	2.5	ESTs
2.0	5.9	2.7	ESTs
2.0	6.8	2.4	TGFB3
2.0	5.1	2.2	SMPD1

Genes induced in TK6 cells by (4 or 24 hours) exposure to conditioned medium produced by cells irradiated with 5 Gy gamma-rays, as identified from hybridization to 6728 member microarrays.

lymphoid cells, which we previously found to be most sensitive to radiation-induced gene expression changes, with cell-free conditioned media collected 30 minutes after γ-irradiation of HCT116 or MCF-7 cells. Genes showing consistent induction after 4 and 24 hours of exposure to γ-ray conditioned medium are listed in Table I with the magnitude of induction as determined by microarray hybridization. Significant gene induction was also observed in MCF-7 cells similarly treated with MCF-7 conditioned medium, although this response was of lower magnitude, consistent with the response to direct irradiation of this cell line. These results indicate that soluble factors from irradiated cells can have an appreciable effect on gene expression in unirradiated cells of the same and different tissue type. We can conclude from these studies that soluble IR-induced factors do affect gene

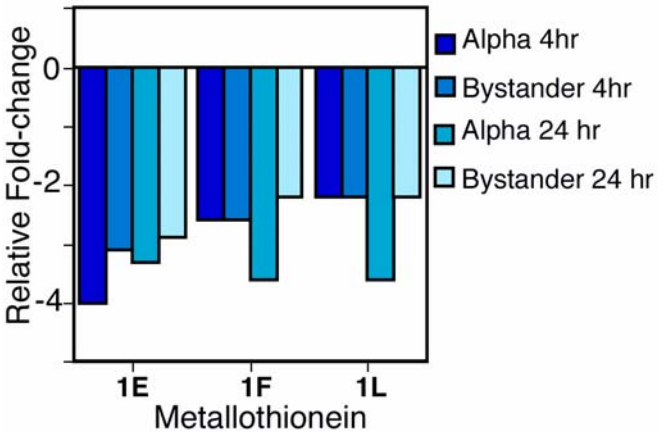

Fig. 2. Relative decrease in expression of metallothionein genes 1E, 1F, and 1L in MCF7 directly and bystander irradiated with 2.5 Gy α-particles, as measured by microarray 4 and 24 hours after irradiation.

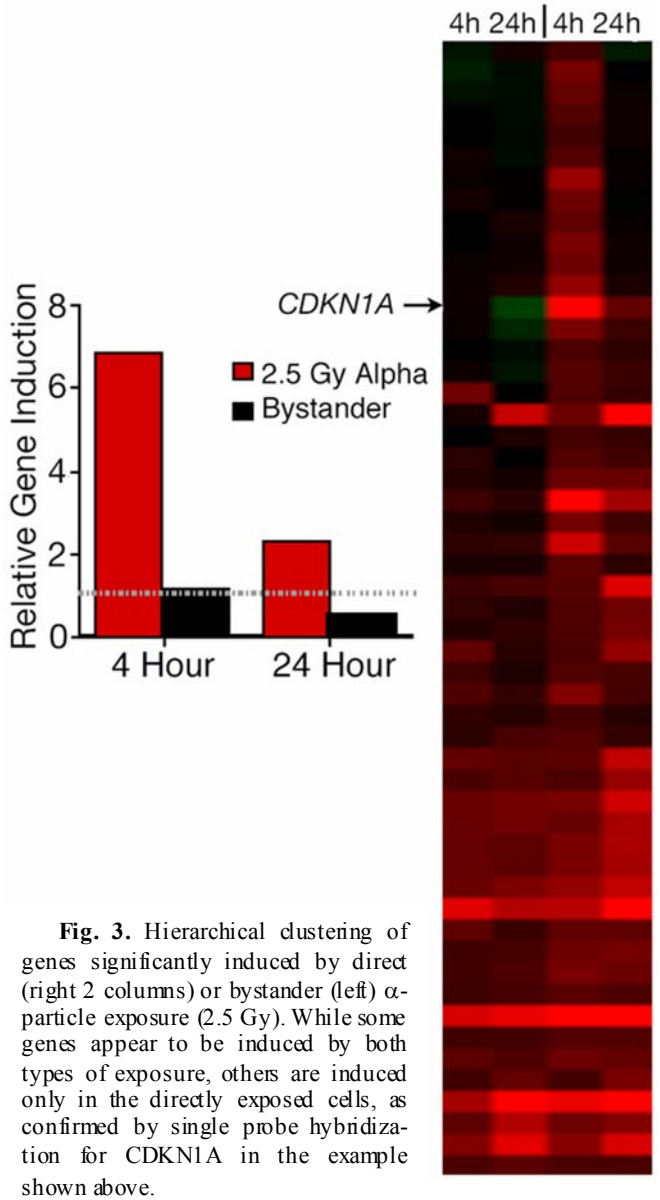

Fig. 3. Hierarchical clustering of genes significantly induced by direct (right 2 columns) or bystander (left) α-particle exposure (2.5 Gy). While some genes appear to be induced by both types of exposure, others are induced only in the directly exposed cells, as confirmed by single probe hybridization for CDKN1A in the example shown above.

expression in bystander cells.

A pilot study using the track segment facility at RARAF has also indicated bystander gene responses following alpha-particle irradiation. In this experiment, MCF7 cells were grown in mylar-bottomed dishes, and half of each dish was irradiated with 2.5 Gy 120 keV/μm α-particles, while the other half was shielded using an aluminum mask. A striking feature of the emerging bystander signature was the apparent coordinate down-regulation of a number of metallothionein genes (Figure 2). Hierarchical clustering of the genes induced in the directly irradiated and bystander halves of the dishes is illustrated in Figure 3. While induction of some genes, such as the illustrated *CDKN1A*, occurred only in the directly irradiated cells, other genes did respond in bystander cells.

The bystander effect is likely to be a natural phenomenon with relevance to IR exposures in humans, and careful gene expression profiling experiments have the potential to dramatically shape our understanding of the signaling and response mechanisms involved. As a naturally occurring physiological response of whole organisms, bystander effects should ideally be studied in an *in vivo*-like multicellular system with preserved 3-D tissue micro-architecture and microenvironment. Future experiments will move toward this goal, building on the results of ongoing experiments in well-characterized cell culture systems and our prior gene expression studies (4, 5, 6, 7).

References

1. Schena M, Shalon D, Davis RW and Brown PO. Quantitative monitoring of gene expression patterns with a complementary DNA microarray. *Science* **270**:467-70, 1995.
2. Narayanan PK, LaRue KE, Goodwin EH and Lehnert BE. Alpha particles induce the production of interleukin-8 by human cells. *Radiat Res* **152**:57-63, 1999.
3. Iyer R and Lehnert BE. Factors underlying the cell growth-related bystander responses to alpha particles. *Cancer Res* **60**:1290-8, 2000.
4. Amundson SA, Shahab S, Bittner M, Meltzer P, Trent J and Fornace AJ Jr. Identification of potential mRNA markers in peripheral blood lymphocytes for human exposure to ionizing radiation. *Radiation Res* **154**:342-6, 2000.
5. Amundson SA, Bittner M, Chen YD, Trent J, Meltzer P and Fornace AJ Jr. cDNA microarray hybridization reveals complexity and heterogeneity of cellular genotoxic stress responses. *Oncogene* **18**:3666-72, 1999.
6. Amundson SA, Do KT and Fornace AJ Jr. Induction of Stress Genes by Low Doses of Gamma Rays. *Radiat Res*. **152**:225-31, 1999.
7. Amundson SA, Lee RA, Koch-Paiz CA, Bittner ML, Meltzer P, Trent JM, Fornace AJ Jr. Differential responses of stress genes to low dose-rate gamma irradiation. *Mol Cancer Res* **1**:445-52, 2003. ■

The Bystander Response in C3H 10T½ Cells: The Influence of Cell-to-Cell Contact

Stephen A. Mitchell, Stephen A. Marino, David J. Brenner and Eric J. Hall

It is now widely accepted that radiation-induced heritable effects in mammalian cells are not solely the result of direct DNA damage and there is now evidence for a number of non-targeted effects, including the bystander response, which do not require a direct nuclear exposure (1). The bystander effect is defined as the observation of a biological response in cells which have not been directly traversed by ionizing radiation but which results from signals initiating in cells in which energy has been deposited.

Although reproducible bystander effects have now been demonstrated for a range of biological endpoints, the mechanisms by which the biological insult is transmitted from targeted to non-targeted cells have not been fully elucidated and may be dependent on the experimental protocol employed (reviewed in (2)). One causative agent may be the secretion from irradiated cells of a soluble factor(s) into the media which then elicits a biological response in unirradiated cells, often over some considerable distance (3). Alternatively, in densely-irradiated cultures the signal may be transmitted by cell-to-cell communication between adjacent cells via gap junctions (reviewed in (4)).

Previous studies using the Columbia microbeam have shown a significant bystander effect for the endpoints of clonogenic survival and oncogenic transformation in C3H 10T½ cells (5, 6). The aim of the present study was to assess whether the magnitude of this effect observed for both endpoints was dependent upon cell-to-cell proximity at the time of irradiation. To achieve this, cells were plated at both high and low density and targeted with a range of 6 MeV α-particles aimed at the centroid of the nucleus. When approximately 2000 cells were plated on a microbeam dish, the vast majority (>90%) of the cells were in direct contact with neighbors via membranes and intercellular gap junctions when irradiated 18 h later. In contrast, when 200 cells were plated using the same protocol, very little contact between cells (<10%) was seen with the majority of cells appearing

as isolated entities, separated by many tens of microns from their neighbors.

The experimental protocol and results for clonogenic survival have been reported previously (http://crr-cu.org/reports2002/b4.htm). Briefly it was observed that at both cell densities, the surviving fractions fell progressively as more α-particles traversed the nucleus but the amount of cell killing was significantly greater at the high cell density compared with low-density cultures ($P<0.0001$). The study has now been extended to examine the influence of cell density on oncogenic transformation. To assess this parameter, 10% of the cells were exposed to 8 α-particles. Following irradiation, cells were replated into 100 mm culture dishes at a low density of about 300 viable cells per dish. The cells were incubated for 7 weeks with culture medium changed every 12 days, before being fixed and stained with Giemsa to identify morphologically-transformed types II and III foci, as described elsewhere (7).

Results are shown in Table I. In these studies, a total of approximately 3.1×10^5 cells were individually imaged, positioned and irradiated. At high density, a transformation frequency of $9.6/10^4$ viable cells was seen, which is similar to that found previously in high-density cultures (5). Using previously published data (8) it is possible to calculate that when 10% of the cells in a population are irradiated with 8 α-particles, the expected transformation frequency in the absence of a bystander effect would be $2.1/10^4$ viable cells. This is lower than that seen in the present study at both cell densities, although again the difference is only significant in the case of the high-density cultures ($P<0.0001$ vs. $P=0.28$ at low density). A statistically significant three-fold decrease in the transformation frequency was observed in the low relative to high cell-density cultures ($P<0.0004$).

These data indicate that the magnitude of the bystander effect is cell-density dependent in C3H 10T½ cells, implicating the involvement of gap junction mediated intercellular communication in transmitting the bystander effect. Several studies have now shown that inhibition of this gap-junction activity in cells irradiated in close contact results in decreased levels of the bystander effects for a variety of biological endpoints (9, 10). An alternative, but unlikely, explanation is that the observed effect is due to some factor released into the media, which, because of a very short half-life can only migrate small distances from the irradiated cell. This is unlikely because it has been estimated that for the irradiation protocol used in the present study, any bystander signal induced could travel over a large distance through the media during irradiation (approximately 600-700 μm) (11).

The results obtained for low-density cultures did deviate from those expected in the absence of a bystander effect, suggesting that such an effect may still be operative. Considering oncogenic transformation, in the absence of a bystander effect a transformation frequency of $2.1/10^4$ viable cells is expected which is less (although not significantly) than the observed frequency of 3.3 (Table I). A similar result was seen previously for clonogenic survival with a non-significant increase in cell killing. However, any bystander effect evident in the low-density cultures is likely to result from interaction of a secreted cytotoxic factor with unirradiated cells, rather than direct communication due to the very low frequency of cell-to-cell contact. This has been confirmed in a previous study on low-density cells where a random distribution of damaged cells throughout the population was seen, suggestive of an extracellular factor (12).

In conclusion, the present study confirms that when cells are exposed to low doses of α-particles the degree of cell-to-cell contact at the time of irradiation is important in transmission of the bystander signal. When cells are in close contact, gap-junctions play a major role, whereas if the degree of contact is poor, the bystander effect is mediated by the release of factors into the surrounding environment.

Table I.

Clonogenic survival rates, number of dishes exposed, numbers of viable cells exposed in transformation studies, number of transformed clones produced, and transformation frequencies for microbeam irradiations.

No. of cells plated, No. of α-particles	Clonogenic surviving fraction (plating efficiency) (±SEM)	No. of dishes exposed	No.* of viable cells exposed/ 10^4	No. of transformants produced	Transformation frequency/ 10^4 surviving cells
200, 0α	(0.23±0.02)	71	0.9	1	1.1
2000, 0α	(0.17±0.03)	60	2.1	1	0.5
200, 8α	0.93±0.02	155	1.8	6	3.3
2000, 8α	0.81±0.01	73	1.5	14	9.6

* *Estimated, accounting for plating efficiency and clonogenic survival.*

References

1. Mothersill C and Seymour C. Low-dose radiation effects: Experimental hematology and the changing paradigm. *Exp Hematol* **31**:437-45, 2003.
2. Morgan WF. Non-targeted and Delayed Effects of Exposure to Ionizing Radiation: I. Radiation-Induced Genomic Instability and Bystander Effects In Vitro. *Radiat Res* **159**:567-80, 2003.
3. Mothersill C and Seymour C. Medium from irradiated human epithelial cells but not human fibroblasts reduces the clonogenic survival of unirradiated cells. *Int J Radiat Biol* **71**:421-7, 1997.
4. Ballarini F, Biaggi M, Ottolenghi A and Sapora O. Cellular communication and bystander effects: a critical review for modelling low-dose radiation action. *Mutat Res* **501**:1-12, 2002.
5. Sawant SG, Randers-Pehrson G, Geard CR, Brenner DJ and Hall EJ. The bystander effect in radiation oncogenesis: I. Transformation in C3H 10T1/2 cells in vitro can be initiated in the unirradiated neighbors of irradiated cells. *Radiat Res* **155**:397-401, 2001.
6. Sawant SG, Randers-Pehrson G, Metting NF and Hall

EJ. Adaptive response and the bystander effect induced by radiation in C3H 10T(1/2) cells in culture. *Radiat Res* **156**:177-80, 2001.
7. Reznikoff CA, Bertram JS, Brankow DW and Heidelberger C. Quantitative and qualitative studies of chemical transformation of cloned C3H mouse embryo cells sensitive to postconfluence inhibition of cell division. *Cancer Res* **33**:3239-49, 1973.
8. Miller RC, Randers-Pehrson G, Geard CR, Hall EJ and Brenner DJ. The oncogenic transforming potential of the passage of single alpha particles through mammalian cell nuclei. *Proc Natl Acad Sci USA* **96**:19-22, 1999.
9. Zhou H, Randers-Pehrson G, Waldren CA, Vannais D, Hall EJ and Hei TK. Induction of a bystander mutagenic effect of alpha particles in mammalian cells. *Proc Natl Acad Sci USA* **97**:2099-104, 2000.
10. Azzam EI, de Toledo SM and Little JB. Direct evidence for the participation of gap junction-mediated intercellular communication in the transmission of damage signals from alpha-particle irradiated to nonirradiated cells. *Proc Natl Acad Sci USA* **98**:473-8, 2001.
11. Nikjoo H and Khvostunov IK. Biophysical model of the radiation-induced bystander effect. *Int J Radiat Biol* **79**:43-52, 2003.
12. Belyakov OV, Malcolmson AM, Folkard M, Prise KM and Michael BD. Direct evidence for a bystander effect of ionizing radiation in primary human fibroblasts. *Br J Cancer* **84**:674-679, 2001. ■

The Bystander Effect and Adaptive Response in C3H 10T½ Cells

Stephen A. Mitchell, Gerhard Randers-Pehrson, David J. Brenner and Eric J. Hall

Evidence has now emerged for a number of biological phenomena which may be important in determining the cellular response to low doses of radiation (1). These include but are not limited to the bystander effect and adaptive response. Although both these phenomena are important at low doses, they have opposite effects on cell survival with the bystander effect transmitting damage from irradiated to non-hit cells while the adaptive response confers resistance to radiation following an initial low priming dose. Therefore they may operate in opposite directions to produce an overall biological effect, but to date there are only limited studies concerning their direct interaction (2, 3).

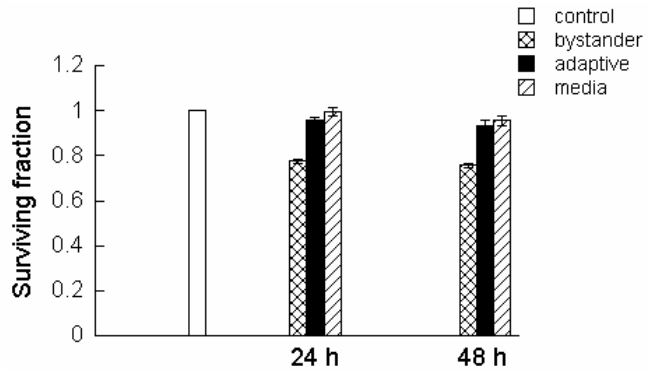

Fig. 1. Surviving fraction of bystander C3H 10T½ cells co-cultured either with cells ('bystander') or culture media ('media') irradiated with 5 Gy of α-particles. Results are also shown for bystander cells pretreated with a 2 cGy priming dose 5 h prior to co-culture with irradiated cells ('adaptive'). Data were pooled from at least three independent experiments (mean ± SEM).

We used a novel radiation setup to examine the relationship between these two processes for the endpoints of clonogenic survival and oncogenic transformation. The experimental protocol employed has been described previously (4).

As shown in Figure 1, a significant decrease in surviving fraction from control levels was observed in the non-hit bystander cells following both 24 h and 48 h co-culture with cells irradiated with 5 Gy of α-particles (24 h: SF=0.77±0.01; $p<0.0001$). There was no significant difference in survival between the two time points studied. At the density at which the cells were plated, the vast majority of cells (>90%) were in close contact at the time of irradiation. Therefore it is possible that the irradiated cells could transmit the bystander signal to non-hit cells either through the secretion of a soluble extracellular factor into the medium and/or through direct cell-to-cell communication via gap junctions. However co-culture of cells with irradiated medium alone had no effect on survival of the non-hit bystander cells at either time point (24 h: SF=1.00±0.02). When cells were exposed to a 2 cGy priming dose 5 h prior to being co-cultured with irradiated cells, the majority of the bystander killing was lost and the surviving fraction was not significantly different from control levels at both time points (24 h: SF=0.96±0.02). This confirms the findings of previous microbeam-based experiments in this laboratory (2, 3).

Table 1 shows the oncogenic transformation frequencies obtained following 24 h of co-culture with irradiated cells. Bystander cells showed a significant increase in transformation frequency over spontaneous control levels ($p<0.0001$). As was observed for clonogenic survival, cells pretreated with the priming dose showed a 2.7-fold significant decrease in transformation frequency from that observed in bystander

Table I.

Clonogenic survival rates, numbers of viable cells exposed in transformation studies, number of transformed clones produced, and transformation frequencies for bystander C3H 10T½ cells co-cultured for 24h with cells ('bystander') or media ('media') exposed to 5 Gy α-particles. Results are also shown for cells irradiated with a 2 cGy priming dose 5h prior to co-culture with irradiated cells ('adaptive'). Data were pooled from at least three independent experiments (mean ± SEM).

Irradiation conditions	Clonogenic surviving fraction (plating efficiency)	*No. of viable cells exposed/ 10^4	No. of transformants produced	Transformation frequency/ 10^4 surviving cells
0 Gy	(0.45±0.004)	11.2	6	0.5
Media	1.0±0.02	8.5	5	0.6
Bystander	0.77±0.01	14.7	51	3.5
Adaptive	0.96±0.02	11.2	14	1.3

** Estimated, accounting for plating efficiency and clonogenic survival.*

Table II.

Clonogenic survival rates, numbers of viable cells exposed in transformation studies, number of transformed clones produced, and transformation frequencies for C3H 10T½ cells. Cells were either directly exposed to 4Gy X-rays or: (i) supernatant from sham-irradiated cells (sham/4 Gy); (ii) supernatant from cells exposed to 2 cGy of X-rays (media/4Gy); or (iii) a 2 cGy priming dose (2 cGy/4Gy). Following a further 5 h incubation at 37°C, these cells were challenged with 4 Gy and processed immediately.

Irradiation conditions	Clonogenic surviving fraction (plating efficiency)	*No. of viable cells exposed/ 10^4	No. of transformants produced	Transformation frequency/ 10^4 surviving cells
0Gy	(0.48±0.01)	7.2	3	0.4
4Gy	0.34±0.01	11.7	78	6.7
Sham/4Gy	0.35±0.01	8.7	54	6.2
Media/4Gy	0.33±0.02	8.3	23	2.8
2cGy/4Gy	0.34±0.01	9.0	27	3.0

** Estimated, accounting for plating efficiency and clonogenic survival.*

cells ($p<0.0001$) to a level that was not significantly different from control levels. Again, no significant increase in transformation frequency was seen following co-culture with irradiated medium only.

Both an adaptive response (5, 6) and bystander effect (7) have been shown to be induced via the transfer of supernatant from irradiated cells onto unirradiated cells. In the present study, we set out to confirm whether such effects could be demonstrated in C3H 10T½ cells.

To examine the adaptive response, confluent, density-inhibited C3H 10T½ cells were sham-irradiated or exposed to a 2 cGy dose of x-rays and 18 h after exposure the supernatants were transferred onto unirradiated cells. Cells treated with the transferred culture medium were then exposed to a 4 Gy dose of x-rays 5 h later and immediately trypzinised for assessment of clonogenic survival and oncogenic transformation as described previously. For comparison, cells were also directly irradiated with 2 cGy and challenged 5 h later with 4 Gy.

The results are shown in Table II. Pretreatment of cells for 5 h with irradiated-conditioned medium prior to the 4 Gy challenge dose had no significant effect on clonogenic survival compared with cells directly irradiated with 4 Gy or treated with sham-irradiated medium. This is in contrast to previous studies (5, 6) and highlights the cell phenotype specific nature of the adaptive and bystander responses. However, an approximate two-fold reduction in the oncogenic transformation frequency was observed in cells treated with irradiated supernatant compared with directly irradiated cells or those treated with sham-irradiated medium, although it did not quite reach statistical significance ($p=0.06$). This suggests that supernatant from cells exposed to 2 cGy of x-rays may contain a factor(s) which acts on unirradiated, bystander cells, reducing their susceptibility to oncogenic transformation, but not cell killing. A similar result was seen for both endpoints when cells were directly irradiated with 2 cGy prior to being exposed to the challenge dose.

It is interesting to note that in the present study, cells directly irradiated with a 2 cGy priming dose followed by a subsequent 4 Gy challenge dose showed no increase in survival (Table II), in contrast to bystander cells in the double-ring experiments which were treated with a priming dose followed by co-culture with irradiated cells and which showed a significant adaptive response for survival (Figure 1). This suggests that following exposure to a priming dose of x-rays and consequent induction of the adaptive mechanism(s), C3H 10T½ cells are less sensitive to the deleterious effects of a bystander signal, but just as susceptible to damage from direct, high-dose exposure to x-rays.

The protocol used to assess the induction of a bystander response via media transfer has been described elsewhere (7). Figure 2 shows the clonogenic survival obtained when unirradiated cells were treated with either irradiated (5 Gy) or unirradiated medium taken from cells 18 h post irradiation. Growth in irradiated medium significantly reduced the clonogenic survival of the cells ($p<0.002$; SF = 0.90±0.03). This has been seen in previous studies and is suggestive of the fact that irradiated cells secrete a cytotoxic factor into the medium which is then able to elicit a bystander effect in unirradiated cells (7). Cells treated with medium from unirradiated control flasks had a non-significant increase in survival (SF=1.08±0.04). This may be due to the medium becoming conditioned from the high-density cultures during the 18 h incubation period and then conferring a survival

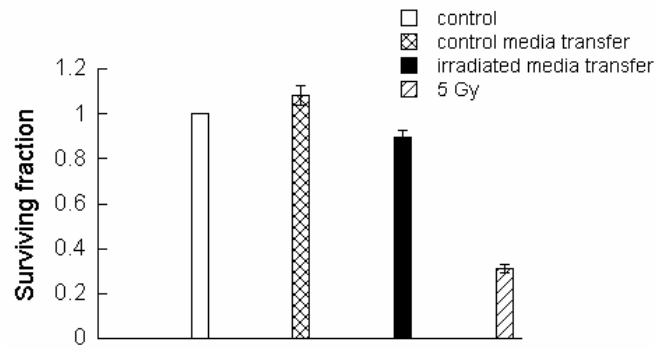

Fig. 2. Surviving fraction of unirradiated C3H 10T½ cells cultured in media from either unirradiated donor cells or cells irradiated with 5 Gy of X-rays 18 h prior to donation. Survival for cells directly irradiated with 5 Gy are also shown. Data were pooled from at least three independent experiments (mean ± SEM).

advantage on the cells to which it is transferred.

Although there are several differences in the protocols used making a direct comparison difficult, the amount of bystander cell killing seen in the medium transfer experiments was two-fold less than that seen when using the double-ring protocol (Figure 2 vs. Figure 1). This may be a result of the bystander signal being transmitted between cells via gap junctions in addition to the secretion of a cytotoxic factor into the medium in the high-cell density double-ring protocol. This may lead to a subsequent increase in cell killing confirming the importance of cell-to-cell contact at the time of irradiation in transmitting the bystander response (8, 9).

In conclusion, these results indicate that following radiation exposure, the resulting biological effect is dependent upon the interaction between the adaptive response and the bystander effect.

References

1. Upton AC. The state of the art in the 1990's: NCRP Report No. 136 on the scientific bases for linearity in the dose-response relationship for ionizing radiation. *Health Physics* **85**:15-22, 2003.
2. Sawant SG, Randers-Pehrson G, Metting NF and Hall EJ. Adaptive response and the bystander effect induced by radiation in C3H 10T(1/2) cells in culture. *Radiation Research* **156**:177-80, 2001.
3. Zhou H, Randers-Pehrson G, Geard CR, Brenner D, Hall EJ and Hei TK. Interaction between radiation induced adaptive response and bystander mutagenesis in mammalian cells. *Rad Research* **160**:512-6, 2003.
4. Stephen A. Mitchell, Stephen A. Marino, David J. Brenner and Eric J. Hall. The Bystander Effect in Radiation Oncogenesis. *Center for Rad. Research Annual Report* p. 20-1, 2002 [http://crr-cu.org/reports2002/b5.htm].
5. Iyer R and Lehnert BE. Alpha-particle-induced increases in the radioresistance of normal human bystander cells. *Radiation Research* **157:**3-7, 2002.
6. Iyer R and Lehnert BE. Low dose, low-LET ionizing radiation-induced radioadaptation and associated early responses in unirradiated cells. *Mutation Research* **503:**1-9, 2002.
7. Mothersill C and Seymour C. Medium from irradiated human epithelial cells but not human fibroblasts reduces the clonogenic survival of unirradiated cells. *International Journal of Radiation Biology* **71:**421-7, 1997.
8. Azzam EI, De Toledo SM and Little JB. Direct evidence for the participation of gap junction-mediated intercellular communication in the transmission of damage signals from alpha-particle irradiated to nonirradiated cells. *Proceedings of the National Academy of Sciences* **98:**473-8, 2001.
9. Zhou H, Randers-Pehrson G, Suzuki M, Waldren CA and Hei TK. Genotoxic damage in non-irradiated cells: contribution from the bystander effect. *Radiation Protection Dosimetry* **99**:227-32, 2002. ■

Stimulation of Clonogenic Survival in Radiation Induced Bystander Cells

Rajamanickam Baskar, Adayabalam S. Balajee and Charles R. Geard

"Bystander effect" is an interesting phenomenon where cells directly targeted by radiation transmit the damaging signal to the non-targeted cells. Bystander effect can be mediated either through gap-junctions or through soluble factors released from irradiated cells. There has been a considerable amount of data obtained on "bystander effects" from various cell types in culture following low and high LET radiation exposure. Available reports on bystander effects show alterations in growth potential, cell killing, gene mutation and modifications in gene expression (1). Radiation-induced bystander effects are multifaceted and often appear to be cell type and genotype dependent, suggesting a need for more studies to understand the molecular mechanism(s) for radiation induced bystander effects. In the present study,

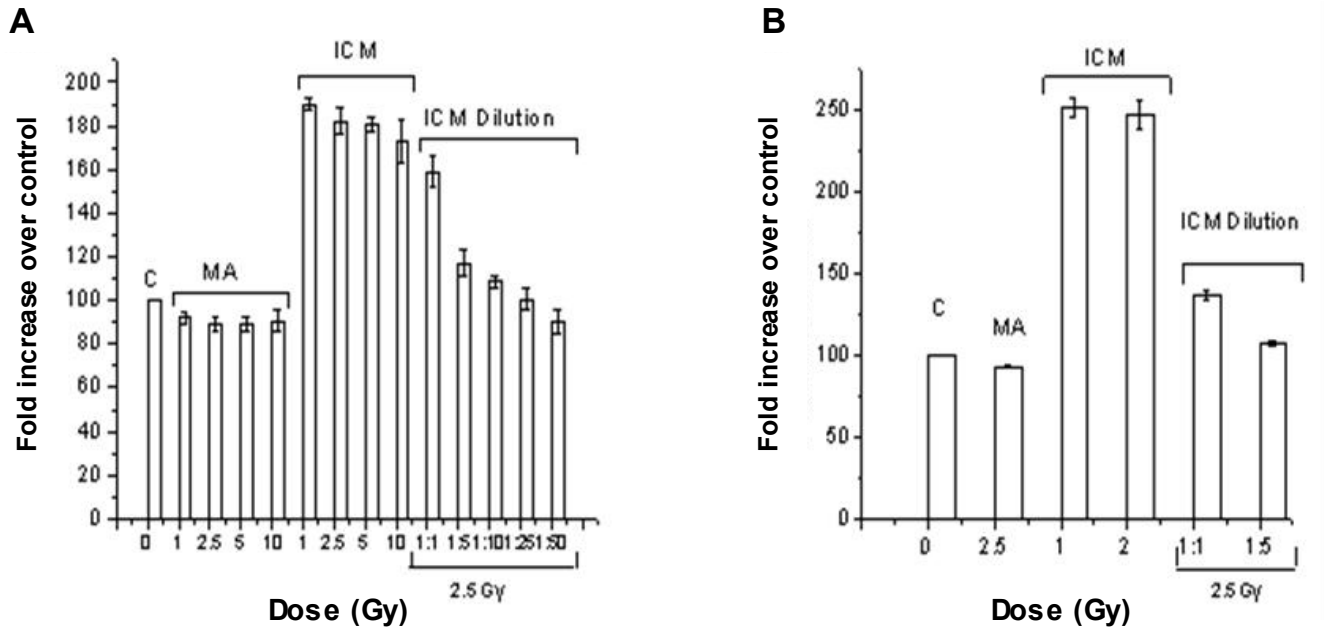

Fig. 1 Stimulation of clonogenic survival in bystander cells. **A.** Survival of the GM637H cells treated with ICM derived from irradiated MRC-5 cells. **B.** Survival of the GM637H cells treated with ICM derived from irradiated GM637H cells. C - Control; MA - Medium alone without cells, irradiated and transferred; ICM - Irradiated conditioned medium with cells; ICM Dilution - ICM (2.5 Gy) was diluted to different concentrations. Each data point represents the mean ± SE of three independent determinations.

using gamma rays as a DNA damaging agent, we have evaluated the role of bystander effect on the clonogenic potential of human fibroblasts.

Primary and SV40 transformed fibroblasts derived from normal (MRC-5 and GM637H) cells were procured from the Coriell Cell Repository, in Camden, New Jersey. Cells were maintained in 2X Eagle's minimal essential medium (EMEM) supplemented with 15% fetal bovine serum, vitamins, essential amino acids, non-essential amino acids and antibiotics (Gibco BRL). The cultures were maintained at 37°C in a humidified 5% CO_2 atmosphere. MRC-5 cells, synchronized at G1 phase by growing them to confluence, were irradiated with different doses (1, 2.5, 5 and 10 Gy) of gamma rays using a ^{137}Cs source at a dose rate of 0.98 Gy/min (Gammacell 40, Atomic Energy of Canada, Canada). The irradiated MRC-5 cells were incubated for 1 hr at 37°C, and the medium collected from the irradiated cells (designated as irradiated conditioned medium, ICM) was used to treat the unirradiated cells for determining of bystander effects. A clonogenic survival assay was used for assessing the growth potential in bystander cells. For this purpose, GM637H cells were seeded at a density of 750 cells/6 cm dish 24 hrs prior to treatment. As a negative control, complete medium alone was irradiated with different doses of gamma rays and incubated for 1 hr at 37°C.

Colonies were fixed in 70% ethanol after two weeks and stained with coomassie blue solution (0.5%). The number of colonies obtained for untreated control cells was considered as 100% and the colonies observed in the treated samples were normalized to the control cells for determining the effect on clonogenic survival. Bystander cells treated with ICM of different radiation doses showed a 1.7 to 1.8-fold enhancement in clonogenic survival (Figure 1A). Cells treated with medium alone did not show any increase in cell survival indicating that the signal released from the irradiated cells is chiefly responsible for an elevated clonogenic potential. If the soluble factors released from the irradiated cells are responsible for clonogenic stimulation in bystander cells, dilution of the factors with unirradiated medium is expected to diminish the bystander effects. To test this possibility, ICM (2.5 Gy irradiated) was serially diluted with complete medium. The findings presented in Fig-1A showed a gradual decline with increasing ICM dilution. Similar results were obtained when ICM derived from 1 Gy and 2.5 Gy gamma rays treated GM637H cells was used (Figure 1B).

Studies using different repair proficient and deficient (primary *vs.* transformed) human cells are in progress to characterize the biochemical nature of the factor(s) responsible for the clonogenic stimulation in bystander cells.

References

1. Mothersill C and Seymour CB. Radiation-induced bystander effects: Past history and future directions. *Radiat Res* **15**:759-67, 2001. ■

Mechanisms of the Bystander Effect: Assessment of Low LET Radiation-Induced Bystander Effect in a Three-Dimensional Culture Model

Rudranath Persaud, Hongning Zhou, Tom K. Hei and Eric J. Hall

The radiation-induced Bystander effect has been demonstrated for a variety of endpoints, using a range of rodent and human cell culture models, mainly with high LET alpha particles. However, there is a need to ascertain whether a similar response can be observed with low LET radiation at doses relevant to environmental exposure. It is equally desirable to determine if such a response can be demonstrated in a three-dimensional culture system, modeling a normal tissue microenvironment. In the present study, a three-dimensional cell culture model comprised of human-hamster hybrid (A_L) and Chinese hamster ovary (CHO) cells as multi-cellular clusters was used to investigate low LET radiation-induced bystander genotoxicity. Separation of A_L and CHO cells was achieved with ~99% efficiency using a magnetic cell separation technique (MACS). Briefly, CHO cells were mixed with A_L cells in various proportions ranging from 10 to 50% and centrifuged briefly to produce a spheroid of 4 x 10^6 cells. Clusters were incubated overnight, resuspended into single cell suspensions, passed twice through MACS separation columns and the efficiency of separation determined using Fluorescence-Activated Cell Sorter (FACS) analysis.

To establish if low LET radiation induces bystander toxicity, CHO cells were labeled with tritiated thymidine (^{3}HdTTP, 30μCi) for 12 hrs and subsequently incubated with A_L cells in multi-cellular spheroids for 24 hrs at 11°C. Labeled CHO cells showed a 50% survival, while the non-labeled, bystander A_L cells showed a surviving fraction of 80% compared to similarly treated controls (Figure 1), thus demonstrating a significant bystander effect induced by irradiation of neighboring cells with low LET electrons.

To determine whether low LET radiation can induce bystander mutation using this spheroid model, CHO cells were labeled with 12 μCi ^{3}HdTTP for 12 hrs and subsequently incubated with A_L cells for 24 hrs at 11°C. Subsequent to magnetic separation, the bystander A_L cells were subjected to a 7-day expression period and mutants were scored utilizing the CD59 Antibody-Complement Cell Lysis Assay. Since the separation of A_L and CHO cells within the cluster may not be entirely efficient, mutant colonies were detected by implementing a centromeric probe toward the human chromosome 11 present in the hybrid A_L cells. Preliminary results have indicated a dose of 12 μCi ^{3}HdTTP induces 169 mutants/10^5 survivors (Figure 2). Additional experiments are underway to establish whether similar mutations can occur at the low dose range of 0.5 to 1.0 μCi ^{3}HdTTP.

Results of the present study should provide important information on the relevance of the bystander effect under *in vivo* conditions. Furthermore, mechanism(s) underlying the bystander effect are likely to be complex and may involve both primary and secondary signaling events. A better understanding of the biochemical and molecular changes governing the bystander process will help in radiation risk assessment and management. ■

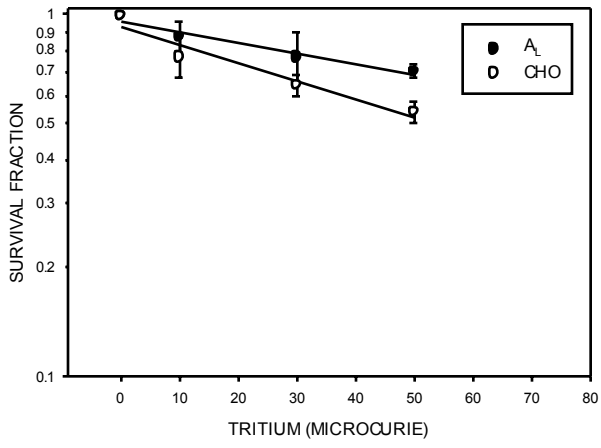

Fig. 1. Survival fraction of A_L and CHO cells treated with Tritium (0-50 microcurie).

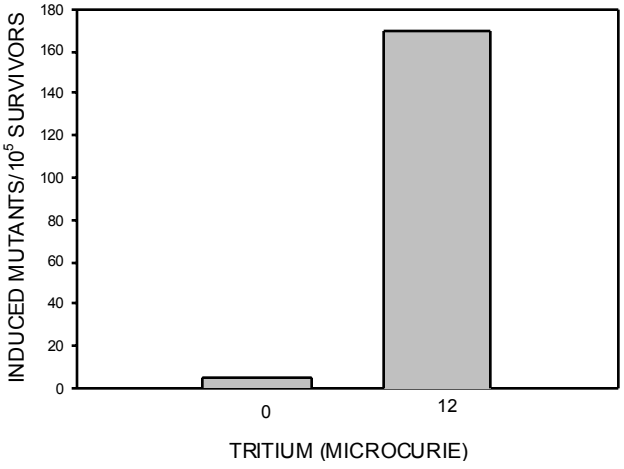

Fig. 2. Mutation induction by Tritium in bystander A_L cells.

Radiation Induced Bystander Effects in Normal Human Fibroblasts

Hongning Zhou, Rudranath Persaud and Tom K. Hei

Based principally on the cancer incidence found in survivors of the atomic bombs in Japan, the International Commission on Radiation Protection (ICRP) and the United States National Council on Radiation Protection and Measurements (NCRP) have recommended that estimates of cancer risk for low dose exposure be extrapolated from higher doses where data are available using a linear, no-threshold model (1, 2). This recommendation is based on the dogma that the DNA of the nucleus is the main target for radiation-induced genotoxicity and, as fewer cells are directly damaged, the deleterious effects of radiation proportionally decline. However, evidence is now emerging that extra-nuclear or extra-cellular targets may also be important in mediating the genotoxic effect of irradiation. Early evidence for this bystander effect came from studies in which the frequency of SCE in populations of cells exposed to low fluences of alpha particles was significantly higher than expected from target theory calculations of the number of cells that had actually received an alpha particle (3, 4). Furthermore, such biological effects as induction of micronuclei (5), gene mutation (6-8), expression of stress-related genes (9-11), and malignant transformation *in vitro* (12) can occur in a significantly higher proportion of cells than in those traversed by an alpha particle. In addition, medium from cultures of cells irradiated with gamma rays can kill unirradiated cells. Cells in contact with cells internally irradiated by short-range ^{3}H-β particles also have a reduced clonal survival (13). However, the mechanism and nature of these bystander signaling processes remain unclear.

The newly designed strip mylar dishes will be used in this experiment. Briefly, the bottom of the well-fit outer and inner stainless rings is covered with 6 μm and 38 μm thick mylar sheets, respectively. The mylar of the inner rings is cut as strips with a specifically designed tool. Exponentially growing normal human lung fibroblasts are seeded in the specially constructed dishes and allowed to grow to confluence. Cells are irradiated with graded doses of alpha particles from the bottom using the track segment mode as described (14-16). Since the fibroblasts seeded on the 38 μm thick mylar strips will not be irradiated due to the short penetrating distance of the alpha particles, these cells will effectively be the bystander cells seeded right next to cells plated on the 6 μm mylar dishes that are directly irradiated. We found that alpha particle irradiation would induce a bystander response in non-irradiated bystander cells using the strip dishes (Figure 1). This unique method provides a sufficient number of bystander cells as well as irradiated cells for further investigation.

Using cDNA signal transduction pathway finder array Analysis (Super Array, MD), preliminary experiments have shown that the COX-2 gene was up-regulated in the bystander cells, while the IGFBP-3 gene was significantly down-regulated in the bystander cells (Figure 2A). Using technique based on RT-PCR, we confirm the finding of down-regulation of the IGFBP-3 gene (Figure 2B). The IGFBP-3 gene is 8.9kb in length and is expressed in a large number of tissues. In addition to its demonstrated growth-promoting roles, IGFBP-3 is also a well-documented in-

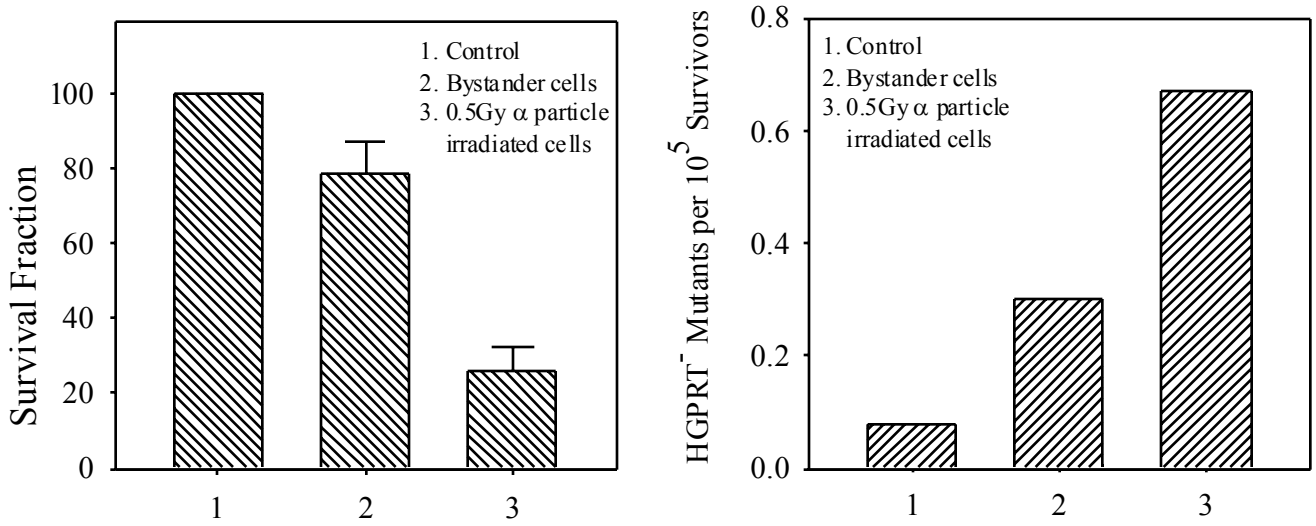

Fig. 1. Survival fraction and *HGPRT* mutation of bystander and directly irradiated cells (0.5 Gy alpha particle radiation) in strip dishes. Data are pooled from 2-3 independent experiments. Bars represent ± SD.

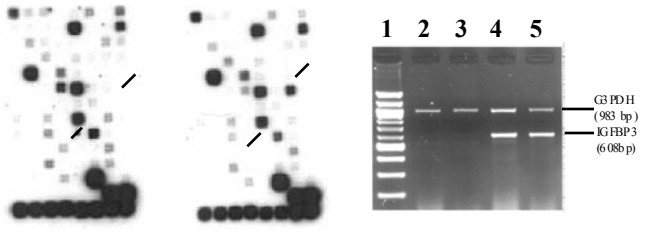

Fig. 2. A. Preliminary data showing differentially expressed signaling genes between control and bystander normal human lung fibroblasts using Super Array cDNA signal transduction pathway finder array. **B.** Confirmation of IGFBP3 down regulation in bystander cells by RT-PCR. Lane 1: 100bp marker; Lanes 2 and 3: bystander cells from different experiments; Lanes 4 and 5: control cells from different experiments.

hibitor of cellular proliferation. It has been reported that over-expression of a transfected IGFBP-3 gene strongly inhibits cell proliferation, with or without added IGF (17). Blocking IGFBP-3 expression with antisense IGFBP3 oligodeoxynucleotides can also attenuate the potent antiproliferative action induced by transforming growth factor-β (TGF-β). More recently, Levitt et al found that IGF-1 inhibited the anti-proliferative effects of celecoxib, COX2 inhibitor, on pancreatic cancer cells, and IGFBP-3 enhanced celecoxib-induced growth inhibition, implying the possible interaction between IGFBP-3 and COX2 (18). In contrast to the expression of COX1, COX2 is not detected in most normal tissues. However, it is induced by mitogenic and inflammatory stimuli, which results in enhanced synthesis of prostaglandins in neoplastic and inflamed tissues. There is considerable evidence that links COX2 to the development of cancer (19). Since the COX2 gene plays an important role in arachidonic acid metabolism, the finding of COX2 overexpression implied that small soluble molecules associated with the arachidonic cascade are essential in mediating the bystander signaling process.

References

1. International Commission on Radiological Protection, Recommendations, Report no. 60 (New York: Pergamon Press), 1991.
2. National Council on Radiation Protection and Measurements, Report 116 (Bethesda, Md., NCRP), 1993.
3. Nagasawa H and Little J. Induction of sister chromatid exchanges by extremely low doses of α-particles. *Cancer Res* **52**:6394-6, 1992.
4. Deshpande A, Goodwin EH, Bailey SM, Marrone BL and Lehnert BE. Alpha-particle-induced sister chromatid exchange in normal human lung fibroblasts: evidence for an extranuclear target. *Radiat Res* **145**:260-7, 1996.
5. Prise KM, Belyakov OV, Folkard M and Michael BD. Studies of bystander effects in human fibroblasts using a charged particle microbeam. *Int J Radiat Biol* **74**:793-8, 1998.
6. Nagasawa H and Little J. Unexpected sensitivity to the induction of mutations by very low doses of alpha-particle radiation: evidence for a bystander effect. *Radiat Res* **152**:552-7, 1999.
7. Zhou H, Randers-Pehrson G, Waldren CA, Vannais D, Hall EJ and Hei TK. Induction of a bystander mutagenic effect of alpha particles in mammalian cells. *Proc Natl Acad Sci USA* **97**:2099-104, 2000.
8. Zhou H, Randers-Pehrson G, Suzuki M, Waldren CA, Vannals D, Chen G, Trosko JE and Hei TK. Radiation risk to low fluences of α-particles may be great than we thought. *Proceeding of National Academy of Science USA* **98**:14410-5, 2001.
9. Hickman AW, Jaramillo RJ, Lechner JF and Johnson NF. α-Particle-induced p53 protein expression in a rat lung epithelial cell strain. *Cancer Res* **54**:5797-800, 1994.
10. Azzam EI, de Toledo SM, Gooding T and Little JB. Intercellular communication is involved in the bystander regulation of gene expression in human cells exposed to very low fluencies of alpha particles. *Radiat Res* **150**:497-504, 1998.
11. Azzam EI, de Toledo SM, Spitz DR and Little JB. Oxidative metabolism modulates signal transduction and micronucleus formation in bystander cells from alpha-particle-irradiated normal human fibroblast cultures. *Cancer Res* **62**:5436-42, 2002.
12. Sawant SG, Randers-Pehrson G, Geard CR, Brenner DJ and Hall EJ. The bystander effect in radiation oncogenesis: I. Transformation in C3H 10T1/2 cells in vitro can be initiated in the unirradiated neighbors of irradiated cells. *Radiat Res* **155**:397-401, 2001.
13. Bishayee A, Rao DV and Howell RW. Evidence for pronounced bystander effects caused by nonuniform distributions of radioactivity using a novel three-dimensional tissue culture model. *Radiat Res* **152**:88-97, 1999.
14. Zhou H, Zhu LX, Li K and Hei TK. Radon, Tobacco Specific Nitrosamine and Mutagenesis in Mammalian Cells. *Mutation Research* **430**:145-53, 1999.
15. Hei TK, Piao CQ, Willey JC, Thomas S and Hall EJ. Malignant transformation of human bronchial epithelial cells by radon-simulated alpha-particles. *Carcinogenesis* **15**:431-7, 1994.
16. Zhu LX, Waldren CA, Vannais D and Hei TK. Cellular and molecular analysis of mutagenesis induced by charged particles of defined linear energy transfer. *Radiat Res* **145**:251-9, 1996.
17. Kelley KM, Oh Y, Gargosky SE, Gucev Z, Matsumoto T, Hwa V, Ng L, Simpson DM and Rosenfeld RG. Insulin-like growth factor-binding proteins (IGFBPs) and their regulatory dynamics. *Int J Biochem Cell Biol* **28**:619-37, 1996.
18. Levitt RJ and Pollak M. Insulin-like growth factor-I antagonizes the antiproliferative effects of cyclooxygenase-2 inhibitors on BxPC-3 pancreatic cancer cells. *Cancer Res* **62**:7372-6, 2002.
19. Subbaramaiah K and Dannenberg AJ. Cyclooxygenase 2: a molecular target for cancer prevention and treatment. *Treads in Pharmacol Sci* **24**:96-102, 2003. ■

Analysis of Radiation-Induced Bystander Effects in Mouse Embryonic Stem Cells Differing in the Status of *Mrad9* Reveals Complexities in the Process

Aiping Zhu, Hongning Zhou, Charles R. Geard, Tom K. Hei and Howard B. Lieberman

It has recently been found that multiple cellular responses to ionizing radiation are not limited to those cells directly exposed, but can often be demonstrated in neighboring "bystander" cells (for review see ref. 1, 2). This bystander effect involves the production of a biological response in cells neighboring those that are actually "hit" by radiation. This implies that cells directly exposed to radiation can transmit a signal to other cells nearby, thus in a sense amplifying the initial damage signal. In essence, this suggests that models taking into account only direct hits in mediating a biological response underestimate the true deleterious effects of radiation exposure, including potential health risks.

The bystander effect was first suggested by Nagasawa and Little (3, 4) when they reported that the calculated, expected nuclear traversal of 1% of cells in a population by a flux of alpha particles caused 30% of the cells to undergo sister chromatid exchanges. Subsequently, bystander effects have been demonstrated for cell survival, mutation and oncogenic transformation (for review see 1). The use of a microbeam to target alpha particles to individual cells also provided more evidence that a cell does not have to be hit directly by an alpha particle to demonstrate mutation or changes in survival. These experiments have been performed by using either of two strategies. In the first, a lethal 20-hit dose of alpha particles could be delivered to 5% of the cells in a population, and mutations would arise in frequency similar to that observed when 100% of cells are hit with a single particle (5). Alternatively, Zhou et al. (6) showed that when 10% of a population is exposed to a single alpha particle, which is sublethal, many more cells in the population demonstrated chromosome aberrations and mutation than just the small percentage exposed. Interestingly, the mutation spectrum for bystander cells differed from that obtained spontaneously or after cytoplasmic irradiation, suggesting that different mutagenic mechanisms are involved (5).

Genetic makeup is also important in terms of understanding how a cell or individual will respond to irradiation. Hundreds of genes participating in multiple DNA repair and cell cycle checkpoint control pathways have been identified and, when mutated, reduce radioresistance and increase the mutagenic or oncogenic potential of radiation exposure (7). Genes involved in signal transduction pathways often have multiple roles in promoting cell survival after radiation exposure, and in maintaining genomic stability in treated cells or even those not exposed to an exogenous DNA damaging agent. Such gene alterations can have dire consequences, including the generation of a high frequency of chromosome aberrations, mutation and cancer. Interestingly, Nagasawa and Little (5) demonstrated that an *xrs-5* mutation in CHO cells significantly enhances chromosome aberration yields due to bystander effects induced by low fluences of alpha particles. They interpreted their results by stating that the *xrs-5* mutation reduced repair of double strand DNA breaks caused by the alpha particles, and this prolonged a signal that mediates the bystander effect. These results suggest that there is a genetic control component to the bystander response, perhaps at the level of damage processing or at another stage. However, regardless of the mechanism responsible, the array of genes involved and their precise roles have not been determined.

The *RAD9* gene, first identified in the fission yeast *Schizosaccharomyces pombe* (8, 9), then subsequently found as orthologues in human *HRAD9* (10) and mouse *Mrad9* (11), is an important genetic element that regulates multiple radioresponses as part of signal transduction pathways. The human and mouse genes partially complement the sensitivity of *S. pombe rad9::ura4+* cells to ionizing radiation, UV and the DNA synthesis inhibitor hydroxyurea, as well as the associated cell cycle checkpoint defects. We created homozygous *Mrad9* knockout mouse ES cells and demonstrated that they are highly sensitive to ionizing radiation, UV and HU (data not shown), and also show defects in the maintenance of ionizing radiation-induced G2/M checkpoint and UV-induced delays in DNA replication, similar to several specific point mutants of the fission yeast *rad9* gene (12). Furthermore, WT human *HRAD9* or mouse *Mrad9* complements the sensitivity defects of the *Mrad9*-/- mouse cells.

The protein encoded by the human *HRAD9* gene is a nucleoprotein, and a nuclear localization signal (NLS) has been identified within (13). We also found in collaboration with Dr. Eva Lee's group at the University of Texas, San Antonio, that ATM can phosphorylate HRAD9 on Ser-272 and the event is important for G1 checkpoint control (14). In collaboration with Dr. Hong-Gang Wang's group at the Moffitt Cancer Center in Tampa, FL, we demonstrated that HRAD9 protein (and surprisingly *S. pombe* rad9 as well) contains a BH3-like domain at its N-terminal region that can bind the anti-apoptotic proteins BCL-2 and BCL-xL, and can cause apoptosis when aberrantly expressed in human cells (15, 16). Therefore, RAD9 regulates two fundamental responses to DNA damage, cell cycle checkpoint control and apoptosis.

The goal of this project is to assess whether mouse embryonic stem (ES) cells express a bystander effect, and to define the role of the cell cycle checkpoint control gene

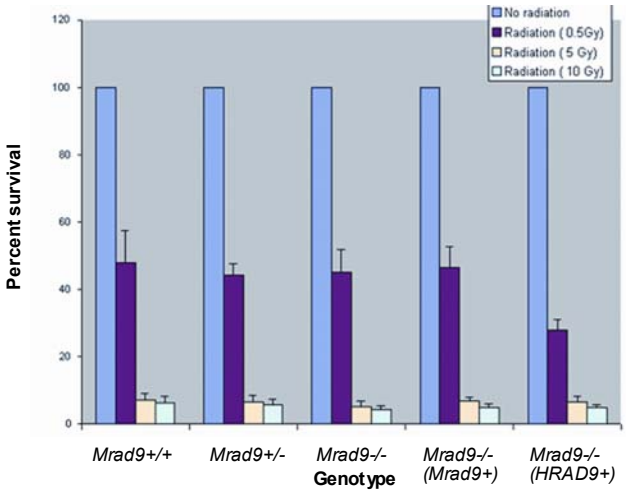

Fig. 1. Radiation-induced cell killing. Radiosensitivity was assessed by measuring colony formation in irradiated versus unirradiated populations. Points represent the average of three trials, +/- S.D.

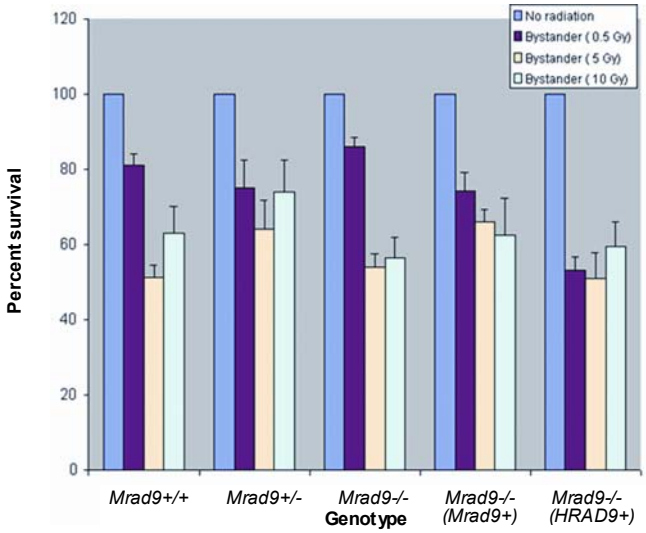

Fig. 2. Radiation-induced bystander cell killing. Radiosensitivity was assessed by measuring colony formation in indirectly irradiated versus unirradiated populations. Points represent the average of three trials, +/- S.D.

Mrad9 in the process. In this report, mouse ES cells differing in the status of *Mrad9* were examined for bystander survival, micronuclei formation and apoptosis in response to broad beam 120 keV alpha particle treatment, using specially designed mylar strip dishes.

When cells differing in the status of *Mrad9* were directly exposed to alpha particles, all the populations demonstrated essentially equivalent killing curves (Figure 1). Interestingly, since *Mrad9*+/- cells are more sensitive than *Mrad9*+/+ cells to gamma rays, and the homozygous deletion mutant shows even greater sensitivity (data not shown), these results indicate that the role of *Mrad9* in mediating the cellular response to ionizing radiation is LET dependent. In addition, we found that all cells, regardless of *Mrad9* status, demonstrated an equivalent bystander reduction in survival after alpha particle exposure (Figure 2).

We also examined these cells for apoptosis, induced both by direct exposure to alpha particles and as a bystander effect. And as indicated in Figure 3, all cell populations examined demonstrated an increased frequency of apoptosis after direct irradiation. For most exposures, induction was dose dependent. Interestingly also is the fact that even *Mrad9*-/- cells showed an induction of apoptosis, contrary to what would be expected by the deletion of the mouse orthologue of the human gene *hRAD9*, shown previously to be a pro-apoptotic element. Likewise, all cells demonstrated an alpha particle-induced bystander apoptotic effect (Figure 4). These results for apoptosis are consistent with the gene not influencing cell survival after exposure to alpha particles (Figure 1, 2).

Micronuclei formation was also examined in the cells differing in *Mrad9* status. As indicated in Figures 5 and 6, background levels of micronuclei were relatively high in the *Mrad9*-/- cells. However, direct exposure to alpha particles induced micronuclei approximately equally above background in all the cells examined. Interestingly, there was little or no bystander effect with regard to micronuclei formation in all the populations examined except those contain-

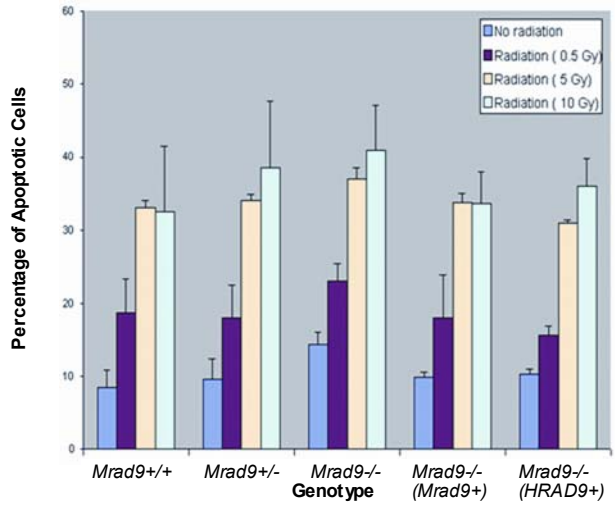

Fig. 3. Radiation-induced apoptosis. Cells either mock treated or irradiated were processed using the Annexin V-FITC Apoptosis Detection Kit from Oncogene. Flow cytometry was used to assess apoptosis in a minimum of 10,000 cells from each population, and points represent the average of three trials, +/- S.D.

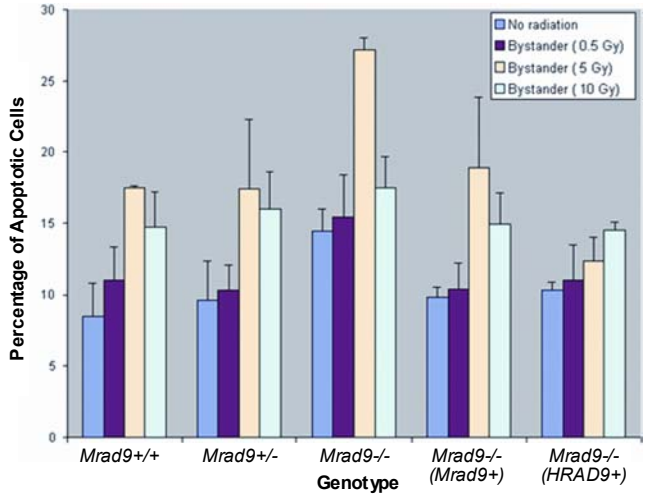

Fig. 4. Radiation-induced bystander apoptosis. Cells either mock treated or irradiated indirectly were processed using the Annexin V-FITC Apoptosis Detection Kit from Oncogene. Flow cytometry was used to assess apoptosis in a minimum of 10,000 cells from each population, and points represent the average of three trials, +/- S.D.

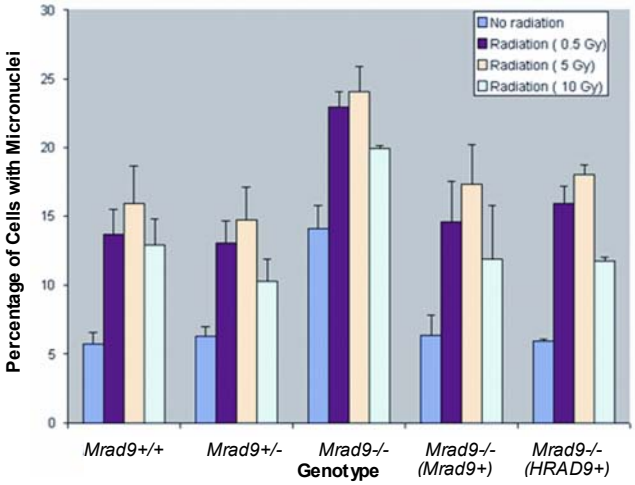

Fig. 5. Radiation-induced micronuclei formation. Irradiated or mock-treated cells were fixed, stained with DAPI, and then scored for micronuclei. Between 500 and 2000 cells were scored per population per experiment. Points represent the average of three trials, +/- S.D.

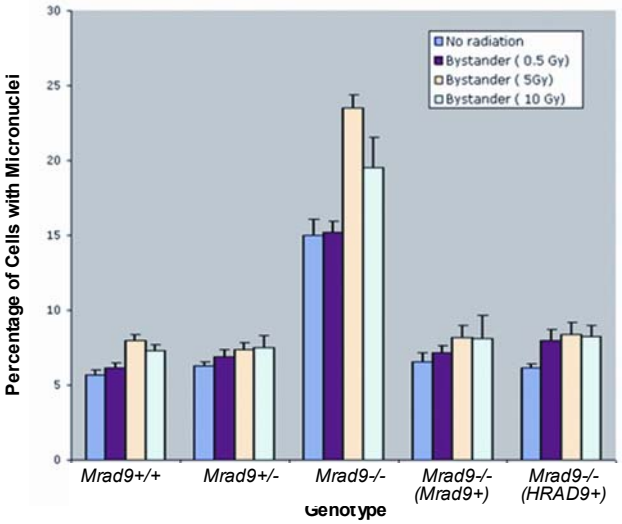

Fig. 6. Radiation-induced bystander micronuclei formation. Indirectly irradiated or mock-treated cells were fixed, stained with DAPI, and then scored for micronuclei. Between 500 and 2000 cells were scored per population per experiment. Points represent the average of three trials, +/- S.D.

ing the *Mrad9*-/- mutation (Figure 6).

In summary, we found that wild-type mouse ES cells are capable of expressing an alpha particle induced bystander effect for cell survival and apoptosis, but not for micronuclei formation. Interestingly, although *Mrad9*-/- cells demonstrated high background levels of apoptosis, the mutation did not effect the bystander induction of programmed cell death or cell killing. In contrast, wild-type ES cells did not exhibit a bystander effect with regard to micronuclei formation, but the *Mrad9*-/- mutation allowed such an effect to be observed. These results suggest that the mechanism of bystander induction is complex and may differ with regard to different endpoints examined.

References

1. Morgan WF. Non-targeted and delayed effects of exposure to ionizing radiation: II. Radiation-induced genomic instability and bystander effects in vivo, Clastogenic factors and transgenerational effects. *Radiat Res* **159**:581-596, 2003a.
2. Morgan WF. Non-targeted and delayed effects of exposure to ionizing radiation: I. Radiation-induced genomic instability and bystander effects in vitro. *Radiat Res* **159**:567-80, 2003b.
3. Nagasawa H and Little JB. Induction of sister chromatid exchanges by extremely low doses of alpha-particles. *Cancer Res* **52**:6394-6, 1992.
4. Nagasawa H and Little JB. Bystander effect for chromosomal aberrations induced in wild-type and repair deficient CHO cells by low fluences of alpha particles. *Mutat Res* **508**:121-9, 2002.
5. Zhou H, Randers-Pehrson G, Waldren CA, Vannais D, Hall EJ and Hei TK. Induction of a bystander mutagenic effect of alpha particles in mammalian cells. *Proc Natl Acad Sci USA* **97**:2099-104, 2000.
6. Zhou H, Suzuki M, Randers-Pehrson G, Vannais D, Chen G, Trosko JE, Waldren CA and Hei TK. Radiation risk to low fluences of alpha particles may be greater than we thought. *Proc Nat Aca Sci USA* **98**:14410-5, 2001.
7. Friedberg EC, Walker GC and Siede W. *DNA Repair and Mutagenesis*. ASM Press, Washington, D.C., 1997.
8. Murrray JM, Carr AM, Lehmann AR, Watts FZ. Cloning and characterisation of the rad9 DNA repair gene from Schizosaccharomyces pombe. *Nucl Acids Res* **19**:3525-31, 1991.
9. Lieberman HB, Hopkins KM, Laverty M and Chu HM. Molecular cloning and analysis of *Schizosaccharomyces pombe rad9*, a gene involved in DNA repair and mutagenesis. *Mol Gen Genet* **232**:367-76, 1992.
10. Lieberman HB, Hopkins KM, Nass M, Demetrick D and Davey S. A human homologue of the *Schizosaccharomyces pombe rad9*+ checkpoint control gene. *Proc Natl Acad Sci USA* **93**:13890-5, 1996.
11. Hang H, Rauth SJ, Hopkins KM, Davey SK and Lieberman HB. Molecular cloning and tissue-specific expression of Mrad9, a murine orthologue of the *Schizosaccharomyces pombe rad9*+ checkpoint control gene. *J Cell Physiol* **177**:241-7, 1998.
12. Hang H, Rauth SJ, Hopkins KM and Lieberman HB. Mutant alleles of Schizosaccharomyces pombe rad9(+) alter hydroxyurea resistance, radioresistance and checkpoint control. *Nucleic Acids Res* **28**:4340-9, 2000.
13. Hirai I and Wang HG. A role of the C-terminal region of human Rad9 (hRad9) in nuclear transport of the hRad9 checkpoint complex. *J Biol* **277**:25722-7, 2002.
14. Chen M-J, Lin Y-T, Lieberman HB, Chen G and Lee EY-HP. ATM-dependent phosphorylation of human Rad9 is required for ionizing radiation-induced checkpoint activation. *J Biol Chem* **276**:16580-6, 2001.
15. Komatsu K, Miyashita T, Hang H, Hopkins KM, Zheng W, Cuddeback S, Yamada M, Lieberman HB and Wang H-G. Human homologue of S. pombe Rad9 interacts with Bcl-2/Bcl-xL and promotes apoptosis. *Nature Cell Biol* **2**:1-6, 2000a.
16. Komatsu K, Hopkins KM, Lieberman HB and Wang H-G Schizosaccharomyces pombe Rad9 contains a BH3-like region and interacts with the anti-apoptotic protein Bcl-2. *FEBS Letters* **481**:122-6, 2000b. ■

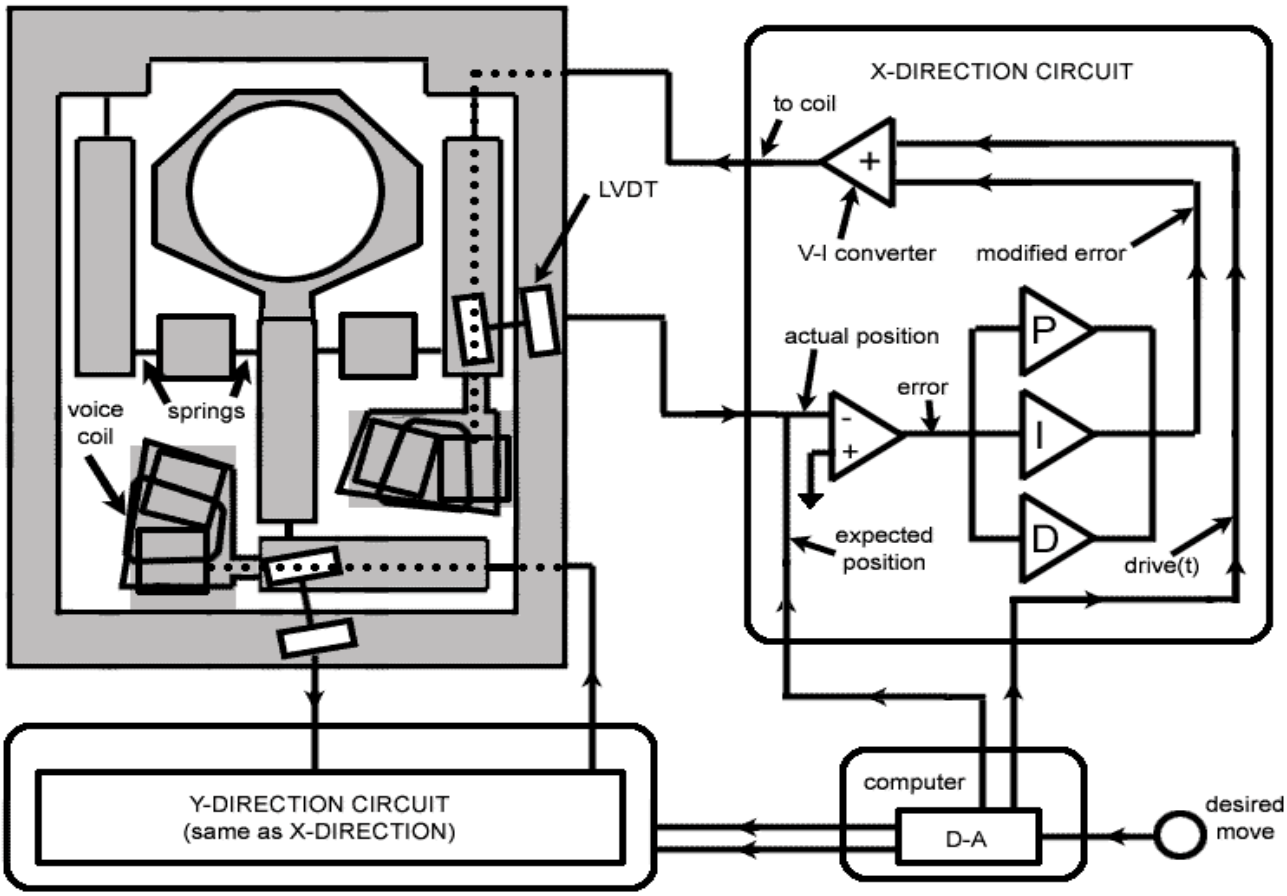

Fig. 5. The Voice-Coil Stage and its control electronics. Dotted lines represent the continuation of the input current from the current driver to the coil.

Extension to 3-dimensional Motion

The VCS with MPC is capable of x-y motion and is being extended to include z motion, for a variety of projects requiring sub-micron-precision z motion, such as phase shifting interference microscopy (which requires a variable path length between the cell sample dish and objective lens), multi-photon imaging (which gives 3-dimensional imaging capability of live cells and tissues, necessitating movements of the sample through the focal plane of the scanning laser), future plans for self-referencing polarographic electrodes (Serp) (which use either monolayer or multiple layer tissue samples), and lowering samples even closer to the exit window after the x-y motion and immediately before irradiation, thereby further reducing any scattering effects.

Construction is underway of a custom coarse x-y stage with cross-roller bearings for rigidity controlled by DC actuators, designed and constructed in-house, which holds a custom LP-200 nano-positioner from Mad City Labs (Madison, WI), and a 3-axis fine motion stage which is currently at RARAF under testing for speed, precision and accuracy (Figure 5). We anticipate a z range of motion of 100 μm with a z-axis resolution of 1.4 nm.

References

1. James B. Rawlings 1999. Tutorial: Model Predictive Control Technology. *Proceedings of the American Control Conference*, San Diego, California, 1 June, 1999. ■

Arsenite Induces Programmed Cell Death by Different Mechanisms

Vladimir N. Ivanov and Tom K. Hei

Inorganic arsenic compounds are environmental toxins, which are associated with the higher risk of different forms of human cancer. Arsenite is a definitive human carcinogen that causes skin, lung, bladder and liver cancer. On the other hand at higher doses, arsenite induces programmed cell death by apoptosis or necrosis. This was a reason to use arsenic in the treatment of leukemia for over a century. Recently we demonstrate that low to moderate concentrations of arsenite (2-10μM) that have little or no effects on either normal melanocytes or fibroblasts may induce apoptosis of human melanomas, including highly metastatic ones, in spite of low surface Fas receptor levels in metastatic melanomas (Ivanov and Hei, submitted). The two prerequisites that dictate apoptotic response of melanomas upon arsenite treatment are low nuclear NF-κB activity and an endogenous expression of TNFα. Under these conditions, melanoma cells acquired sensitivity to TNFα-mediated killing. On the other hand, signaling pathways including those of PI3K-AKT, ERK, and MAPK p38 play a protective role against arsenite-induced oxidative stress and apoptosis, partially via positive control of heme oxygenase-1 (HO-1) expression, which possess strong anti-apoptotic activities.

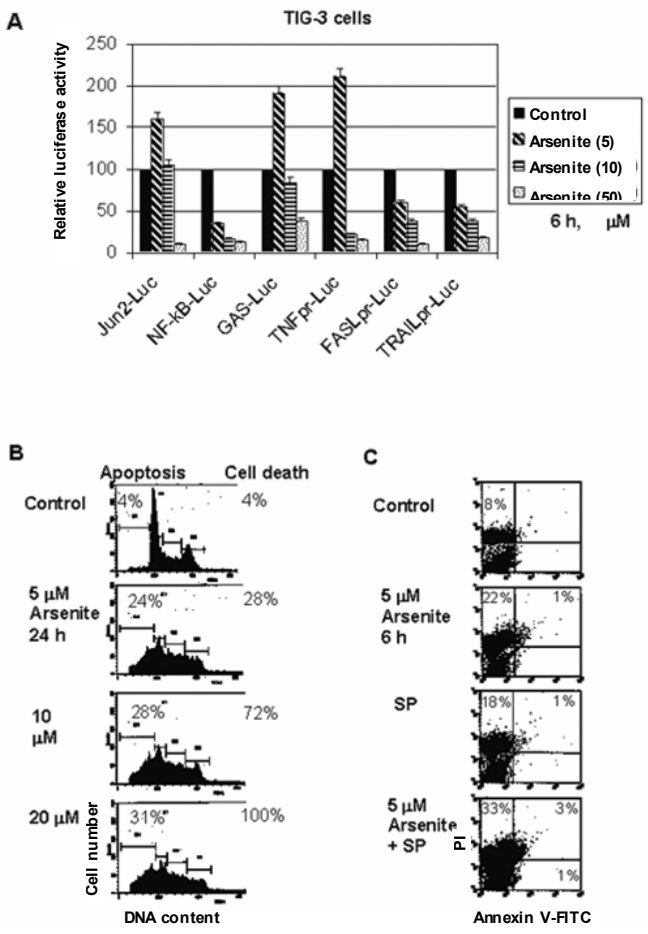

Fig. 1. Arsenite treatment of TIG-3 cells affects transcription factor activities and levels of cell death.

In order to elucidate other possible connections between gene expression and sensitivity to arsenite treatment, we determined changes in the promoter activities driven by the master transcriptional regulators, AP-1, NF-κB and STAT's, using transfection of the reporter constructs Jun2-Luc, NF-κB-Luc and GAS-Luc, respectively, followed by arsenite treatment. Furthermore, we determined effects of arsenite (in the range of concentration 2-50μM) on the promoter activities of the particular genes, which are important for the induction of apoptosis: Fas-Ligand (FasL), TRAIL and TNFα (Figure 1A) using immortalized TIG-3 normal human lung fibroblasts with high transfection efficiency. The maximal positive effects on several promoter activities (Jun2-Luc, GAS-Luc, TNFpr-Luc) have been observed after 5μM arsenite treatment, although the other reporters, especially NF-κB-Luc, were negatively regulated by arsenite in these conditions (Figure 1A). While an increase in the arsenite concentration (up to 10μM) had no negative effects for Jun2-Luc and GAS-Luc activities, it dramatically decreased NF-κB-dependent transcription after 6 h of treatment (Figure 1A). Finally, 50μM arsenite negatively affected all used reporter activities (Figure 1A). In contrast to normal human lung fibroblasts, TIG-3 cells were sensitive to cytotoxic effects of arsenite, showing moderate levels of apoptotic cell death following 5μM arsenite treatment (Figure 1B). Additional increase in arsenite dose (10-20μM) sharply accelerated levels of necrotic death of fibroblasts (Figure 1B). Necrotic commitment of TIG-3 cells 6 h after arsenite treatment was clearly detected by the use of Annexin V-FITC + PI staining and flow cytometry (Figure 1C). Inhibition of JNK activity by SP600125 additionally increased necrotic death of TIG-3 cells (Figure 1C), indicating a protective role of JNK activation against necrosis of TIG-3 cells. Introduction of inhibitory antibodies against TNFα, TRAIL or FasL into cell cultures had no protective effects, indicating that arsenite-induced death of these cells is not mediated by canonical death receptor-dependent pathways (Figure 2A). Data obtained may suggest a role of mitochondria-targeting pathways in the apoptotic response of TIG-3 cells to arsenite treatment, as was previously described for other cell systems (1, 2).

One of the primary effects of arsenite in the cell is induction of oxidative stress, which is mediated by assembling of the active Rac1-NADPH oxidase complex. Oxidative

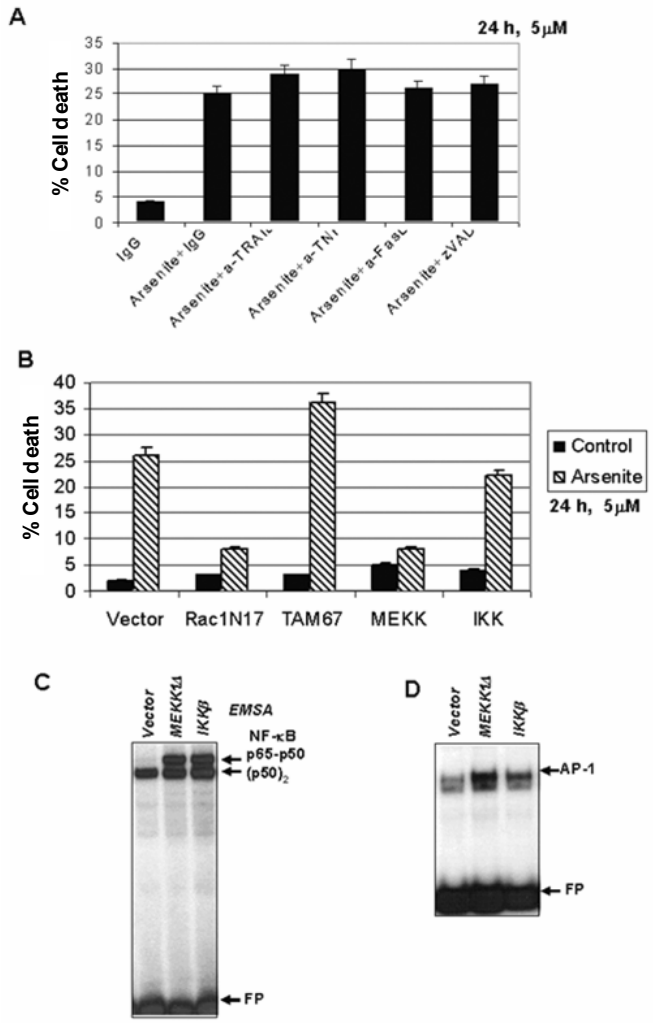

Fig. 2 Dominant-negative Rac1N17 suppressed arsenite-induced death of TIG-3 cells.

stress is followed by the development of apoptosis (3-6). We determined effects of dominant-negative Rac1N17 (which suppresses superoxide production) on the arsenite-induced apoptosis of TIG-3 cells. We also used in these experiments TAM67, a dominant negative expression construct for c-Jun (7) and expression constructs encoding permanently active MEKK1Δ and IKKβ (IKK^{S178E}). Rac1N17 profoundly inhibited arsenite-induced death of TIG-3 cells demonstrating a general dependence of arsenite-induced apoptosis from Rac1 activation (Figure 2B). By contrast, TAM67–transfected cells acquired a higher sensitivity to arsenite treatment, indicating some protective role of c-Jun in arsenite-induced death of human fibroblasts (Figure 2B). MEKK1Δ has several final targets in the cell, including JNK-c-Jun and IKK-IκB-NF-κB (8), while IKKβ activates NF-κB by targeting IκB for degradation (9). As expected, nuclear NF-κB activity was notably induced in both MEKK1Δ– and IKKβ–transfected TIG-3 cells (Figure 2C). Dramatic increase of AP-1 activity was observed in MEKK1Δ-transfected TIG-3 cells, compared to slight changes of AP-1 activity in IKKβ-transfected cells (Figure 2D). This was accompanied by down-regulation of arsenite-induced apoptosis for MEKK1Δ–, but not for IKKβ-transfected cells (Figure 2B), excluding a role of activation of IKKβ/NF-κB in the resistance to arsenite treatment for TIG-3 cells.

References

1. Larochette N, Decaudin D, Jacotot E, Brenner C, Marzo I, Susin SA, Zamzami N, Xie Z, Reed J and Kroemer G. Arsenite induces apoptosis via a direct effect on the mitochondrial permeability transition pore. *Exp Cell Res* **249**:413-21, 1999.
2. Costantini P, Jacotot E, Decaudin D and Kroemer G. Mitochondrion as a novel target of anticancer chemotherapy. *J Natl Cancer Inst* **92**:1042-53, 2000.
3. Ozaki M, Deshpande SS, Angkeow P, Suzuki S and Irani K. Rac1 regulates stress-induced, redox-dependent heat shock factor activation. *J Biol Chem* **275**:35377-83, 2000.
4. Verma A, Mohindru M, Deb DK, Sassano A, Kambhampati S, Ravandi F, Minucci S, Kalvakolanu DV and Platanias LC. Activation of Rac1 and the p38 mitogen-activated protein kinase pathway in response to arsenic trioxide. *J Biol Chem* **277**:44988-95, 2002.
5. Smith KR, Klei LR and Barchowsky A. Arsenite stimulates plasma membrane NADPH oxidase in vascular endothelial cells. *Am J Physiol Lung Cell Mol Physiol* **280**:L442-9, 2001.
6. Martindale JL and Holbrook NJ. Cellular response to oxidative stress: signaling for suicide and survival. *J Cell Physiol* **192**:1-15, 2002.
7. Brown PH, Chen TK and Birrer MJ. Mechanism of action of a dominant-negative mutant of c-Jun. *Oncogene* **9**:791-9, 1994.
8. Lee FS, Hagler J, Chen ZJ and Maniatis T. Activation of the IkappaB alpha kinase complex by MEKK1, a kinase of the JNK pathway. *Cell* **88**:213-22, 1997.
9. Karin M and Lin A. NF-kappaB at the crossroads of life and death. *Nat Immunol* **3**:221-7, 2002. ■

Susceptibility of Human Breast to Parathion, an Organophosphorous Pesticide and Estrogen

Gloria M. Calaf, Gertrudis Cabello[1] and Tom K. Hei

Organophosphorous compounds are the most widely used pesticides by virtue of their biodegradable nature and short persistence. Such compounds make up more than 50% of insecticides currently used in the US, due to their low toxicity and low cost. The etiology of breast cancer remains unidentified. Epidemiological studies have demonstrated the association between cancer in humans and agricultural pesticide exposure. Recently two agricultural pesticides, parathion and malathion, have been used to control mosquito populations in large cities such as New York and Los Angeles to decrease the incidence of the West Nile Virus. The primary target in insects is the nervous system where pesticides take action by inhibiting the release of the enzyme acetylcholinesterase at synaptic junctions. Atropine is a parasympatholytic alkaloid used as an antidote to acetylcholinesterase inhibitors (1). The aim of this work was to examine the susceptibility of human breast epithelial cells MCF-10F to parathion and estrogen.

In vitro model systems have been extensively used in the study of initiation of cancer (2-9). It is not established that parathion, an organophosphorous pesticide, is a human carcinogen; however, it has recently been reported that this substance induced mammary tumors after subcutaneous injection in rats (10).

The present results show that an organophosphorous pesticide, such as parathion, could induce malignant transformation in human breast epithelial cells. Parathion and 17-beta estradiol increased cell proliferation, induced anchorage independent growth, invasive capabilities (Figure 1), and altered PCNA, mutant p53, beta-catenin, and Rho A protein expression (Figure 2), among others, in comparison to control MCF-10F. Atropine inhibited such effects. Other authors (11) have addressed the question of a putative relevance of Rho proteins in tumor progression and analyzed the protein expression in breast tumors. They found that the protein expression level of a modulator of actin cytoskeleton and cell adhesion, such as Rho A, was increased in all breast samples as compared to normal tissues from the same individuals.

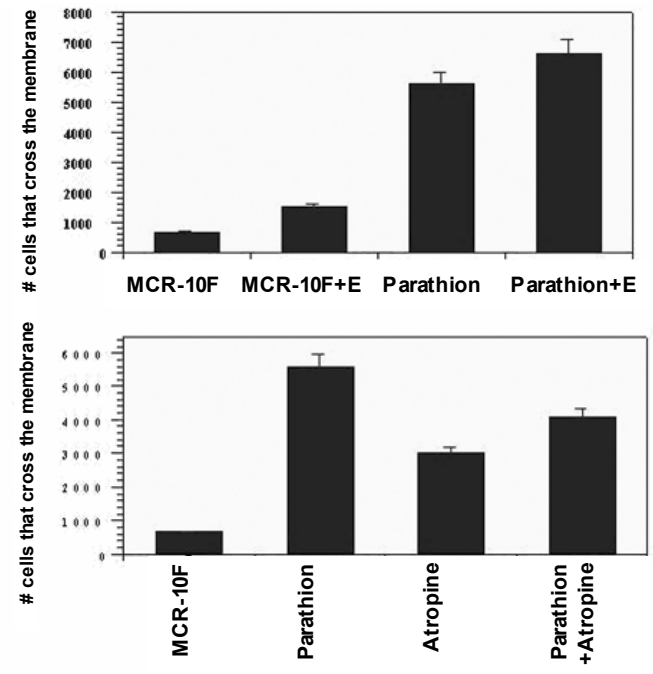

Fig. 1. Invasive characteristics of MCF-10F cells, after various treatments, were scored, 20 hrs after plating onto the matrigel membrane. Invasiveness was determined using modified Boyden's chambers constructed with multiwell cell culture plates and cell culture inserts.

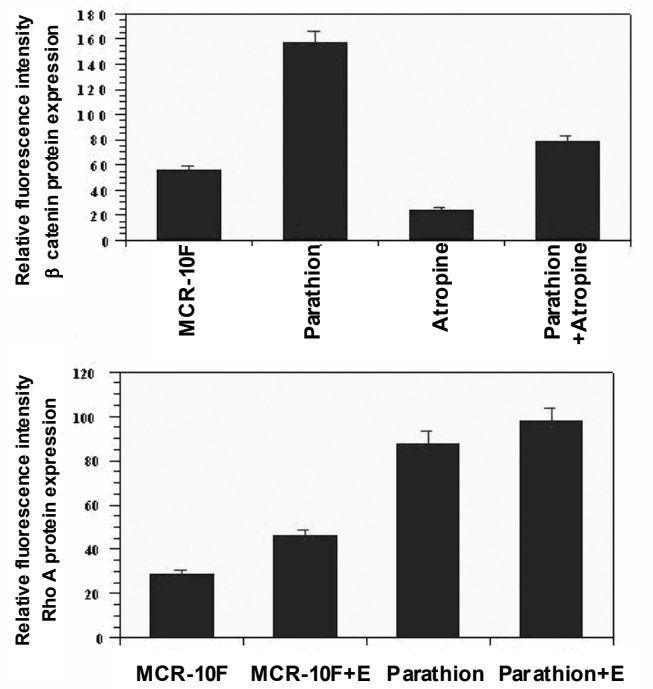

Fig. 2. Average relative amounts of a) beta catenin and b) Rho A protein expressed by MCF-10F cells after treatments. Protein expression of cells was determined by immunofloures-cent staining and quantified using confocal microscopy and a computer program, which gives the area of the intensity of the staining. The primary antibodies used were mouse monoclonal antibodies (Santa Cruz Biotechnology Inc., Santa Cruz, CA).

[1] *University of Tarapaca, Arica, Chile.*

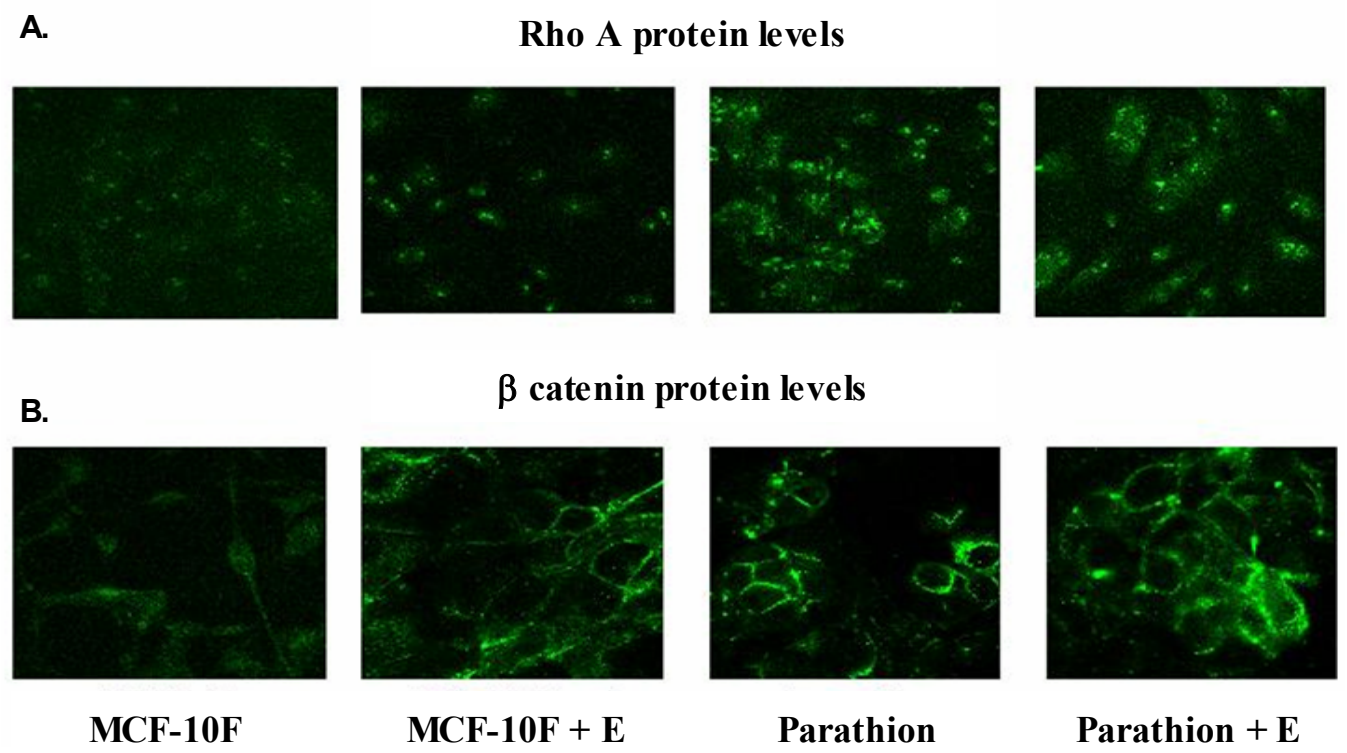

Fig. 3. Representative immunofluorescent imaging staining of a) Rho A and b) beta catenin protein levels in treated cell lines.

Rho A seems also to be a potential marker for small breast carcinomas with metastatic ability (12). Rho A may have a role in the invasive capabilities observed in MCF7-pesticide treated cell lines, since it also altered cell polarity and motility (13, and Figure 3A).

Beta-catenin, as a component of a complex signal transduction pathway, may serve as a common switch in central processes that regulate cellular proliferation and differentiation (14). Beta-catenin was not expressed in the normal cell line MCF-10F cells, but was expressed after estrogen treatment (Figure 3B). A strong reaction was seen following the parathion, either alone, or combined with estrogen in comparison to estrogen and control, indicating the involvement of the pesticide in the regulation of the transformed phenotype. Significant evidence indicates that the E-cadherin-catenin complex is the target of many growth factor and hormone-dependent signaling pathways that regulate its function and expression. The function of the cadherin-catenin system in cell adhesion as well as in intracellular signaling appears to be subjected to multifactorial control by a variety of different mechanisms. It may be suggested that it has a role in the E-cadherin/alpha-catenin complex due to the invasive capabilities observed in these two cell lines. Modulating cell-cell and cell-matrix adhesive properties of invasive colon carcinoma cells have been reported (15). The effects of another organophosphorous pesticide, malathion, on cell adhesion complex E-cadherin/beta catenin and Rho from the human mammary carcinoma cell line MCF-7 have been observed (13). Those cells also showed an increase in levels of Rho A protein.

In summary, these studies showed that an organophosphorous pesticide, such as parathion, in combination with estrogens, induced a cascade of events indicative of cell caracteristics observed in human breast epithelial cells, suggesting that these factors may contribute to the initiation of breast cancer.

References

1. Taylor P. Anticholinesterase agents. In: *The Pharmacological Basis of Therapeutics,* Goodman Gilman A, Rall TW, Nies AS, Taylor P (eds), NY, New York, Pergamon Press Inc **7**:131-47, 1990.
2. Thraves PJ, Salehi Z, Dritschilo A and Rhim JS. Neoplastic transformation of immportalized human epidermal keratinocytes by ionizing radiation. *Proc Natl Acad Sci USA* **87**:1174-7, 1990.
3. Hall EJ and Hei TK. Genomic instability and bystander effects induced by high-LET radiation. *Oncogene* **22**:7034-42, 2003.
4. Rhim JS and Dritschilo A. Neoplastic transformation in human cell systems – An overview. In *Neoplastic Transformation in Human Cell Culture: Mechanisms of Carcinogenesis*, Rhim JS, Dritschilo A (eds), Totowa NJ. Human Press: 11-31, 1993.
5. Calaf G and Russo J. Transformation of human breast epithelial cells by chemical carcinogens. *Carcinogenesis* **14**:483-92, 1993.
6. Riches AC, Herceg Z, Bryant PE and Wynford-Thomas D. Radiation-induced transformation of SV40-immortalized human thyroid epithelial cells by single and fractionated exposure to gamma-irradiation in vitro. *Int J Radial Biol* **66**:757-65, 1994.
7. Hei TK, Piao CQ, Willey JC, Thomas S and Hall EJ.

Malignant transformation of human bronchial epithelial cells by radon-simulated alpha-particles. *Carcinogenesis* **15**:431-7, 1994.
8. Calaf G and Hei TK. Establishment of a radiation and estrogen induced breast cancer. *Carcinogenesis* **21**:769-76, 2000.
9. Calaf G and Hei TK. Oncoprotein expressions in human breast epithelial cells transformed by high LET radiation. *Int J Radiation Biol* **77**:31-40, 2001.
10. Cabello G, Valenzuela M, Rudolph I, Hrepic N and Calaf GM. A rat mammary tumor model induced by the organophosphorous pesticides, parathion and malathion, possibly through acetylcholinesterase inhibition. *Environ Health Perspect* **109**:471-9, 2001.
11. Fritz G, Brachewtti C, Bahlmann F, Schmidt M and Kaina B. Rho GTPases in human breast tumors: expression and mutation analyses and correlation with clinical parameters. *Br J Cancer* **87**:635-44, 2002.
12. Kleer CG, Van Golen KL, Zhang Y, Wu ZF, Rubin MA and Merajver SD. Characterization of Rho C expression in benign and malignant breast disease: a potential new marker for small breast carcinomas and metastatic ability. *Am J Pathol* **160**:579-84, 2002.
13. Cabello G, Galaz S, Botella L, Calaf GM, Pacheco M, Stockert JC, Villanueva, Canete M and Juarranz A. The pesticide malathion induces alterations in actin cytoskeleton and in cell adhesion of cultured breast carcinoma cells. *Int J Oncol* **23**:697-700, 2003.
14. Takayama T, Shiozaki H, Shibamoto S, Oka H, Kimura Y, Tamura S, Inoue M, Monden T, Ito F and Mondem M. Beta-catenin-expression in human cancers. *Amer J Pathol* **148**:39-46, 1996.
15. Breen R, Steele G Jr and Mercurio AM. Role of the E-cadherin/alpha-catenin complex in modulating cell-cell, cell-matrix adhesive properties of invasive colon carcinoma cells. *Ann Surg Oncol* **2**:378-85, 1995. ■

Induction of Nitrotyrosine by Arsenite in Mammalian Cells

Su X. Liu and Tom K. Hei

Arsenic is a well-established human carcinogen. Epidemiological data has shown that chronic exposure of humans to inorganic arsenite is associated with an increased incidence of cancer of the lung, skin, bladder, and liver. Its carcinogenic mechanism, however, is not clear. We showed previously that arsenite induces predominantly multilocus deletions using the human hamster hybrid (A_L) cell assay, and that reactive oxygen species mediate its genotoxic response. It has been suggested that production of peroxynitrite, a strong oxidant formed from the coupling of nitric oxide and superoxide anion was significantly increased in the cells exposed to sodium arsenite. Since peroxynitrite promotes nitration and oxidation of phenolic compounds such as tyrosine, and the formation of 3-nitrotyrosine, the presence of nitrotyrosine in biological samples has been used as a marker for the presence of peroxynitrite anions. In this study, nitrotyrosine expression as analyzed with immuno-cytochemical staining and Western blotting for the A_L cells exposed to graded doses of arsenite. The suppressive effect of L-NMMA (N^G-methyl-L-argine), a competitive inhibitor of the enzyme nitric oxide synthase, in nitrotyrosine expression was examined. A_L cells were maintained in Ham's F12 medium, supplemented with 8% heat-inactivated fetal bovine serum, 25μg/ml gentamycin, and 2X normal glycine (2×10^{-4} M), at 37°C in a humidified 5% CO_2 incubator.

Exponentially growing A_L cells were treated with 0.5, 1.0 and 1.5 μg/ml of sodium arsenite for 24 hrs when used in the immuno-cytochemical staining assay and with 1.0 and 2.0 μg/ml of arsenite for 24 hrs for the Western blot analysis. To ascertain the role of peroxynitrite anions in the process, cells were pretreated with 2 mM of L-NMMA for 1 hr before concurrent treatment with arsenite. Rabbit anti-nitrotyrosine antibody (Upstate Biochemical, Lake Placid, N.Y.) was used for both the immunochemical staining and Western blot analysis. For immunochemical staining, cells were grown in chamber slides for 3 days and fixed with acetone for 20 min. at -20°C. The rabbit anti-nitrotyrosine antibody coupled with Vectastain ABC kit and DAB substrate kit (Vector) were used according to the manufacturer's instructions. For the Western blot, proteins were extracted from both control cultures and arsenite treated cells and the concentration of the protein was determined using the Bradford assay (Bio-Rad). From each treatment group, 30 μg of protein were fractioned by SDS-PAGE gel, transferred onto Hybond membranes, and immunoblotted with rabbit anti-nitrotyrosine antibody at 4°C. Peroxidase-conjugated anti-rabbit IgG (1:10,000, Jackson Labs., Maine) was used to detect nitrotyrosine levels by the enhanced chemiluminescence (ECL) procedure (Amersham, Arlington Heights, IL).

Figure 1 shows the immunohistochemical staining-pattern of 3-nitrotyrosine in control and arsenic treated A_L cells. At low doses of arsenite, the majority of the stain was found to be perinuclear in nature (Figure 1-2). However, at higher arsenite concentrations (Figure 1-5) and with the positive peroxynitrite control (Figure 1-6), the staining

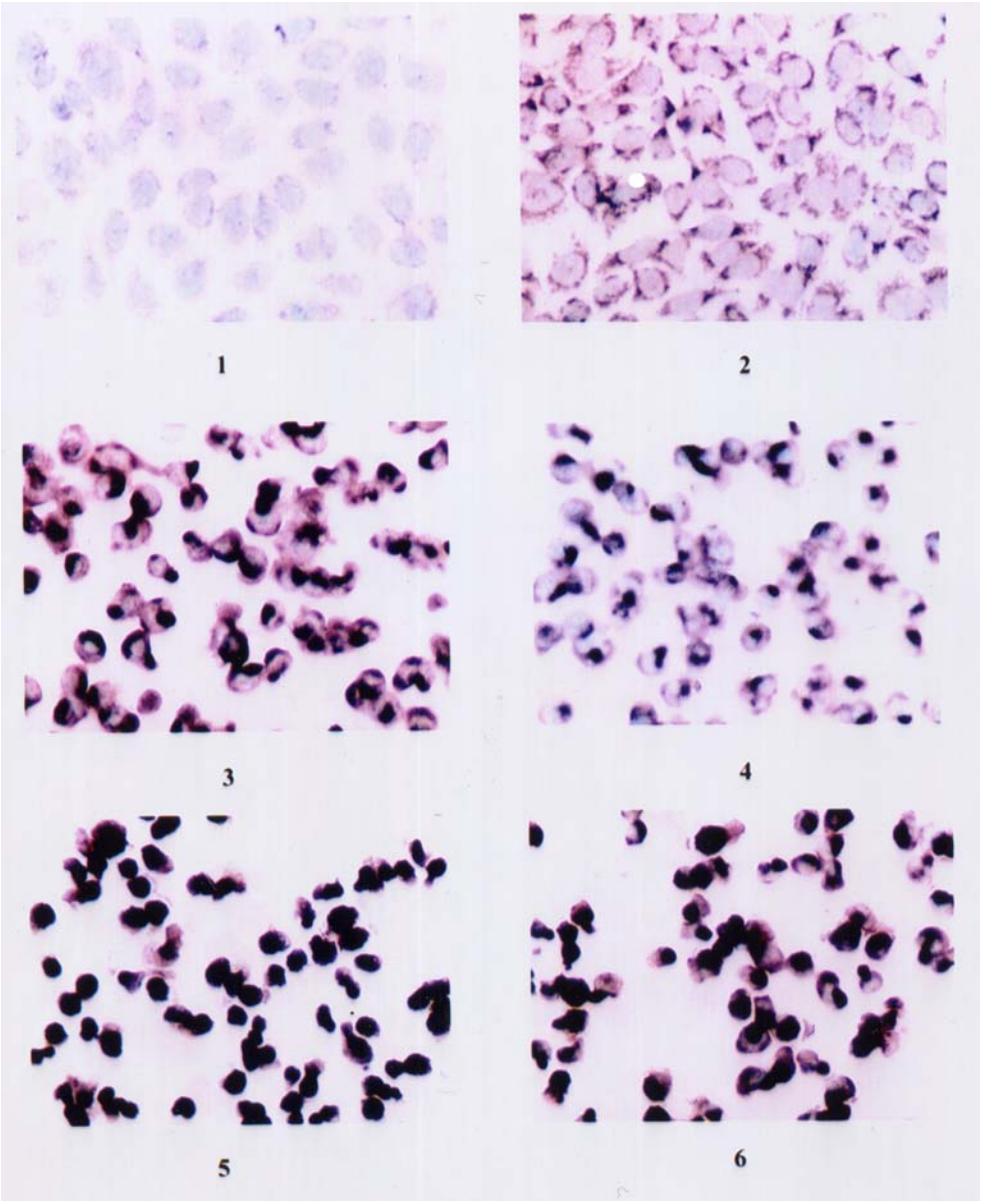

Fig. 1. Immuno-cytochemical staining of 3-nitrotyrosine in A_L cells treated with sodium arsenite. 1) Control; 2) 0.5 μg/ml; 3) 1 μg/ml; 4) 1 μg/ml + 2mM L-NMMA; 5) 1.5 μg/ml; 6) Positive control (40 μM peroxynitrite overnight treatment) 100X.

pattern was diffused to include the nuclei as well. Concurrent treatment with L-NMMA significantly reduced the 3-nitrotyrosine staining in arsenite treated cultures (Figure 1-3 versus Figure 1-4, $p<0.001$). The result of Western blot analysis also showed dose response induction of nitrotyrosine in arsenite-treated A_L cells. Figure 2 shows the dose response induction of 3-nitrotyrosine in arsenite-treated (24 hr) A_L cells. Peroxynitrite (40μM overnight treatment) was used as a positive control. Addition of L-NMMA to the arsenite treated group (2μg/ml) reduced the protein level by more than 60% and attested to the peroxynitrite origin of the reaction. ■

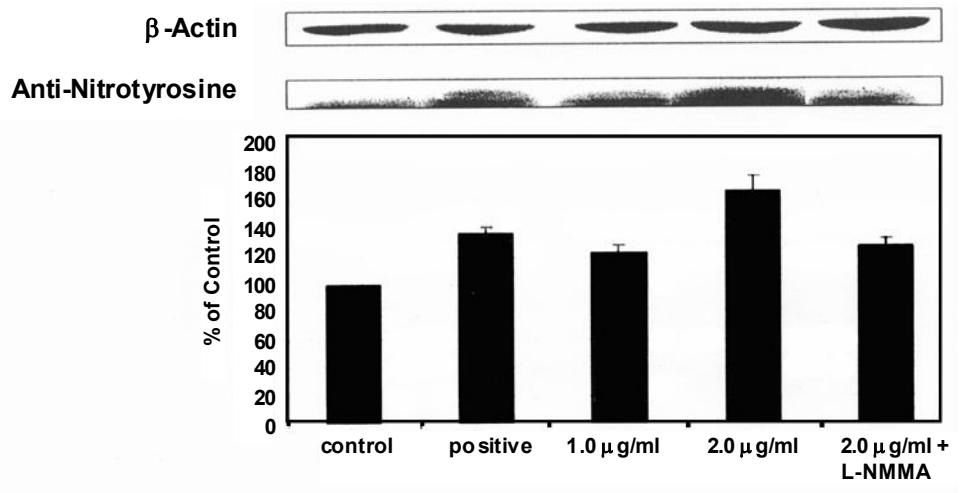

Fig. 2. 3-Nitrotyrosine expression by Western blot in A_L cells treated with sodium arsenite.

Induction of Transformation by Arsenite in hTERT-Immortalized ASEC Cells

Chang Q. Piao and Tom K. Hei

Epidemiologic studies have demonstrated that exposure to inorganic arsenic is associated with increased risk of human cancer of the skin, urinary bladder, respiratory tract, liver, and kidney, etc. Although several hypotheses have been proposed, the mechanisms responsible for arsenic carcinogenesis have not been established, partly because carcinogenesis in rodent models has never been convincingly demonstrated, and no human models in cell culture were available. In this study, an hTERT-immortalized human small airway epithelial cell line was established, and treated with sodium arsenite to study the multi-stage phenotype and molecular mechanism in the process of arsenite-induced transformation.

Normal human small airway epithelial cells (SAEC), from a female donor, was purchased from Clonetics (Walkersville, MD). These cells were transfected with hTERT by retrovirus-mediated gene transfer. In the construct of pBabest2, the cDNA encoding hTERT was subcloned into the retroviral vector pBabe under the control of the promoter present in the Molony murine leukemia virus LTR. The retroviral constructs were packaged using the highly efficient and helper free cell line Phoenix A (ATCC). Phoenix A cells were plated in 10 cm diameter dishes and transfected when reaching 80% confluence, with 4 μg/ml retroviral plasmid DNA in 10 ml medium using lipofectAMINE plus reagent (Gibco-BRL), according to instructions of manufacturer. Clones resistant to 400 μg/ml G418 were selected. The hTERT-expressing cells (SAEhF) at passage 10 after G418 selection were treated with 2 μg/ml for 4 weeks, and then were continuously cultured for more than 150 PDs to confirm immortalization (SAEhF-A). The immortalized SAEhF-A cells did not obtain the transformed phenotype in

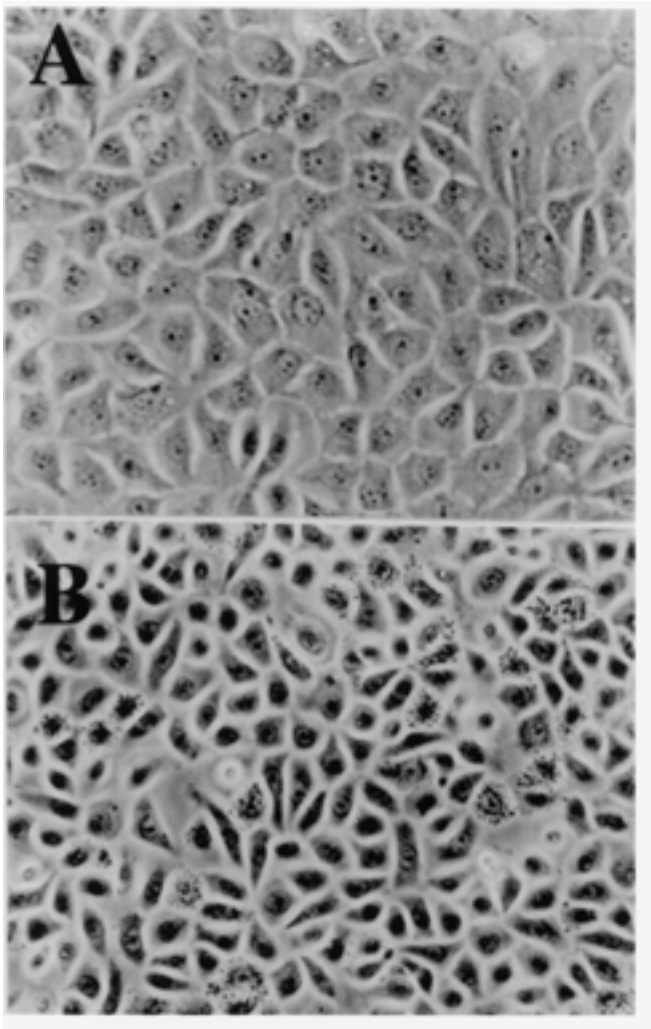

Fig. 1. Morphological alteration. **A.** SAEhF; **B.** SAEhF-2A.

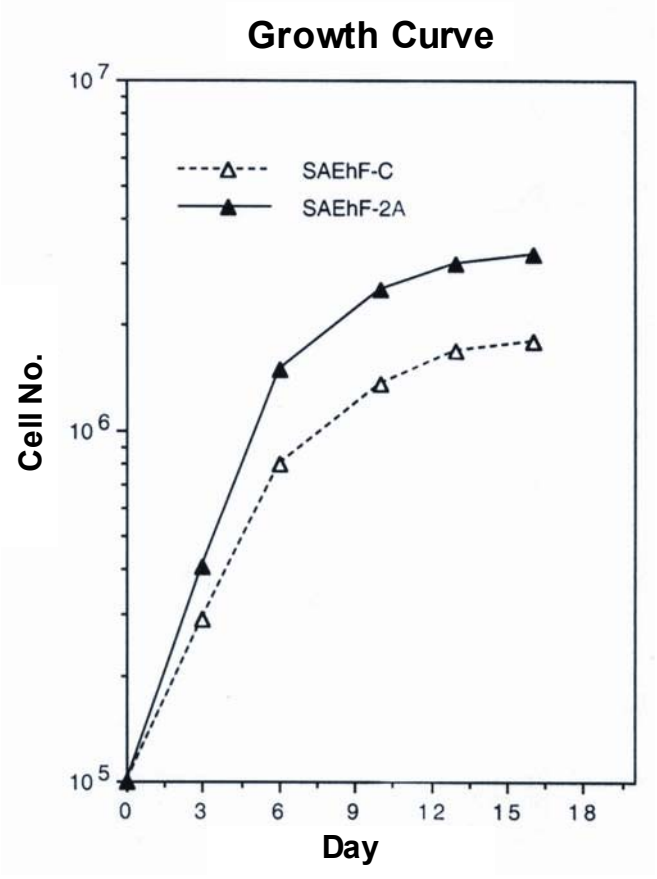

Fig. 2. Growth curve. Higher proliferation rate and saturation density in SAEhF-2A compared with the control SAEhF-C.

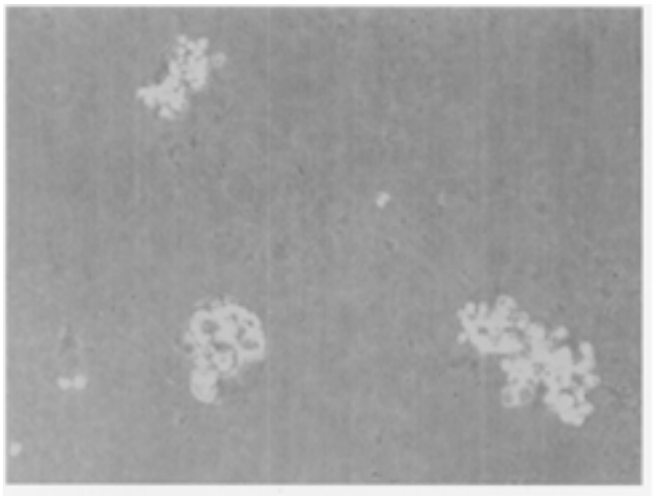

Fig. 3. Colonies of SAEhF-2A grown in soft agar.

anchorage independent analysis. The SAEhF-A cells were treated with 2 μg/ml of sodium arsenite for 4 weeks again (SAEhF-2A). The SAEhF-2A cells were continuously cultured for 8 weeks after secondary arsenite treatment. The size of the cells became much smaller, and had a higher proliferation rate and saturation density than parental cells (Figures 1 and 2). The SAEhF-2A cells also obtained the transformation phenotype of anchorage independent growth in agar analysis (Figure 3). Tumorigenicity in nude mice and alterations of gene type analysis were in the study. ■

Ectopic Expression of Betaig-h3 Gene Abrogates the Tumorigenicity of H522 Human Lung Cancer Cells

Yong L. Zhao and Tom K. Hei

Lung cancer is one of the most common and deadly malignancies in the United States. At the time of cancer diagnosis, almost 50% of patients have already developed metastasis (1). Therefore, a better understanding of the molecular mechanisms responsible for the acquisition of invasive and metastatic ability is pivotal to a better diagnosis and treatment of this disease. Using papillomavirus-immortalized human bronchial epithelial (BEP2D) cells, we have previously shown that downregulation of the Betaig-h3 gene is causally related to the tumorigenicity of BEP2D cells induced by either α-particle radiation or asbestos fiber treatment. In addition, a decrease or absence in expression of the Betaig-h3 gene was found in 14 human tumor cell lines when compared with normal human cells or tissues. The data suggest that loss of Betaig-h3 expression is a frequent event and may function as a tumor suppressor not only in an asbestos/radiation-transformed tumor model but in human cancer cells as well. In this report, the functional role of the Betaig-h3 gene was investigated in H522 lung cancer cells in which Betaig-h3 expression was deleted (2). We further provide evidence that the Betaig-h3 gene functions as a tumor suppressor in human lung cancer cells (3).

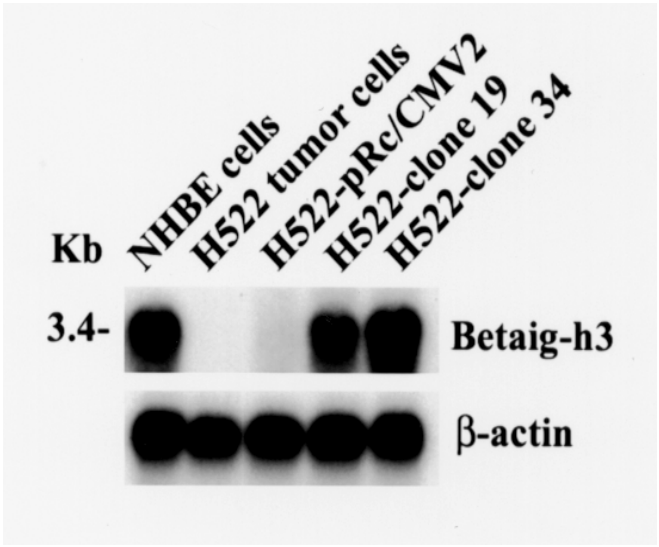

Fig. 1. Ectopic expression of the Betaig-h3 gene in H522 human lung cancer cells by transfection.

To ascertain the tumor suppressive effect of the Betaig-h3 gene, we ectopically re-expressed the gene in H522 human lung cancer cells using pRc/CMV2-Betaigh3 expression vector. Two G418 resistant colonies (19 and 34) that expressed different levels of the Betaig-h3 gene were chosen for further studies. From the Northern blotting result (Figure 1), the parental H522 cells and H522-pRc/CMV2 cells expressed a low but similar level of Betaig-h3 gene. After transfection, the expression of the Betaig-h3 gene in clone 19 was restored to a level similar to that of control NHBE cells, whereas in clone 34 cells it was about 50% higher than the control.

To determine whether ectopic expression of the Betaig-h3 gene in H522 cells suppresses tumor formation in vivo, we inoculated parental H522 and clone 19 and 34 cells

subcutaneously into nude mice for a tumorigenicity assay (Figure 2). The results showed that mice injected with H522 (12/12 mice) and empty vector-transfected H522 cells (12/12 mice) produced progressively growing tumors at 2 months, with the average tumor volume of 446.75 mm^3 and 641.8 mm^3, respectively. In contrast, half of the sites injected with Betaig-h3 transfected cells formed small nodules at 1-2 weeks after inoculation. However, all these nodules were regressed in one month and no tumors were found when monitored for more than three months (0/24 mice). Three independent experiments were carried out. The data indicate that recovery of Betaig-h3 gene expression in H522 cancer cells totally abrogate their tumorigenicity in nude mice.

Our data provide further evidence that loss of Betaig-h3 expression functions as a tumor suppressor not only in the asbestos/radiation-induced tumorigenic process, but also in human lung cancer cells.

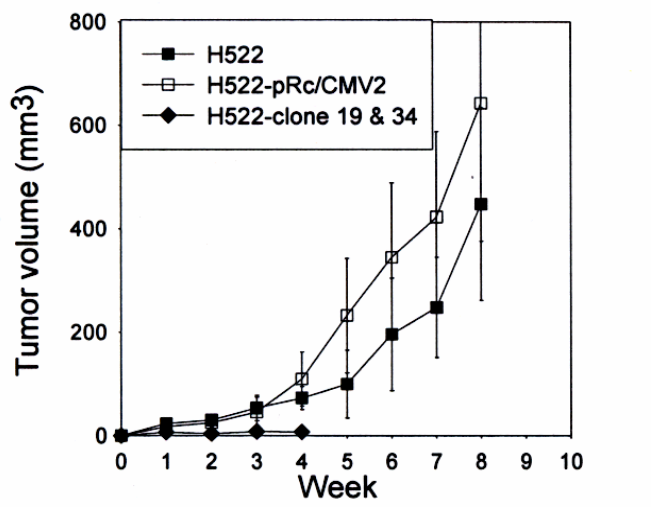

Fig. 2. Suppression of tumorigenicity in H522 tumor cells by Betaig-h3 gene transfection.

References

1. Feinstein MB and Bach PB. Epidemiology of lung cancer. *Chest Surg Clin N Am* **10**:653-61, 2000.
2. Zhao YL, Piao CQ, Hall EJ and Hei TK. Mechanisms of radiation-induced neoplastic transformation of human bronchial epithelial cells. *Radiat Res* **155**:230-4, 2001.
3. Zhao YL, Piao C and Hei TK. Downregulation of Betaig-h3 gene is causally linked to tumorigenic phenotype in asbestos treated immortalized human bronchial epithelial cells. *Oncogene* **21**:7471-7, 2002. ■

Malignant Transformation of Human Bronchial Epithelial Cells with the Tobacco-Specific Nitrosamine, 4-(Methylnitrosamino)-1-(3-Pyridyl)-1-Butanone

Hongning Zhou, Gloria M. Calaf and Tom K. Hei

There is a great body of literature clearly demonstrating that cigarette smoking is causally associated with various types of human cancers such as lung and those of the upper digestive tract (1). In the U.S., approximately 90% of deaths from lung cancer among men and 79% of those among women are associated with smoking (2). While tobacco smoke contains about 3,800 chemical and physical agents, including at least 40 known human carcinogens, it is the tobacco-associated nitrosamines that are the most potent carcinogenic component (3). Tobacco-specific nitrosamines are formed from nicotine and related tobacco alkaloids. Two nitrosamines in this category, 4-(methylnitrosamino)-1-(3-pyridyl)-1-butanone (NNK) and N′-nitrosonornicotine (NNN), have been shown to be strong carcinogens in laboratory animals (reviewed in refs. 4, 5), and can induce tumors both locally and systematically. Importantly, it has also been shown that the amount of NNK in tobacco smoke is high enough such that the total estimated doses to smokers and long-term snuff-dippers are similar in magnitude to the total doses required to produce cancer in laboratory animals. These exposures thus represent an unacceptable risk to cigarette smokers and non-smokers exposed to years of environmental tobacco smoke.

The cellular and molecular mechanisms for human bronchial carcinogenesis by tobacco-specific N-nitrosamines are not clear. It would be ideal to use a human bronchial cell line that has been exposed to these carcinogenic agents to assess the various transformation stages leading to malignancies. However, no primary human cell model is available for this area of study. First, the frequency of human cell transformation is too low to be reproduced in any laboratory setting (6); second, due to telomere shortenings, primary cultures senesce before they undergo neoplastic transformation (7). The BEP2D cell line established clonal population of HPV-18-immortalized human bronchial epithelial cells was used in this experiment. BEP2D cells have an epithelial morphology in culture, a near diploid karyotype, a relatively stable genotype, are anchorage-dependent, and non-tumorigenic in nude

mice (8).

NNK treatment of BEP2D cells for a 24-hour period was largely non-toxic. However, in cells treated with NNK continuously for 7 days, toxicity significantly increased as the concentration of NNK increased such that treatment of cells with an 800 µg/ml dose of NNK resulted in a surviving fraction of ~50%. After NNK treatment, the cells from either 100 or 400 µg/ml and 7-day-treatment groups were subcultured for a period of several months, at which time they were tested for resistance to serum-induced terminal differentiation and for anchorage independent growth. Three months post-treatment, there were no alterations in any of the phenotypes assayed. However, NNK-treated BEP2D cells subsequently demonstrated a gradually reduced response to serum-induced terminal differentiation and an increased colony forming efficiency in soft agar. The results from 8 months of subculture, post-NNK treatment, indicated that in the presence of serum, the plating efficiency of control BEP2D cells decreased to 2% from its original value of 35% in serum-free medium. In contrast, NNK treated cells were much more resistant to serum induced terminal differentiation. Similarly, these NNK treated cells were able to grow in soft agar, which reflected their anchorage independent nature. The doubling times of the NNK treated cells were significantly shorter than that of control BEP2D cells, indicating their faster growth rate.

Upon inoculation into nude mice, NNK treated cells (13 months post-NNK treatment) produced tumors with a latency period of approximately 9 weeks. Four months post-injection, when the tumors had attained a size of 8-10 mm in diameter, they were excised, and the tumor cell lines were established as described above. Characterization by routine hematoxylin and eosin staining of paraffin embedded sections indicated the nodules to be carcinogenic in nature. Histologically, the tumor was composed of variably sized nests and chords of polyhedral cells that often formed large cores of keratin. Under higher magnification small nests of cells were found to be divided by a thin stroma and the moderately pleomorphic cells varied from round to elongated. Nuclei were prominent and there were often multiple nucleoli. Individual cells frequently formed keratin and there were intercellular bridges. There were five to six mitotic figures per high field of magnification. These findings were consistent with a squamous cell or epidermoid carcinoma since approximately 30 to 40 percent of human bronchogenic carcinomas fall under this sub-classification. Among the 10 animals injected with control BEP2D cells, no tumors were formed in nude mice for up to 9 months post injection. Four NNK-induced primary tumor cell lines, two from each 100 µg/ml and 400 µg/ml 7-day treatment groups, were successfully established. Immunofluorescent staining of keratin expression confirmed the cells' epithelial origin. When these primary tumor cell lines were inoculated into nude mice, they induced tumors at the injected site with a shorter latency (~4 weeks) than the parental tumor cells. Two secondary tumor cell lines were similarly established from these secondary tumors.

The expression of several selected proteins frequently associated with lung cancer was determined in the NNK-treated BEP2D cells and in the tumor cell lines subsequently generated, as shown in Figure 1. Quantification of the immunofluorescent imaging of stained cells showed a signifi-

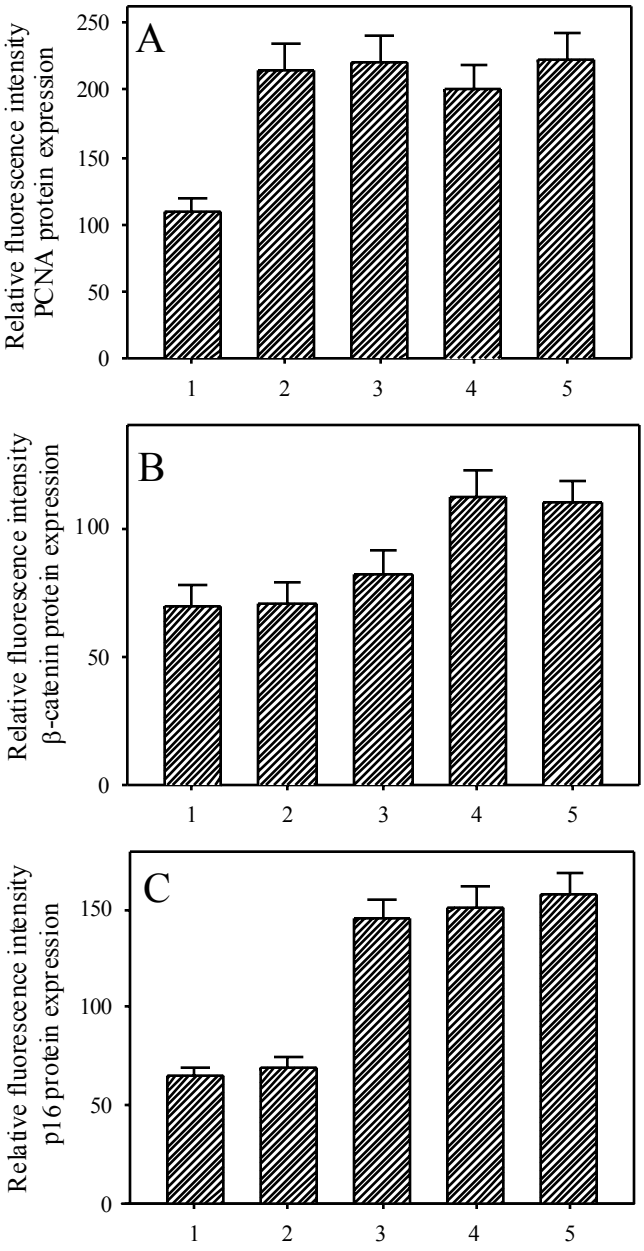

Fig. 1. Relative amount of PCNA, β-catenin and p16 expression was determined by the use of a computer program that gives the area and intensity of the staining obtained under confocol microscopy. 1. BEP2D cells. 2. Earlier passage after NNK-treated BEP2D cells (passage 9 after treatment, no phenotypic changes identified at this stage). 3. Later passage BEP2D cells post NNK treated (passage 38 after treatment, cells were resistant to serum-induced terminal differentiation and exhibited anchorage independent growth, but not tumorigenic). 4. Tumor cell line 1 (from 100 µg/ml NNK treatment for 7 days, passage 3 after cell line was established). 5. Tumor cell line 2 (from 400 µg/ml NNK treatment for 7 days, passage 3 after cell line was established).

cant increase in PCNA expression in early passage cultures (passage 8-12 after NNK treatment) of NNK treated cells when compared with controls, but these cells were not resistant to serum-induced terminal differentiation, showed no anchorage independent growth, and did not undergo tumorigenesis. This high expression level continued to be observed among late passage cultures (passage 36-40 after NNK treatment which became resistant to serum induced terminal differentiation and anchorage independent growth, but were not tumorigenic), and in tumor cell lines. In contrast to the PCNA expression, expression of β-catenin was similar to controls in the early passage NNK-treated cells. However, among the late passage cells, β-catenin showed a slight increase in expression and the level was significantly amplified in the tumor cell lines. Finally, p16 expression was found to increase only in the late passage cultures and the two-fold increase observed was not different from those of the tumor cell lines generated.

In addition, there is evidence that human papillomavirus-immortalized human bronchial epithelial cell lines may have greater relevance than their Simian Virus40 (SV40)-immortalized counterpart in studying of human disease. It has been reported that as much as 20% of primary bronchogenic carcinoma tissue contains HPV sequences (9). It is possible that exposure to tobacco products may present a higher risk for individuals bearing an overt or occult HPV infection of the respiratory epithelium. Using human-hamster hybrid cells, we reported previously that NNK, either alone or in combination with a single 25 cGy dose of radon alpha particles, would induce mutation in the *CD59* locus, and that NNK induced mostly deletion mutations at moderately high doses in the cells (10). The results presented here indicate that NNK induces a stepwise neoplastic transformation of the immortalized human bronchial epithelial cells. These studies could be extremely useful in elucidating mechanisms involved in the initiation and progression of NNK-induced cancer, and provide a useful model for further investigation of the molecular mechanisms of NNK carcinogenesis.

References

1. Hoffmann D, Brunnemann KD, Prokopczyk B and Djordjevic MV. Tobacco-specific N-nitrosamines and areca-derived N-nitrosamines: chemistry, biochemistry, carcinogenicity, and relevance to humans. *J Toxicology and Environmental Health* **41**:1-52, 1994.
2. Gupta PC, Mutri PR and Bhonsle RB. Epidemiology of cancer by tobacco products and the significance of TSNA. *Critical Reviews in Toxicology* **26**:183-98, 1996.
3. Hecht SS, Carmella SG, Foiles PG and Murphy SE. Biomarkers for human uptake and metabolic activation of tobacco-specific nitrosamines. *Cancer Res* **54**:1912s-7s, 1994.
4. Hoffmann D and Hecht SS. Nicotine-derived N-nitrosamines and tobacco-related cancer: current status and future directions. *Cancer Res* **45**:935-44, 1985.
5. Hecht SS and Hoffmann D. The relevance of tobacco-specific nitrosamines to human cancer. *Cancer Surv* **8**:273-94, 1989.
6. Hei TK, Piao CQ, Han E, Sutter T and Willey JC. Radon-induced neoplastic transformation of human bronchial epithelial cells. *Radiat Oncol Invest* **3**:398-403, 1996.
7. Kang MK and Park NH. Conversion of normal to malignant phenotype: telomere shortening, telomerase activation, and genomic instability during immortalization of human oral keratinocytes. *Crit Rev Oral Biol Med* **12**:38-54, 2001.
8. Willey JC, Broussoud A, Sleemi A, Bennett WP, Cerutti P and Harris CC. Immortalization of human bronchial epithelial cells by papillomaviruses 16 or 18. *Cancer Res* **51**:5370-7, 1991.
9. Ostrow RS, Manias DA, Fong WJ, Zachow KR and Faras AJ. A survey of human papillomavirus DNA by filter hybridization. *Cancer* **59**:429-434, 1987.
10. Zhou H, Zhu LX, Li K and Hei TK. Radon, tobacco-specific nitrosamine and mutagenesis in mammalian cells. *Mutation Res* **430**:145-53, 1999. ■

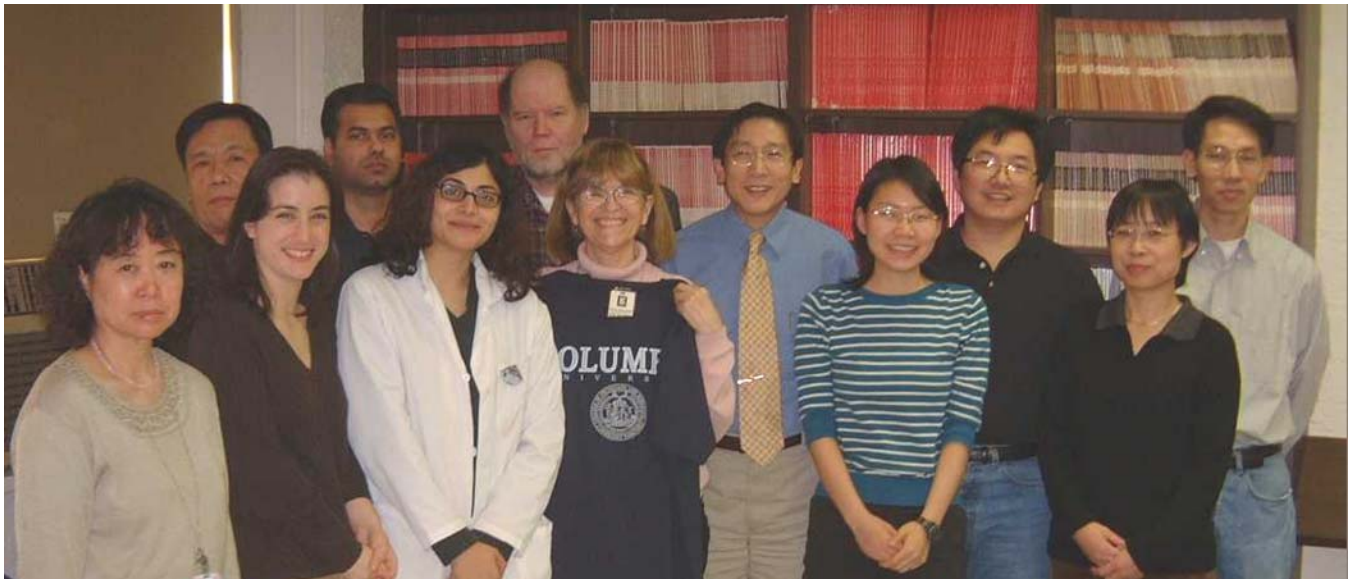

A farewell party for Dr. Gloria Calaf, who accepted a professorship at the University of Tarapaca in Chile, and left Dr. Hei's Laboratory in December, 2003. Good luck Gloria!

A commemorative picture of Dr. Tom Hei with Dr. Donald Malins, a seminar speaker during the spring term of this year.

Dr. Tom Hei, advisor to the Chinese medical exchange students from Fudan University, from left, Ms. Xian Cao, Ms. Ding Ding and Ms. Zheng Chenr.

Dr. Hei with his collaborator of over 20 years, Dr. Charles Waldren and his wife Diane. Together they published over 30 peer reviewed articles.

A reunion in Japan: Dr. Hei proudly presents two of his former research fellows, Dr. Ryuichi Okayasu (left), now a team leader at the NIRS in Japan, and Dr. Keiji Suzuki, an associate professor at Nagasaki University.

A high school summer student, Mr. Gary Chan of Pomona High School in Suffern, New York, hard at work at the bench.

Use of Multicolor Fluorescence in Situ Hybridization (M-FISH) For Detecting Spontaneous and Radiation Induced Chromosomal Instability in DNA Repair Defective Mouse Cells

Adayabalam S. Balajee and Charles R. Geard

The technique of multicolor fluorescence in situ hybridization (M-FISH) involves the use of PCR generated chromosome specific probes that are labeled differentially with various fluorescent dyes in different proportions. The combination of dyes (DEAC, FITC, Spectrum Orange, Texas Red and Cy5) enables the detection of all the chromosomes simultaneously with a single hybridization procedure. The separation of different excitation and emission spectra is achieved by appropriate filter sets (DAPI, DEAC, FITC, Spectrum Orange, Texas Red and Cy5). The resulting unequivocal color signature for each chromosome enables the analysis of hidden or complex chromosome aberrations. The M-FISH probes for mouse chromosomes were obtained from Meta Systems, Germany and the hybridization procedure followed was essentially the same as described by the manufacturers. M-FISH requires 3-4 days for hybridization and the analysis of a single metaphase takes about 30 min. Microscopic analysis was performed using an Axioplan II imaging microscope (Zeiss, Germany) equipped with an HBO 100 Mercury lamp and filter sets for DAPI, DEAC, FITC, Spectrum Orange, Texas Red and Cy5. Images were captured and processed using the Isis/M-FISH imaging system. A typical M-FISH pattern obtained for all the mouse chromosomes with each of the fluorochromes separately as well as in combination is illustrated in Figure 1.

After optimizing the M-FISH technique, we investigated the spontaneous and radiation induced chromosomal instability in ATM (ataxia telangiectasia mutated) heterozygous

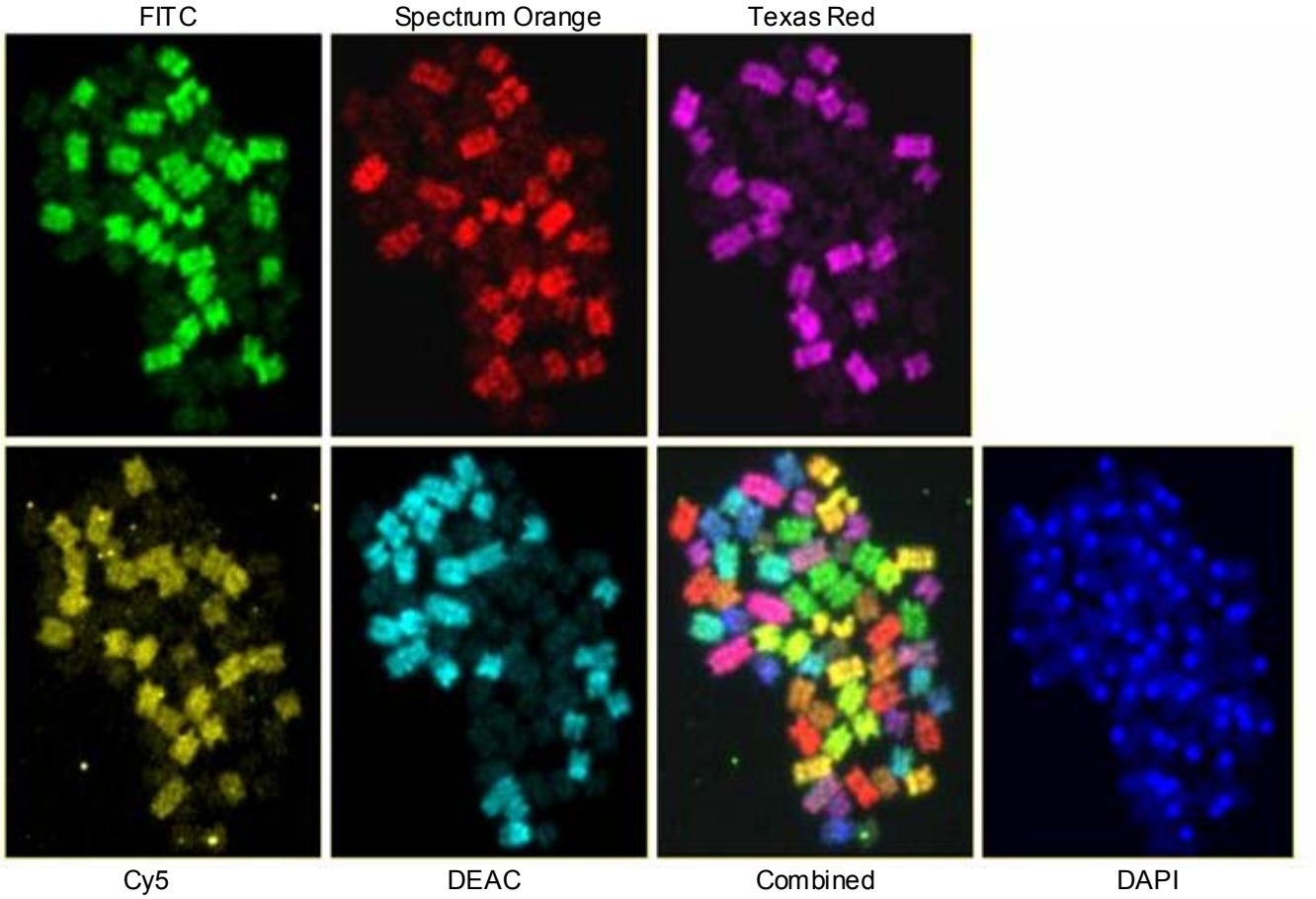

Fig. 1. A typical M-FISH pattern obtained for all the mouse chromosomes with each of the fluorochromes separately as well as in combination.

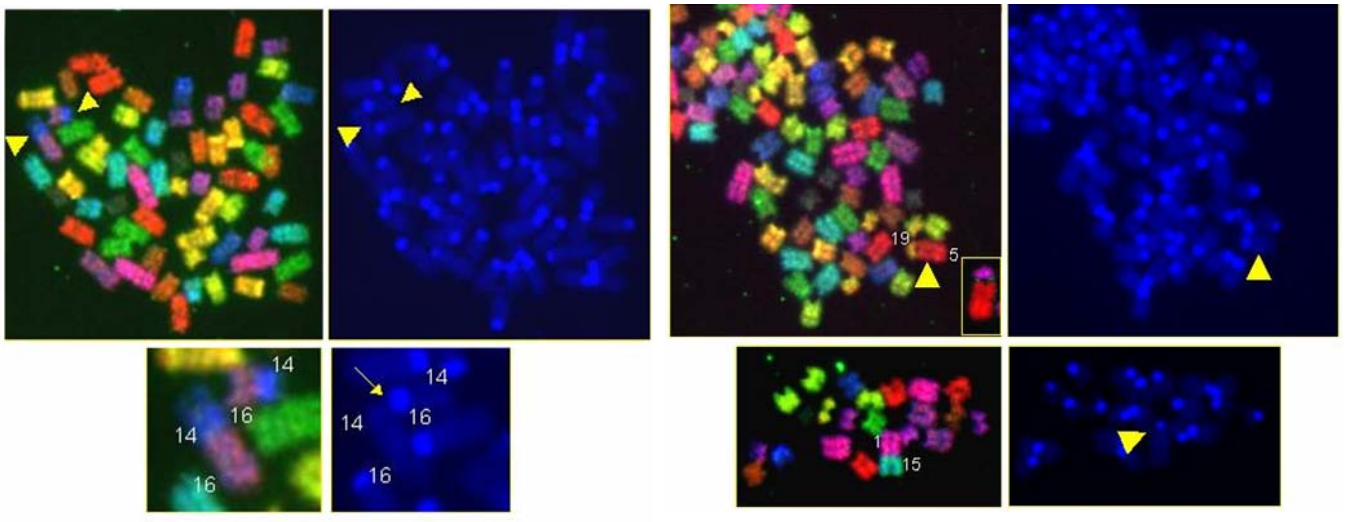

Fig. 2 Examples showing the reciprocal translocation induced by 0.1 Gy of irradiation involving chromosomes 14/16, 5/19 and 1/15. The arrowheads mark the chromosomes involved in exchanges. The merged color image of the chromosome showing the translocation (between 5 and 19) is shown in the inset.

mouse embryonic fibroblast (MEF) cells. Cells were irradiated with different doses of alpha particle irradiation (0.1, 1 and 2 Gy). Metaphase chromosomes prepared from control and irradiated cells were then processed for M-FISH. Simple and complex chromosomal changes induced by radiation were detected at the overall genome level by the application of the M-FISH technique. Complex chromosomal aberrations involving translocations, dicentrics with and without the fragments were observed. Complex chromosomal changes involving translocations between chromosomes and the acentric fragments (usually undetectable with conventional cytogenetic techniques) were detected by M-FISH. Examples showing the reciprocal translocation induced by 0.1 Gy of radiation involving chromosomes 14/16, 5/19 and 1/15 are illustrated in Figure 2. The arrowheads mark the chromosomes involved in exchanges. The merged color image of the chromosome showing the translocation (between 5 and 19) is shown in the inset.

We are planning to use M-FISH in mouse cells defective in specific pathways of DSB repair (non-homologous end joining (NHEJ) and homologous recombination repair) to determine whether there are any genotype specific unique chromosomal changes induced by different qualities of radiation. ■

Stable Intra-Chromosomal Biomarkers of Past Exposure to Densely-Ionizing Radiation in Several Chromosomes of Exposed Individuals

Catherine R. Mitchell, Tamara V. Azizova,[1] M. Prakash Hande,[2] Ludmilla E. Burak,[1] Josephine M. Tsakok,[3] Valentin F. Khokhryakov,[1] Charles R. Geard and David J. Brenner

mBAND analysis was used to investigate the levels of intra and inter-chromosomal aberrations in chromosomes 1 and 2 in the Mayak cohort. This cohort of radiation workers was from the Mayak Production Association nuclear weapons facility, near Ozyorsk, Russia (1). A substantial number of workers were occupationally exposed to plutonium, to γ-rays, or to both from 1949 onwards and due to the reliable dosimetric and medical information available for each individual, and because of the very low mobility rates of the Mayak workers, this cohort offers a unique opportunity to study the effects of radiation exposure to different radiation qualities (1).

In a previous study on this cohort carried out at Columbia, a biomarker for past high-LET radiation exposure, in the form of an increase in the number of intra-chromosomal

[1] *Southern Urals Biophysics Institute, Ozyorsk, Russia.*
[2] *National University of Singapore.*
[3] *Dept. of Environmental Health Sciences, Joseph Mailman School of Public Health, Columbia University.*

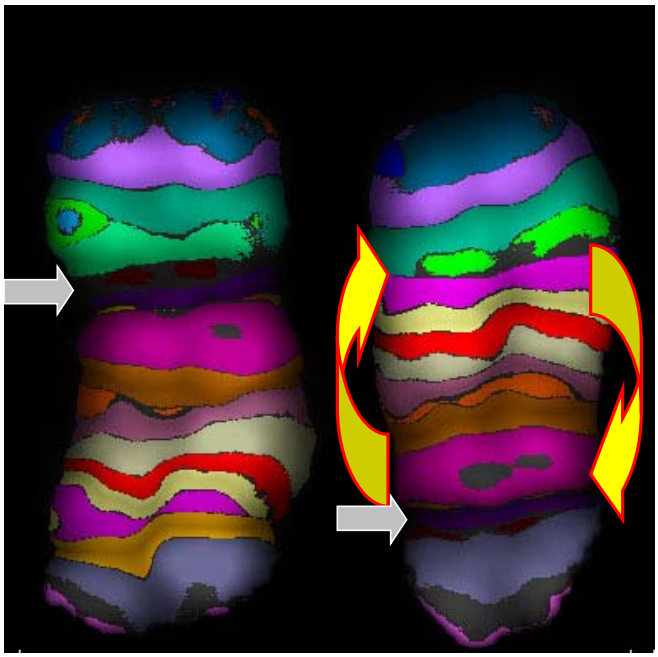

Fig. 1. Intra-chromosomal aberration detected in chromosome 2 of a PBL of a highly-exposed plutonium worker. Left chromosome is normal and the right shows the aberration. Grey arrows denote the centromeres. Yellow arrows indicate the region of the chromosome which was inverted, as indicated by the reversal in the sequence of band colors. This is an example of an inter-arm intra-chromosomal aberration (pericentric inversion).

aberrations, was found to be present in chromosome 5 of the plutonium-exposed Mayak workers (2). The presence of such a biomarker would potentially increase the accuracy of epidemiological estimates of high-LET radiation exposed individuals such as nuclear workers, airline flight crew, astronauts and patients undergoing neutron radiotherapy. The aim of this study was to examine whether this biomarker was present in chromosomes 1 and 2 of the same individuals. As these chromosomes are larger and have a higher DNA content, a larger number of aberrations would be expected than were found in chromosome 5.

Peripheral blood lymphocytes (PBLs) were examined from 26 healthy radiation workers from the Mayak Production Association. Eleven of these workers were exposed to high doses of α particles ($\geq$0.4 Gy bone marrow dose) as a consequence of plutonium inhalation, 11 were exposed to high doses of γ-rays ($\geq$1.5 Gy bone marrow dose) but no plutonium, and 4 were exposed to moderate doses (<0.4 Gy bone marrow dose) of both plutonium and γ-rays. Five control individuals, who were unexposed workers at the Mayak plant, were also examined. Blood samples were taken at the Southern Urals Biophysics Institute and metaphase spreads of PBLs were produced (3). The slides were then shipped to the USA and hybridized with mBAND probes and scored for chromosome aberrations

The multicolor banding FISH (mBAND) technique used for detecting intra-chromosomal aberrations allows single chromosomes to be "painted" with a series of colored bands along the axis (4, 5). These "paints" or probes are hybridized with chromosomes in metaphase preparations on slides. After hybridization, the chromosomes can be visualized. mBAND is based on region-specific chromosome paints (RSCP) combined with quantitative color ratio analysis: Each RSCP is labeled using a unique fluorochrome combination. The fluorochromes are sequentially excited by filtered light using a fluorescent microscope. Returning to the ground state the fluorochromes emit light of a certain wavelength and the light is captured via a camera and the images fed to a computer. The partial overlap in fluorochromes, between adjacent RSCPs results in a "merged color" continuously changing fluorescence pattern along the chromosome axis, quantified as a continuous change of color ratios. The software can detect differences in the emitted light and assigns "pseudo colors" to chromosome sections with similar color ratios, resulting in a reproducible color banding pattern. Loss or rearrangements of the bands indicate an intra-chromosomal aberration (4, 6). Figure 1 shows an example of an inter-arm inversion (pericentric) found in chromosome 2 from one of the high Pu-exposed workers.

The intra-chromosomal aberrations were scored manually based on the pseudo color images and it is important to assess the degree of observer dependence inherent in this process. To do this, all the slides were independently scored by two different observers. The results previously reported for chromosome 5 (2) were also rescored by two further observers.

Figure 2 shows the pooled data for stable intra-chromosome aberrations in chromosomes 1 and 2, as well as the corresponding data for chromosome 5 (which includes the results reported earlier (2), augmented with repeat scoring by two further observers). A large yield of intra-chromosomal aberrations was observed in all three chromo-

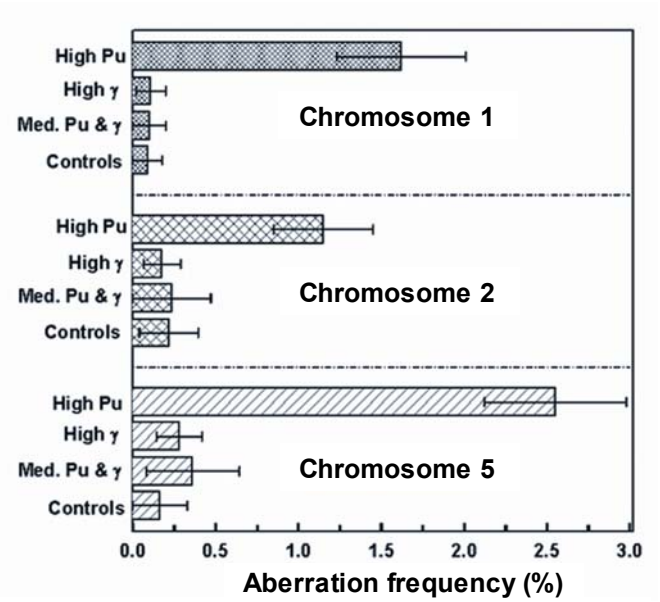

Fig. 2. Measured yields of stable intra-chromosomal aberrations in PBLs of individuals following high exposure to plutonium ($\geq$0.4 Gy bone marrow dose), high exposure to γ-rays ($\geq$1.5 Gy bone marrow dose and zero plutonium), medium exposure to both plutonium and γ-rays (<0.4 Gy Pu dose, <0.4 Gy γ dose), and unexposed controls. The mean numbers of intra-chromosomal aberrations are shown.

somes of the individuals exposed to high doses of plutonium (chromosome #1: 1.62 ± 0.39%, #2: 1.15 ± 0.30%; #5: 2.55 ± 0.43%). Taken together, 5.3% of the cells examined contained such aberrations in one of the three chromosomes examined. Extrapolated to the whole genome, this implies that about 24±5% of the cells of the individuals in the high-plutonium group contain large intra-chromosomal aberrations. There was no significant increase over the (low) background control rate in the population who were exposed to high doses of γ-rays. Fisher's exact test was used to investigate whether there were systematic differences between the results of the two observers. No statistically significant differences were seen.

These results for chromosome 1 and 2 confirm and extend previously published data for chromosome 5; however, the intra-chromosomal aberration frequencies observed in the present study for chromosomes 1 and 2 are somewhat lower than that observed for chromosome 5. The difference in intra-chromosomal aberration yields between chromosomes 1 and 2 and chromosome 5 are barely statistically significant, but the differences in intra-chromosomal yield per unit DNA content of each chromosome are significant, with chromosome 5 having a larger yield per unit DNA content ($12.7\pm2.1/10^5$Mb) than either chromosome 1 ($5.6\pm1.4/10^5$Mb) or chromosome 2 ($4.5\pm2.1/10^5$Mb). This difference, though not large, is surprising as the yield of intra-chromosomal aberrations would be expected to be approximately proportional to the DNA content of the chromosome, analogous to the dependencies on DNA content observed for inter-chromosomal aberrations (7, 8).

In conclusion, we have confirmed by examining chromosomes 1 and 2 the previous conclusion for chromosome 5 that intra-chromosomal aberrations represent a sensitive, long-lived, quantitative, low-background biomarker of exposure in human populations exposed to densely-ionizing radiation many years earlier. Even many years after occupational exposure, about a quarter of the PBLs of the healthy plutonium workers contain large (≥6Mb) intra-chromosomal rearrangements; the various control groups contained very few such intra-chromosomal aberrations. Quantification of this large-scale chromosomal damage in human populations exposed many years earlier should lead to new insights into the mechanisms of cytogenetic damage, as well significantly enhancing epidemiological studies.

References

1. Anspaugh LR, Degteva MO and Vasilenko EK. Mayak Production Association: introduction. *Radiat Environ Biophys* **41**:19-22, 2002.
2. Hande MP, Azizova TV, Geard CR, Burak LE, Mitchell CR, Khokhryakov VF, Vasilenko E and Brenner DJ. Past exposure to densely ionizing radiation leaves a unique permanent signature in the genome. *Am J Hum Genet* **72**:1162-70, 2003.
3. Burak LE, Kodama Y, Nakano M, Ohtaki K, Itoh M, Okladnikova ND, Vasilenko EK, Cologne JB and Nakamura N. FISH examination of lymphocytes from Mayak workers for assessment of translocation induction rate under chronic radiation exposures. *Int J Radiat Biol* **77**:9018, 2001.
4. Chudoba I, Plesch A, Lorch T, Lemke J, Claussen U and Senger G. High resolution multicolor-banding: a new technique for refined FISH analysis of human chromosomes. *Cytogenet Cell Genet* **84**:156-60, 1999.
5. Boei JJ, Vermeulen S, Moser J, Mullenders LH and Natarajan AT. Intrachanges as part of complex chromosome-type exchange aberrations. *Mutat Res* **504**:47-55, 2002.
6. Johannes C, Chudoba I and Obe G. Analysis of X-ray-induced aberrations in human chromosome 5 using high-resolution multicolour banding FISH, mBAND. *Chromosome Res* **7**:625-33, 1999.
7. Cornforth MN, Greulich-Bode KM, Loucas BD, Arsuaga J, Vazquez M, Sachs RK, Bruckner M, Molls M, Hahnfeldt P, Hlatky L and Brenner DJ. Chromosomes are predominantly located randomly with respect to each other in interphase human cells. *J Cell Biol* **159**:237-44, 2002.
8. Johnson KL, Brenner DJ, Nath J, Tucker JD and Geard CR. Radiation-induced breakpoint misrejoining in human chromosomes: random or non-random? *Int J Radiat Biol* 75:131-41, 1999. ■

Chromosomal Analysis of Lymphocytes in Airline Pilots Using mFISH and mBAND Techniques

Catherine R. Mitchell, M. Prakash Hande,[1] Carol S. Griffin,[2] Josephine M. Tsakok,[3] Elaine Ron,[4] Alice J. Sigurdson,[4] Lee Yong,[5] Charles R. Geard and David J. Brenner

Airline personnel are exposed to cosmic rays during flights. A large number of flying hours at high altitudes may increase doses of high-LET neutrons and gamma rays. The mean annual dose equivalent has been estimated to be 1-3mSv (1, 2) but varies according to flight altitude, latitude and solar activity. This dose may lead to increases in chromosomal aberrations and a potential increase in cancer risk. This study examines the yield of stable inter and intra-chromosomal aberrations from peripheral blood lymphocytes (PBLs) of 5 long haul airline pilots using mFISH and mBAND techniques. The aim was to investigate whether pilots had a higher number of chromosomal aberrations than controls and to look for the presence of intra-chromosomal aberrations present due to the exposure to high-LET neutrons.

PBLs were taken from 5 healthy male long-haul airline pilots. Metaphase spreads were produced, chromosomes hybridized with mFISH and mBAND probes and scored for inter and intra-chromosomal aberrations. Chromosomes 1, 2 and 5 were studied using mBAND.

A slight increase in inter-chromosomal aberration frequency was observed for the pilots after analysis with mFISH (1.4% compared with the background 0.7%) although it did not reach statistical significance. Analysis of the mBAND data, looking at just one chromosome, found an intra-chromosomal aberration frequency of 2.5 ± 0.8% which is higher than that of our controls from our Mayak study (0 ± 0.3%). This result is not significant, but is highly suggestive that airline pilots have an increased number of intra-chromosomal aberrations compared with grounded controls.

This study suggests that occupational exposure to high-LET radiation in the form of cosmic rays, as is usual in the case of airline pilots, may lead to an increase in chromosomal aberrations. This may or may not increase the risk of cancer. More exposed individuals, along with more appropriate controls, need to be studied in order to elucidate this further.

[1] *National University of Singapore.*
[2] *Medical Research Council, Radiation and Genome Stability Unit, Harwell, UK.*
[3] *Dept. of Environmental Health Sciences, Joseph Mailman School of Public Health, Columbia University.*
[4] *Radiation Epidemiology Branch, National Cancer Institute, NIH, Bethesda, MD.*
[5] *The National Institute for Occupational Safety and Health, CDC, Cincinnati, Ohio.*

References

9. Bouville A and Lowder WM. Human population exposure to cosmic radiation. *Radiation Protection and Dosimetry* **24**:293-9, 1988.
10. Montagne C, Donne JP, Pelcot D, Nguyen VD, Bousset P and Kerlau G. In-flight radiation measurements aboard French airliners. *Radiation Protection and Dosimetry* **48**:79-83, 1993. ■

mFISHing in Russia

Catherine Mitchell, Charles Geard and David Brenner Travel to Ozyorsk, Russia for a Meeting with Their Collaborators

Catherine R. Mitchell, photography by Nathalie Latham

For several years now there has been a successful collaboration between the CRR and the Southern Urals Biophysics Institute (SUBI) in Ozyorsk, Russia. Up until 12 years ago Ozyorsk was a closed, secret city, but in 1992 it was no longer designated secret, but still remained closed. In practical terms this means that a fence runs around the perimeter of the city and people are not permitted to move freely into Ozyorsk.

Ozyorsk is a factory city and most of its inhabitants are employed in areas related to the Mayak nuclear facility. From 1949 onwards, the Mayak facility was involved in the production of nuclear weapons. In the past, safety proce-

Fig. 1. In front of the Southern Urals Biophysics Institute on the first day of our visit. Left to right: Alexander (our interpreter), David Brenner, Charles Geard, Catherine Mitchell.

dures were not rigorously enforced which resulted in some workers being exposed to high levels of Plutonium (Pu) and gamma rays. The Mayak facility does not now produce nuclear weapons, but instead manufactures radioisotopes for medical and industrial use. However, many of the previously exposed workers remain in Ozyorsk and their health is regularly monitored by doctors at SUBI. This, together with the fact that the dosimetry of their exposure is well documented makes the Mayak workers an ideal cohort for the study of radiation exposure *in vivo*.

The collaboration between SUBI and the CRR focuses on the study of chromosome aberrations in the lymphocytes of people who have had past-exposure to radiation. The blood from exposed individuals and controls is taken during routine examination at SUBI. The lymphocytes are stimulated to grow *in vitro* and metaphase spreads are produced. These slides are then sent from Russia to New York where they undergo mFISH and mBAND hybridization and chromosomes are captured and analyzed. Studies so far have proved the existence of a "biomarker" for past exposure to high-LET irradiation, *i.e.*, an increase in intra-chromosomal aberrations were observed in people exposed to Pu in comparison with those exposed to gamma rays and controls (1).

In December 2003, David Brenner, Charles Geard, Catherine Mitchell and Nathalie Latham (a photographer interested in recording details of the study) travelled to SUBI to discuss future research and to demonstrate mFISH and mBAND hybridizations and analysis. The trip proved fruitful and interesting both from a work perspective and also because it allowed us a rare opportunity to experience, albeit briefly, this fascinating city.

Friday, December 5

Due to heavy snow in New York the flight from JFK to Frankfurt was delayed by 4 hours. The plane finally took off at 1.30 a.m. arriving in Frankfurt one hour after the connecting flight to Ekaterinburg had already left. Not an auspicious start!

Saturday, December 6

The next direct flight to Ekaterinburg from Frankfurt was scheduled for the following Tuesday, which due to the shortness of the planned trip was not a practical option. Fortunately, it was possible to travel to Moscow and then on to Ekaterinburg via Aeroflot. So after meeting Nathalie in Frankfurt we caught the flight to Moscow where we had less than one hour to make the connection to Ekaterinburg. Nathalie managed to find a way through the diplomatic entrance, avoiding a long queue at customs. We then paid $40 for a taxi to the next terminal. After a further 2-hour flight we finally arrived in Ekaterinburg at 5 a.m. local time, 8 hours later than we had planned.

Sunday, December 7

After a much-needed 4-hour sleep in our hotel we met our interpreter, Alex, and made our way to the "Cathedral of the Blood." This was a very ornate church built near the site where Tsar Nicholas II and Tsarina Alexandra and their children were executed in the basement of a house in 1918. We met up with Sergey Romanov and Tamara Azizova from SUBI after lighting candles (to pray for a successful trip). We were taken to the Ekaterinburg museum where a selection of the many gems found locally in the Ural Mountains are displayed together with iron statutes from the local town of Kystin. We dined in a local Uzbekistani restaurant and then embarked on the 3-hour journey back to Ozyorsk. The conditions were treacherous and the car containing David and Tamara with Alex driving accidentally skidded and drove into a ditch leaving the passengers very shaken. Fortunately, the driver of the other car produced a towrope and managed to pull the car out of the ditch and back onto the motorway. On arriving at Ozyorsk we had to pass through a "checkpoint" before entering the closed city. We were then taken to our hotel.

Monday, December 8

Alex picked us up at 9 a.m. and took us to SUBI where we met Tamara and were introduced to Ludmilla, Alena and Maria who were involved in research at SUBI. The workers at SUBI had prepared slides for us to take back to New York to undergo mFISH and mBAND analysis. Charles examined each slide by microscopy to determine whether the meta-

Fig. 2. Ludmilla and Catherine carrying out an mBAND hybridization.

Fig. 3. Charles verifying slides.

Fig. 4. Left–right: Alena, Ludmilla, Alexander, Tamara & David looking at mBAND chromosome images.

phase spreads were of sufficient quality to attempt hybridization.

Catherine attempted to carry out a hybridization within the lab at SUBI accompanied by Ludmilla, Alena and Alex.

David spent time with Tamara to discuss the future direction of the project and Nathalie spent time taking photographs of Charles, Catherine and David at work.

That evening we were taken to the canteen usually used by Mayak workers for dinner. Our two SUBI drivers Igor and Sacha joined us and were able to tell us about themselves and life in Ozyorsk.

Tuesday, December 9

Charles and Catherine spent the morning examining slides that Ludmilla had prepared and selected the best ones for the latest study.

After lunch Catherine and Nathalie donned lab coats and were taken by Tamara to visit some of the workers from Mayak who were in SUBI for their routine medical checks. They were introduced to two female ex-workers Vera and Nina. Nathalie asked them questions about their lives and their work at Mayak. They were shown photographs of their families and were very eager to talk about their lives and work at Mayak.

Laden down with gifts of homemade jam and garlic they moved onto a second ward containing three male workers. The eldest, Sergey, had previously been exposed to radiation at Mayak. At first he was somewhat reticent until Nathalie assured him that the photographs she took would not show them in a bad light. He talked about his family and told us he was an avid reader of Faust. The two other men were confusingly both named Yuri. One of the Yuris was keen on ice-fishing and underwater hunting with a spear! Meeting these workers certainly put added a human dimension to the research. Later in the day David and Catherine met with Dr Valentin Khokhryakov who provided the dosimetry concerning the Mayak workers in the study.

In the evening we visited a pained silk Batik factory. It was very impressive to see how Alex could alternate between translating discussions concerning chromosomes and biology (from the lab), families and hobbies (from the Mayak workers), complex physics equations and dosimetry (from the meeting with Dr Khokhrykov) and then the fine art of silk painting (in the Batik factory). We ended the evening having dinner in a restaurant with Alex and Tamara.

Wednesday, December 10

Catherine showed the SUBI lab workers mFISH and mBAND images she had captured in New York. In the afternoon we went to the Mayak museum where we were escorted around by a very enthusiastic guide. He was very proud of the burial of nuclear waste and that the levels of Pu exposure are at present much lower than in previous decades. After this we went for dinner and bowling at the casino. At the end of the evening Tamara presented each of us with a book entitled "Plutonium in Madens' Hands" written entirely in Russian. It told the story of young female Mayak workers in the 1940s who had been exposed to Plutonium.

Thursday, December 11

In the morning the drivers took us to the spectacular frozen lake where the ice was up to 1.5 meters thick. It was possible to walk on the surface and there were several small huts on the ice where fishermen would sit all night in their attempt to catch fish. The temperature was as low as -20°C

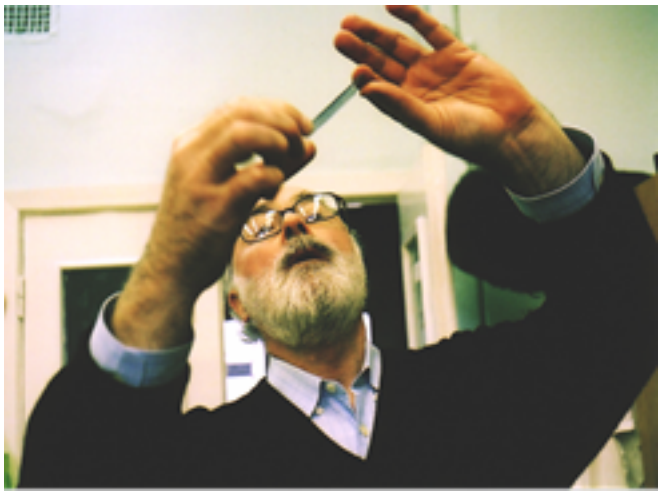

Fig. 5. Charles examining an archival slide.

Fig. 6. Ludmilla next to blood sample archives of Mayak workers dating back to over 40 years.

Fig. 7. Mayak Museum: David Brenner and Charles Geard in front of painting of Mayak Plutonium complex (foreground of painting) and the town of Ozyorsk in background surrounded by lakes.

and some of our cameras froze!

We are attempting to carry out a study performing mFISH analysis on archival slides. SUBI has a large collection of slides from individuals, from up to 20 years ago and we plan to examine chromosomes from the same individual over a long period of time to observe whether there is any change in the aberration frequency in their cells. At present the hybridization of these old slides has not been consistent as the DNA has degraded over time. Charles spent a large part of the day examining these slides to check their quality.

Catherine carried out the second part of the hybridization procedure and the mFISH and mBAND pictures were shown to everyone in the lab.

In the evening the SUBI and CRR workers returned to the same canteen as on Monday evening. An illuminated notice board outside displayed the date, temp (-11°C), pressure and the dose rate (13 μroentgens per minute).

A formal dinner of hot and cold smoked fish and shashlick (barbecued meat) was served. Many toasts were made to celebrate the very successful trip and even more vodka was drunk. Alex entertained everyone with his wide repertoire of traditional Russian and modern western songs on the guitar.

Friday, December 12

The week passed so quickly and following brunch at SUBI it was time for our final goodbyes. We were driven back to Ekaterinburg airport and whilst Charles, David and Catherine flew directly back to New York (without any delay!), Nathalie remained in Ekaterinberg for two further days for her direct flight back to Paris.

The trip proved to be very productive from several perspectives. It was interesting to see the labs at SUBI, to meet the Mayak workers and to have an opportunity to spend some time in this unique city. We are very grateful to everyone at SUBI for their hospitality and appreciated the lengths they went to make our short stay so memorable.

References

1. Hande MP, Azizova TV, Geard CR, Burak LE, Mitchell CR, Khokhryakov VF, Vasilenko EK and Brenner DJ. Past exposure to densely ionizing radiation leaves a unique permanent signature in the genome. *Am J Hum Genet* 72:1162-70, 2003. ■

Fig. 8. Sergey, a retired engineer from Mayak, at hospital for his annual check up.

Fig. 9. Catherine, David and Charles on a frozen lake surrounding Ozyorsk.

Mrad9 Is Essential for Mouse Embryogenesis

Kevin M. Hopkins, Wojtek Auerbach,[1] Xiangyuan Wang, Debra J. Wolgemuth,[2] Alexandra L. Joiner[1] and Howard B. Lieberman

We have cloned mouse genomic and cDNA orthologues of the fission yeast *S. pombe* cell cycle checkpoint control gene *rad9*. The *rad9* gene of *S. pombe* is involved in the repair of damaged DNA caused by exposure to ionizing radiation and ultraviolet light. *S. pombe* cells containing *rad9*::*Ura4*$^{+}$ are highly sensitive to these DNA damaging agents, and are unable to delay cycling in late G2 after exposure to radiation. Therefore, these cells lack G2/M check-

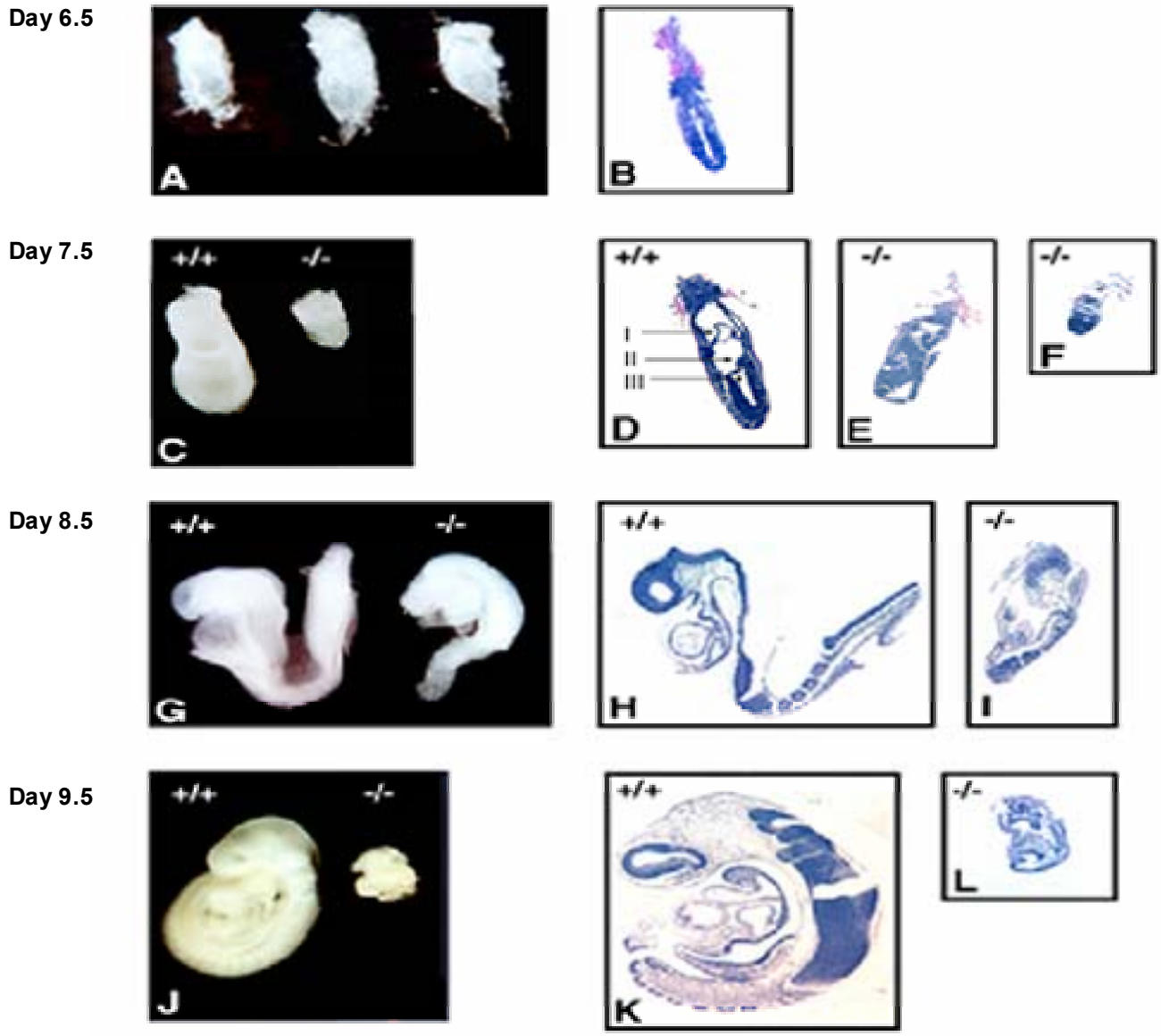

Fig. 1. Gross morphology and thin sections of mouse embryos derived from *Mrad9*+/- X *Mrad9*+/- crosses. Photographs of intact or thin-sectioned embryos from E6.5 (A, B), E7.5 (C, D, E, F), E8.5 (G, H, I) and E9.5 (J, K, L) are presented. Labeling for D is as follows: I, extra-embryonic component of the chorion; II, allantois; III, neural ectoderm (neuroepithelium) in the primitive streak region. Genotypes: +/+, *Mrad9*+/+; -/-, *Mrad9*-/-.

[1] *Skirball Institute of Biomedical Medicine and Howard Hughes Medical Institute, Developmental Genetics Program, New York University School of Medicine, New York, NY.*

[2] *Depts. of Genetics & Development and Obstetrics & Gynecology, and the Institute for Human Nutrition, Columbia University.*

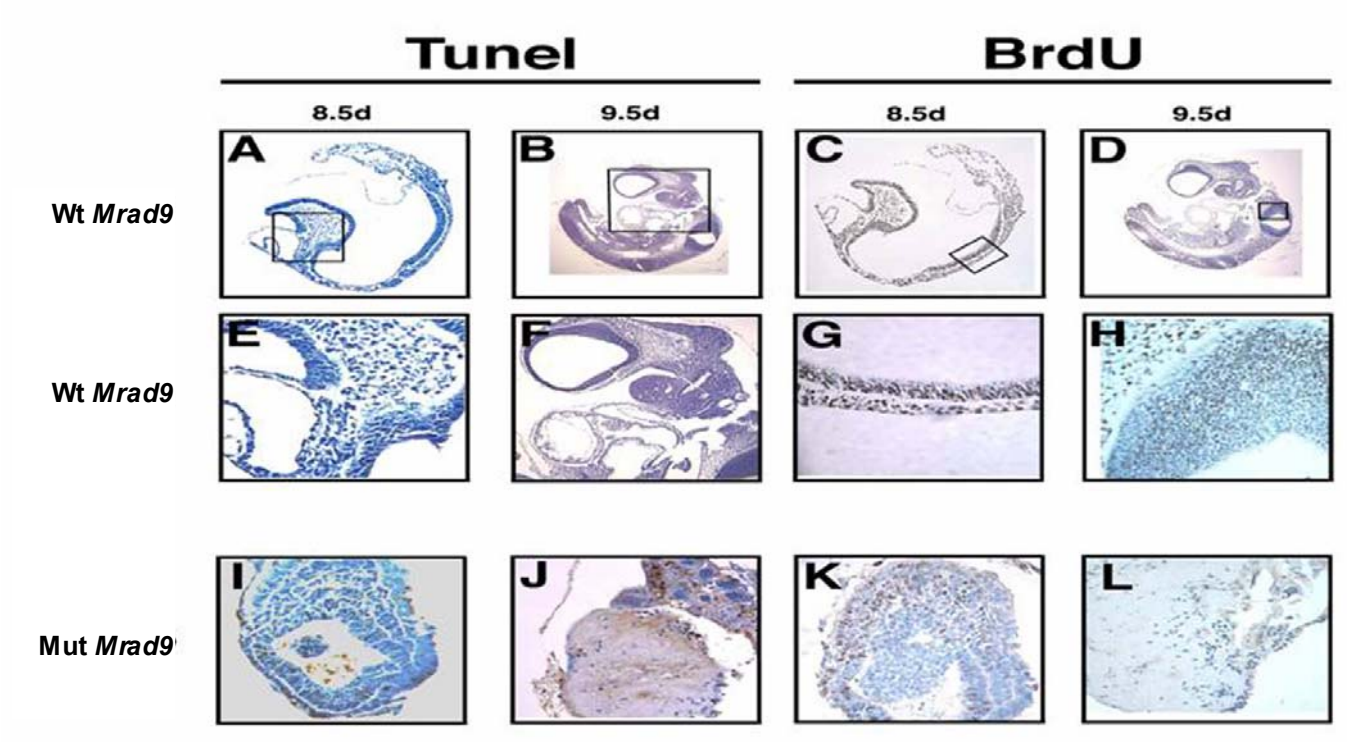

Fig. 2. Cross sections of TUNEL stained d8.5 wild type *Mrad9* (A and E), d8.5 homozygous mutant *Mrad9* (I), d9.5 wild type *Mrad9* (B and F) and d9.5 mutant *Mrad9* (J) embryos. E and F are higher magnification views of the boxed regions in A and B respectively. Sections of BrdU *in utero* labeled d8.5 wild type *Mrad9* (C and G), d8.5 mutant *Mrad9* (K), d9.5 wild type *Mrad9* (D and H) and d9.5 mutant *Mrad9* (L) embryos. G and H are higher magnification views of the boxed regions in C and D respectively.

point control. To determine the role of a mammalian version of this gene in radioresistance and cell cycle checkpoint function, we used the cloned *Mrad9* gene to generate *Mrad9* deleted mouse embryonic stem (ES) cells and adult heterozygous *Mrad9* deleted mice. To accomplish this goal, the first two exons of *Mrad9* in ES cells were surrounded by loxP sites, using gene targeting techniques, and subsequently deleted by expressing Cre, a site specific recombinase that recognizes and processes loxP sites. These cells were then used to make heterozygous *Mrad9* mice.

Although heterozygous *Mrad9* mice were generated, paired heterozygous *Mrad9* matings produced no mutant *Mrad9* mice among 419 offspring examined. This provided strong evidence that the loss of *Mrad9* leads to embryonic lethality. To characterize the embryonic lethality in more detail, we analyzed the morphology of embryos, at different stages of development, obtained from timed matings between heterozygous *Mrad9* mice. Starting at day 7.5, homozygous deleted Mrad9 embryos appear smaller than their heterozygous mutant or wild type counterparts (Figure 1C). There is also loss of distinct morphological features, including well-defined, identifiable structures at this time (Figure 1, D-F).

Using the TUNEL assay, we determined that day 8.5 and day 9.5 mutant *Mrad9* embryos contain regions that are apoptotic (Figure 2, I and J). There were no detectable apoptotic regions in wild type embryos at the same time in development (Figure 2, E and F). We also checked if embryonic cells were still synthesizing DNA at these times. Embryos were labeled with BrdU *in utero*, thin sectioned and stained with anti-BrdU antibodies. The wild type day 8.5 and day 9.5 embryos were synthesizing DNA throughout all regions of the embryo (Figure 2, G and H). For the day 8.5 and day 9.5 *Mrad9*-/- embryos, DNA synthesis was still occurring but not as robust as is observed for the wild type embryos (Figure 2, K and L).

We have been able to establish MEF cultures from *Mrad9*+/+ and *Mrad9*-/- embryos. However, MEFs from *Mrad9*-/- embryos fail to grow. ■

Creation of *Mhus1b* Knockout ES Cells and Mice

Haiying Hang

Human cell cycle checkpoint genes *Hhus1, Hrad1* and *Hrad9* were identified recently. Their protein products Hhus1, Hrad1 and Hrad9 can form a heterotrimer, a ring structure resembling a PCNA DNA sliding clamp. Knocking out each of their counterparts *hus1, rad1* and *rad9* in the fission yeast *S. pombe* renders the cells extremely sensitive to γ-rays, UV light and hydroxyurea, a DNA replication inhibitor. These mutant cells are also defective in S/M and G2/M checkpoint control. *Mhus1*$^{-/-}$ and *Mrad9*$^{-/-}$ mouse cells are also sensitive to genotoxic agents and have defective cell cycle checkpoint control. *Hhus1b*, a paralogue of *Hhus1,* has been identified and preliminarily characterized in the PI's laboratory. The expression levels of the two genes parallel across human tissues. Our initial study indicates that *Hhus1* and *Hhus1b* manifest distinct features in three aspects. First, HUS1b can only directly interact with RAD1 while HUS1 can directly bind to both. Second, overexpression of *HUS1b,* but not *HUS1,* leads to cell death. Third, *HUS1b* is significantly less conserved than *HUS1* from mouse to human. These data suggest that Hhus1b and Hhus1 play distinct molecular roles in the same processes, including cell cycle checkpoint control and genome stabilization as well as tumor suppression. In order to define the roles of *HUS1b* in these functions, we have created mouse cells and mice in which *Mhus1b* (the mouse version of *HUS1b*) has been deleted.

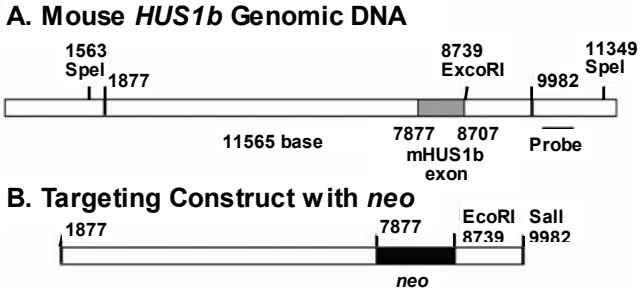

Fig. 1. Mouse *Mhus1b* Genomic DNA and *Mhus1b* Gene Targeting Constructs: (A) The 11.6 kb mouse genomic DNA contain an 831 bp intronless *Mhus1b* open reading frame. The fragment between 1877 and 9982 has been used to make targeting constructs. The fragment located at the right of the base 9982 will be used as a probe in Southern blotting to detect *Mhus1b* gene deletion. **(B)** The *neo*-containing targeting construct, in which a *neo* gene replaced the entire coding region of *Mhus1b*.

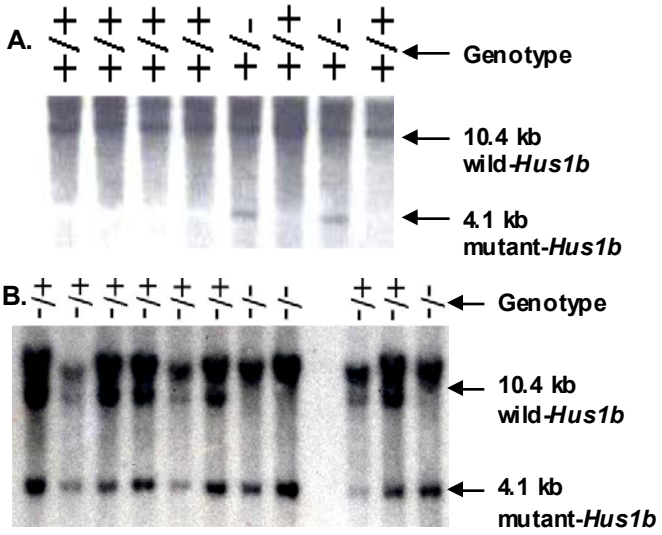

Fig. 2. Generation of *Mhus1b*-knockout ES cells. The method to replace wild type *Mhus1b* alleles with a targeting construct is described in the text. **(A)** Two *Mhus1b*$^{+/-}$ clones were identified out of 180 clones examined in the first round screening. DNA isolated was cut with *Spe*I, and then subject to Southern blot analysis using the probe indicated in Figure 1. A targeted clone displays two bands while a wild type clone only shows a high MW band (10.4kb). **(B)** A second round screening yielded 25% *Mhus1b*$^{-/-}$ clones from *Mhus1b*$^{+/-}$ cells. Three *Mhus1b*$^{-/-}$ clones are shown here.

The construct for targeting *Mhus1b* in ES cells is shown in Figure 1. The *neo*-containing construct was introduced into mouse ES cells by electroporation to replace a wild type *Mhus1b* allele, and then ES cell colonies, formed in medium in the presence of 200 μg/ml G418, were screened for *Mhus1b*$^{+/-}$ clones. We successfully acquired two *Mhus1b*$^{+/-}$ clones (Figure 2A). One *Mhus1b*$^{+/-}$ ES cell clone was expanded and incubated in medium containing high concentration G418 (2mg/ml), and cell colonies were screened again

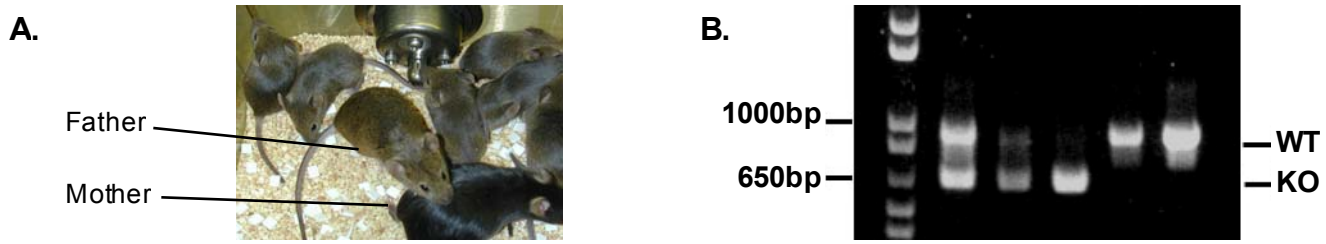

Fig. 3. *Mhus1b* knockout mice. (A) A B6 black female mated with a male *Mhus1b* chimera and produced agouti pups (brown). **(B)** Genotyping indicates that some of the pups are *Mhus1b*$^{+/-}$ mice (lanes 2 and 3). Mating between these *Mhus1b*$^{+/-}$ offspring has successfully produced *Mhus1b*$^{-/-}$ pups (lane 4). PCR was used to genotype the pups.

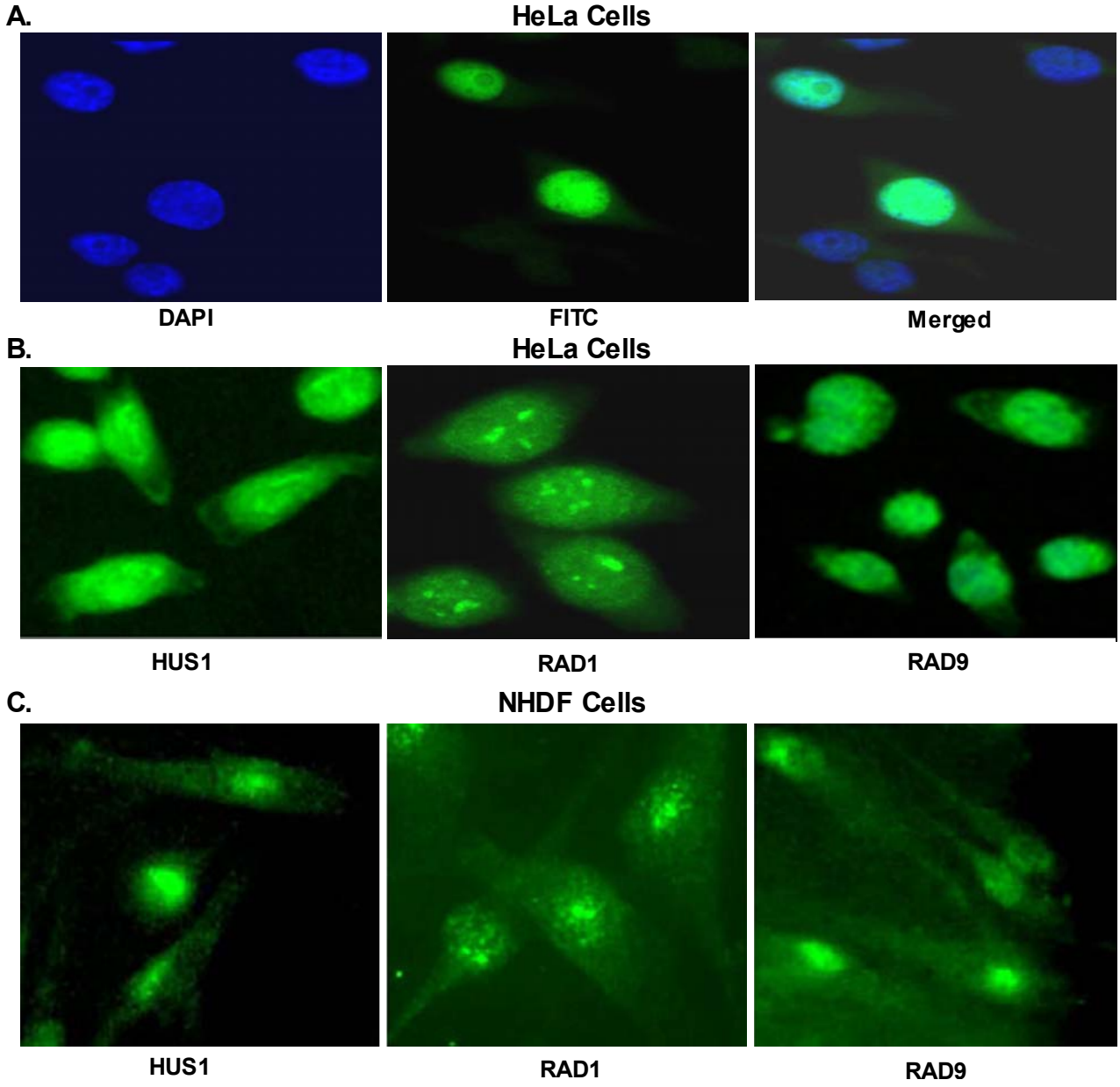

Fig. 4. HUS1b is localized in the nucleus. HUS1b (A) and the three other related proteins HUS1, RAD1 and RAD9 (B and C) are localized in the nucleus. **(A)** Flag-HUS1b was overexpressed in HeLa cells. After fixation, cells were probed with FITC-conjugated anti-Flag antibody. The FITC fluorescence was overlapped with DAPI staining, suggesting that HUS1b locates in the nucleus. **(B)** and **(C)** anti-HUS1, anti-RAD1 and anti-RAD9 sera were used to probe fixed HeLa cells and normal human dermal fibroblasts (NHDF), and subsequently FITC-conjugated secondary antibody was applied to reveal the locations of these proteins. They are mainly localized in the nucleus.

for *Mhus1b*$^{-/-}$ clones. We have generated 3 *Mhus1b*$^{-/-}$ clones in this way (Figure 2B).

Mhus1b$^{+/-}$ ES cells (129 strain) were also used for injection into blastocysts of B6 mice. Male chimera pups (brown and black mixture) born from the B6 female mice were selected to mate with other female B6 mice again, and agouti pups (brown) from the mating were screened for *Mhus1b*$^{+/-}$ genotype (Figure 3A). Further mating between *Mhus1b*$^{+/-}$ mice yielded *Mhus1b*$^{-/-}$ mice (Figure 3B).

Like the four other related cell cycle checkpoint proteins, HUS1b is localized in the nucleus (Figure 4; RAD9b localization in ref. 1), suggesting that HUS1b may work coordinately with the four proteins (RAD1, RAD9, RAD9b and HUS1b) in repairing DNA damage, maintaining genome stability and safeguarding cell cycle checkpoints.

With *Mhus1b*$^{-/-}$ cells and mice, we will be able to investigate the roles of *Mhus1b*$^{-/-}$ in DNA protection, cell cycle checkpoint controls and tumor suppression.

References

1. Hopkins KM, Wang X, Berlin A, Hang H, Thaker HM and Lieberman HB. Expression of mammalian paralogues of HRAD9 and Mrad9 checkpoint control genes in normal and cancerous testicular tissue. *Cancer Res* **63**:5291-8, 2003. ■

Paralogue of HRAD9 Is a Nuclear Protein and Coimmunoprecipitates with HRAD9, HRAD1, HHUS1 and HHUS1B*

Xiaojian Wang, Kevin M. Hopkins and Howard B. Lieberman

Human RAD9 was isolated as a homologue of fission yeast *Schizosaccharomyces pombe rad9*. It functions as a G2 checkpoint control protein in the cell cycle (1). Recently, Human (*HRAD9*) and mouse (*Mrad9*) ortholog of this gene have been isolated by our group and called *HRAD9B* and *Mrad9B* respectively. The results have shown that similar to HRAD9, HRAD9B is a nuclear protein and physically interacts with checkpoint control proteins HRAD9, HRAD1, HHUS1 and HHUS1 paralogue HHUS1B (2).

HRAD9B protein has 414 amino acids, among which, 55% are similar and 35% are identical to HRAD9. HRAD9 is a located in the nucleus. To determine whether HRAD9B is also localized in the cell nuclear compartment, immunofulorescence experiments were performed. Both HRAD9 and HRAD9B were fused with FLAG epitope, these tagged genes were overexpressed in Hela cells. Protein subcellular localization was visualized under fluorescence microscopy. Since FLAG antibody was commercially conjugated with fluorescence dye FITC. As seen in Figure 1, FITC green staining is co-localized with control DAPI blue staining, which suggested that HRAD9B is a nuclear protein.

HRAD9 can form complexes with other nucleus-located checkpoint control proteins, HHUS1 and HRAD1, sometimes referred to as 9-1-1 complex or RHR heterotrimer (3). Recently isolated Human HUS1 paralogue HHUS1B can also coimmunoprecipitate with this heterotrimer (4).

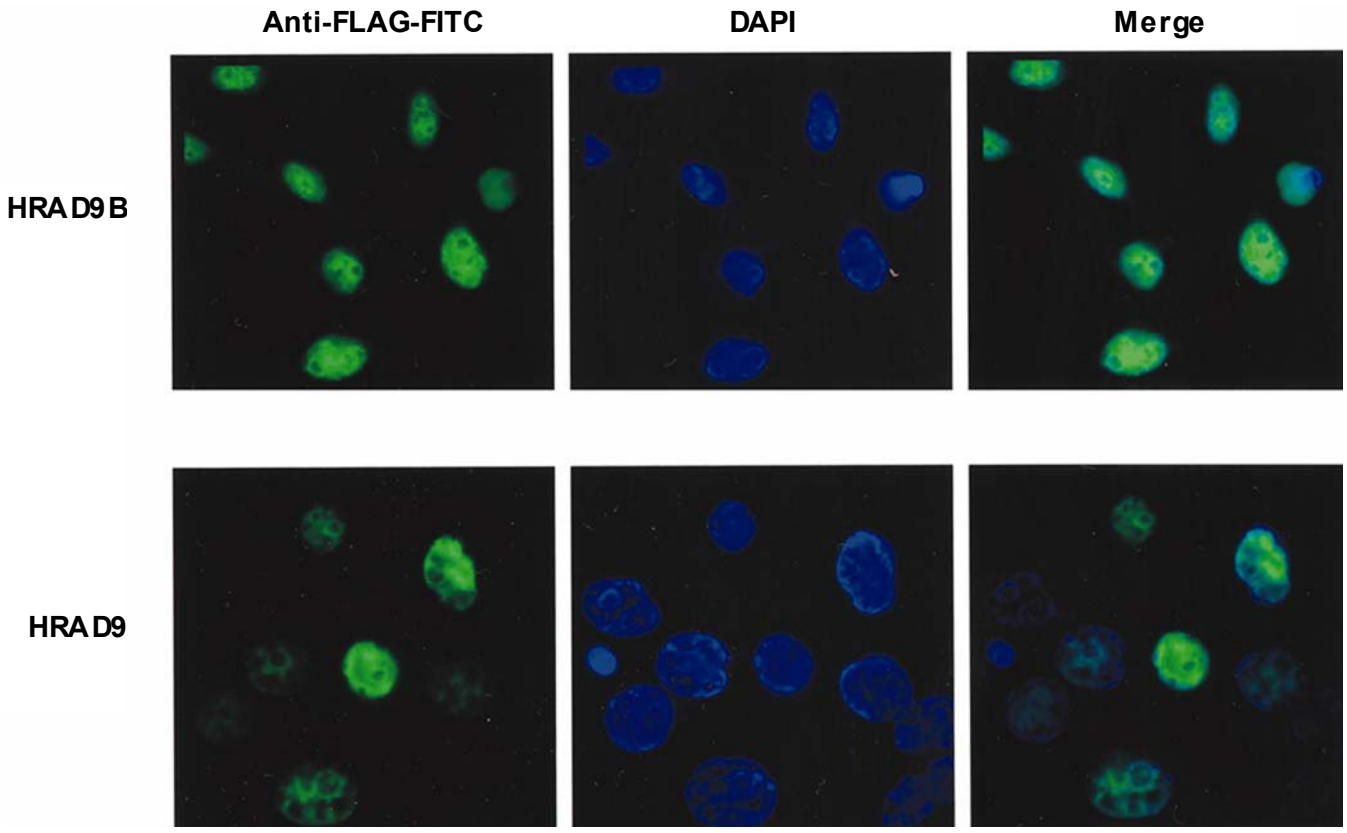

Fig. 1. Localization of HRAD9B and HRAD9 in the nucleus. Hela cells were transfected with a plasmid encoding FLAG-tagged HRAD9B or HRAD9, and after 24h, cells were stained with anti-FLAG antibodies to visualize these proteins or stained with DAPI to detect DNA in the nucleus. The untransfected control cells contained an undetectable FLAG signal (data not shown). As indicated, both HRAD9B and (as reported previously) HRAD9 localize in the nucleus.

* *Data shown here are published in Ref. 2.*

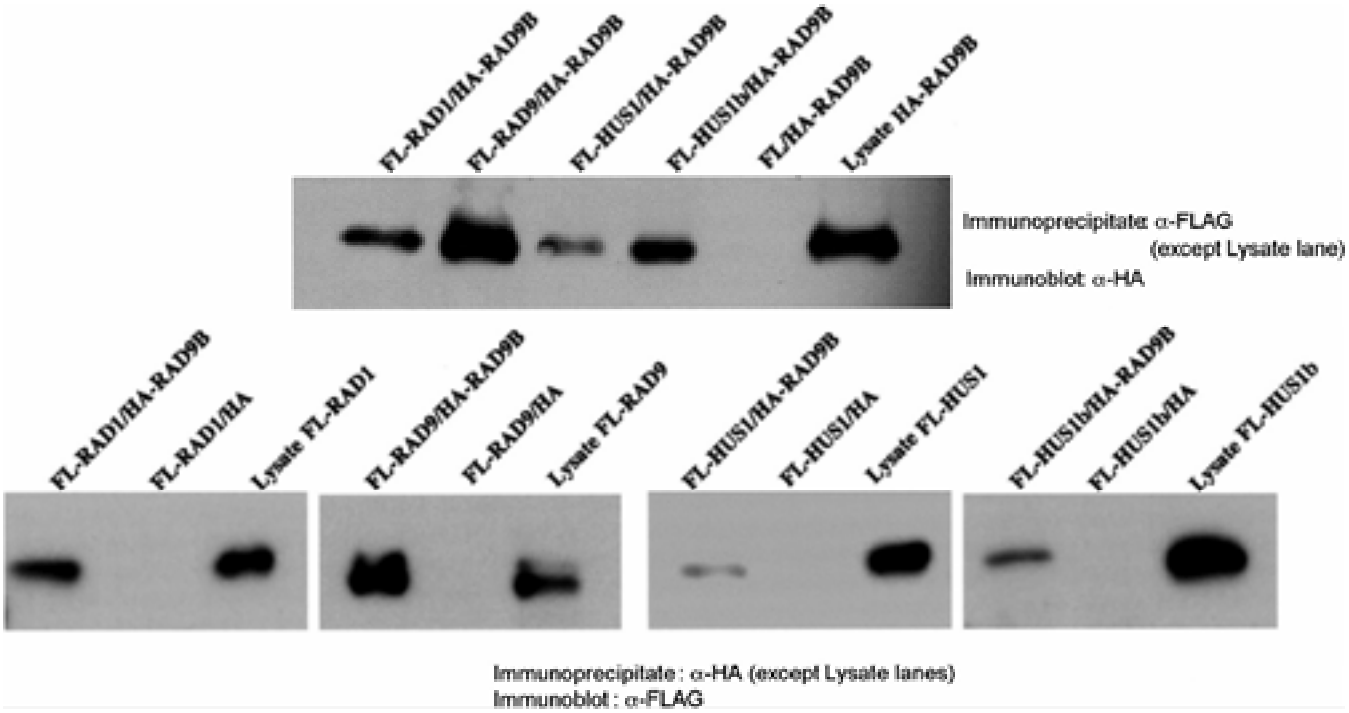

Fig. 2. Western analysis demonstrating that HRAD9B coimmunoprecipitates with the human checkpoint proteins HRAD9, HRAD1, HHUS1, and HHUS1B. *Top* shows HRAD9B on the Western blot; *bottom* shows the other proteins cited.

Although the mechanism of the complex regulating checkpoint is unclear, one hypothesis is that this complex forms a PCNA-like (proliferating cell nuclear antigen-like) heterotrimer clamp, clamp loader HRAD17 complex may load it onto damaged DNA and start cell cycle machinery or facilitate damage repair (2). Coimmunoprecipitate experiments were performed to determine whether HRAD9B shares similar properties (Figure 2). All these proteins were tagged with epitopes, HA or FLAG and overexpressed in 293 cells. When FLAG tagged HRAD9, HRAD1, HUS1, or HHUS1B was immunoprecipitated with anti-FLAG conjugated beads, anti-HA always detected HA-HRAD9B via western blotting. However, when the reverse coimmunoprecipitations were performed, that is anti-HA beads were used for immunoprecipitation, and anti-FLAG was used for protein presence detection, HHUS1B was not always detected. This suggests HRAD9B and HHUS1B may physically interact weakly and quickly or the antibodies don't work well under this particular situation. Whether HRAD9B is also engaged in checkpoint control and other similar biochemical reactions needs further investigation (5).

References

1. Lieberman HB, Hopkins KM, Nass M, Demetrick D and Davey S. A human homologue of the *Schizosaccharomyces pombe rad9+* checkpoint control gene. *Proc Natl Acad Sci USA* **93**:13890-5, 1996.
2. Hopkins KM, Wang X, Berlin A, Hang H, Thaker H and Lieberman HB. Expression of mammalian paralogues of *HRAD9* and *Mrad9* checkpoint control genes in normal and cancerous testicular tissue. *Cancer Research* **63**:5291-8, 2003.
3. Ellison V and Stillman B. Biochemical characterization of DNA damage checkpoint complexes: clamp loader and clamp complexes with specificity for 5' recessed DNA. *PLOS Biology* **1**:231-243, 2003.
4. Hang H, Zhang Y, Dunbrack RL Jr, Wang C and Lieberman HB. Identification and characterization of a paralog of human cell cycle checkpoint gene, HUS1. *Genomics* **79**:487-92, 2002.
5. Dufault VM, Oestreich AJ, Vroman BT and Karnitz LM. Identification and characterization of RAD9B, a paralog of the RAD9 checkpoint gene. *Genomics* **82**:644-51, 2003. ■

The Role of *Mrad9B* in Radioresistance, Cell Cycle Control and Maintaining Genomic Integrity

Corinne Leloup, Aiping Zhu, Kevin Hopkins and Howard B. Lieberman

Human *HRAD9B* and mouse *Mrad9B* were identified in our laboratory as paralogs of the cell cycle checkpoint control genes *HRAD9* and *Mrad9*, respectively (1). But, the molecular and biological functions of these paralogs have not yet been defined in detail. The ability of the *HRAD9B* gene product to coimmunoprecipitate with the checkpoint proteins HRAD1, HRAD9, HHUS1 and HHUS1B suggests that it could also be involved in cell cycle control. Both human and mouse *RAD9B* are expressed predominantly in normal testis. However, the level of *HRAD9B* is dramatically reduced in testicular cancerous tissues. These characteristics indicate that *RAD9B* could play a role in maintaining genomic integrity and mediating this type of cancer. In order to learn more about the function of *Mrad9B*, a construct was made to delete the first two exons of the gene by homologous recombination in mouse embryonic stem cells, thereby inactivating the endogenous gene (Figure 1).

The response of cells with altered *Mrad9B* status to radiation and other genome-damaging agents will be examined in regard to cell cycle regulation and genome stability.

If RAD9B is indeed involved in cell cycle control, knocked-out cells will predictably display an abnormal cell cycle pattern, especially after irradiation, when the cycle is delayed to allow more time for DNA repair. Moreover we will examine whether Mrad9B is involved more directly in DNA repair, for instance by mediating histone H2AX phosphorylation. The role of the gene in neoplastic transformation will also be examined.

References

1. Hopkins KM, Wang X, Berlin A, Hang H, Thaker HM and Lieberman HB. Expression of Mammalian Paralogues of HRAD9 and Mrad9 Checkpoint Control Genes in Normal and Cancerous Testicular Tissue. *Cancer Res* **63**:5291-8, 2003. ■

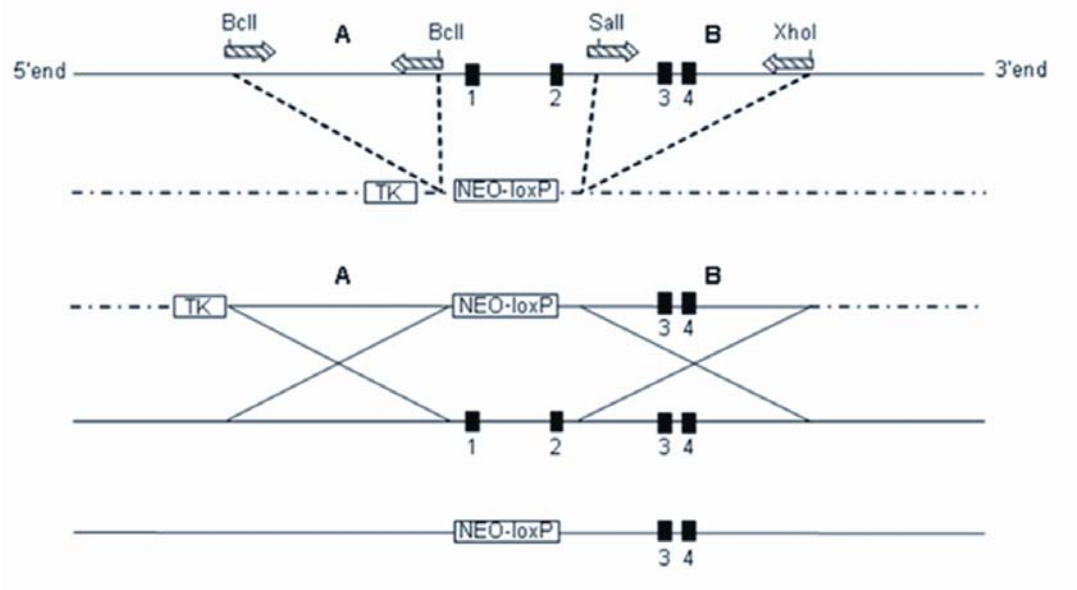

Fig. 1. Targeted disruption of the mouse *Mrad9B* gene: The arrows represent probes for PCR amplification; the black boxes are the first four exons of the *Mrad9B* gene. Vector-derived sequences are shown as stippled lines whereas genomic DNA is shown as full lines. **A** and **B** are the two genomic fragments that were amplified by PCR and inserted into the plasmid. Homologous recombination of the targeting construct is depicted by the large " Xs."

Gene Expression Profiles Following Low Dose-Rate Ionizing Radiation Exposure of Human Cells

Sally A. Amundson, R. Anthony Lee,[1] Christine A. Koch-Paiz,[1] Michael L. Bittner,[2] Paul Meltzer,[2] Jeffrey M. Trent[2] and Albert J. Fornace, Jr.[1]

Environmental radiation exposures tend to be to low doses protracted over time, and today's environment of increasing nuclear power and radiological applications increases occupational exposures and the risk of accidents. In addition, fears of radiological terrorism have also recently come to the fore. The effects of protracted low dose-rate exposures cannot be entirely predicted by extrapolation from acute high-dose exposures, however. Early experiments using fractionation to mimic low dose-rates found increased cellular survival compared with single acute exposures (1). This sparing effect was confirmed in later low dose-rate experiments, and related to the DNA repair capacity of cell lines. While wild-type parental cell lines showed markedly increased survival with dose protraction, repair deficient mutants including mouse lymphoma LY-S (2), *xrs5* and *xrs6* (3), *irs20* (4) and fibroblasts from AT patients (5) showed little or no dose-rate effects for survival. Mutation and cell transformation, endpoints with possible relevance to long-term risk in humans, have also been studied in terms of dose-rate effects. While some studies reported protection against mutation induction both *in vivo* (6) and *in vitro* (7) by dose protraction, other investigations have revealed inverse dose-rate effects for mutagenesis. In this case, decreasing the dose-rate actually increased mutation induction (8, 9), a phenomenon possibly linked to windows of extreme sensitivity within the cell cycle (10, 11). Despite such studies, there is still insufficient data to fully understand the impact such low dose-rate effects may have on human health in terms of carcinogenesis or other endpoints, and risk assessment predictions continue to be based largely on studies of high dose acute exposures.

As low dose-rate irradiation results in complex effects on endpoints of potential relevance to human risk, gene expression profiling in the context of dose-rate may reveal early indicators of differential signal transduction pathway activation. While a limited number of studies have begun to address gene induction by low dose-rate irradiation (12, 13, 14), no coherent picture has yet emerged. Direct studies of low dose exposures in the relatively responsive ML-1 cell line have shown that changes in gene expression are detectable following doses of gamma-rays as low as 2 cGy in human cells (15). The sensitivity of this system made it ideal for the extension of these studies to low dose-rate exposures (16), and indeed, linear induction of *CDKN1A, GADD45A* and *MDM2* was found to occur between 2 and 50 cGy when the rate of exposure was decreased across three orders of magnitude.

In this study, low dose-rate exposure reduced the magnitude of induction of *CDKN1A* and *GADD45A*, while *MDM2* was induced to the same extent regardless of the rate of radiation delivery (Figure 1). Microarray analysis was then performed to compare the behavior of a large number of genes following irradiation at different dose-rates. This identified additional low dose-rate-inducible genes with two general patterns of low dose-rate response (Figure 2). One group of genes was induced in a dose-rate dependent fashion, similar to *GADD45A* and *CDKN1A*. Functional annotation of this gene cluster indicated a preponderance of genes with known roles in apoptosis regulation. A second group of genes responded with dose-rate independent induction, similar to *MDM2*. In this case, functional annotation revealed that the majority of these genes were involved in cell cycle regulation. Two of the genes identified in this dose-rate-independent cluster, *BTG2* and *PHLDA3*, were selected for further study. Dose-response experiments confirmed that both these genes were indeed induced to the same extent independent of the rate of exposure (Figure 3).

Since the functional annotation of the two categories of low dose-rate-induced genes was so striking, we examined the effects of protracting radiation exposure on the cellular endpoints of apoptosis and cell cycle progression. While lowering the rate of exposure resulted in protection against apoptosis induction, there was no effect on either the magnitude or duration of cell cycle delay (Figure 4). These cellular responses mirrored the known functions of the genes found to be responding to low dose-rate irradiation in either a dose-rate dependent or dose-rate independent fashion. This apparent differential regulation of stress signaling pathways and

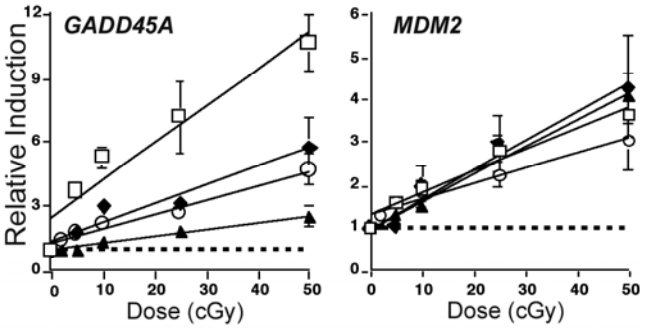

Fig. 1. Gene induction 2 h after γ-irradiation at 290 (□), 29 (◆), 2.4 (○) or 0.28 (▲) cGy/min. Points, mean of at least 4 independent experiments, errors, SEM. The dashed line indicates the level of expression in untreated cells.

[1] *NIH, National Cancer Institute, Division of Basic Science, Bethesda, MD.*
[2] *NIH, National Human Genome Research Institute, Bethesda, MD.*

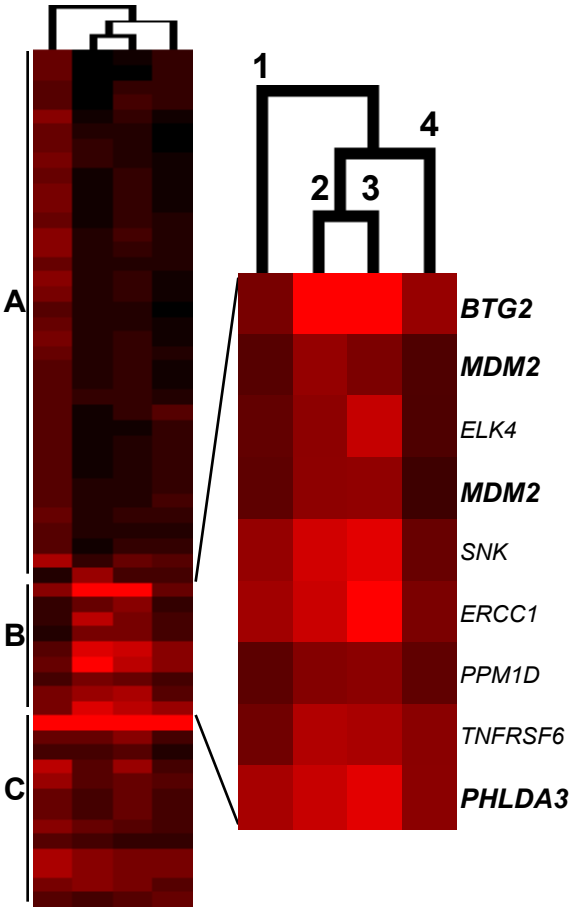

Fig. 2. Clustering of genes induced two hours after 50 cGy γ-rays: (1) 290 cGy/min, (2) 29 cGy/min, (3) 2.4 cGy/min or (4) 0.28 cGy/min. Brighter red indicates larger relative induction. The Dendrogram shows the similarity between the treatment conditions as determined by hierarchical clustering. A) genes responding only to acute exposure; B) cluster of genes exhibiting dose-rate independent regulation; C) genes with marked dose-rate dependent regulation. Genes studied in detail are listed in bold face type.

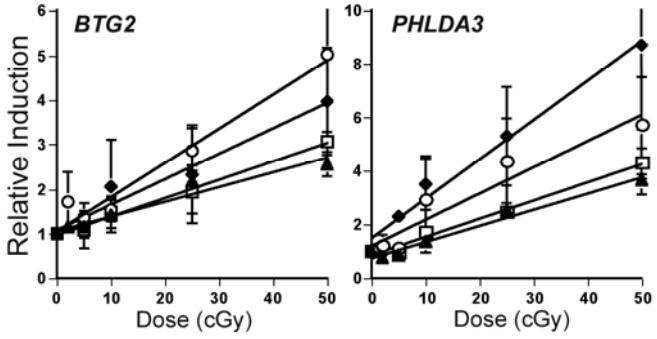

Fig. 3. Gene induction 2 h after γ-irradiation at 290 (□), 29 (◆), 2.4 (○) or 0.28 (▲) cGy/min. Points, mean of at least 4 independent experiments, errors, SEM. The dashed line indicates the level of expression in untreated cells.

specific cellular responses as a result of protracted radiation exposure suggests qualitatively different mechanisms of response to low and high dose-rate irradiation that could not have been predicted from classical high dose studies.

While these findings suggest that low dose-rate irradiation could be an informative tool for the study of the intertwined signaling events responding to radiation exposure, the differential cellular responses to low dose-rate irradiation may also have serious implications for the carcinogenic risk of such exposures. If cells damaged by protracted irradiation escape apoptosis while undergoing normal cell cycle arrest, critically damaged cells that would be eliminated following an acute exposure may be more prone to misrepair and continue proliferating. Such a situation could increase the early DNA damage and mutational events escaping surveillance, and enhance tumor promotion through increasing the survival of cells with accumulating damage or mutations in an environment of continued low dose-rate radiation exposure.

References

1. Elkind MM and Sutton H. X-ray damage and recovery in mammalian cells in culture. *Nature* **184**:1293-5, 1959.
2. Evans HH, Horng MF, Mencl J, Glazier KG, Beer JZ. The influence of dose rate on the lethal and mutagenic effects of X-rays in proliferating L5178Y cells differing in radiation sensitivity. *Int J Radiat Biol Relat Stud Phys Chem Med* **47**:553-62, 1985.
3. Nagasawa H, Chen DJ and Strniste GF. Response of x-ray-sensitive CHO mutant cells to gamma radiation. I. Effects of low dose rates and the process of repair of potentially lethal damage in G1 phase. *Radiat Res* **118**:559-67, 1989.
4. Stackhouse MA and Bedford JS. An ionizing radiation-sensitive mutant of CHO cells: irs-20. II. Dose-rate ef-

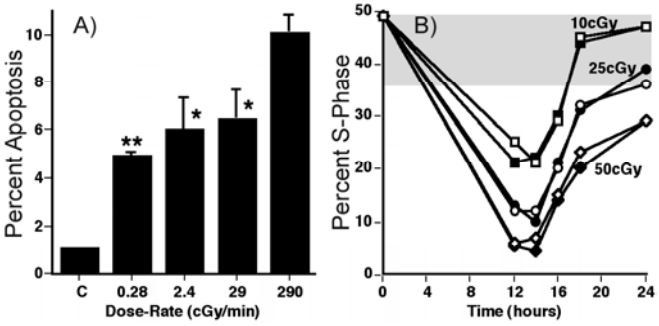

Fig. 4. A) Apoptosis scored by DAPI staining 48 hours after 0.5 Gy γ-rays delivered at different dose-rates. "C" indicates the level of apoptosis in untreated controls. Bars are the mean of 3 experiments +/- SEM. Apoptosis induced by low dose-rate irradiation was significantly different from that induced by acute exposure (* $p<0.05$; ** $p<0.001$). B) Cell cycle progression after low dose-rate irradiation plotted as the percentage of cells in S-phase following acute (2.9 Gy/min: filled symbols) or low dose-rate (0.0028 Gy/min: open symbols). The shaded area indicates the range of S-phase in untreated cells through the experiment.

fects and cellular recovery processes. *Radiat Res*, **136**:250-4, 1993.
5. Nagasawa H, Little JB, Tsang NM, Saunders E, Tesmer J and Strniste GF. Effect of dose rate on the survival of irradiated human skin fibroblasts. *Radiat Res*, **132**:375-9, 1992.
6. Lorenz R, Deubel W, Leuner K, Gollner T, Hochhauser E and Hempel K. Dose and dose-rate dependence of the frequency of HPRT deficient T lymphocytes in the spleen of the 137Cs gamma-irradiated mouse. *Int J Radiat Biol* **66**:319-26, 1994.
7. Evans HH, Nielsen M, Mencl J, Horng MF and Ricanati M. The effect of dose rate on x-radiation-induced mutant frequency and the nature of DNA lesions in mouse lymphoma L5178Y cells. *Radiat Res* **122**:316-25, 1990.
8. Furuno-Fukushi I, Ueno AM and Matsudaira H. Mutation induction by very low dose rate gamma rays in cultured mouse leukemia cells L5178Y. *Radiat Res* **115**:273-80, 1988.
9. Amundson SA and Chen DJ. Inverse dose-rate effect for mutation induction by gamma-rays in human lymphoblasts. *Int J Radiat Biol* **69**:555-63, 1996.
10. Rossi HH and Kellerer AM. The dose rate dependence of oncogenic transformation by neutrons may be due to variation of response during the cell cycle. *Int J Radiat Biol Relat Stud Phys Chem Med* **50**:353-61, 1986.
11. Brenner DJ, Hahnfeldt P, Amundson SA and Sachs RK. Interpretation of inverse dose-rate effects for mutagenesis by sparsely ionizing radiation. *Int J Radiat Biol* **70**:447-58, 1996.
12. de Toledo SM, Azzam EI, Gasmann MK and Mitchel RE. Use of semiquantitative reverse transcription-polymerase chain reaction to study gene expression in normal human skin fibroblasts following low dose-rate irradiation. *Int J Radiat Biol* **67**:135-43, 1995.
13. Ross HJ, Canada AL, Antoniono RJ and Redpath JL. High and low dose rate irradiation have opposing effects on cytokine gene expression in human glioblastoma cell lines. *Eur J Cancer* **33**:144-52, 1997.
14. Melkonyan HS, Ushakova TE and Umansky SR. Hsp70 gene expression in mouse lung cells upon chronic gamma-irradiation. *Int J Radiat Biol*, **68**:277-80, 1995.
15. Amundson SA, Do KT, Fornace AJ Jr. Induction of Stress Genes by Low Doses of Gamma Rays. *Radiat Res* **152**:225-31, 1999.
16. Amundson SA, Lee RA, Koch-Paiz CA, Bittner ML, Meltzer P, Trent JM and Fornace AJ Jr. Differential responses of stress genes to low dose-rate gamma irradiation. *Mol Cancer Res*. **1**:445-2, 2003. ■

Gene Expression Responses to Neutron Irradiation

Sally A. Amundson

While cellular context is one critical factor in determining the signaling responses triggered by ionizing radiation (1), the profiling of gene expression responses to diverse stress stimuli can also provide important information and insights. The molecular responses to diverse genotoxic insults were early on assumed to be broadly similar, and to result from activation of a general cellular stress or damage signal. However, exposure to genotoxic agents is now known to trigger numerous complex and overlapping signaling networks, many of which are mediated through alterations in gene expression. Studies utilizing functional genomics approaches are now revealing distinct gene expression signatures that are characteristic of exposure to different classes of stress agents (2, 3).

In gene expression studies of over 65 human cell lines and primary cells, we have consistently found the highest degree of ionizing radiation-responsiveness in cells of lymphoid or myeloid lineage. A pilot study comparing gene induction in the human myeloid ML-1 cell line by low doses of γ-rays and 0.43 MeV neutrons produced at the RARAF facility revealed differences in the magnitude of induction of previously characterized radiation-response genes (Figure 1). Preliminary microarray experiments also suggested there

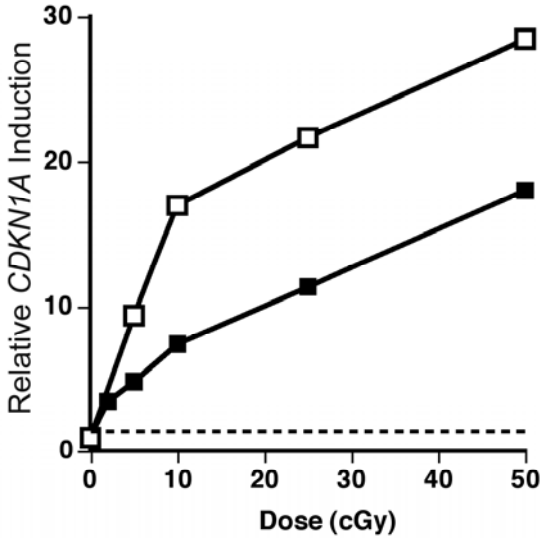

Fig. 1. Relative induction of *CDKN1A* in ML-1 at 2 hours after exposure to γ-rays (■) or 0.43 MeV neutrons (□). The dashed line represents the basal level of expression in mock-irradiated controls.

may be qualitative differences in the genes induced, but further confirmation will be needed. Neutrons of 0.43 MeV were chosen for this study as this energy has been reported to have the highest RBE for a number of endpoints. Since the biological effects of this energy appear most different from those of low LET, it seemed reasonable that if distinct damage signaling pathways are triggered by high LET, their resultant gene expression patterns might be most discernable in such a comparison.

The human B-lymphoblastoid TK6 cell line also shows a robust gene-expression response to low LET radiation, while

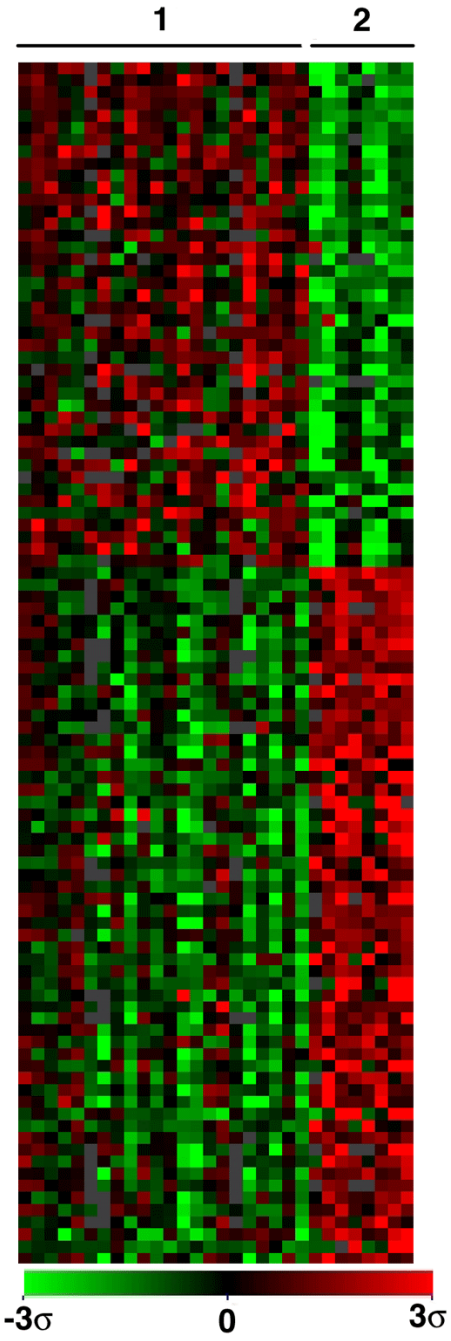

Fig. 2. Hierarchical clustering of genes differentially expressed following DNA-damaging treatments (1, see text for specific agents) and non-genotoxic agents (2, see text). Red indicates over-expression of a gene, green under-expression, compared to the mean response according to the scale below the figure. Grey boxes indicate poorly hybridizing genes with a quality score < 0.5.

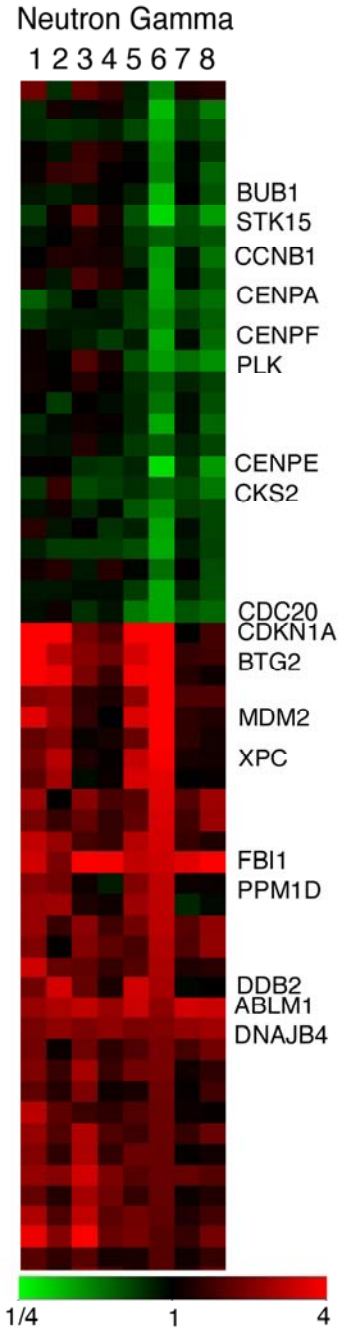

Fig. 3. K-means clustering of genes with differential expression following gamma and neutron irradiation. Each column represents a different experiment with either 0.5Gy 0.43 MeV neutrons (RARAF): 1: TK6 4h, 2: TK6 24h, 3: NH32 4h, 4: NH32 24h, or with 2.5 Gy γ-rays: 5: TK6 4h, 6: TK6 24h, 7: NH32 4h, 8: NH32 24h. The intensity of red or green represents an individual gene's induction or repression respectively as indicated in the scale below the figure. Variation with type of radiation, p53 status and time can all be discerned. For interest, a sampling of genes with different patterns of regulation has been annotated with names.

NH32, a targeted p53 knock-out cell line derived from TK6 (4), adds additional power to this model system by enabling studies targeted at this key signaling pathway and modulator of carcinogenesis. In a much broader study, TK6 and NH32 cells have been exposed to similarly lethal levels of 12 different agents. The gene expression profiles revealed by microarray hybridization contain both broad similarities and specific patterns of early gene expression changes four hours after exposure. For instance, a set of genes was identified that broadly discriminated between agents primarily causing DNA damage (0.43 MeV neutron, γ-ray, UVB, methyl methanesulfonate (MMS), adriamycin, camptothecin, cisplatin, arsenite and hydrogen peroxide) and non-genotoxic agents (heat shock, osmotic shock and Tetradecanoylphorbol 13-acetate (TPA) exposure). Hierarchical clustering of this DNA-damage discriminating gene set is illustrated in Figure 2. Different sets of genes were also identified that could discriminate between specific agents within either the genotoxic or non-genotoxic groups of treatments, with very strong signatures being identified for both TPA and arsenite treatments. Furthermore, the inclusion of NH32 in these studies allowed detection of strong p53-dependent gene expression response signatures that varied among agents, and were almost completely absent among non-DNA-damaging stresses.

While the response to γ-rays and neutrons showed broad similarity to other DNA-damaging agents, a small group of genes appeared to distinguish ionizing radiation from other types of DNA damaging agents. A number of genes also appeared to show differential expression following low LET γ-ray and high LET neutron exposure (Figure 3). Although there are too few experiments in this study to truly define a signature of high LET, and further confirmatory studies will be needed, the results are encouraging, and support the hypothesis that unique patterns of gene expression may occur in response to high LET exposure, as well as in response to more diverse agents.

References

1. Amundson SA, Bittner M, Chen YD, Trent J, Meltzer P and Fornace AJ Jr. cDNA microarray hybridization reveals complexity and heterogeneity of cellular genotoxic stress responses. *Oncogene* **18**:3666-72, 1999.
2. Jelinsky SA, Estep P, Church GM and Samson LD. Regulatory networks revealed by transcriptional profiling of damaged Saccharomyces cerevisiae cells: Rpn4 links base excision repair with proteasomes. *Mol Cell Biol* **20**:8157-67, 2000.
3. Hamadeh HK, Bushel PR, Jayadev S, DiSorbo O, Bennett L, Li L, Tennant R, Stoll R, Barrett JC, Paules RS, Blanchard K and Afshari CA. Prediction of compound signature using high density gene expression profiling. *Toxicol Sci* **67**:232-40, 2002.
4. Chuang YY, Chen Q, Brown JP, Sedivy JM and Liber HL. Radiation-induced mutations at the autosomal thymidine kinase locus are not elevated in p53-null cells. *Cancer Res* **59**:3073-6, 1999. ■

Hypofractionation for Prostate Cancer Radiotherapy – What Are the Issues?

David J. Brenner

You can't open a radiation journal these days without someone debating the α/β ratio for prostate cancer (1-21). Why the debate? What are the issues? What might they mean for prostate cancer radiotherapy? In brief, the arguments have gone as follows:

1. One of the main motivations for delivering a treatment in many fractions is that late sequelae are generally more sensitive than early effects (such as tumor control) to changes in fractionation. So increasing the number of fractions generally spares late-responding tissues more than the tumor. This can be quantified in terms of the α/β ratio:
   - A small α/β ratio (1-4 Gy), typical of late sequelae, means large sensitivity to changes in fractionation.
   - A large α/β ratio (>8 Gy), typical of tumor control, means low sensitivity to changes in fractionation.
2. It is generally assumed that the mechanistic basis for the different fractionation response of tumors and late-responding normal tissues relates to the larger proportion of cycling cells in tumors. But prostate tumors contain unusually small fractions of cycling cells (22). So, back in 1999, Brenner and Hall (1) and Duchesne and Peters (2) reasoned that prostate tumors might not respond to changes in fractionation in the same way as other cancers; both papers hypothesized that prostate tumors might respond to changes in fractionation more like a late-responding normal tissue. In mathematical terms, the suggestion was that the α/β ratio for prostate cancer might be low, comparable to that for late sequelae. If so, much of the rationale for using many fractions, or using low dose rate, would disappear for prostate radiotherapy.
3. A first estimate of α/β for prostate cancer was made in 1999 (1), by comparing results from external beam RT (EBRT) with those from brachytherapy (BT). Consistent with the theoretical hypotheses (see above), the estimated value of α/β was 1.5 Gy [95% C.I.: 0.8–2.2 Gy], comparable to α/β values for late-responding normal tissues, and much smaller than those for most tumors.
4. The problem with this estimate (1) of the α/β value for prostate, and almost all subsequent ones (3-11, 13-19) is that they involve comparing or equating EBRT results with BT results. There are many pertinent differences between EBRT and BT (different dose distributions, different RBE's, different overall times, different institutions, different PSA distributions, hypoxia), any or all of which could bias the α/β estimate. Much of the debate has centered around the significance of these biases, and how to take them into account. Despite these problems, there does seem to be consensus among most of the analyses which have taken this approach that the α/β value for prostate cancer is indeed quite low, probably in the 1 to 4 Gy range (1-2, 4-11, 13-16, 18-19), which is similar to the values for most late-responding tissues.
5. One analysis has also been performed (12) which avoided many, though not all, of the potential biases involved in comparing EBRT and BT. Here, EBRT + a 2-fraction HDR BT boost was compared with EBRT + a 3-fraction HDR boost, all done with the same technique at the same institution. The resulting estimated α/β ratio for prostate cancer was 1.2 Gy [95% C.I.: 0.03–4.1 Gy], again comparable with α/β values for late-responding normal tissues.
6. If the α/β value for prostate cancer is indeed similar to that for the surrounding late-responding normal tissue, one could use fewer fractions (i.e., hypofractionate), or HDR, and yet, by choosing the right dose, produce:
   - comparable tumor control and late sequelae to conventional fractionation / protraction
   - reduced early urinary sequelae (5)
   - patient convenience
   - financial / resource advantages
   - potential for biologically-based individualized treatments.
7. The arguments presented above really relate to the α/β value for prostate cancer *in relation to the* α/β *value for the relevant late-responding normal tissue*. Just what is the appropriate α/β value for late rectal complications? Extensive evidence from animal studies (23-29) suggests that for late rectal sequelae $\alpha/\beta > 4$ Gy – i.e., higher than for most other late sequelae. While one must always be cautious of extrapolations from rodents to man, this higher value for late rectal damage is supported by clinical results which suggest that much late rectal injury is actually consequential of early effects (30-32), and thus a high α/β value for late rectal damage is not unreasonable.
8. The potentially high value of α/β for late rectal complications (together with the low value of α/β for prostate cancer) has two consequences:
   - It becomes less likely that the α/β value for prostate cancer is greater than that for late rectal complications – the situation where hypofractionation or HDR would be sub-optimal.
   - It becomes more likely that the α/β value for prostate cancer is actually less than that for late rectal complications – the situation where hypofractionation or HDR would be optimal.
9. If, then, the α/β value for prostate cancer is actually less than that for the surrounding late-responding normal tissue, now hypofractionation or HDR, at the appropriate dose, would also yield:
   - increased tumor control for a given level of late complications, or

Fig. 1. Sir Laurence Olivier was treated in London in 1967 for prostate cancer with a hypofractionated 6×6 Gy protocol, reported no major sequelae, and lived a further 22 years.

- decreased late complications for a given level of tumor control.

The implication of these considerations is that either hypofractionated EBRT or HDR BT, at the appropriate dose, has the potential to yield improved clinical results for prostate cancer, compared with conventional fractionation or LDR.

Hypofractionation in a curative setting, even when the dose is appropriately lowered, is a *prima-facie* unsettling idea, particularly as the literature has many examples of large dose per fraction resulting in unacceptable late effects (33-36). None of these reports are for prostate cancer, however. To the contrary, there is a report of 22 years experience (1962-84) with 232 prostate cancer patients treated in London with a 6×6 Gy protocol (37): even with the much poorer dose distributions than are now routine, minimal long-term urologic or bowel morbidity was reported.

As an aside, Sir Laurence Olivier (Figure 1) was treated in London in 1967 for prostate cancer with a hypofractionated 6×6 Gy protocol, reported no major sequelae, and lived a further 22 years (38).

There is also extensive experience from the Christie Hospital, Manchester, of treating prostate cancer with a 15×3.1 Gy protocol, both before and since the era of conformal therapy, again with satisfactory results and without excess late sequelae (7). A five-year outcome analysis of freedom from disease (bNED) in 700 patients treated this way (15×3.1 Gy) between 1995 and 1998 (21) yields results consistent with an α/β value in the range from 0.5 to 3 Gy, but inconsistent with a 'conventional' α/β value of 8 to 10 Gy.

For prostate cancer (and these considerations are unique to prostate cancer*), hypofractionation or HDR deserve serious consideration. The London and Manchester experiences, together with the analyses summarized here, suggest that conservatively designed clinical trials (20), with a minimum of about 10 fractions, would be low-potential-risk/high-potential-gain studies.

---

* *These considerations may possibly also apply to melanoma (39).*

References

1. Brenner DJ and Hall EJ. *Int J Radiat Oncol Biol Phys* **43**:1095, 1999.
2. Duchesne GM and Peters LJ. *Int J Radiat Oncol Biol Phys* **44**:747, 1999.
3. King CR and Mayo CS. *Int J Radiat Oncol Biol Phys* **47**:536, 2000.
4. Brenner DJ and Hall EJ. *Int J Radiat Oncol Biol Phys* **47**:538, 2000.
5. Brenner DJ. *Int J Radiat Oncol Biol Phys* **48**:315, 2000.
6. Fowler JF, Chappell RJ and Ritter MA. *Int J Radiat Oncol Biol Phys* **50**:1021, 2001.
7. Logue JP, Cowan RA, Hendry JH. *Int J Radiat Oncol Biol Phys* **49**:1522, 2001.
8. King CR and Fowler JF. *Int J Radiat Oncol Biol Phys* **51**:213, 2001.
9. D'Souza WD and Thames HD., *Int J Radiat Oncol Biol Phys* **51**:1, 2001.
10. King CR and Fowler JF. *Int J Radiat Oncol Biol Phys* **54**:626, 2002.
11. Dale RG and Jones B. *Int J Radiat Oncol Biol Phys* **52**:1427, 2002.
12. Brenner DJ, *et al*. *Int J Radiat Oncol Biol Phys* **52**:6, 2002.
13. Lee WR. *Int J Radiat Oncol Biol Phys* **53**:1392; author reply 1393, 2002.
14. Wang JZ, Guerrero M and Li XA. *Int J Radiat Oncol Biol Phys* **55**:94, 2003.
15. Amer AM, *et al*. *Int J Radiat Oncol Biol Phys* **56**:199, 2003.
16. Lindsay PE, Moiseenko VV, Van Dyk J and Battista JJ. *Phys Med Biol* **48**:507, 2003.
17. Nahum AE, Movsas B, Horwitz EM, Stobbe CC and Chapman JD. *Int J Radiat Oncol Biol Phys*, 2003.
18. Kal HB and Van Gellekom MPR. *Int J Radiat Oncol Biol Phys*, 2003.
19. Wang JZ, Li XA, Yu CX and DiBiase SJ. *Int J Radiat Oncol Biol Phys* **57**:1101, 2003.
20. Fowler JF, Ritter MA, Chappell RJ and Brenner DJ. *Int J Radiat Oncol Biol Phys* **56**:1093, 2003.
21. Livsey JE, *et al*. *Int J Radiat Oncol Biol Phys* **57**:1254, 2003.
22. Haustermans KM, *et al*. *Int J Radiat Oncol Biol Phys* **37**:1067, 1997.
23. Terry NH and Denekamp J. *Br J Radiol* **57**:617, 1984.
24. van der Kogel AJ, Jarrett KA, Paciotti MA and Raju MR. *Radiother Oncol* **12**:225, 1988.
25. Dewit L, Oussoren Y, Bartelink H and Thames HD.

Radiother Oncol **16**:121, 1989.
26. Gasinska A, *et al. Radiother Oncol* **26**, 244, 1993.
27. Dubray BM and Thames HD. *Radiother Oncol* **33**:41, 1994.
28. Brenner D, Armour E, Corry P and Hall EJ. *Int J Radiat Oncol Biol Phys* **41**:135, 1998.
29. van den Aardweg GJ, Olofsen-van Acht MJ, van Hooije CM and Levendag PC. *Radiat Res* **159**:642, 2003.
30. Wang CJ, *et al. Int J Radiat Oncol Biol Phys* **40**:85, 1998.
31. Dorr W and Hendry JH. *Radiother Oncol* **61**:223, 2001.
32. Jereczek-Fossa A, Jassem J and Badzio A. *Int J Radiat Oncol Biol Phys* **52**:476, 2002.
33. Bates TD and Peters LJ. *Br J Radiol* **48**:773, 1975.
34. Peters LJ and Withers HR. *Br J Radiol* **53**:170, 1980.
35. Hatlevoll R, Host H and Kaalhus O. *Int J Radiat Oncol Biol Phys* **9**:41, 1983.
36. Cox JD. *Cancer* **55**:2105, 1985.
37. Collins CD, Lloyd-Davies RW and Swan AV. *Clin Oncol (R Coll Radiol)* **3**:127, 1991.
38. Cottrell J. *Laurence Olivier* (Prentice-Hall, Englewood Cliffs, NJ, 1975.
39. Bentzen SM, *et al. Radiother Oncol* **16**:169, 1989. ■

Mortality Patterns in British and US Radiologists – What Can We Really Conclude?

David J. Brenner and Eric J. Hall

There have been several studies of age-specific and cause-specific mortality among radiologists, with the goal of quantifying the effects of their radiation exposure. The most recent report, published by Doll and colleagues (1), assessed 100 years of observations in terms of mortality from cancer and from other causes. Relative to all male physicians, male British radiologists who entered the field between 1897 and 1979 showed a small but significant increase overall in cancer mortality (standardized mortality ratio, SMR=1.16) and a small but significant decrease in non-cancer mortality (SMR=0.86). The increased cancer risk is not surprising in that estimated annual doses to the early radiologists were typically in the range of 1 Gy/yr (2).

When the British radiologists are stratified by time-of-entry into the profession, the most recent cohort (1955-70) showed a decrease in cancer mortality compared to the physicians control group (32 observed, 45 expected, SMR=0.71), though this difference in cancer mortality was not statistically significant (1). In addition, there was a significant decrease in non-cancer mortality (SMR=0.64) in the British radiologists, compared to all physicians. These decreases in risk relative to all physicians have attracted much interest (3-5), leading to speculation that low doses of radiation could increase longevity.

The corresponding, but much larger, study of male US radiologists (6, 7) has, surprisingly, received much less attention. Some comparisons between the two studies, both of which are retrospective cohort studies, are given in Table I (in which we only consider radiologists who entered the profession after 1920, when at least minimal radiation protection practices were in place). There are advantages and disadvantages to both studies: the British study has a longer follow up and included radiologists who entered the field more recently; the US study has the advantage of considerably larger numbers and a more direct analysis of the "all physicians" control groups (in the British studies the control mortality rates for "all male medical practitioners" were estimated indirectly from census data).

Some comparison of results between the two studies are shown in Table 1. If we look at both cohorts of radiologists who entered the field after 1920, the US study shows good evidence of significantly increased standardized mortality

Table I.

	British radiologists study [1][a]	US radiologists study [6,7]
Number of radiologists	2,629	6,510
Control physicians	Rates estimated from census data	23,215
Profession entry years	1920 - 1979	1920 -1969
Last year of follow up	1996	1974
No. of radiologists deceased	837 (35%)	1,871 (29%)
SMR for all cancer mortality[b]	1.04 (n.s.)	1.31 (s.s)
SMR for non-cancer mortality[b]	0.86 (s.s.)	1.18 (s.s.)
SMR for all cancer mortality[b] for most recent entry cohort	0.71 (n.s.) (profession entry 1955-1979)	1.15 (n.s.) (profession entry 1940-69)

n.s., not statistically significant ($p>0.05$).
s.s., statistically significant ($p<0.05$).
[a] Restricted to radiologists who entered the profession after 1920.
[b] SMRs relative to all physicians; this is the most appropriate comparison group as death rates in 25-74 year old British physicians are about half those of the general public [8]).

ratios, relative to all physicians, both for cancer and non cancer mortality. The British study shows no evidence for a different SMR between the radiologists and all physicians for cancer mortality, and a significant decrease in SMR for non-cancer mortality.

If we stratify each study just by its most recent cohort (1955-79 in the British study, 1940-69 in the US study), neither show a significant SMR for cancer mortality compared to all physicians, though, again, the SMRs are lower for the radiologists in the British study.

How are we to interpret these somewhat smaller radiation risks estimated from the British, compared with the US, radiologists? The British study included radiologists who entered the field up to 1970, compared with 1960 in the US study; clearly radiation risks do decrease for radiologists who entered later (1), due to lower doses and shorter follow up. On the other hand, if we directly compare risks in British and US radiologists who entered the field during the same time period, the SMRs are still somewhat lower in the British study than the US study; for example, among radiologists entering the field in the 1920s and 1930s, the cancer SMRs were 1.24 for the British cohort and 1.38 for the US cohort. Year for year, however, the doses to the two cohorts were probably quite similar: estimated mean annual doses to British radiologists decreased from 5 mGy in 1964 (9) to 0.5 mGy in 1984 (10), compared with estimated mean annual doses to US radiologists from 1972 to 1978 respectively of 1.2, 0.7, 1.1, 3.6, 3.2, 1.3 and 1.7 mGy (11).

Although it is beyond the scope of this communication to undertake a formal meta-analysis, an appraisal of the SMR data in Table I would suggest that, if the US and British studies were appropriately combined:

a) the SMR for all radiologists entering the field after 1920 compared to all physicians would probably be significantly greater than unity for cancer, but would be close to unity for non-cancer mortality;
b) for the more recent lower-dose cohorts, the estimated SMR for cancer mortality, compared to all physicians, would not be significantly different from unity.

Support for this last point comes from a more detailed analysis of causes of death in a cohort of 20,000 British consultants employed in the National Health Service between 1962 and 1979 (8), i.e., when mean annual occupational doses to radiologists and radiotherapists would have been at most a few mGy (9, 10). For the 1,600 radiologists and radiotherapists in this cohort, their risk of dying from any cause (from 1962 to 1992) was 1.03 [95% C.I.: 0.92-1.15] compared to all consultants; the corresponding relative risk for cancer mortality in the radiologists and radiotherapists was 0.99 [95% C.I.: 0.80-1.23].

In short, in the early "pre-shielding" era, radiation risks to radiologists were large and easily demonstrable. In the current era, where annual doses are more than a thousand-fold lower, the radiation effects may be below the limit of detectability for a retrospective cohort study, and arguably for any current epidemiological method. Thus it is entirely to be expected that some studies will produce null results, some will produce slightly positive results, and others will produce slightly negative results – which is the case for the studies discussed here (1, 6-8).

Estimating the risks to a human population from low doses of radiation is difficult. Usefully estimating risks to a population receiving annual occupational doses of less than 1 mGy is extraordinarily difficult, because the SMRs are close to unity. The fact that a low-dose epidemiological study yields results indistinguishable from the controls provides no evidence one way or the other as to whether there are, in fact, health consequences – though it does rule out large risks or large benefits.

References

1. Berrington A, Darby SC, Weiss HA and Doll R. 100 years of observation on British radiologists: mortality from cancer and other causes 1897-1997. *Br J Radiol* **74**:507-19, 2001.
2. Braestrup CB. Past and present radiation exposure to radiologists from the point of view of life expectancy. *Am J Roentgenol*, *Rad Ther Nucl Med* 78:988-92, 1957.
3. Cameron LS. Radiation increases the longevity of British radiologists. *Brit J Radiol* **75**:637-9, 2002.
4. Sherwood T. 100 years' observation of risks from radiation for British (male) radiologists. Lancet 358:604, 2001.
5. Daunt S. Decreased cancer mortality of British radiologists. *Brit J Radiol* **75**:639-40, 2002.
6. Matanoski GM, Sternberg A and Elliott EA. Does radiation exposure produce a protective effect among radiologists? *Health Phys* **52**:637-43, 1987.
7. Matanoski GM. Risk of cancer associated with occupational exposure in radiologists and other radiation workers. In: *Cancer – achievements, challenges and prospects for the 1980s* [Burchenal JH, Oettgen HF, eds] New York: Grune and Stratton 241-54, 1981.
8. Carpenter LM, Swerdlow AJ and Fear NT. Mortality of doctors in different specialties: findings from a cohort of 20000 NHS hospital consultants. *Occup Environ Med* **54**:388-95, 1997.
9. Webb GAM. Radiation exposure to the public – current levels in the United Kingdom, London: *HMSO*, 1974.
10. Hughes JS and Roberts CC. The radiation exposure to the U.K. population – 1984 review. *NRPB Report* R173. Chilton: National Radiological Protection Board, 1984.
11. *United Nations Scientific Committee on the Effects of Atomic Radiation (UNSCEAR).* Ionizing Radiation: Sources and Biological Effects. 1982 Report. New York, NY: United Nations, 1982. ■

Estimated Radiation Risks Potentially Associated with Full-Body CT Screening

David J. Brenner and Carl D. Elliston

There is increasing interest, particularly from independent radiology clinics, in the use of full-body CT screening of healthy adults. The technique is intended to be an early detection device for a variety of diseases including lung cancer, coronary artery disease, and colon cancer. At present the evidence for the utility of this technique is anecdotal, and there is considerable controversy regarding its efficacy: to date, no studies have yet been reported indicating a life-prolonging benefit.

While the potential benefits and risk have been debated in terms of disease detection *vs.* false positives, less attention has been paid to the potential radiation risks associated with full-body CT scanning. The radiation issue is pertinent because CT scans by their nature result in much larger organ doses compared with conventional single-film x rays.

Typical doses from a single full body scan are about 9 mGy to the lung, 8 mGy to the digestive organs, and 6 mGy to the bone marrow. The effective dose, which is a weighted average of doses to all organs, is about 7 mSv. If, for example, 10 such scans were undertaken in a lifetime, the effective dose would be about 70 mSv, i.e., 10 times larger.

To put these doses in perspective, in the most recent report on cancer incidence in the A-bomb survivors, individuals in the dose category from 5 to 100 mSv (mean 29 mSv) show a statistically-significant increase in solid cancer risk, with similar results more recently being reported for cancer mortality. The lowest dose category in the exposed A-bomb survivor population (5-50 mSv, mean 20 mSv) is also associated with an increased cancer mortality risk, though of marginal statistical significance (p=0.15).

Table I.
Estimated organ doses for typical full-body scan (from C-3 vertebra through the symphysis pubis) with Siemens Volume Zoom scanner operated at 120 kV and 130 mAs, with a pitch of 1.75.

Organ	Organ Dose (mGy)
Thyroid	15.2
Bone Surface	9.8
Esophagus	9.3
Lung	8.9
Stomach	8.2
Liver	8.0
Bladder	7.9
Breast (female)	7.0
Gonads (female)	7.0
Colon	6.6
Red bone marrow	5.9
Skin	4.5
Gonads (male)	1.5

Based on low-dose risk estimates ultimately derived from A-bomb data, we provide here risk estimates for both single and annual full-body CT scans. The low-dose risk estimates are based on a linear fit to the dose-response data in the A-bomb survivors. It is important to note that the doses of relevance here (~7-200 mGy) correspond to a region where data on increased radiation risks are directly available from the A-bomb survivors. Of course the risk estimates for multiple (e.g., annual) full-body scans, where the dose is correspondingly higher, will be considerably more robust.

The estimated organ doses for a typical full-body scan technique, using a Siemens Volume Zoom scanner, are given in Table I. Relevant organ doses are in the range from 6 to 9 mGy, and average to an effective dose (i.e., a weighted average over all relevant organs) of about 7 mSv. To put this in perspective, a typical screening mammogram produces about 2.6 mGy to the breast, with a corresponding effective dose of about 0.13 mSv – a factor of around 50 times less. Another comparison would be with the annual natural background exposure, where a typical effective dose is around 3 mSv.

These estimated organ doses were then used to calculate mortality risks. Figure 1 shows the estimated lifetime cancer mortality attributable to a single full-body CT examination at a given age. From Figure 1 it is clear that radiation-induced lung cancer is the dominant cause of cancer mortality in this context. The estimated lifetime cancer mortality

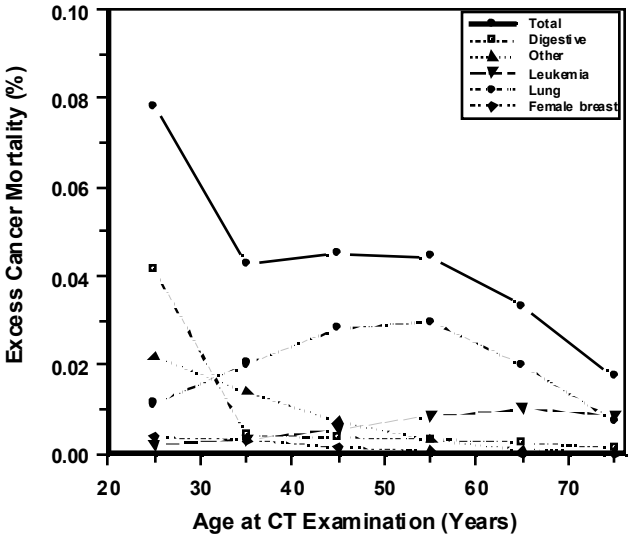

Fig. 1. Excess cancer mortality risks estimated here to be associated with the radiation from a single full-body CT scan undertaken at a given age. Estimated 95% credibility limits are approximately a factor of 3.2 in either direction.

risks from a single full-body scan are about 4.5 x 10^{-4} (about 1 in 2,200) for a 45-year-old, and about 3.3 x 10^{-4} (about 1 in 3,000) for a 65 year old. To put these values in perspective, the odds of an individual dying in a traffic accident in the U.S. during the single year 1999 were about 1 in 5,900. Of course there is uncertainty in the radiation risk estimate: we estimate that the 95% credibility limits for the radiation risk estimate are about a factor of 3.2 in either direction – thus the lifetime risk from a full body scan to a 45 year old could be as low as 1.4 x 10^{-4} or as high as 1.4 x 10^{-3}.

Figure 2 shows the corresponding risks for annual full-body CT scans, from a given age up to (but not including) age 75. For example, a 45 year old who plans 30 annual full-body scans would potentially accrue an estimated lifetime cancer mortality risk of 1.1% (about 1 in 90). Correspondingly, a 60 year old planning 15 annual full-body scans would potentially accrue an estimated lifetime cancer mortality risk of 1 in 390. Again for comparison, the lifetime odds of an individual born in the US in 1999 dying in a traffic accident are estimated to be 1 in 77. Due to the larger doses involved for multiple scans, the credibility limits on the risk estimate are narrower, typically about a factor of 2 in either direction for 30 scans. The risks from multiple full-body scans can, of course, be reduced by undertaking fewer scans, and/or starting at a later age.

Because of the comparatively low doses associated with full-body scans, the risk estimates provided here have non-negligible uncertainties associated with them. However, despite these uncertainties – factors of 2 to 3 – these risk estimates are sufficiently robust to be useful in the assessment of the efficacy of full-body scans, both from an individual and from a public-health perspective. ■

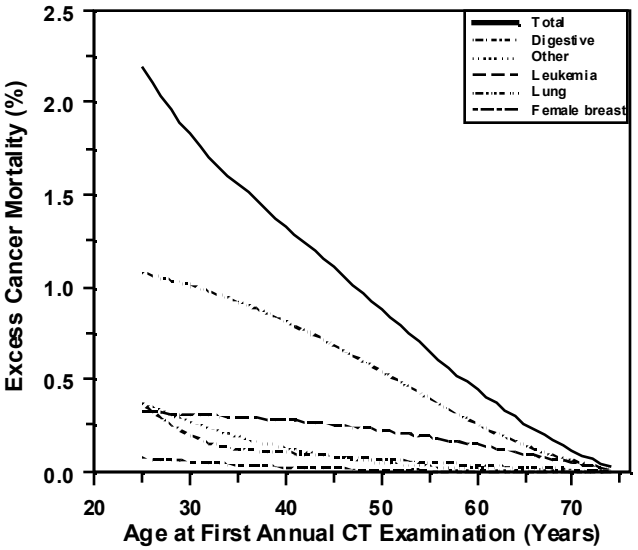

Fig. 2. Excess cancer mortality risks estimated here to be associated with the radiation from *annual* full-body CT scans. Annual scans are assumed to commence at the specified age and continue until age 75.

What Is the Lowest Dose of X- or Gamma Rays for Which There Is Good Evidence of Increased Cancer Risks in Humans?

David J. Brenner, Richard Doll,[1] Dudley T. Goodhead,[2] Eric J. Hall, Charles E. Land,[3] John B. Little,[4] Jay H. Lubin,[5] Dale L. Preston,[6] R. Julian Preston,[6] Jerome S. Puskin,[7] Elaine Ron,[3] Rainer K. Sachs,[8] Jonathan M. Samet,[9] Richard B. Setlow[10] and Marco Zaider[11]

The biological effects of low levels of radiation have been investigated and debated for more than a century. As we discuss, there is little question that intermediate and high doses of ionizing radiation, say above 100 mSv, given acutely or over a prolonged period, produce deleterious consequences in humans including, but not exclusively, cancer. However at lower doses, the situation is less clear. For example most radiological examinations produce doses in the range from 3 to 30 mSv. Understanding the risks of low doses of radiation remains of societal importance in relation to issues as varied as screening tests for cancer, the future of nuclear power, frequent-flyer risks, occupational radiation exposure, manned space exploration, and radiological terrorism. Here we ask (1) what is the lowest dose of x or gamma rays for which there is convincing evidence of significantly elevated cancer risks in humans?

[1] *Radcliffe Infirmary, Oxford, UK*
[2] *Radiation and Genome Stability Unit, Medical Research Council, Harwell, UK.*
[3] *Radiation Epidemiology Branch, NCI, Bethesda, MD.*
[4] *Harvard School of Public Health, Boston.*
[5] *Biostatistics Branch, NCI, Bethesda, MD.*
[6] *Radiation Effects Research Foundation, Hiroshima, Japan.*
[7] *Environmental Carcinogenesis Division, US EPA, Research Triangle Park, NC.*
[8] *Office of Radiation and Indoor Air, US EPA, Washington, DC.*
[9] *Department of Mathematics, University of California, Berkeley.*
[10] *Department of Epidemiology, Johns Hopkins, Upton, NY.*
[11] *Memorial Sloan-Kettering Cancer Center, New York, NY.*

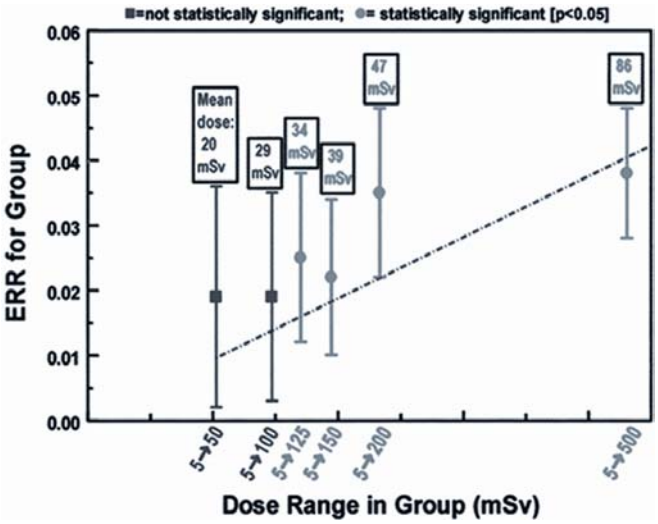

Fig. 1. Estimated excess relative risk (±1 SE) of mortality (1950–97) from solid cancers among groups of survivors in the Life-Span Study cohort of atomic-bomb survivors, who were exposed to low doses (<500 mSv) of radiation (2). The groups correspond to progressively larger maximum doses, with the mean doses in each group indicated above each data point. The first two data points (in blue) are not statistically significant (p=0.15 and 0.3, respectively) compared to the comparison population who were exposed to less than 5 mSv, while the remaining 4 higher-dose points (in red) are statistically significant (p<0.05). The dashed straight line represents the results of a linear fit (2) to all the data from 5 to 4,000 mSv (higher dose points not shown).

Acute low-dose exposures

The epidemiological study with the highest statistical power for evaluating low dose risks is the Life Span Study (LSS) cohort of atomic-bomb survivors (2) – because the cohort is large, follow-up is both complete and very long, and the survivors were exposed to a wide range of reasonably well-characterized radiation doses. While the A-bomb survivor analyses have often been considered as high-dose studies, in fact the mean dose in the exposed group on the LSS cohort is only 200 mSv, with over 50% of the exposed individuals in the cohort (>25,000 individuals) having doses below 50 mSv. Cancer incidence (3), cancer mortality (2), and non cancer-related mortality (2) have been studied, though almost half the exposed population – and a larger fraction of the individuals exposed as children – are still alive.

In the LSS study, organ dose estimates are available for all individuals included in the analysis, and the results are presented in dose group categories; a comparison population is used who were sufficiently far from the explosions that their doses were <5 mSv. Figure 1 shows low-dose risk estimates (2) for solid-cancer mortality in the A-bomb survivors (1950-1997). The individuals in the dose category from 5 to 125 mSv (mean dose 34 mSv) show a significant (p=0.025) increase in solid-cancer related mortality. There is the possibility of bias in these low-dose cancer mortality risk estimates; for example, individuals nearer the blast might be more likely to have cancer recorded on their death certificates. There is less potential for such bias in the cancer incidence studies (3); here, the A-bomb survivors in the dose range from 5 to 100 mSv (mean dose 29 mSv) show a significantly-increased solid cancer incidence (p=0.05) compared with the population who were exposed to <5 mSv.

The A-bomb survivor risks discussed above represent an average over all exposed individuals. There is good evidence that there are subpopulations at greater or lower risk than the average, depending on age (4), genetic status (5), or other factors (6). As well as the practical implications for population-wide radiation protection, low-dose studies on potentially radiosensitive subpopulations may result in a higher signal (risk) to noise (background) ratio, allowing low-dose risks to be more clearly established in these groups. One approach in this regard is to focus on *in-utero* or childhood exposure: radiation risks are expected to be higher due to the higher proportion of dividing cells in younger individuals, and also because of the longer lifespan available for a potential cancer to be expressed. Childhood cancer risks after prenatal x-ray exposure have been extensively studied: A detailed analysis of the many studies of childhood cancer risks from diagnostic *in utero* exposures concluded that a 10 mSv dose to the embryo and fetus does indeed cause a significant and quantifiable increase in the risk of childhood cancer (7); Mole (8) has argued that the most reliable risk estimate from these studies comes from prenatal examinations in Britain during the period 1958-61, for which the estimated mean fetal dose is 6 mSv and the odds ratio for childhood cancer deaths is 1.23 (95% CI: 1.04-1.48).

Protracted low-dose exposures

Much attention has been given to studies of large numbers of radiation workers who were chronically exposed to low radiation doses. Results have been reported from a pooled analysis of studies of nuclear workers in three countries [US, Canada, UK (9)], an enlarged UK study of nuclear workers (10), and from studies of Canadian radiation workers (11, 12). These studies have recently been reviewed by Gilbert (13). Statistically significant excess cancer incidence and mortality risks for solid cancers were found in the Canadian studies (mean dose 6.5 mSv). In contrast, neither the pooled analysis nor the UK study (both of which had higher mean doses, 40 mSv and 30 mSv respectively) showed a significant increase in solid cancer risk. However, all three studies found an increased risk for leukemia, which was statistically significant in the pooled study, borderline significant in the UK study, and non-significant in the Canadian studies.

As with the acute exposures, it is informative to examine childhood exposure, as the risks are expected to be higher and thus easier to quantify. The US scoliosis cohort study (14) of females exposed under age 20 to multiple diagnostic x rays (mean breast dose 108 mSv in 25 exposures) demonstrated a statistically significant increased risk for breast cancer (relative risk, RR=1.6, 95% CI: 1.1-2.6); the excess risk remained significant when the analysis was limited to individuals with breast doses between 10 and 90 mSv.

Ron *et al.* (15) studied children who received fractionated irradiation of the scalp (five fractions, mean total thyroid dose 62 mSv, dose range 40-70 mSv); compared to

matched, unirradiated comparison subjects, they showed a statistically significant increase in thyroid cancer risk, (RR=3.3, 95% CI: 1.6-6.7). Higher risks were seen when the age at exposure was limited to under 5 years (RR=5.0, 95% CI: 2.7-10.3). A subsequent pooled analysis (16) of five cohort studies of thyroid cancer after childhood exposure to external radiation (four of these studies, including the scalp irradiation study described above, were of fractionated exposure) showed clear evidence of an increased risk of thyroid cancer (RR=2.5, 95% CI: 2-4) at a mean dose to the thyroid of 50 mSv (dose range 10 to 90 mSv).

At still lower doses, there is a suggestion (17) of an increase in leukemia risk in children under age 5 who were exposed to fallout from nuclear weapons testing (estimated fallout marrow dose 1.5 mSv, RR=1.11; 95% CI: 1.00-1.24). No individual doses were estimated in this study, but it is difficult to see how the biases that are common in ecologic studies could have affected the temporal correlation between the dose from fall-out and the incidence of the disease. These results are consistent with an earlier case-control study (18) of leukemia in Utah in relation to fallout from the Nevada nuclear test site; here a significant excess risk for acute leukemia was seen in individuals who died aged under 20 and who received bone-marrow doses from 6 to 30 mGy (odds ratio 5.8; 95% CI: 1.6-22).

Summary of doses at which there is clear evidence of cancer risks

For x or gamma rays, there is good evidence of an increase in risk for cancer at acute doses above 50 mSv, and reasonable evidence for an increase in some cancer risks at doses above about 5 mSv. As expected from basic radiobiology, the doses above which statistically significant risks are seen are somewhat higher for protracted exposures than for acute exposures; specifically, there is good evidence of an increase in some cancer risks for protracted doses above 100 mSv, and reasonable evidence for an increase in cancer risk at protracted doses above about 50 mSv.

It seems unlikely that we will be able to directly estimate risks at significantly lower doses than these, because of the practical limits of epidemiology discussed above. Of course the fact that risks cannot be directly estimated at doses below, say, 5 mSv, does not imply any conclusion as to whether or not there actually are risks at these lower doses.

References

1. Brenner DJ, Doll R, Goodhead DT, Hall EJ, Land CE, Little JB, Lubin JH, Preston DL, Preston RJ, Puskin JS, Ron E, Sachs RK, Samet JM, Setlow RB and Zaider M. Cancer risks attributable to low doses of ionizing radiation: assessing what we really know. *Proc Natl Acad Sci USA* **100**:13761-6, 2003.
2. Preston DL, Shimizu Y, Pierce DA, Suyama A and Mabuchi K. Studies of mortality of atomic bomb survivors. Report 13: Solid cancer and noncancer disease mortality: 1950-1997. *Radiat Res* **160**:381-407, 2003.
3. Pierce DA and Preston DL. Radiation-related cancer risks at low doses among atomic bomb survivors. *Radiat Res* **154**:178-86, 2000.
4. Pierce DA. Age-time patterns of radiogenic cancer risk: their nature and likely explanations. *J Radiol Prot* **22**:A147-54, 2002.
5. Risk estimation for multifactorial diseases. A report of the International Commission on Radiological Protection. *Ann ICRP* **29**:1-144, 1999.
6. Herold DM, Hanlon AL and Hanks GE. Diabetes mellitus: a predictor for late radiation morbidity. *Int J Radiat Oncol Biol Phys* **43**:475-9, 1999.
7. Doll R and Wakeford R. Risk of childhood cancer from fetal irradiation. *Br J Radiol* **70**:130-9, 1997.
8. Mole RH. Childhood cancer after prenatal exposure to diagnostic X-ray examinations in Britain. *Br J Cancer* **62**:152-68, 1990.
9. Cardis E, Gilbert ES, Carpenter L, Howe G, Kato I, Armstrong BK, Beral V, Cowper G, Douglas A and Fix J. Effects of low doses and low dose rates of external ionizing radiation: cancer mortality among nuclear industry workers in three countries. *Radiat Res* **142**:117-32, 1995.
10. Muirhead CR, Goodill AA, Haylock RG, Vokes J, Little MP, Jackson DA, O'Hagan JA, Thomas JM, Kendall GM, Silk TJ, Bingham D and Berridge GL. Occupational radiation exposure and mortality: second analysis of the National Registry for Radiation Workers. *J Radiol Prot* **19**:3-26, 1999.
11. Ashmore JP, Krewski D, Zielinski JM, Jiang H, Semenciw R and Band PR. First analysis of mortality and occupational radiation exposure based on the National Dose Registry of Canada. *Am J Epidemiol* **148**:564-74, 1998.
12. Sont WN, Zielinski JM, Ashmore JP, Jiang H, Krewski D, Fair ME, Band PR and Letourneau EG. First analysis of cancer incidence and occupational radiation exposure based on the National Dose Registry of Canada. *Am J Epidemiol* **153**:309-18, 2001.
13. Gilbert ES. Invited commentary: studies of workers exposed to low doses of radiation. *Am J Epidemiol* **153**:319-22; discussion 323-4, 2001.
14. Morin Doody M, Lonstein JE, Stovall M, Hacker DG, Luckyanov N and Land CE. Breast cancer mortality after diagnostic radiography: findings from the U.S. Scoliosis Cohort Study. *Spine* **25**:2052-63, 2000.
15. Ron E, Modan B, Preston D, Alfandary E, Stovall M and Boice JD Jr. Thyroid neoplasia following low-dose radiation in childhood. *Radiat Res* **120**:516-31, 1989.
16. Ron E, Lubin JH, Shore RE, Mabuchi K, Modan B, Pottern LM, Schneider AB, Tucker MA & Boice JD Jr. Thyroid cancer after exposure to external radiation: a pooled analysis of seven studies. *Rad Res* **141**:259-77, 1995.
17. Darby SC, Olsen JH, Doll R, Thakrar B, Brown PD, Storm HH, Barlow L, Langmark F, Teppo L and Tulinius H. Trends in childhood leukaemia in the Nordic countries in relation to fallout from atmospheric nuclear weapons testing. *BMJ* **304**:1005-9, 1992.
18. Stevens W, Thomas DC, Lyon JL, Till JE, Kerber RA, Simon SL, Lloyd RD, Elghany NA and Preston-Martin S. Leukemia in Utah and radioactive fallout from the Nevada test site. A case-control study. *JAMA* **264**:585-91, 1990. Erratum in: *JAMA* 265:461, 1991. ■

Progress towards Monte Carlo Simulations and Dosimetry in ATOM Phantoms

Carl D. Elliston and David J. Brenner

We have acquired 20 Thompson-Nielson high-sensitivity MOSFET dosimeters (model TN-1002RD) and three "ATOM" heterogeneous anthropomorphic dosimetry phantoms – an adult male (model 701-D), a pediatric ten-year old (model 706-D), and a pediatric one-year old (model 704-D) – made of tissue-equivalent (TE) plastics that simulate soft tissue, bone, lung, breast, and brain (Figure 1). The phantoms are sectional (25-mm slabs), and provide relocatable dosimeter positions corresponding to 19 internal organs, enabling our MOSFET dosimeters to be easily and precisely placed. For example Figure 2 shows a single phantom slice with 16 MOSFET dosimeters placed to measure the dose to the lung, adrenals, spleen, and liver. We use 20 MOSFET dosimeters at once.

Fig. 1. Three "ATOM" heterogeneous anthropomorphic dosimetry phantoms.

In order to perform dosimetry calculations, the Thompson-Nielson high-sensitivity MOSFET dosimeters must first be calibrated. This has been accomplished using a Perspex phantom, for which we made special MOSFET inserts.

Experiments performed with our MOSFET dosimeters will ultimately be used to verify our computational models of the ATOM phantoms. We will then be able to perform Monte-Carlo simulations using our computational models to calculate different organ doses for a variety of CT examinations from a variety of CT machines. Monte Carlo calculations will be performed in MCNPX, for which we have become beta testers. MCNPX adds to the extensively used MCNP4B many new features including mesh tallies, a method that can calculate dose on a rectangular (or other shaped) grid overlaid on top of standard problem geometry.

In order to perform Monte Carlo simulations of our phantoms, we have first to construct a computational body model from tomographic images. This has been accomplished as follows:

We CT scanned the three phantoms using a Siemens Sensation 16 scanner (Figure 3). The result of each of these CT scans is a series of several hundred digital image slices (DICOM images). Each image slice is an array of pixels in a two-dimensional geometry. A pixel's value represents the electron density of the material scanned (CT number). By multiplying the pixel size by the slice thickness of an image, three-dimensional volume elements, called voxels, are obtained.

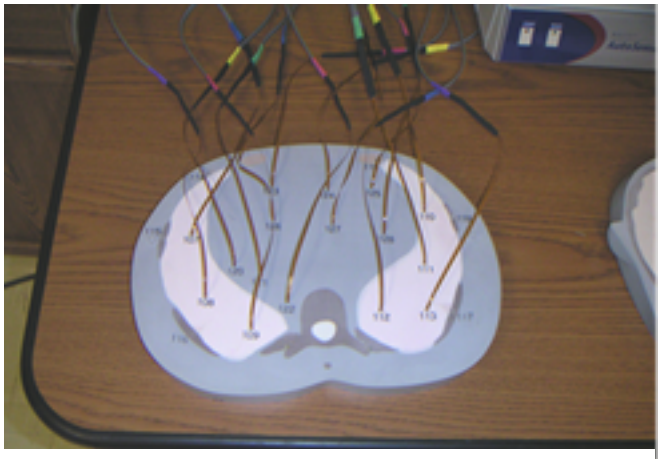

Fig. 2. A single phantom slice with 16 MOSFET dosimeters placed to measure the dose to the lung, adrenals, spleen, and liver.

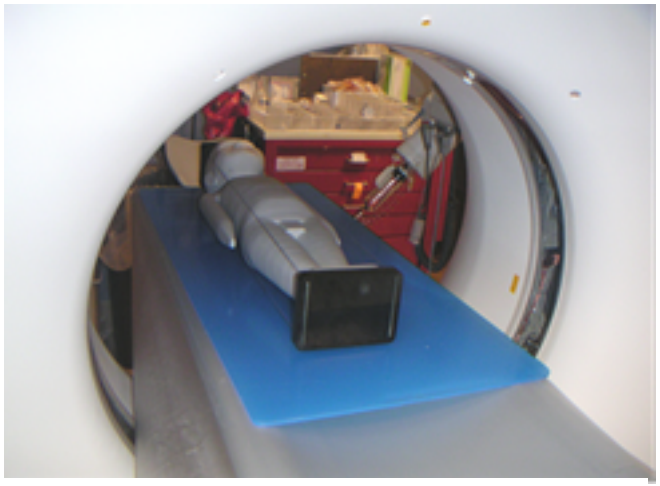

Fig. 3. CT scanning a phantom using a Siemens Sensation 16 scanner.

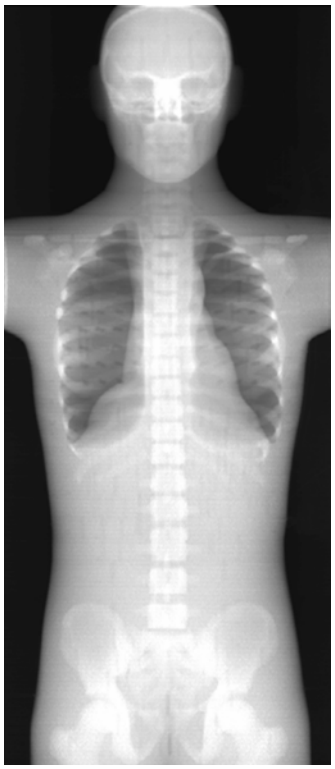

Fig. 4. A reconstruction from the CT scan of our adult phantom.

Fig. 5. Segmentation being performed using the CT visualization software 3D-Doctor.

Shown in Figure 4 is a reconstruction from the CT scan of our adult phantom. In our CT scans the dimensions of each individual voxel are .9 mm x .9 mm x 1 mm for the adult phantom and .5 mm x .5 mm x 1 mm for each of the pediatric phantoms. This resolution results in nearly 200 million pixels for the 1-year old phantom. Using such a large number of pixels is not possible in MCNPX at this time. However, we easily reduced the pixel resolution by increasing the voxel size to make computation times in MCNPX reasonable. A resolution of 3 mm x 3 mm x 3 mm is currently used. Nonetheless, the quality of the original CT scan is crucial in the construction of a computational model. The resolution of the original images determines the ability to perform segmentation accurately and to model the human anatomy.

Segmentation has been performed using the CT visualization software 3D-Doctor (Figure 5). Each pixel in each DICOM image has been identified as being of a particular material type – soft tissue, brain, bone, breast, lung, detector, or air – by a semi-automated procedure. The results of this procedure are illustrated in the picture to the right. The DICOM image in the upper left panel contains nearly 2000 different CT numbers. After processing, the new DICOM image, shown in the upper right panel, contains only 6 CT numbers – one each for breast, soft tissue, air, detector, lung, and bone. The processed DICOM images were subsequently converted into an ASCII format that MCNPX can read. We have successfully translated a single CT slice into MCNPX as a rectangular lattice using its repeated structures feature, and we have extended this procedure to convert multiple image slices into MCNPX.

The conversion of DICOM images into MCNPX input described above was performed using 3D-Doctor and a simple FORTRAN program we have written for this purpose. However, we have also learned to use ITK – a powerful open-source software suite capable of manipulating DICOM files. With this software we will streamline the segmentation process and add simulated human organs.

For the latter task we have enlisted the assistance of Dr. Celina Imielinska, an expert in using ITK to develop semi-automated organ segmentation routines. As a part of the Columbia University Vesalius Project, she has already segmented many organs, including the prostate (left), from data made available through the Visible Human Project (supported by the National Library of Medicine). The goal of the Visible Human Project is the creation of complete, anatomically detailed, three-dimensional representations of the normal male and female human bodies. Our objective is to take the geometry of the Visible Human organs, rescale them, and overlay these organs onto our computational body model, in order to estimate organ doses from CT scans. These estimated doses will then be readily testable experimentally using our MOSFET dosimeters with our ATOM phantoms. ■

The Radiological Research Accelerator Facility

AN NIH-SUPPORTED RESOURCE CENTER – WWW.RARAF.ORG

Director: David J. Brenner, Ph.D., D.Sc.
Manager: Stephen A. Marino, M.S.
Chief Physicist: Gerhard Randers-Pehrson, Ph.D.

During this past year, we have achieved several significant accomplishments:

- Irradiation of three-dimensional tissue.
- Our first focused microbeam irradiation.
- Our first microbeam irradiation using protons.
- The first charged particle beam as well as the first focused microbeam in the new microbeam facility.
- Another significant development is a grant from the National Center for Research Resources (NCRR) of the National Institutes of Health (NIH) for the purchase of an accelerator to replace the Van de Graaff that is now over 50 years old.
- Recently, the grant supporting the developmental projects at RARAF has been shifted from the NCRR to the National Institute of Biomedical Imaging and Bioengineering (NIBIB).

Research Using RARAF

Interest continues to remain quite strong in the "bystander" effect, in which only some cells are irradiated and a response is obtained that is greater than would be expected for the fraction irradiated. Several experiments examining this effect were continued and new ones initiated, observing a variety of endpoints to determine the size of the effect and the mechanism by which it is transmitted. Evidence has been obtained for both direct cell-cell gap junction communication through cell membrane contact and indirect, long-range communication through media transfer. In some experiments, the unirradiated cells can be identified due to different staining and scored directly. In other experiments, unirradiated cells are physically separated from the irradiated cells during irradiation. Both the microbeam and the track segment facilities continue to be utilized in various investigations of this phenomenon. The single-particle microbeam facility provides precise control of the number and location of particles but is somewhat limited in the number of cells that can be irradiated. The track segment facility provides broad beam irradiation that has a random pattern of charged particles but allows large numbers of cells to be irradiated and multiple users in a single day.

In Table I are listed the experiments performed at RARAF from May 1, 2002 through October 31, 2003 and the number of days each was run in this period. The reporting period comprises 18 months in order to better align it with the date of the Annual Report. Seventeen different experiments were run during this period, about the same as the average for 1997-2002. Ten experiments were undertaken by members of the CRR, supported by grants from the NIH and the Department of Energy (DOE). Seven experiments were performed by outside users, supported by grants and awards from the NIH, the National Aeronautics and Space Administration (NASA), the National Science Foundation (NSF) and the Ministry of Education, Science, Sports and Culture of Japan. Brief descriptions of these experiments follow.

Investigations involving the oncogenic neoplastic transformation of mouse C3H 10T½ cells (Exp. 73) were continued by Eric Hall, Stephen Mitchell and Richard Miller of the Center for Radiological Research (CRR). Using the microbeam facility, 10% of the cells were irradiated through the nucleus with 2 to 12 helium ions. Cells were plated at densities of approximately 200 and 2000 per dish to try to observe the relative contribution of cell-cell communication to the bystander effect. Cell killing and transformation were greater for the cells plated at the higher density relative to those plated at the lower density. The results imply that gap junction communication has a greater role in the bystander effect than media transfer. The track segment facility was used to investigate whether there is an adaptive response for the bystander effect. Cells (bystanders) were plated on special track segment dishes made by cutting the Mylar surface into several equal strips and removing alternate strips. The Mylar is thick enough to stop the incident ions. This dish is placed inside a second dish that has a complete Mylar surface. Cells are plated on the combined surface. All the cells were given a dose of 250 kVp x-rays and after 5 hours the nuclei were irradiated with helium ions. Significant reductions in cell killing and transformation were observed for the bystander cells given x-rays relative to those that weren't.

Richard Mauer, David Roth and James Kinnison of Johns Hopkins University continued development of a portable neutron spectrometer system for the energy range 0.5 to 100 MeV (Exp. 89). The spectrometer will be used on the International Space Station and the manned mission to Mars. Emphasis is now on determining the shapes and rise times of the pulses generated by gamma rays and neutrons to perform gamma-ray discrimination. A second detector of borated plastic scintillator to be used on the Messenger probe that will orbit Mercury was irradiated with neutrons for an initial evaluation of the system. In addition, an irradiation with 2.1 MeV neutrons was performed on a charged-coupled device (CCD) to be used to send video signals from the New Horizons probe that will travel past Pluto to the outer asteroid belt. Since the probe will be too far away to use solar panels, there will be an on-board power supply. The effect of neutrons emitted by the power supply on the resolution of the camera was determined.

Sally Amundson of the NIH is investigating radiation-induced gene expression profiles in human cell lines using

Table I.

Experiments Run at RARAF, May 1, 2002–October 31, 2003

Exp. No.	Experimenter	Institution	Exp. Type	Title of Experiment	Days Run
73	S. Mitchell, E.J. Hall	CRR	Biology	Neoplastic transformation of C3H10T½ cells by specific numbers of α particles	27.3
89	R.H. Mauer, et al.	Johns Hopkins U.	Physics	Calibration of a portable real-time neutron spectrometry system	4.5
92	S. Amundson	NIH	Biology	Functional genomics of cellular response to high-LET radiation	1.0
94	B. Ponnaiya, C.R. Geard	CRR	Biology	Single cell responses in hit and bystander cells: single-cell RT-PCR and protein immunofluorescence	8.0
103	G. Jenkins, C.R. Geard	CRR	Biology	Damage induction and characterization in known hit versus non-hit human cells	11.9
106	B. Ponnaiya, C.R. Geard	CRR	Biology	Track segment alpha particles, cell co-cultures and the bystander effect	9.0
108	H. Zhou, T.K. Hei	CRR	Biology	Modulation of adaptive response in alpha-particle-induced bystander effects	2.0
109	A. Balajee, C.R. Geard	CRR	Biology	DNA damage induction in microbeam-irradiated cells assessed by the comet assay	3.7
110	H. Zhou, D. Roy, T.K. Hei	CRR	Biology	Identification of molecular signals of alpha particle-induced bystander mutagenesis	14.4
114	M. Suzuki (Zhou)	Ntnl. Inst. of Radiological Sci., Japan	Biology	Bystander response in primary human bronchial epithelial cells using the G2PCC technique	4.0
115	A. Caldwell, R. Galea	Columbia Univ.; Max Planck Inst., Germany	Physics	Proton cooling studies for the development of a muon ion source for the Muon Collider/Neutrino Factory	27.4
116	O. Belyakov	CRR	Biology	Long-range communication phenomena in 3-D human tissue systems	12.9
117	K. Irzynska, O. Belyakov	Jagiellonian Univ., Poland; CRR	Biology	Studies of direct and bystander radiation effects in V79 cells using broad field and microbeam irradiation	1.0
118	R. Kolesnick, G. Perez	MSKCC; Mass. General Hosp.	Biology	Characterization of the radiosensitive target for cell death in mouse oocytes	1.3
119	D. Lawrence	Los Alamos Natl. Lab.	Physics	Calibration of a neutron spectrometer for planetary studies	5.8
120	R. Persaud, T. Hei	CRR	Biology	Determination of the bystander response for low-LET protons	5.0
121	A. Zhu, H. Lieberman	CRR	Biology	The bystander effect in mouse embryo stem cells with a mutant Mrad9 gene	2.9

Note: Names in parentheses are CRR members who collaborated with outside experimenters.

cDNA microarray hybridization and other methods (Exp. 92). She is characterizing the response of a p53 wild-type and knock-out pair of human cell lines. The profiles generated by cells irradiated with 0.43 MeV neutrons are providing insight into the specificity of ionizing radiation responses, as well as revealing potential candidates for high LET-specific responses.

Two studies investigating the bystander effect were continued by Brian Ponnaiya and Charles Geard of the CRR. In one study (Exp. 94), levels of p21 production were measured in individual normal human fibroblasts using immunofluorescent staining. This procedure permits observation of the variation in response of individual cells to radiation instead of just the average response of a large number of cells. From 1 to 100% of the cell nuclei were irradiated with helium ions using the microbeam facility. The second investigation uses the track segment facility for broad-beam charged particle irradiations of human fibroblasts and epithelial cells immortalized with telomerase (Exp. 106). Special cell dishes are made from stainless steel rings with thin Mylar windows epoxied on both sides. Cells are plated on both inner Mylar surfaces and the dish volume is filled with medium, eliminating any possibility of cell-cell contact between cells on opposing surfaces. Cells on one surface are irradiated with 4He ions; cells on the opposite surface are unirradiated because the particles stop in the medium before reaching them. Cells are observed in situ after irradiation with doses from 1 to 10 Gy of 125 keV/μm ^{4}He ions. Plateau phase cells are scored for cell cycle delay and micronucleus production while log phase cells are scored for chromosomal aberrations. It was observed that irradiated fibroblasts can induce micronuclei in bystander fibroblasts, but bystander epithelial cells are refractory to irradiated epithelial cells. Furthermore, epithelial cells are capable of responding to irradiated fibroblasts, which results in the induction of micronuclei in the bystander epithelial cells. Chromosomal analyses of irradiated fibroblast populations and bystander cells at the first cell division post irradiation demonstrated the induction of gross chromosome aberrations in the irradiated population and chromatid aberrations (of the simple type – breaks and gaps) in the bystander population. Elevated yields of similar types of chromatid type aberrations were also observed in both irradiated and bystander fibroblast populations up to 20 population doublings post irradiation.

Charles Geard and Gloria Jenkins of the CRR are studying the bystander effect in several cell lines using the microbeam facility (Exp. 103). Normal human fibroblasts and human mammary epithelial cells were irradiated with helium ions, targeting 1%, 10% and 100% of the cell nuclei. Endpoints for various experiments included micronucleus production in S phase, production of p21 and p53 in the fibroblasts and production of H2AX in the mammary cells. In some of the experiments the bystander cells were stained

with a different dye than the irradiated cells so that they could be distinguished.

Hongning Zhou and Tom Hei of the CRR continued to use the single-particle microbeam facility for two experiments investigating the bystander effect. A study examining adaptive response in bystander effects in human-hamster hybrid (A_L) cells (Exp. 108) was completed. After low-dose x-ray irradiation, 10% of the cells were traversed by 1 or 20 helium ions. There was a decrease in the bystander effect for mutation when neighbor cells are traversed by one particle and a somewhat smaller decrease for traversal by 20 particles. . In addition, they found that the bystander cells showed an increase in sensitivity to a subsequent, challenging dose of x-rays. The mutation spectra are being analyzed and should provide some evidence for understanding the mechanism of bystander mutagenesis and adaptive response. With Debasish Roy of the CRR, they are trying to identify the signaling transduction pathways involved in radiation-induced bystander mutagenesis (Exp. 110). Hybrid A_L cells, normal human lung fibroblasts, mitochondrial deficient cells, and other functional deficiency cell lines are irradiated using the microbeam facility. A fraction of the cells is irradiated with a single alpha particle. Initially, the irradiated (stained) cells were separated from the unirradiated cells by a cell sorter and accumulated from experiments over four consecutive days. This method proved logistically to be quite difficult. Presently, the cells are kept *in situ* for 2, 6, 24 or 48 hours after irradiation, thereby increasing the number of cells and the time for interaction. In addition, some experiments have been performed using the track segment facility using the "strip" dishes described for Experiment 73. The mRNA extracted from the cells is analyzed using microarrays. Preliminary data show some gene expression changes in the bystander cells.

Investigations of damage induction in normal human fibroblasts and *Ataxia Telangiectasia* cells (Exp. 109) by Adayabalam Balajee and Charles Geard of the CRR included a search for foci of damage and repair proteins. Cells were irradiated through the nucleus with helium ions using the microbeam facility. The *AT* cells were scored using the comet assay to determine chromosome breakage. The fibroblasts were stained and examined to observe the repair proteins, which should cluster around the helium ion track. Fluorescence of stained irradiated cells was 2-3 times greater than in the controls, implying a significant increase in repair proteins, and formed foci, although the number of foci was not the same as the number of ion traversals in the nuclei.

Masao Suzuki of the National Institute of Radiological Science, Japan is trying to determine whether alpha particle irradiation can induce a bystander response in primary human bronchial epithelial cells using the G2PCC technique (Exp. 114). Ten percent of the cells were irradiated in the nucleus with helium ions using the microbeam facility. The cells then accumulated and were harvested in the G2 phase of the cell cycle, and the process of premature chromosome condensation was used to observe chromatin aberrations.

Initial studies for the development of a muon ion source (Exp. 115) were undertaken by Alan Caldwell and Raphael Galea, originally at the Physics Department of Columbia University (working at the Nevis Laboratory) and now at the Max Planck Institute in Munich, Germany. Pions produced by high-energy proton bombardment of a target will be allowed to decay into muons that must be forced to travel in the same direction, slowed down (cooled) and bunched with a minimum spread in energy and time. As a first test of the method, low energy protons from the Van de Graaff were used to determine the energy spread and timing. The source will eventually be used for the Muon Collider/Neutrino Factory, whose location is yet undetermined.

An investigation of the bystander effect in three-dimensional model human tissue systems was begun by Oleg Belyakov of the CRR (Exp. 116). Several novel artificial human skin tissue systems were obtained from the MatTek Corporation: epidermis, cornea and tracheal/bronchial epithelium, allowing the modeling of the conditions present *in vivo*. The tissues were irradiated using the microbeam facility with 10 helium ions deposited 17 to 400 locations in a line 8-10 mm long across the sample (20 to 500 μm spacings) and with 2.75 MeV protons at 100-300 μm spacings. Irradiations were also performed using the track segment facility to irradiate samples with 125 keV/μm ^{4}He ions and 12 keV/μm protons with doses that resulted in approximately 0.5 to 2 particles per cell nucleus. The microbeam samples were embedded in paraffin and cut into 5 μm-thick sections to observe the bystander effect as a function of distance. For all experiments, three endpoints were studied: an *in situ* apoptosis assay, epidermal differentiation and a proliferation assay. He has observed a clear bystander response, established dose dependency and studied the role of differentiation vs. damage induction processes.

Katarzyna Irzynska, an undergraduate student from Jagiellonian University in Krakow, Poland performed experiments on direct and bystander effects in V79 cells (Exp. 117). Under the tutelage of Oleg Belyakov of the CRR, cells were irradiated with helium ions using the microbeam facility and 11-keV/μm protons using the track segment facility. Irradiated and bystander cells were scored for "total cellular damage" (TCD), defined as the sum of the fraction of cells with micronuclei and those that became apoptotic.

Richard Kolesnick of the Memorial Sloan Kettering Cancer Center (MSKCC) and Gloria Perez of Massachusetts General Hospital are trying to characterize the radiosensitive target for mouse oocyte killing (Exp. 118). Is it the DNA, the plasma membrane or the cytoplasm? Understanding what the target is would help in the development of protective therapies to prevent the side effects of radiotherapy on female germ cells. For these experiments they are using the mouse strain C57BL/6 because oocytes from these mice show low rates of spontaneous apoptosis. Mature and immature oocytes are irradiated in the DNA, the cytoplasm or the cell membrane using the microbeam facility. Because the oocytes are spherical with a uniform diameter of about 80 μm, they are irradiated with protons because the range of the helium ions is insufficient to penetrate much more than half way through the cells.

David Lawrence of Los Alamos National Laboratory performed a calibration of a neutron spectrometer to be used on the Messenger mission, a space probe for investigations

of the planet Mercury (119). The detector comprises a pair of borated plastic scintillators that were irradiated with monoenergetic neutrons from 0.5 to 2.0 MeV to obtain response functions and efficiencies. The detectors were also tested for angular response.

An investigation of the bystander effect using low-LET radiation (Exp. 120) was begun by Tom Hei and Rudranath Persaud of the CRR. A_L cells were irradiated with 3.1 MeV protons (~12 keV/μm) using the microbeam facility. Approximately 20% of the population was irradiated with 200 protons per nucleus. Preliminary results for this experiment indicate that the protons did not induce a bystander effect. The mutant yield for the control group was 200, whereas for the irradiated group it was 160.

Howard Lieberman and Aiping Zhu of the CRR have begun experiments to investigate the bystander effect in mouse embryo stem cells with a mutation in the Mrad9 gene (Exp. 121), which promotes radiation resistance and helps regulate the cell cycle and apoptosis. Cells plated on the special "strip" dishes are irradiated with 1 to 10 Gy of helium ions using the track segment facility and observed for cell survival, micronucleus production and apoptosis. Cells with the mutated gene show an enhanced bystander effect for some of the endpoints.

Development of Facilities

One of the major recent developments has been the receipt of a grant from the National Center for Research Resources (NCRR) of the NIH for the purchase of an accelerator to replace our present 4.2-MV Van de Graaff, which is over 50 years old and has problems with a vacuum leak in the acceleration tube and an aged charging belt. Many parts for the accelerator are custom-made or no longer commercially available and the voltage regulation is only ±2-4 kV. We have ordered a new 5 MV Singletron accelerator from High Voltage Engineering Europa in the Netherlands that will meet or exceed our present capabilities. The charging system is electronic, similar to that of a Cockroft-Walton, so there are no moving parts (belts, chains) in the charging system. Terminal voltage ripple will be 200 V or less. The higher voltage will provide ion beams with longer ranges and lower LETs. Better voltage stability will result in a smaller beam spot for our double lens system since energy spread in the beam reduces focusing. An RF ion source will produce protons, deuterons, ^{3}He ions, and ^{4}He ions with beam currents of at least 100 μA. Control of valves and power supplies in the terminal is performed through a light link rather than by motors with strings, as in our present system. Terminal parameters are monitored through this light link rather than by a TV camera or monocular. Control of the accelerator is through a computer interface. The accelerator should arrive in May, 2005. Removal of the Van de Graaff and installation of the Singletron will require at least a partial dismantling and reconstruction of the extension on the west side of the building and take 3-6 months.

During the past 18 months, our development effort has increased markedly. Not only was on-line development time increased by more than 60% over last year, but two more people were added to the development team: Greg Ross and Guy Garty. Development continued or was initiated on the microbeam facilities and a number of extensions of their capabilities:

- Assembly of the beam line and end station for the new microbeam facility
- Development of focused microbeams
- Voice-coil and precision z-motion stages
- New microbeam irradiation slides
- Laser ion source
- Secondary emission ion microscope (SEIM) for viewing focused beam spots
- Source-based microbeam
- Non-scattering particle detector
- Advanced imaging systems
- Focused x-ray microbeam

The beam line from the new 90-degree bending magnet into the new microbeam laboratory has been completed. Valves, an ion pump, energy regulation slits and a module with a series of object apertures for the lens have been assembled into the beam line. Also installed is an x-y adjustment for the tube inside the beam line in which the two lenses will be mounted, so that the pair of lenses can be aligned with the beam. In order to assemble the beam line and have access to it, a scaffold that can accommodate two people was erected surrounding the beam line and the 90-degree magnet below it. This proved to be more difficult than anticipated because of the braces for the magnet stand as well as the horizontal beam line and associated components. A hole was made in the ceiling of the microbeam room and a winch mounted on the roof so that the 2.5-m long tube containing the lenses could be lowered into the beam pipe.

Construction of the new microbeam facility on the floor over the exit of the Van de Graaff has been essentially completed. The on-line microscope has been modified so that it can be rotated in and out of place over the irradiation port. When off-line, the movable portion of the microscope sits on its original base and is usable as a standard fluorescence microscope. The camera, image analysis system, and microscope stage have all been integrated into the microbeam irradiation control program. The exit port has a SiN window with a 1-mm square section only 100 nm thick to minimize scattering. This will be more important for the 0.5-μm diameter beam that will be produced by the compound lens system. Until the compound lens is constructed, we will use a single quadrupole quadruplet to produce a beam with a diameter of 3 μm for cell irradiations.

Testing of the single electrostatic quadrupole quadruplet continued, using the existing microbeam facility. A beam approximately 3 μm in diameter was obtained using a lens with rods only having a titanium coating (no gold). A second lens constructed with gold plating over the titanium was also able to produce a beam 3 μm in diameter. This lens was used in the original microbeam facility to perform our first focused microbeam irradiations of cells with helium ions and our first microbeam irradiations using low-LET protons. Unfortunately, the lens has developed a problem and has had to be removed from service for repair. The lens with the titanium-coated rods has been mounted in the alignment tube

for the double lens system and placed in the beam line for the new microbeam facility. It has focused the beam to less than 10 μm diameter. We are still in the process of optimizing the focus and should be able to obtain a beam spot of 3 μm or less and begin microbeam experiments on the new beam line. Measurements are being made of the voltages required to obtain various beam spot geometries when all and only some of the lens elements are used. This information will be used by our consultant, Alexander Dymnikov, at the University of Louisiana to calculate parameters for the double quadrupole triplet lens assembly that will be used to focus the ion beam to a diameter of 0.5 μm. Final machining of the rods for the lens electrodes will start as soon as the results of these calculations are received. For these measurements to be most useful, the energy and energy spread of the beam must be known accurately. A thin nickel target has been constructed and mounted on the T2 beam line to use the extremely narrow (<90 eV) Ni(p,γ) resonance at 1.844 MeV to define the beam energy and energy spread. Eventually, the measurements will be repeated on the microbeam line itself using an extremely thin (0.1 μm) layer of Ni on a thin Pt (2 μm) target backing.

Our custom-designed Voice-Coil Stage (VCS), which uses thin coils in permanent magnetic fields to move the microscope stage, has been integrated into the new microbeam facilities and has been shown to position the stage reliably under normal use to within ±0.4 μm, with a settling time of ~50 ms. Development is continuing to improve its performance. The circuitry for the linear variable differential transformer (LVDT) feedback system for the voice-coil stage has been tested and is being built into a NIM module. This stage will provide both more accurate and faster positioning than the present stage, which is moved by stepping motors. We have purchased a high-precision stage from Mad City Labs in Wisconsin that also has a vertical motion. This stage has a range of motion of 200 μm in the x and y directions and 100 μm in the z direction, with nanometer positioning. This stage exceeds the accuracy needed for the 0.5 μm diameter beam, however because of its limited range of motion in the horizontal plane, we will have to mount it within a coarser stage in order to be able to access the entire surface area on which cells are plated. The vertical motion is required for the imaging techniques described below. The stage will also be used to raise and lower the sample over the exit window during movement to minimize the separation and thereby reduce beam spread due to scattering in the window.

In parallel with our improved spatial properties of the microbeam, it became essential to develop corresponding improvements in the substrate on which cells are grown and imaged. Our prime requirements for improvements are improved optical properties, minimal background fluorescence, and strong adherence to the supporting dish or slide. We are using a thermoplastic polymer called parylene, the generic name for a family of polymers that are formed on surfaces exposed to a rarified gas in a vacuum. Standard plastic microscope slides with ¼"-diameter holes are sandwiched around a glass slide that has been coated with a water-soluble release agent. The slides are plated with parylene using a coating system we have purchased and the assemblies separated by soaking in water. Strong, flat coverings over the holes in the slides have been achieved; however the surfaces have many inclusions. Development is continuing on producing films without the surface defects that make them unsuitable for microscopy.

The laser ion source is nearing completion. The spherical lens to focus the ions on the entrance of the acceleration tube was completed last year. The rotating laser target assembly has been designed and constructed. The mounts for the mirrors and lens to direct and focus the laser beam on the target are being designed. When the mounts are received, testing of the system will begin. An evaporable getter was purchased to replace the titanium sublimation pump that was originally going to be used to maintain the vacuum in the source. Unlike the sublimation pump, the getter doesn't require a large power supply, reducing the amount of space required in the accelerator terminal, the amount of weight the column has to support and the amount of terminal power consumed. The reduction in weight and power consumption made the source much more compatible with the new accelerator that is on order. The terminal of the Singletron is being designed to accommodate the ion source without any modification to our present design. We have decided not to install the source in the Van de Graaff, which could take up to a month for modifications to the terminal and testing, because the accelerator will be decommissioned next April.

As we improve the spatial characteristics of the microbeam system, it becomes increasingly important to be able to assess the beam quality in order to adjust the system to its optimum capabilities. A secondary electron ion microscope (SEIM) has been designed and is currently being constructed. This device will enable us to measure the beam profile and position in real time with sub-micron resolution and sensitivity to single projectile particles (1-5 MeV protons, as well as heavier ions). We expect to interchange the SEIM and the cell-imaging microscope rather frequently. To this end a special mount has been designed and built (see Figure 1). The SEIM design was inspired by the technique of

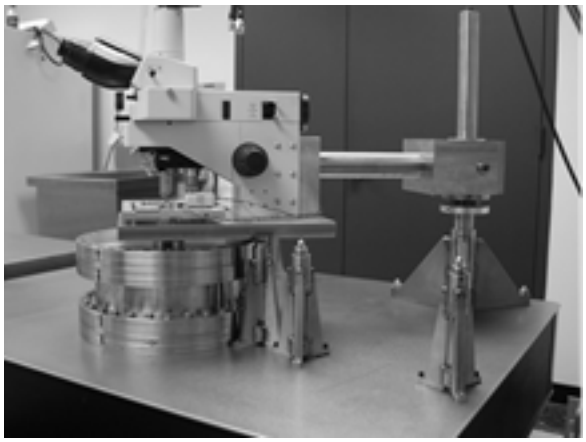

Fig. 1. The new microbeam irradiation station. On the right is the pivot arm for moving the microscope between the online and off-line positions. It will also be used to move the SEIM online and off line. The stands in the lower middle and right are to support the microscope when in the off-line position. The voice coils stage is in place on the microscope.

photoelectron microscopy (PEM) and we gratefully acknowledge the advice of a world expert in PEM, Dr. Gertrude Rempfer, in finalizing our design. The SEIM is based on secondary electrons emitted by a film on which the ions in the beam are incident. The ejected electrons are focused to form a magnified image on an image-intensified CCD. We have developed a novel "folded" design for the SEIM using a mirror lens to maintain a long path for the electrons with a more compact instrument. Calculations indicate a magnification of ~500 can be achieved, yielding a resolution of 0.1-0.2 μm.

Calculations have been performed for the design of a free-standing microbeam (FSM) based on a small, low activity radioactive alpha-particle emitter (0.1 μCi ^{210}Po) plated on the tip of a wire. Alpha particles emitted from the source are focused into a 5μm spot using a compound magnetic lens made from commercially available permanent magnets, since only a single type and energy of particle will be focused. A compound lens system similar to the one designed for the new microbeam will be used, the only difference being that it will use magnetic lenses, rather than electrostatic lenses. The FSM will replace the accelerator in our original microbeam laboratory and will be fitted with a voice coil stage for placement of the cells to be irradiated. It also will be fitted with the existing electrostatic beam deflector, used to enable fast opening and closing of the beam, enabling single particle irradiations. This facility will be used to perform microbeam irradiations during the period when the Van de Graaff is being removed and the Singletron installed. The design would also be useful for groups that desire to perform microbeam experiments at their home institutions but lack an appropriate accelerator. It is estimated that a complete FSM system, including the microscope, could be built for ~$100k.

To irradiate thick samples, such as model tissue systems or oocytes, or to use particles with very short ranges, such as the heavy ions from the laser ion source, a completely non-scattering upstream particle detector is necessary. A novel particle detector has been designed on the basis of a long series of inductive cells coupled together into a delay line. The Lumped Delay Line Detector (LD^2) will consist of 300 silver cylinders 3 mm long with a 2.2 mm inside diameter connected by inductors and capacitively coupled to ground. The cylinders are glued to a semi-cylindrical tube of dielectric material 1 m long for mechanical support. The dielectric has a semi-cylindrical metal tube around it that can be rotated about its axis to adjust the capacitance. If the individual segment delays are set (by adjustment of the capacitance) such that the propagation velocity of the pulse equals the projectile velocity, the pulses induced in all segments will add coherently, giving a fast electron pulse at one end of the delay line that is 150 times larger than the charge induced on a single cylinder. This easily detectable charge of at least 150 electrons will be amplified to provide the detection pulse for the particle counter. The inductors and the cylinders have been purchased; the rest of the detector parts await machining. It is anticipated that this detector will become the standard detector for all the irradiations on the new microbeam facility.

Development has begun on new imaging techniques to view cells without stain and to obtain three-dimensional images. Two different techniques are being investigated: phase-shifted interference microscopy and quantitative non-interference phase microscopy. In phase-shifted interferometry, images are obtained with a Mirau interferometric objective at a sequence of path (phase) differences between the sample and the lens: 0, $\lambda/4$, $\lambda/2$, and $3\lambda/4$, where λ is the wavelength of the incident light. It is important that the substrate for the cells is an optically flat, reflecting surface. Parylene dishes with aluminum plated on the outside will be used as the substrate. The combined images can be used to produce a topographic image by solving for the phase shifts at each point. The essence of the algorithm for determining the phase shifts is to solve for three variables with an over-determined system of four equations. The Mirau lens has been purchased and the substrate system is being developed. The other method being investigated is a relatively new technique that can generate phase images and phase-amplitude images using a standard microscope. To obtain a quantitative phase image, an in-focus image and very slightly positively and negatively defocused images are collected. The resulting data can be used to yield the phase distribution by Fourier-transform methods. Test images sent to the software manufacturer yielded surprisingly good resultant images. We are evaluating a trial copy of the Fourier transform-based software for generating phase images or phase-amplitude images from the three microscope images. The Mad City stage will be able to provide the vertical motion required by both these methods to obtain the necessary images for different distances between the sample and the lens.

We have investigated expanding the microbeam repertoire to include soft x-rays (Al k_α, 1.49 keV). Microbeam studies with high-energy x-rays or gamma rays are not feasible due to Compton scattering effects, so we are limited to x-ray energies where the predominant mode of interaction is photo-electron absorption. A proton beam will be focused onto an aluminum foil using the compound electrostatic lens. The characteristic x-rays produced in the foil will be focused to a diameter of 1 μm using a zone plate with a focal length of 12.7 mm. Calculations performed indicate that a 1 nA proton beam should produce a dose rate of 0.1 Gy/sec of x-rays, adequate for the biological studies envisioned. The end of the microbeam line will be modified so that the target and zone plate can be rotated into or out of the beam path to change irradiation modalities quickly.

Accelerator Utilization and Operation

Accelerator usage is summarized in Table II. Use of the accelerator for radiobiology and associated dosimetry decreased by about 25% over 2001-2002. Only about half the accelerator use for all experiments was for microbeam irradiations. Because of the relatively low number of cells that can be irradiated in a day, microbeam experiments often require considerable beam time to obtain sufficient biological material, especially for low probability events such as transformation and mutation, and therefore normally constitute a large fraction of the experimental use. These changes

RARAF staff (l-r), sitting: Dr. Alan Bigelow, Dr. Gerhard Randers-Pehrson, Dr. Charles Geard. Standing: Mr. Stephen Marino, Mr. Gregory Ross, Dr. David Brenner, Dr. Guy Garty, Mr. David Cuniberti and Mr. Gary Johnson.

in usage resulted in large part from lens development. Until August 2003, when the new microbeam line was in place and had a lens mounted in it, switching between biology experiments using a collimated beam and development using the lens was very inefficient. Three to four days were lost each time in the changes to the end of the beam line required for the two arrangements. To increase efficiency, no microbeam experiments were performed between January and July 2003, allowing us to fully concentrate on lens development.

Utilization of the accelerator by radiological physics increased greatly this past year, primarily due to the experiment on proton cooling (Exp. 115) that comprised about 20% of all the time used for experiments. On one visit, this experiment ran continuously for 3½ days. As usual, there were no chemistry experiments this reporting period.

Use of the accelerator for online development increased by 60% over last year to almost half of all available time (8 hours/day, 5 days /week, excluding holidays), mainly due to the concentration on development from January to July 2003. For several months, many more than the usual number of extra shifts was worked in the evening, on weekends and holidays, bringing total use of the accelerator to 100% of the normally available time.

Accelerator maintenance and repair time declined by a third over last year but was still somewhat higher than the long-term average due to continued problems in the power supply in the terminal used to spray negative charge on the charging belt. Despite several modifications to the supply to reduce sparking, one of two strings of high voltage diodes in the supply shorts out. The vacuum leak in one of the sections of the acceleration tube is a problem that has troubled us for several years. No replacement of the section is planned because the accelerator will be dismantled in about 15 months to make room for the new one. No major repairs or modifications to the accelerator were performed. Once the new accelerator is installed, we anticipate much less accelerator maintenance, not only because the accelerator will be new, but also because the accelerator will be charged electronically and will have few moving parts (no belt or chains). It has an RF ion source that also should require less maintenance than the Duoplasmatron source we are presently using.

Table II.

Accelerator Use, May 2002–October 2003
Percent Usage of Available Days

Radiobiology and associated dosimetry	29%
Radiological physics and chemistry	9%
On-line facility development and testing	48%
Off-line facility development	11%
Safety system	2%
Accelerator-related repairs/maintenance	11%
Other repairs and maintenance	1%

Personnel

The Director of RARAF is Dr. David Brenner. The Van de Graaff accelerator facility is operated by Mr. Stephen Marino and Dr. Gerhard Randers-Pehrson. Our ranks have now swelled to a total of seven physicists, an increase of two.

- Dr. Alan Bigelow, now an Associate Research Scientist, is continuing the development of the laser ion source, parylene coatings for microbeam slides and an optical system for 3-dimensional viewing of cells.
- Dr. Furu Zhan, a postdoctoral fellow from China, is assisting in running the accelerator, performing microbeam irradiations and developing the facility.
- Mr. Kurt Michel, an undergraduate student from Pace University, was a part-time intern until May 2003, assisting with the development of the voice coil positioning stage for the microbeam facility and parylene coatings.
- Mr. Greg Ross is a Programmer/Analyst who arrived in January, 2003. He is assisting with various programming tasks and is working on the development of the voice coil stage for the microbeam facility and a neutron target for the bomb detection system.
- Mr. Guy Garty, a Staff Associate, arrived from Israel in June 2003. He is working on the development of a focused x-ray microbeam, a source-based microbeam and an inductive detector for single ions.

Biologists from the Center for Radiological Research are stationed at the facility in order to perform experiments:

- Dr. Charles Geard, the Associate Director of the CRR, continues to spend most of each working day at RARAF. In addition to his own research, he collaborates with some of the outside users on experiments using the sin-

gle-particle microbeam facility.

- Dr. Brian Ponnaiya is an Associate Research Scientist performing experiments using the track segment and microbeam irradiation facilities.
- Ms. Gloria Jenkins, a Biology Technician, performs experiments on the microbeam facility for Dr. Geard.
- Dr. Stephen Mitchell, a Postdoctoral Fellow, continues to perform research involving neoplastic transformation of cells.
- Dr. Oleg Belyakov, another Postdoctoral Fellow, left in June 2003. He was performing experiments on the track segment and microbeam facilities using model tissue culture systems.
- Dr. Richard Miller, an Associate Professor, returned in June 2003 as a Research Scientist, but left again in October. He was working with Stephen Mitchell on experiments involving cell transformation.
- Ms. Allison Groome, an undergraduate student from Pace University working as an intern assisting Drs. Geard and Ponnaiya on a part-time basis, left in 2003.

Recent Publications of Work Performed at RARAF (2002-2003)

1. Amundson SA, Lee RA, Koch-Paiz CA, Bittner ML, Meltzer P, Trent JM and Fornace AJ Jr. Differential responses of stress genes to low dose-rate α-irradiation. *Molecular Cancer Research* **1**:445-52, 2003.
2. Bigelow AW, Randers-Pehrson G, Michel KA, Brenner DJ and Dymnikov AD. Sample targeting during single-particle single-cell irradiation. AIP Conference Proceedings for the Seventeenth International Conference on the Application of Accelerators in Research and Industry (CAARI), Denton, Texas, November 12-16, 2002. *AIP Conference Proceedings* **680**:347-50, 2003.
3. Bigelow AW, Randers-Pehrson G and Brenner DJ. Laser ion source for the Columbia University microbeam, 9th International Conference on Nuclear Microprobe Technology and Applications, ICNMTA 2002. *Nuclear Inst and Meth in Phys Res B* **210**:65-9, 2003.
4. Brenner DJ and Sacks RK. Domestic radon risks may be dominated by bystander effects – but the risks are unlikely to be greater than we thought. *Health Phys* **85**:105-8, 2003.
5. Brenner DJ and Sacks RK. Are bystander effects important? *6th International Workshop on Microbeam Probes of Cellular Radiation Response,* Oxford, UK, March 29-31, 2003.
6. Brenner DJ, Sawant SG, Hande MP, Miller RC, Elliston CD, Fu Z, Randers-Pehrson G and Marino SA. Routine screening mammography: how important is the radiation-risk side of the benefit-risk equation? *Int J Radiat Biol* **78**:1065-7, 2002.
7. Geard CR. Cellular responses to low doses using modern microbeams. Proceedings of the *Workshop on Networking Radiation Sciences in Health, Safety, and the Environment*, McMaster University, Hamilton, Ontario, November 25-26, 2002. To be published in *Radiat Res.*
8. Geard CR, Jenkins-Baker G, Bigelow A, Brenner DJ, Hall EJ, Hei TK, Marino S, Randers-Pehrson G and Ponnaiya B. Single cell gene expression and microbeam irradiation: the concept of the average cell. *6th International Workshop on Microbeam Probes of Cellular Radiation Response,* Oxford, UK, March 29-31, 2003.
9. Geard CR, Ponnaiya B, Jenkins-Baker G, Hei TK, Brenner DJ, Hall EJ and Randers-Pehrson G. Microbeam mediated cellular effects: Observations and implications for low dose radiation risk assessment. In *Molecular Mechanisms for Radiation-induced Cellular Response and Cancer Development*, Tanaka, K, Takabataka, T, Fujikawa, K, Matsumoto, T and Sato, F, Eds. Institute for Environmental Science, Japan, p. 82-8, 2002.
10. Hall EJ. How Many Bystander Effects Are There? *6th International Workshop on Microbeam Probes of Cellular Radiation Response*, Oxford, UK, March 29-31, 2003.
11. Hande MP, Azizova TV, Geard CR, Burak LE, Mitchell CR, Khokhryakov VF, Vasilenko EK, Brenner DJ. Past exposure to densely ionizing radiation leaves a unique permanent signature in the genome. *Am J Hum Genet* **72**:1162-70, 2003.
12. Horowitz YS, Oster L, Biderman S and Einav Y. Localized transitions in the thermoluminescence of LiF:Mg,Ti: potential for nanoscale dosimetry. *J Phys D Appl Phys* **36**:446-59, 2003.
13. Katanic J. Electron Spin Resonance Characterization of Human Tooth Enamel Response to Proton, Neutron, and Ultraviolet Radiation, Ph.D. thesis, Purdue University, August, 2003.
14. Kinnison JD, Maurer RH, Roth DR and Haight RC. High energy neutron spectroscopy with thick silicon detectors. *Radiat Res* **159**:154-60, 2003.
15. Maurer RH, Kinnison JD, Roth DR and Goldsten JO. Neutron spectroscopy on the international space station. *AIAA Conference on International Space Station Utilization*, Cape Canaveral, FL, 16 October, 2001. Proceedings published on CD ROM, AIAA paper 2001-5059.
16. Maurer RH, Roth DR, Kinnison JD, Goldsten JO, Gold RE and Fainchtein R. Mars Neutron Energy Spectrometer (MANES): an instrument for the Mars 2003 lander. *Acta Astronaut.* **52**:405-10, 2003.
17. Mitchell SA, Marino SA, Brenner DJ and Hall EJ. The bystander effect and adaptive response in C3H 10T½ cells. Submitted to *Radiat Res* 2003.
18. Mitchell SA, Randers-Pehrson G, Brenner DJ and Hall EJ. The bystander response in C3H 10T½ cells: the influence of cell-to-cell contact. Submitted to *Radiat Res.*
19. Morgan WF, Hartmann A, Limoli CL, Nagar S and Ponnaiya B. Bystander effects in radiation-induced genomic instability. *Mutat Res* **504**:91-100, 2002.
20. Zhou H, Randers-Pehrson G, Geard CR, Brenner DJ, Hall EJ and Hei TK. Interaction between radiation-induced adaptive response and bystander mutagenesis in mammalian cells. *Radiat Res* **160**:512-6, 2003.
21. Zhou HN, Randers-Pehrson G, Waldren C and Hei TK. Radiation induced bystander effect and adaptive response: implication for low dose radiation risk assessment. *Advances Space Research* (in press). ■

RADIATION SAFETY OFFICE 2003

Members of the RSO staff at an outing to the U.N. (l-r): James Dolan, Olga Loukhton, Dong Michelle Kang, Salmen Loksen, Dae-In Kim, Mutian Zhang, Roman Tarasyuk and Tom Juchnewicz.

PROFESSIONAL STAFF

Salmen Loksen, M.S., CHP, DABR; Director, Radiation Safety Officer
Ahmad Hatami, M.S., DABR, DABMP; Assistant Director
Thomas Juchnewicz, M.S., DABR; Assistant Radiation Safety Officer
Jacob Kamen, Ph.D., NRRPT, CHP; Assistant Radiation Safety Officer
Bruce Emmer, M.S., DABMP, DABR; Physicist
Mutian Zhang, M.S.; Acting Radiation Protection Supervisor
Dae-In Kim, M.S.; Junior Physicist
Shuntong Guo, M.S., CHP; Junior Physicist

TECHNICAL STAFF

Olga Loukhton, M.S.; Chief Technician
Roman Tarasyuk; Technician B
James Dolan; Technician B
Dong Michelle Kang, M.S.; Technician A

ADMINISTRATIVE AND SECRETARIAL STAFF

Diana Morrison; Administrative Assistant, assigned to the JRSC
Yvette Acevedo, A.A.S.; Administrative Aide
Raquel Garcia; Clerk B
Milvia Perez, A.A.S.; Clerk B
Stephen Benson, B.A.; Administrative Assistant

Top (l-r): Ahmad Hatami and Salmen Loksen. Bottom: Tom Juchnewicz and Jacob Kamen.

Table of Contents

Administrative and secretarial staff (l-r): Yvette Acevedo, Raquel Garcia, Milvia Perez and Stephen Benson.

Technicians (l-r): Dong Michelle Kang and James Dolan. Mutian Zhang. Dae-In Kim.

RADIATION SAFETY OFFICE 2003

INTRODUCTION

On May 19, 1957, the President of Columbia University distributed a memo entitled "Directive to All University Departments Having a Source of Ionizing Radiation," advising all parties of the expanded function of the Radiation Safety Committee.

Later, a notice entitled "Radiation Safety Guide for Columbia University," dated February 10, 1959, named Philip M. Lorio as the Health Physics Officer for University Departments and Laboratories other than the College of Physician & Surgeons, where Dr. Edgar Watts was the named Health Physics Officer. The Chairman of the Radiation Safety Committee was Dr. Gioacchino Failla, who initiated the Radiological Research Laboratory in the Department of Radiology of Columbia University Medical Center (CUMC).

By agreement between The Presbyterian Hospital in the City of New York (PH) and Columbia University (CU), the Radiation Safety Office (RSO) was established as an autonomous unit in 1962 for the purpose of maintaining radiation safety. The Joint Radiation Safety Committee (JRSC), appointed by the Medical Board of the Presbyterian Hospital in the City of New York and the Vice President for Health Sciences of Columbia University, is charged with the responsibility of defining and ensuring enforcement of proper safeguards in the use of sources of ionizing radiation.

Dr. Harald H. Rossi, Director of the Radiological Research Laboratories, was appointed Chairman of the Joint Radiation Safety Committee. Under his direction, this committee developed a "Radiation Safety Code and Guide," the administration of which is assigned to the Radiation Safety Officer. Dr. Eric J. Hall, the present Director of the Center for Radiological Research, now chairs the JRSC.

The present Joint Radiation Safety Committee of the Columbia University Medical Center and the New York State Psychiatric Institute came into existence through an agreement made on February 12, 1991 between New York State Psychiatric Institute (NYSPI), the College of Physicians and Surgeons of Columbia University (P&S), and The Presbyterian Hospital in the City of New York (PH). This agreement combined several overlapping clinical and educational programs, including all programs for ensuring radiation safety. The current Director of the Radiation Safety Office and Radiation Safety Officer, Salmen Loksen, C.H.P., D.A.B.R., was appointed on December 16, 1996.

The Radiation Safety Office reports to and advises the Joint Radiation Safety Committee of Columbia University Medical Center, New York Presbyterian Hospital and the New York State Psychiatric Institute. The Committee meets on a quarterly basis. For administrative purposes, the Radiation Safety Office reports to Dr. Richard Sohn, Associate Dean for Research Administration and Director of Grants and Contracts. The Radiation Safety Office participates in the review of research protocols for the Radioactive Drug Research Committee under the jurisdiction of the U.S. Food and Drug Administration.

Radiation Safety Office staff are Columbia University employees. New York Presbyterian Hospital, Columbia University College of Physicians and Surgeons, and New York State Psychiatric Institute fund the Radiation Safety Office budget via a cost sharing payback arrangement.

A full-asset merger between The Presbyterian Hospital in the City of New York and New York Hospital on December 1, 1997, created a single entity known as New York Presbyterian Hospital with facilities in two major Manhattan locations, Columbia University Medical Center at West 168th Street in Washington Heights and New York Weill Cornell Center at East 68th Street on the Upper East Side.

OVERVIEW OF RADIATION SAFETY OFFICE RESPONSIBILITIES

The Columbia University Medical Center hosts a large health sciences campus with extensive teaching, research, and clinical facilities. The basic goal of the Radiation Safety Office is to ensure the implementation of all protective measures necessary to keeping the dose from ionizing radiation to patients, visitors, students, faculty and staff on campus, and to the general community at large As Low As Reasonably Achievable (ALARA). Major entities of the campus supported by the Radiation Safety Office are:

- Columbia University, Health Sciences Campus
- Columbia University, College of Physicians & Surgeons
- New York Presbyterian Hospital
- New York State Psychiatric Institute
- New York Presbyterian Hospital, Allen Pavilion
- Columbia Cyclotron Facility - PET Net Pharmaceuticals, Inc.
- Audubon Biomedical Science and Technology Park (Audubon I)
- Russ Berrie Medical Science Pavilion (Audubon II).

Reporting to the Joint Radiation Safety Committee of Columbia University Medical Center and New York State Psychiatric Institute, the Radiation Safety Officers and the staff of the Radiation Safety Office are responsible for obtaining and maintaining licenses authorizing the possession and use of radioactive materials and obtaining and maintaining registrations and permits for the operation of radiation producing equipment. In addition, the Radiation Safety Office is responsible for obtaining and maintaining those permits necessary for the safe disposal of research or medical wastes containing low levels of radioactivity or their controlled discharge to the environment.

The Radiation Safety Office ensures the compliance of the authorized users of radioactive materials or radiation producing equipment with all governmental regulatory requirements and guidelines by means of: training, education, consultation, and by a program of internal audits and inspections of facilities. Regulatory agencies charged with oversee-

ing the possession, use, or disposal of radioactive materials or radiation producing machines are:

- United States Food and Drug Administration
- United States Nuclear Regulatory Commission
- New York State Department of Environmental Conservation
- New York State Department of Health
- New York City Department of Health, Office of Radiological Health.

The New York City Department of Health, the New York State Department of Environmental Conservation, and the United States Food and Drug Administration conduct periodic inspections and audits of the Columbia University Medical Center and New York State Psychiatric Institute facilities operating under their licenses or permits. The Radiation Safety Office works continuously to ensure that regulatory violations are prevented and to ensure those that do occur are swiftly corrected.

The Radiation Safety Office also ensures compliance with institutional policies and procedures published in the "Radiation Code and Guide of Columbia University Medical Center and New York State Psychiatric Institute."

SUMMARY OF RADIATION SAFETY OFFICE OPERATIONS FOR 2003

A representative summary of activities performed and services provided by the Radiation Safety Office is presented below. While inclusive of most major activities and services, the summary is by no means exhaustive, but is intended to provide an overview of departmental operations. An unabridged compilation of Radiation Safety Office activities and services may be found in Minutes of the Quarterly Meeting of the Joint Radiation Safety Committee of Columbia University Medical Center and New York State Psychiatric Institute.

Statistical data presented are from the fiscal year, July 1, 2002 through June 30, 2003. Activities are covered for the period through the end of December 2003.

Maintenance of New York City Department of Health Office of Radiological Health Licenses, Registrations, and Permits, Audits and Inspections

A primary activity of The Radiation Safety Office is the continued maintenance of the City of New York Radioactive Materials Licenses, the Certified Linac Registration, and the Diagnostic X-Ray Permits**.** Currently this includes:

- Radioactive Materials License No. 75-2878-01 (Broad Scope Human Use)
- Radioactive Materials License No. 92-2878-02 (Teletherapy)
- Radioactive Materials License No. 74-2878-03 (Non-Human Use)
- Radioactive License No. 52-2878-04 (Cyclotron Facility)
- Radioactive Materials License No. 93-2878-05 (Gamma Knife)
- City of New York Therapeutic Radiation LINAC Unit Certified Registration No. 77-0000019.
- Columbia-Presbyterian Hospital Radiation Installation Permit H96 0076353 86
- Columbia-Presbyterian NMC-Allen Pavilion Radiation Installation Permit H960076383 86.

Significant activities performed in 2003 to maintain the City of New York Licenses, Registrations and Permits include:

1. On August 28, 2003, the Radiation Safety Office filed with the New York City Department of Health, Office of Radiological Health, an application for the renewal of City of New York Linac Certified Registration 77-0000019 for an additional five-year period. This application is to allow the continued operation of the three therapeutic linear accelerators in the Department of Radiation Oncology. The request for renewal is submitted for review and approval by a quorum of the Joint Radiation Safety Committee.

2. On April 3, 2003, the Radiation Safety Office filed with the New York City Department of Health applications for the renewal of City of New York Radioactive Materials License Number 52-2878-04 (Cyclotron and Radioligand Laboratory). In June 2003, the Radiation Safety Office received a notice of the renewal of Radioactive Materials License 52-2878-04 for a period of five years.

3. On September 26, 2002, the Radiation Safety Office received an amended Radioactive Materials License No. 74-2878-03 (Non-Human Use) authorizing possession of SMP Model PET Gallium/Gernanium-68 sealed sources for calibration of a Concorde MicroPET scanner. And on November 1, 2002, the Radiation Safety Office received an amended License No. 75-28787-01 (Human Use) authorizing possession of Strontium-90 in several new models of the Noveste Beta-Cath intravascular brachytherapy device. Each License Amendment request had been approved by the Joint Radiation Safety Committee prior to submission to the New York City Department of Health.

4. Department of Health applications for the amendment The Radiation Safety Office filed with the New York City of City of New York Radioactive Materials License Numbers 92-2878-02 (Teletherapy), 93-2878-05 (Gamma Knife) and Linac Certified Registration 77-0000019 adding Gerald Kutcher, Ph.D., DABR as a therapy physicist. On May 19, 2003, the RSO received the amendments to Radioactive Materials License 92-2878-02, 93-2878-05 and Linac Certified Registration 77-0000019. On July 7, 2003, a quorum of the Joint Radiation Safety Committee voted to approve the addition of Sandra Russo, M.D., and Richard Gewanter, M.D., Department of Radiation Oncology, as authorized users to Radioactive Materials License Numbers 75-2878-01 (Broad Scope Human Use), 92-2878-02 (Teletherapy), 93-2878-05 (Gamma Knife), and Certified Linac Registration 77-0000019. In addition, on July 7, 2003, a quorum of the Joint Radiation Safety Committee voted to approve the addition of Robert Mooji, Ph.D., D.A.B.R., Department of Radiation Oncology, as a therapy physicist to Radioactive Materials Licenses Numbers 75-2878-01 (Human Use), 92-2878-02 (Teletherapy), 93-2878-05 (Gamma Knife) and Certified Linac Registration 77-0000019. The Radiation Safety Office is in the process of preparing the appropriate amendment applications.

5. As reported to the Joint Radiation Safety Committee in the Quarterly Report of the Radiation Safety Office dated April 3, 2003, the Radiation Safety Office filed with the New York City Department of Health applications for the amendment of City of New York Radioactive Materials License Numbers 75-2878-01 (Human Use), 92-2878-02 (Teletherapy), 93-2878-05 (Gamma Knife) and Linac Certified Registration 77-0000019 adding Yoichi Watanabe, Ph.D., D.A.B.R., Tian Liu, Ph.D., D.A.B.R., and Dennis Mah, Ph.D., D.A.B.R. as therapy physicists. On May 19, 2003, the RSO received an amendment to Radioactive Materials License 75-2878-01 (Human-Use), 92-2878-02 (Teletherapy), 93-2878-05 (Gamma Knife) and Linac Certified Registration 77-0000019.

6. The New York City Department of Health, Office of Radiological Health conducts periodic unannounced audits of records and inspections of facilities at the Columbia University Medical Center operating under the Radioactive Material Licenses, the Certified Linac Registration, and the Diagnostic X-ray Registrations. In 2003, these audits and inspections included:

- July 10, 2002 through July 12, 2002, License 93-2878-05 (Gamma Knife)
- November 10 and 12, 2003, License 52-2878-04 (Cyclotron & Radioligand)
- September 10, 2002 through November 14, 2002, License 74-2878-03 (Non-Human Use)
- September 18, 2002 through September 24, 2002, License 75-2878-01 (Human Use)
- June 2, 2003, Certified Linac Registration 77-00000019
- August 5, 2003, Radioactive Materials License 92-2878-02 (Teletherapy).

7. The New York City Department of Health, Office of Radiological Health reports the results of these audits and inspections to representatives of the Management of Columbia University and the New York Presbyterian Hospital, New York State Psychiatric Institute, and the Radiation Safety Office. All records and activities were deemed to be in compliance with the Rules of the City of New York, Article 175, Radiation Control and the Conditions of the Licenses and Certified Registration with the possible exception of a single calibration performed in the Department of Radiation Oncology. On December 7, 2002, the Radiation Safety Office provided documentation to a New York City Department of Health Administrative Tribunal that this calibration was performed in full compliance with Article 175. The Radiation Safety Office is awaiting the decision of the Department of Health in this matter.

8. The RSO prepared a request to the NYC Department of Health to authorize the removal of a number of high personnel radiation dosimetry readings obtained in the PET Imaging Suite during the First Quarter of 2003. In the Quarterly Report dated July 7, 2003, the Radiation Safety Office reported to the Committee that an investigation of the dosimetry readings revealed that they did not represent actual personnel radiation doses but were due to storing the dosimetry next to a radioactive check source.

9. As reported to the Joint Radiation Safety Committee in the Quarterly Report of the Radiation Safety Office dated July 7, 2003, the New York State Education Department's Office of the Professions has directed that medical physicists must apply for a New York State professional License in order to continue to practice in New York State. Licenses are required for the practice of diagnostic radiologic physics, medical health physics, medical nuclear physics and therapeutic radiological physics. It is essential that all medical physicists and medical physics assistants working under their supervision obtain appropriate licensure in order to continue their work at the Medical Center. Departments and individuals requiring information or assistance regarding licensure are encouraged to contact the Radiation Safety Office. At present, all senior officers of the Radiation Safety Office are certified either by the American Board of Health Physics, the American Board of Medical Physics, and/or the American Board of Radiology and are licensed to practice as Medical Physicists by the State of New York.

10. As reported to the Joint Radiation Safety Committee in the Quarterly Report of the Radiation Safety Office dated July 7, 2003, in accordance with the requirements of RCNY 175 and the Conditions of the City of New York Radioactive Materials Licenses and Therapeutic Radiation Linac Certified Registrations, the Radiation Safety Office again reminded all Authorized Users that any proposed changes to: statements, representations and procedures; facilities; quantities of radionuclides and their chemical or physical forms; authorized users, therapy physicists and radiation safety officers; the receipt and use of radioactive materials for medical purposes, from those permitted or referenced by the current License or Registration must be submitted to the Joint Radiation Safety Committee in a timely manner for review and approval prior to their planned implementation. Minor or "ministerial" changes must be submitted for review and approval by the Joint Radiation Safety Committee (RCNY 175.103(b)(3)(ii)(C) & (D), (iii), (iv)). Substantial changes require review and approval by the Joint Radiation Safety Committee prior to being submitted to the Office of Radiological Health for amendment of the License or Registration (RCNY 175.103(a)(4), (b)(3)(ii)(B) & (E), (iii), (iv)).

In addition, the Radiation Safety Office reminded all Authorized Users that Conditions of certain City of New of York Radioactive Materials Licenses may require certain functions or procedures performed only by or under the supervision and in the physical presence of specific Authorized Users, Authorized Technical Personnel, Therapy Physicists, and Physicians named on the License.

11. The Radiation Safety Office reminded all Authorized Users that RCNY 175 requires all misadministrations be reported to and investigated by the Radiation Safety Officer. RCNY 175.103(2) requires that: "(ii) The radiation safety officer shall: (A) investigate overexposures, misadministrations, accidents, spills, losses, thefts, unauthorized receipts, uses, transfers, and disposals, and other deviations from approved radiation safety practice and implement corrective actions as necessary."

12. From July 10, 2002 through July 12, 2002, the New York City Department of Health, Office of Radiological Health, Radioactive Materials Section conducted an audit of

records and an inspection of facilities authorized under New York City Radioactive Materials License 93-2878-05 (Gamma Knife). On September 27, 2002, the Radiation Safety Office received from the Office of Radiological Health, Notice of Violation, Docket #17847-02X0 citing Columbia University Medical Center for two violations resulting from the Gamma Knife inspection.

The Hearing Officer requested that additional documentation of Dosimetry system calibrations be provided by Columbia University Medical Center and adjourned the Administrative Tribunal until January 16, 2003.

On January 16, 2003, the Administrative Tribunal was called to order, and Columbia University Medical Center provided the Hearing Officer with all documentation requested. The Administrative Tribunal was adjourned pending the decision of the Hearing Officer. Since the last report made to the Joint Radiation Safety Committee on July 7, 2003, there has been no further action on this issue.

13. In compliance with Office of Radiological Health Information Notice N.2001-1, the Radiation Safety Office prepared a list of all analytical x-ray equipment at Columbia University Medical Center. The list included equipment such as electron microscopes, analytic x-ray units, x-ray fluorescense units, particle accelerators, and x-ray machines utilized for academic purposes that are non-commercial in nature.

Maintenance of New York State Department of Environmental Conservation Permits, Audits and Inspections

Another primary activity of The Radiation Safety Office is the continued maintenance of New York State Department of Environmental Conservation Radiation Control Permit No. 2-6201-00005/00006.

Under the Conditions of the Radiation Control Permit and in compliance with New York State 6 NYCRR Part 380, Rules and Regulations for Prevention and Control of Environmental Pollution by Radioactive Materials, Columbia University Medical Center conducts medical research and clinical activities that discharge limited and controlled quantities of radioisotopes to the atmosphere and to sewage systems.

The Columbia University Medical Center is sited within a densely populated urban area. The quantities of radioisotopes discharged and the resulting public radiation dose are closely regulated by the New York State Department of Environmental Conservation. Radiation doses to the general public resulting from atmospheric discharges of radioisotopes are required not to exceed the U.S.N.R.C. Constraint Limit of 10 mrem per year.

Columbia University Medical Center and the New York State Psychiatric Institute are currently permitted a total of fifteen (15) atmospheric emission points from which radionuclides are discharged to the atmosphere. Monitoring, analyzing, reporting, and minimizing discharges from these emission points, in order to ensure compliance with the Conditions of the Radiation Control Permit, is one of the major continuing activities of the Radiation Safety Office.

Significant activities performed in 2003 to maintain the New York State Department of Environmental Conservation Radiation Control Permit include:

1. As required by New York State 6 NYCRR Part 380 and the Conditions of the New York State Department of Environmental Conservation Radiation Control Permit, the Radiation Safety Office will be submitting an Annual Report summarizing Discharges of Radioactive Effluents to the Environment from the fifteen atmospheric emission points and by controlled sewer disposal by the end of March 2004. For the calendar year 2002, all atmospheric discharges were within the quantities authorized by the Radiation Control Permit, and the resulting public dose was within the U.S.N.R.C. Constraint Limit of 10 millirem per year. All discharges to sewers were well below the Effluent Concentration Limits as required by Part 380-11.7, Table of Concentrations.

2. On April 3, 2003 the Radiation Safety Office informed the Joint Radiation Safety Committee of the audit and inspection of NYSDEC Radiation Control Permit 2-6201-0005/0006 conducted on March 13, 2003 by the New York State Department of Environmental Conservation. On April 24, 2003, the RSO received from the NYSDEC a Notice of Violation reporting the findings of that inspection. These findings included atmospheric discharges of Fluorine-18 and Nitrogen-13 from the Cyclotron Facility in excess of Permit Limits during the calendar year 2002. In the Notice of Violation, the NYSDEC took note of the corrective actions already put into practice by CPMC, but also required the submission of further documentation of actions taken in four specific areas: commitment to monitoring atmospheric discharges; communications; training; utility support. The Notice stated that though the quantities of F-18 and N-13 exceeded the numerical limits of the Radiation Control Permit the constraint limit dose of 10 mrem per year to the general public from the atmospheric discharge of radioisotopes had not been exceeded. A memorandum dated June 10, 2003, documenting the corrective actions in these four areas was prepared by the Radiation Safety Office and submitted to the NYSDEC.

3. In the Quarterly Report of the Radiation Safety Office to the Joint Radiation Safety Committee, dated July 7, 2003, the Radiation Safety Office reported extensively and in depth on discharges of C-11 from the Cyclotron Facility in June 2003 that exceeded the numerical limits of the Radiation Control Permit. These discharges were reported to the NYSDEC. The Radiation Safety Office received from the NYSDEC a memorandum dated July 2, 2003, confirming their previous verbal authorization to continue operations at the Cyclotron Facility, as the public dose resulting from the discharges did not exceed the constraint limit of 10 mrem per year to the general public from the atmospheric releases of radioisotopes. The NYSDEC memorandum of July 2, 2003, set interim discharge limits of 6 Curies of C-11 and 200 millicuries of N-13 for the Cyclotron Facility exhaust stack. The NYSDEC memorandum of July 2, 2003, further required Columbia University Medical Center to request a permit modification to reflect all physical and procedural changes made in regard to effluent systems, including reassignment of discharge quantities among the emission points on the Milstein Hospital rooftop. The deadline for filing this permit modification request was set by the

NYSDEC to be September 1, 2003.

The Radiation Safety Office received an additional memorandum from the NYSDEC dated August 4, 2003, regarding Notice Of Intent To Modify Permit. This memorandum required the maximum annual quantity of C-11 discharged from the Radioligand lab exhaust stack be reduced from 20 Curies to 12 Curies to balance the re-assignment of additional C-11 discharge capacity to the Cyclotron exhaust stack.

On February 24, 2004, the Radiation Safety Office submitted to the New York State Department of Environmental Conservation, Division of Environmental Permits, Region 2, in a timely manner, a modification request for NYSDEC Radiation Control Permit 2-6201-00005/00006. Calculations included with this permit modification request demonstrate compliance with the constraint limit 10 mrem per year to the general public from the atmospheric discharge of radioisotopes.

4. On August 28, 2003, as requested by Markus Spivak, Environmental Radiation Specialist, NYSDEC in correspondence to Salmen Loksen, Director, Radiation Safety Office, dated June 17, 2003, the Radiation Safety Office sent Mr. Spivak a complete incident report of the discharges of C-11 in June 2003. The report, taken principally from the Quarterly Report of the Radiation Safety Office to the Joint Radiation Safety Committee, dated July 7, 2003, and from the Report of Norman Simpson, Director, Radioisotope and Radioligand Production, dated June 30, 2003, gives the proximate causes of the incident, accounts for all factors contributing to the releases remaining unrecognized, and outlines the steps taken to ensure that this type of incident will be precluded in the future.

5. Acceptance testing on May 18 indicated that the combo target in the Cyclotron could operate with acceptable discharges of F-18 and N-13. However, long-term follow-up over the months of May and June indicates a higher level of discharge of N-13 than previously expected. Approximately 30% of the annual limit for the discharges, were released in May 2003 and by July 7, 2003, the date of the Quarterly Meeting of the JRSC, N-13 releases were at 86% of the Annual Permit Limit. At the previous Quarterly Meeting of July 7, 2003, the Radiation Safety Office recommended to the JRSC that PET Net corporate service address the N-13 discharge problem. The Radiation Safety Office further recommended that if problems with the "Combo-Target" could not be resolved, the single isotope target might need to be reinstalled.

On July 17, 2003, with the "Combo-Target" in operation, stack monitoring analysis detected the discharge of 50.73 mCi of N-13 from the Cyclotron exhaust stack. This put the atmospheric discharge of N-13 from the Cyclotron Facility stack at 137.2% of the annual Permit Limit and 68.6% of the 200 mCi authorized in the NYSDEC memorandum dated July 2, 2003.

On July 19, 2003, and July 20, 2003, at the initiation of the PET Net Cyclotron Manager, the "Combo-Target" was removed from the cyclotron, and a non-vented single isotope target was installed on beam-line #2. On July 20, 2003, graduated test runs of the newly installed single-isotope target were performed. No discharges or elevated radiation levels were observed during the test runs. Continued monitoring of N-13 discharges from the single isotope target reveals satisfactory radiation safety performance to date.

6. On July 25, 2003, the Radiation Safety Office installed a temporary 24" x 24" x 2" coconut charcoal filter in the plenum above the Nuclear Medicine Hot Lab Hood. Installation of this filter allows the discharges of I-131 from this source to be reduced by a factor of 90%. Periodic monitoring of this filter for contamination by Xenon-133 is performed. On July 23, 2003, the Radiation Safety Office obtained from AKF Engineering design drawings for a permanent installation of a charcoal filter housing in the Nuclear Medicine exhaust system in the 10th floor machine area. At present, the Radiation Safety Office has received one bid for this construction and is in the process of obtaining others.

7. As required by 6 NYCRR Part 380 and the conditions of our N.Y.S.D.E.C. Radiation Control Permit, the Radiation Safety Office has reviewed atmospheric discharges of volatile isotopes of Iodine and Xenon-133 gas. All First and Second Quarter discharges of volatile isotopes of Iodine and Xenon gas were well within the Maximum Annual Quantity Authorized in our Permit. Quarterly trends indicate that annual discharges will be under 100% of Permit Limits. Iodine-131 discharged from Emission Point I (Nuclear Medicine Stack, Milstein Hospital Building roof-top) from January 1 through August 31, 2003 was 91.88% of the Permit Limit. Xenon-133 discharged from Emission Point I from January 1 through June 30, 2003 was 6.31% of the Permit. Since the installation of the non-vented single isotope target on July 20, 2003, all discharges from the Cyclotron exhaust stack have been within normal, acceptable limits.

8. The Radiation Safety Office reminded all Authorized Users whose laboratories discharge radioisotopes to the atmosphere that, in accordance with New York State Department of Environmental Conservation, Application Guidelines For Radiation Control Permits For Discharge Of Radioactive Materials In Effluents To Air, E. Permit Modifications, Columbia University Medical Center is required to conduct its Radiation Safety Program in accordance with the statements, representations, and procedures contained in the application and supporting documents of NYSDEC Radiation Control Permit 2-6201-0005/0006. The Guidelines require that, before any changes are made to operations, facilities, equipment, procedures, or radioactive materials that affect discharges, the proposed changes must be submitted to the Joint Radiation Safety Committee for review and approval prior to being submitted to the New York State Department of Environmental Conservation as a Permit Amendment Request.

Administration of Radioactive Material: Receipt, Distribution, and Radioactive Waste Disposal

A major program of the Radiation Safety Office is the centralized administration of all authorized radioactive material use at the Columbia University Medical Center and New York State Psychiatric Institute.

Types of radioisotopes, allowed uses and possession limits for member Institutions and major Departments are au-

thorized under five separate City of New York Radioactive Materials Licenses.

The use of authorized radioisotopes by individual Authorized Users and Responsible Investigators is controlled by the Joint Radiation Safety Committee through the administration of the Radiation Safety Office. Human Use of radioactive materials by Authorized User Physicians is allowed after a review of credentials and a majority vote by a quorum of the Joint Radiation Safety Committee. Non-Human Use of radioactive materials is allowed after a review of credentials and written permission of the Radiation Safety Office. In the Year 2003, thirteen (13) new Responsible Investigators were approved for non-human use of radioactive materials and fifty-eight (58) current Responsible Investigators received renewal of their authorizations.

The Radiation Safety Office maintains a Radioactive Waste Transportation permit with the State of South Carolina in order to allow for transfer of Low-Level Radioactive Waste to a disposal site in Barnswell, South Carolina.

Significant activities performed in 2003 to administer, receive, distribute, and dispose of radioactive materials included:

1. The Radiation Safety Office received and distributed 2872 packages containing radioactive material, excluding shipments to the Nuclear Medicine and Radiation Oncology departments. For all shipments, the Radiation Safety Office conducted package surveys and ensured correct distribution to Authorized Users and Responsible Investigators. The Radiation Safety Office maintains inventory control of all radioactive materials received and distributed through the use of a detailed and extensive computerized database.

2. The Radiation Safety Office provides scheduled pick-ups of radioactive waste generated by the activities of the Authorized Users and Responsible Investigators.

3. On December 11, 2002, the Radiation Safety Office shipped a total of fifty-four 30-gallon drums of Liquid Scintillation Vial waste for disposal by NSSI/Sources and Services of Houston, Texas. Total volume of the shipment was 6.13 cubic meters, weighing 8,100 kilograms. The total activity shipped was 14.8 mCi, in which 12.6 mCi was of tritium (3H) and 2.2 mCi was of other radionuclides.

4. On March 5, 2003, the RSO shipped a total of fifty-four(54) drums of Dry Active Waste (thirteen 55-gallon and forty-one 30-gallon drums) for disposal by Envirocare of Utah via GTS Duratek Super-Compaction. On the same day, the RSO shipped a total of five (5) fiber drums of solid animal carcasses for incineration at Envirocare of Utah. The total volume of the dry waste shipment was 261.91 cubic feet, weighing 5,025 pounds. The total dry waste activity shipped was 57.048 mCi, in which 50.351 mCi was of tritium (^{3}H), 3.096 mCi was of carbon-14. The shipped animal carcasses had total volume of 9.3 cubic feet, weighted 56.70 kilograms and contained 4.21 mCi of tritium.

5. On June 23, 2003, the RSO shipped forty 30-gallon drums of liquid scintillation vials (LSV) for disposal by NSSI Sources & Services of Texas via RADIAC Research Corp. The total volume of the LSV shipment was 160.4 cubic feet, weighing 6,000 pounds. The total activity shipped was 16.608 mCi, in which 13.353 mCi was of tritium (^{3}H), 2.545 mCi was of carbon-14, and 0.708 mCi was of other radionuclides.

6. On August 14, 2003, the RSO shipped fifteen 30-gallon drums of liquid scintillation vials (LSV) for disposal by NSSI Sources & Services of Texas via RADIAC Research Corp. The total volume of the LSV shipment was 60.2 cubic feet, weighing 2,250 pounds. The total activity shipped was 2.627 mCi, in which 1.987 mCi was of tritium (^{3}H), 0.371 mCi was of carbon-14, and 0.269 mCi was of other radionuclides.

7. On October 23, 2003, the RSO shipped thirteen 30-gallon drums and one 55-gallon drum of liquid scintillation vials (LSV) for disposal by NSSI Sources & Services of Texas via RADIAC Research Corp. The total volume of the LSV shipment was 59.5 cubic feet, weighing 2,200 pounds. The total activity shipped was 4.64 mCi, in which 4.561 mCi was of tritium (^{3}H), 0.069 mCi was of carbon-14, and 0.01 mCi was of other radionuclides.

8. As of June 30, 2003, the Radiation Safety Office had disposed of approximately 1,257 cubic feet (35.6 cubic meters) of short half-life radioactive waste through decay-in-storage, and approximately 5,010 liters of low-level aqueous radioactive waste through monitored sewer disposal. The total activity of sewer-disposal aqueous radioactive waste was 46.314 mCi, of which 39.284 mCi was tritium (^{3}H), 6.956 mCi was ^{14}C, and 0.074 mCi was other radionuclides.

9. As of June 30, 2003, the Radiation Safety Office had disposed of approximately 1,257 cubic feet (35.6 cubic meters) of short half-life radioactive waste through decay-in-storage, and approximately 5,010 liters of low-level aqueous radioactive waste through monitored sewer disposal. The total activity of sewer-disposal aqueous radioactive waste was 46.314 mCi, of which 39.284 mCi was tritium (3H), 6.956 mCi was 14C, and 0.074 mCi was other radionuclides.

10. As required by 6 NYCRR Part 380 and the conditions of our NYSDEC Radiation Control Permit, the Radiation Safety Office has reviewed controlled sewer disposal of aqueous radionuclides. During the entire fiscal year, the discharge for all isotopes was well below the concentration limits of 6NYCRR Part 380-11.7 Table II.

11. As of June 30, 2003, the Radiation Safety Office had picked up 1,038 waste containers from research labs, and delivered 1,022 waste containers. During the same period, the Radiation Safety Office picked up 250 bags of patient waste from clinical areas.

12. During the fiscal year of 2003 the RSO reviewed one "Application for the Use of Radioisotopes" and issued 2872 isotope orders. The above orders resulted in the purchase of a total of approximately 16.843 Curies of activity. ^{35}S, ^{3}H, ^{32}P, ^{103} Pd (seeds), and ^{125}I were the five isotopes purchased with the highest activities.

13. RSO and Environmental Health & Safety (EH&S) staff continued to develop a mixed waste program. Supported by the audit section of the RSO, waste area staff has started monitoring liquid waste that might contain hazardous chemicals. As of this quarter, the Radiation Safety Office did not have any known hazardous waste or mixed waste containing toluene or xylene in the storage facilities. Mr. Loksen requested that Mr. Hatami inquire from the NYSDEC as to

their policies regarding liquid mixed waste. The NYSDEC responded that neither the RSO nor researchers are allowed to dilute a mixed waste if it contains more than 24% alcohol by volume. This information will be included in the Policy and Procedure being developed by the RSO and EH&S. All researchers will be informed of the NYSDEC's response by the RSO in the new Policy and Procedure. On December 1, 2003 the RSO sent a memo to all Responsible Investigators regarding the existing policy of not accepting liquid mixed waste for storage in its radioactive waste storage and disposal area. Training is offered to all researchers regarding this policy.

14. On April 10, 2003, the Radiation Safety Office filed a report with the New York State Energy Research and Development Authority for 2002 Low-Level Radioactive Waste.

15. On May 30, 2003, Ahmad Hatami generated a Policy and Procedure Manual issued to the Pathology Department for the Safe Handling of Pathologic Examination of Technetium-99M Labeled Specimens. This policy was reviewed and signed by Salmen Loksen and Ahmad Hatami.

16. On June 16, 2003, Ahmad Hatami, Mutian Zhang, and Michelle Kang attended the Environmental Resource Center's annual Hazardous Waste Training Seminar.

17. On June 19, 2003, Ahmad Hatami, Mutian Zhang, Olga Loukhton, and Dae-In Kim of the RSO attended a one-day course on DOT/IATA Radioactive Shipping Training given by the New Jersey and Greater New York Chapters of the Health Physics Society.

18. During 2003, EH&S developed a Hazardous Materials Transportation Security Plan for shipments of hazardous material regulated under CFR 172.802 including hazardous waste, radioactive materials and radioactive waste. On December 17, 2003, the EH&S officers provided a training lecture on the Security plan and blood borne pathogens to RSO staff.

19. Low-level mixed waste (LLMW), which contains both radioactive materials and hazardous chemicals, is regulated under EPA regulations as well as NRC regulations. In order that the management of liquid waste generated in CUMC, NYPH and NYSPI complies with all of the above regulations, the RSO, together with EH&S, developed a Policy and Procedure for liquid radioactive waste management. On January 6, 2004, the RSO and the EH&S officers held a meeting on the Policy and Procedure for low-level mixed waste. The RSO and EH&S officers are in the process of reviewing the document, and after it is finalized, the RSO will distribute it to all authorized users of radionuclides.

20. The Radiation Safety Office is in the process of planning for the disposal of orphaned radioactive sources from the Radiological Research Lab and throughout CUMC, NYPH and the New York State Psychiatric Institute. On September 10, 2003 Michael Lindstrom from the Los Alamos Lab contacted Mr. Hatami concerning eight Am-241 sealed sources that are located in the medical center and asked for further documentation and pictures of the sources. In response, the RSO is providing the documentation requested by Mr. Lindstrom. On July 22, 2003, a representative from the Los Alamos Lab in charge of Pu/Be recovery requested that, if it is possible, the downtown campus become a storage site for all Pu/Be recovery sources in the metropolitan area for a near future pick-up. The shipment is scheduled for February 10, 2004.

ALARA Program - Personnel Dosimetry, Bioassay, and Area Monitoring

In accordance with regulatory requirements, the Radiation Safety Office operates an ALARA (As Low As Reasonably Achievable) Program to ensure that the radiation doses to all workers at the Columbia University Medical Center and New York State Psychiatric Institute and the radiation doses to the general public resulting from all operations of Columbia University Medical Center and the New York Psychiatric Institute are within the legal limits and As Low As Reasonably Achievable (ALARA).

The principal methods of monitoring radiation dose are the assignment of personnel radiation dosimeters to individuals, the posting of area and environmental dosimeters, and the monitoring of all discharges containing radioactivity.

Immediate action is taken, as appropriate, in response to unusual or high dosimeter readings. Quarterly ALARA Reports are prepared and submitted to the Joint Radiation Safety Committee. The Quarterly ALARA Report presents: the doses of individual workers that exceed ALARA I Limits; the results of investigation of doses to individual workers that exceed ALARA II Limits; and discussions of significant trends within departments that may experience high individual doses. In addition, the Quarterly Environmental ALARA Report is prepared and submitted to the Joint Radiation Safety Committee. The Quarterly Environmental ALARA Report presents the quantities of radionuclides discharged to the atmosphere and the sewer system and the resulting dose to the general public.

In 2003, all doses to individual workers were less than the legal annual reportable limits as specified in RCNY Article 175, Radiation Control, except for one person from PET Suite who left her badge next to a radiation check source. All doses to the general public resulting from atmospheric discharges of radionuclides were less than the U.S.N.R.C. constraint limit of 10 mrem per year.

Significant activities performed in 2003 to maintain the ALARA Program were:

1. The Radiation Safety Office distributed approximately 9,000 personnel radiation dosimeters each quarter, including both monthly and quarterly badges. A total of about 36,000 dosimeters were distributed and collected in 2002. To maintain dosimetry records, the Radiation Safety Office uses dedicated computers with Internet and direct modem access to the database of the dosimeter supplier, Landauer Inc.

2. The Radiation Safety Office received Annual Occupational Exposure Reports (NRC Form 5) from Landauer Inc. for the year 2002 and forwarded these reports to radiation workers as required by the New York City Department of Health regulations.

3. In 2003, the Radiation Safety Office notified 63 employees with ALARA Level 1 readings and investigated 33 cases of ALARA Level II readings as reported by Landauer

Inc. Particular attention was paid to occupational groups that typically exceed the ALARA limits, i.e., workers and researchers at the Cyclotron Facility, Angiography, the Cardiac Cath Lab, and physicians in the PET Suite.

4. In 2003, the Radiation Safety Office performed 38 thyroid bioassays on radiation workers using radioactive isotopes of iodine including: Iodine-123, Iodine-125, and Iodine-131.

5. Since the number of personal radiation dosimeters has been steadily increasing, the process of distributing exposure reports was found to be inefficient and time consuming. As a result of a new agreement between Landauer Inc and CUMC on April 1, 2003, a second copy of exposure reports (without personal information or Social Security number) is now directly sent to each group. This process was implemented during the badge-reporting period of April 2003 and is working efficiently.

6. During fiscal year 2002-2003, 19 radiation workers completed declaration of pregnancy forms. The Radiation Safety Office provided them with health physics counseling about risk factors and additional monitoring of the fetus during their gestation period while continuing to closely follow their personnel radiation exposure reports.

7. The RSO held two meetings on May 27, 2003 and June 2, 2003 for badge coordinators. Attendees were updated on the following issues: the importance of returning badges on time; regulatory requirements; exposure reports and units; ALARA review and investigation of exposures; previous exposure history; annual occupational dose limits; pregnancy policy and fetal dose limits; and proper use and badge wear, including wear during fluoroscopy procedures. An officer of the Radiation Safety Office answered questions and addressed concerns from the audience. The Radiation Safety Office is in the process of planning for the next meeting in the spring of 2004.

Radiation Safety Compliance – Routine Internal Inspections and Audits

A major activity of the Radiation Safety Office is the performance of quarterly inspections of facilities and audits of records of approved clinical departments and research laboratories to ensure compliance with regulatory requirements as authorized by the Joint Radiation Safety Committee.

Significant compliance activities conducted in 2003 include:

1. The RSO completed annual inspections and audits of CUMC and New York State Psychiatric Institute clinical facilities using radioactive materials. The audits and inspections are to ensure compliance with City of New York Radioactive Materials License conditions and with RCNY Article 175, Radiation Control. The facilities audited include: New York Presbyterian Hospital Nuclear Cardiology, NYPH Nuclear Medicine, Allen Pavilion Nuclear Cardiology, and Allen Nuclear Medicine. In addition, The RSO performed the required quarterly inventory and leak testing for all radioactive sources located in the following facilities: Milstein Nuclear Medicine, Allen Pavilion Nuclear Medicine, Cyclotron, and Columbia University Health Sciences (VC-11 Alpha sources, Irradiators, etc.). All were found to be in compliance. Leak Test Certificates were generated and issued for each of the above sealed sources.

2. In 2003, the Radiation Safety Office performed 1,173 routine radiation safety inspections and audits of Columbia University Medical Center and New York State Psychiatric Institute research laboratories using radioactive materials. The results were communicated to the Responsible Investigators. A total of 164 deficiencies were followed up by correction of the cited deficiencies. During the same period, the Radiation Safety Office conducted 69 laboratory clearance and exit and entry surveys.

3. In 2003, the Radiation Safety Office measured airflow rates in 102 fume hoods in which volatile radioactive materials are used. In all rooms where radioactive gases or aerosols are used, ventilation rates were measured and Spill Gas Clearance Times were calculated and posted. Adjustments were made as required to air supply and exhaust systems to obtain negative pressure conditions. The RSO performed face velocity measurements on approximately 57 fume hoods in which radioisotopes are used or stored. Researchers whose hoods did not meet safe flow rate standards were instructed to have their hoods repaired or replaced. There were 34 fume hoods for I-125 or other volatile isotopes. Surveys were conducted for 130 hoods, among which 84 AFV measurements were taken.

4. Some areas, such as Allen Pavilion Room 1-198 (Nuclear Medicine), were found not to be under negative pressure. Adjustment to the air supply and exhaust system was recommended. Nuclear Medicine will inform the RSO when the problem is corrected so that the airflow study can be repeated.

5. In addition to the regular inspections of clinical facilities and research laboratories, the Radiation Safety Office investigates major spills, incidents involving radioactive materials, and misadministrations. In 2003, the Radiation Safety Office responded to 15 spill incidents. The Radiation Safety Office ensured that timely notice of reportable incidents was made to the New York City Department of Health, Office of Radiological Health.

6. The RSO responded to three spill incidents in the Nuclear Cardiology Department, which were minor incidents in terms of the quantity of radioisotopes. After proper decontamination procedures, residual surface contamination was well within the limits of Article 175.

7. On October 17, 2003 a tritium spill occurred in Dr. Sturley's lab, PS 3-426. Four glass syringes containing less then 1 uCi H-3 were broken after being dropped on the floor. The broken glass scattered in an area of about 10 square feet. The floor was carefully cleaned up. Wipe tests gave background readings.

8. On November 12, 2003, a tritium spill occurred in Dr. Clynes' lab, PS 8-440A. The lab reported that about eight liters of H-3 containing solution leaked from a waste carboy. The RSO responded immediately and supervised decontamination. After the room was cleaned, wipe test showed background readings. Personnel survey and bioassay were performed, and no intake or contamination was found. The amount of tritium involved in the incident was ~370 μCi.

Training

In accordance with regulatory requirements the Radiation Safety Office provides initial radiation safety training to all new employees of the Columbia University Medical Center and the New York State Psychiatric Institute prior to their beginning work with radiation equipment or radioactive materials. The Radiation Safety Office provides the required annual refresher training thereafter.

Significant training activities in 2003 included:

1. Pursuant to Article 175 of the New York City Health Code, the following radiation safety courses and training sessions were presented from July 2002 through June 2003:
   - 12 initial training seminars for individual researchers
   - 12 annual refresher seminars for researchers
   - 12 nursing seminars for New York Presbyterian Hospital
   - Training sessions for Dental School residents
   - Training sessions for Radiology residents
   - Training sessions for the Facilities Department.
2. For employees who could not attend the regularly scheduled classes, the Radiation Safety Office designed and implemented a self-study program, including the use of videotapes available at the Health Sciences Library. A passing grade on a quiz administered after viewing the video qualifies an employee working in Non-Human Use applications to be issued a personnel radiation dosimeter and authorizes that employee to begin work with radioactive material or radiation equipment. If the individual's employment involves human use of radioactive material, a passing grade on the quiz results in obtaining a temporary badge until the next regularly scheduled training session is attended.
3. On April 1, 2003, Ahmad Hatami presented an annual refresher course for X-ray, Nuclear Medicine, and Hospital groups.
4. On April 2, 2003, Mr. Hatami gave a radiation safety-training course for the supervisors and ancillary personnel of the Columbia University. The course included a PowerPoint presentation and was conducted in English with handouts in English and Spanish.
5. On April 23, 2003, an annual refresher course was given by Ahmad Hatami for Drs. Greene and Shelanski's groups in the Department of Pathology.
6. In April and May of 2003, Mr. Hatami presented four sessions of ER Training on the Use of Survey Meters for the Adult and Pediatric Emergency Room personnel.
7. From June 21, 2003 through June 26, 2003, Thomas Juchnewicz, Assistant Radiation Safety Officer attended the AAPM Summer School held at Colorado College in Colorado Springs, Colorado. The topic of the Summer School is IMRT and Conformal Therapy. It is anticipated that this training will be of assistance to the RSO's continuing radiation safety support to the Department of Radiation Oncology.

Professional Radiation Safety and Health Physics Support

The Radiation Safety Office provides professional radiation safety and health physics consultation to clinical departments, research laboratories, Authorized Users, and Responsible Investigators to ensure compliance with technical requirements in the regulations and good practice in the safe use of radioactive materials and radiation equipment.

Specific examples of professional support provided by the Radiation Safety Office in 2003 include:

1. In 2003, the Radiation Safety Office provided radiation safety support for 75 brachytherapy and Iodine-131 radiopharmaceutical therapy patients receiving treatment from the New York Presbyterian Hospital Departments of Nuclear Medicine and Radiation Oncology. This support included: room preparation; distribution of personnel radiation dosimeters; performance of patient and room surveys; posting instructions in patient rooms; entering instructions in patient charts; patient discharge surveys; room decontamination; and removal of patient generated wastes for decay-in-storage and disposal.
2. An officer of the Radiation Safety Office participates as a Member of the Animal Care Protocol Review Committee, reviewing all procedures using radionuclides in animal research.
3. In 2003, the Radiation Safety Office performed 37 routine animal radiation surveys in the Institute of Comparative Medicine in order to minimize contamination in animal facilities and cages, protect Animal Care staff, and ensure proper disposal of animal carcasses containing radioactivity.
4. In 2003, the Radiation Safety Office provided calibration and maintenance services for 278 radiation survey instruments used throughout the Columbia University Medical Center and New York State Psychiatric Institute. The Radiation Safety Office maintains a supply of portable survey instruments available for loan to Responsible Investigators.
5. The RSO and EH&S met on May 28, 2003 for a joint session of discussions and cross training. The cross training included classifications of radioactive waste, mixed waste (chemical and radioactive waste combined), laboratory safety and chemical hygiene, clearance procedures, and hazardous waste training.
6. On May 28, 2003, there was a meeting with Salmen Loksen, Ahmad Hatami, and Jake Kamen of the RSO, Kathleen Crowley and Christopher Pinto of EH&S, and Michael van Biema, Interim Director for Purchasing, and Joe Brucia, Interim Associate Director of Purchasing, regarding ordering radioactive materials online using FFE. Using this pilot program, radioactive material requisitions may be reviewed and approved online, resulting in faster requisition response and reduced paperwork. A training meeting for RSO staff will be held on June 23, 2003. Following finalization of the new requisition procedure, Responsible Investigators will be notified on measures for using the new system.
7. The Radiation Safety Office provides continuing radiation safety support for the Columbia University Cyclotron Facility and the Columbia University Radioligand Laboratory for the production and synthesis of PET imaging radiopharmaceuticals. This support includes: basic radiation safety services; personnel dosimetry; area radiation monitoring and analysis of radioisotope releases to the atmosphere; review of Authorized User credentials; and review of system modifications.
8. The Radiation Safety Office is involved in provid-

ing professional health physics expertise for the planned construction of an additional Cyclotron/Radioligand Facility on the Columbia University Health Sciences campus.

9. The RSO continues the process of scanning paper documents into the PaperPort software application. This process is a measure to back-up our paper files with digital copies that may be transferred to CD-ROM or DVD formats. This electronic document system allows for quicker search and retrieval of information, and reduces the quantity of paper documents maintained in the RSO files. During the move to our new location, we have reviewed files to determine which are to be retained, archived, or disposed of after they are converted into digital files.

Professional Radiation Safety and Medical Physics Support for Non-Radiology X-ray Activities

The Joint Radiation Safety Committee in agreement with New York Presbyterian Hospital has assigned the Radiation Safety Office responsibility for Radiation Safety and Medical Physics support for those clinical facilities outside the Department of Radiology that use x-ray equipment. A major part of this program is the quality assurance program for dental radiography.

This quality assurance program is designed to optimize the radiological safety and clinical quality of dental radiography, based on recommendations for quality assurance that have been promulgated by a number of professional organizations, including the National Council on Radiation Protection and Measurements (NCRP), the Bureau of Radiological Health of the Food and Drug Administration, the American College of Radiology (ACR), and the American Academy of Dental Radiology Quality Assurance Committee.

The Radiation Safety Office has primary responsibility for preliminary radiation safety shielding evaluation, acceptance testing, diagnostic quality assurance, and radiation safety surveys on all dental x-ray units installed at the following locations:

- Morningside Dental Associates: 9 intraoral units, and 1 panoramic - cephalographic unit at two locations
- Ambulatory Care Networked Corporation (ACNC): 2 intraoral units and 1 panoramic - cephalographic unit
- Babies Hospital OR: 1 portable intraoral unit
- Vanderbilt Clinic Teaching & Research Areas: 2 panoramic units, 2 panoramic-cephalographic units, 21 intraoral units, and 1 intraoral-cephalographic unit
- Dentcare Clinic (Intermediate School 183): 1 intraoral unit
- New York State Psychiatric Institute: 1 intraoral unit and 1 panoramic unit
- Columbia Eastside: 6 intraoral units, and 1 panoramic-cephalographic unit
- Columbia North: 5 intraoral units, 1 panoramic unit
- Mobile Dental Facility: 2 intraoral units
- Thelma Adir Health Care Center: 5 intraoral units, and 1Panoramic Unit.

Significant activities in this area in 2003 included:

1. The Radiation Safety Office is in the process of upgrading its current Dental QA equipment. After an extensive investigation the RTI Barracuda system was selected as a replacement for obsolete test equipment. RSO personnel are undergoing training in the use of the new system.

2. Audits of non-radiology x-ray facilities were conducted. The departments audited included Animal Care, Endoscopy, Interventional Cardiology, Pain Management, Surgery, and Urology. Audit results were sent to the departments involved, and copies were forwarded to Radiology Medical Physics.

3. On July 2, 2003, Bruce Emmer gave the annual Fellows Lecture to the radiology residents.

4. The RSO coordinates with Radiology Medical Physics the procedures for the audit of non-radiology x-ray facilities, policies for personnel dosimetry for fluoroscopy users, and acceptable methods for calculation of EDE, view box-inspections, and radiation safety checks of protective lead equipment.

University and Hospital Emergency Response & Management of Terrorist Events Involving Radioactive Material

On September 11, 2001, the Radiation Safety Office immediately attempted to contact the New York City Health Department, Office of Radiological Health to offer assistance and inquire about the well being of their personnel located in the downtown Manhattan area. The Radiation Safety Office staff was placed on emergency standby in order to render assistance if requested.

Shortly thereafter, the Radiation Safety Office received a list of pager and home telephone numbers of Office of Radiological Health personnel in order to maintain communications in the event of future disruptions.

As a result of these tragic events, the Joint Radiation Safety Committee formed a new Subcommittee for the Management of Radiation Incidents, chaired by David Brenner, Ph.D., to provide the University and Hospital with professional expertise in the area of possible radiological threats and the appropriate response to them. As always, the Radiation Safety Office provides the professional and technical personnel to support the Joint Radiation Safety Committee's policies and recommendations.

Activities in this new area of responsibility include:

1. On September 3, 2003 Dr. Kamen from the Radiation Safety Office met with Tobias Lickerman and Richard Borri of the New York City Office of Radiological Health regarding the response to radiological emergency incidents. During the meeting, steps were discussed, including raising awareness, training, and development of standard operating procedures. Mr. Lickerman has agreed to come to the CUMC campus and give a training class to emergency response personnel. It was also suggested that a one-day seminar be organized for the emergency personnel, perhaps including a lecturer from the Armed Forces Radiobiological Research Institute (AFRRI).

2. On Saturday, August 23, 2003, the New York City Fire Department joined Columbia University Health Science Division Environmental Health and Safety (EH&S) and the CUMC Radiation Safety Office in a joint unit drill exercise. All the groups met at 10 a.m. on 168th Street in front of the P&S building. All FDNY participants were given a tour of laboratory buildings, radioactive waste storage rooms,

chemical storage rooms, and irradiators. During the tour, questions and concerns from the FDNY were addressed by RSO and EH&S staff. After the tour, individuals participating in this drill gathered in Room 312 of HHSC and reviewed all the lessons learned. One concern that the FDNY raised was that during a real emergency in the basement, it might be difficult to see the signs to the radioactive waste room. They suggested that signs be in a yellow color and of a much larger size. The Radiation Safety Office has completed the process of purchasing and installing these signs.

3. On Friday, September 5, 2003, the Radiation Safety Office met with the Emergency Room Department to conduct a drill in response to a simulated radioactive terrorist attack. In preparation for the drill, the Radiation Safety Office prepared a realistic scenario of multiple Dirty Bomb explosions and their consequential effects throughout New York City. The drill commenced at 10 a.m. in the Emergency Room of Columbia-Presbyterian Medical Center. In attendance from the Radiation Safety Office were Salmen Loksen, RSO Director; Jacob Kamen, Assistant Radiation Safety Officer; and Mutian Zhang, Acting RSO Waste Supervisor. Personnel from the Emergency Room Department proceeded with the drill wearing protective suits and treated simulated victims from four sources of contamination. At its completion, both the Radiation Safety Office and the Emergency Room Department agreed that the drill went smoothly. Additional points that were discussed included the need for survey meters to have improved visible alerts when radiation is detected. Emergency Room personnel who treated simulated radiation victims were not able to hear the indication alert on the survey meters through the protective suits. Also, the emergency showers located outside of the Emergency Room need to be continually maintained and fully functional in the event of an attack.

4. Since April 1, 2003, the Radiation Safety Office has been attending the Emergency Department Subcommittee weekly meetings with regard to preparing for terrorist activities. The Radiation Safety Office ordered portable survey meters dedicated for use at the Emergency Room at New York Presbyterian Hospital. On September 10, 2003, the RSO received the purchased electronic dosimeters for emergency incidents. At this time, these dosimeters are being calibrated and engraved for security purposes before distribution. These instruments will be calibrated and maintained on an ongoing basis by the RSO. A request was made for additional instrumentation to be provided to the Allen Pavilion Emergency Room. In addition, a request was made for specific written guidelines to be provided by the RSO for the monitoring and evaluating of patients presenting at the emergency room with possible radioactive contamination. A request was made by the Chair of the Subcommittee to be invited to the JRSC Subcommittee on the Management of Radiation Incidents. The RSO suggested that, in addition to the pocket dosimeters, unassigned personnel monitoring badges could be immediately made available to the Emergency Room. The RSO indicated that, if additional instrumentation is needed, such instruments are available in the Radiation Safety Office for emergency room use.

5. The Emergency Room of the New York Presbyterian Hospital offered a two-day training class on September 29-30, 2003 on the use of different protective suits for responding to incidents with weapons of mass destruction, involving chemical, biological, and radiological hazardous material. At the suggestion of Raffaela Pia, Associate Director of Nursing at the Emergency Room at NYPH, Salmen Loksen and Jacob Kamen attended this training.

6. The Office of Environmental Health & Safety developed a Hazardous Materials Transportation Security Plan for shipments of hazardous material regulated under CFR 172.802 including hazardous waste, radioactive materials and radioactive waste. On December 17, 2003, the EH&S officers provided a training lecture on the Security plan and blood borne pathogens to RSO staff.

7. On August 14, 2003, New York City, along with much of the Northeastern United States was subject to an electrical power outage. During the entire period of the emergency at Columbia-Presbyterian Medical Center, from August 14, 2003, 4:00 p.m. to August 15, 2003, 4:00 p.m., the Radiation Safety Office maintained professional and technical staff on site. During the power outage, the Radiation Safety Office staff attended Columbia University Emergency Management briefings, inspected the security of radioactive materials facilities, and provided radiation safety support to New York Presbyterian Hospital Facilities personnel responding to a major water leak in a Cyclotron Facility pump system that occurred during the power outage.

RSO Personnel and Facilities

Significant personnel and facilities activities in 2003 included:

1. On June 16, 2003, Ahmad Hatami, Mutian Zhang, and Michelle Kang attended the Environmental Resource Center's annual Hazardous Waste Training Seminar.

2. On June 19, 2003, Ahmad Hatami, Mutian Zhang, Olga Loukhton, and Dae-In Kim of the RSO attended a one-day course on DOT/IATA Radioactive Shipping Training given by the New Jersey and Greater New York Chapters of the Health Physics Society.

3. From August 26, 2003, through August 30, 2003, Dae-In Kim, Health Physicist, Radiation Safety Office, attended operations training for the RDS-112 Cyclotron offered by CTI in Oak Ridge, Tennessee.

4. On September 4, 2003, Radiation Safety Office professional staff attended a meeting with Ronald Van Heertum M.D. and Peter Esser Ph.D. of the Department of Radiology and Steve Derasmo and Henry Meltzer of Stonehill & Taylor to review initial plans for the installation and operation of a PET/CT Trailer on the Columbia University Medical Center campus. The Radiation Safety Office will provide continuing consultation as to radiation safety and regulatory requirements for this project.

5. Mr. Shuntong Guo, M.S., is now a Certified Health Physicist, as recognized by the American Board of Health Physicists.

6. The RSO has moved its main offices to a new location on the fourth floor of the Mailman School of Public Health building, 722 West 168th Street. ■

Professional Affiliations & Activities

AMUNDSON, SALLY A., Ph.D.

Adjunct Faculty
- NCI Radiation Epidemiology Branch, National Institutes of Health, Adjunct Investigator

Member
- Radiation Research Society
- Women in Radiation Research Committee
- Program Committee
- RRS Annual Meeting Program Committee
- EU-US Workshop on Molecular Signatures of DNA Damage Induced Stress Responses Organizing Committee
- Radiation Effects Team Working Group (NASA)

Reviewer
- *Cancer Research*
- *International Journal of Radiation Oncology, Biology, Physics*
- *Radiation Research*
- *Bioinformatics*
- *Radiation Research Study Section -- outside opinion*

BALAJEE, ADAYABALAM S., Ph.D.

Member
- American Association for Advancement of Science
- Radiation Research Society

Reviewer
- *Mutation Research*
- *Advances in Space Research*
- *Medical Science Monitor*

Honors
- Editing a book on "DNA repair and human diseases" for Landes Biosciences, Texas, USA

BIGELOW, ALAN, Ph.D.

Member
- American Physical Society
- Radiation Research Society

BRENNER, DAVID J., Ph.D., D.Sc.

Member
- Columbia University Radiation Safety Committee, *Chairperson*
- National Council on Radiation Protection and Measurements (NCRP)
- NCRP Committee 12 on the use of ionizing radiation to combat terrorism
- Radiation Research Society, *Program Committee*
- American Statistical Association Conference on Radiation and Health 2004, Chairperson
- TV and radio appearances on the subject of pediatric CT examinations, depleted uranium

Editorial Work
- *Radiation and Environmental Biophysics*, Assoc. Editor

CALAF, GLORIA M., Ph.D.

Adjunct Faculty
- University of Tarapaca; Faculty of Sciences; Dept. of Biology and Health, Arica, Chile, *Adjunct Professor*

Member
- Biology Society of Chile
- Mastology Society of Chile
- Chilean Society of Citology
- Chilean Society of Cancer
- New York Academy of Sciences
- Tissue Culture Association
- International Association of Breast Cancer Research
- American Association of Cancer Research
- Society of Experimental Biology and Medicine
- Radiation Research Society

Student Mentoring
- Autonomous University of Madrid, Spain, Ph.D. Advisor

GEARD, CHARLES R., Ph.D.

Member
- American Society of Therapeutic Radiology and Oncology (ASTRO)
- Environmental Mutagen Society
- Associate Member Radiobiology Advisory Team (AMRAT) of the Armed Forces Radiobiology Research Institute (AFRRI)
- Columbia University, Faculty Council, *Voting Member*
- Columbia University, Mailman School of Public Health, Division of Epidemiology Ph.D. Committee
- Advisory Committee on Radiobiology, Brookhaven National Laboratory
- Scientific Peer Review Panel, Breast Cancer Department of the Army, Research Program
- Scientific Instrumentation Review Panel, Research Council, Ontario, Canada

Editorial Work
- *International Journal of Radiation Biology*, Editorial Board

Reviewer
- *British Journal of Cancer*
- *Mutation Research*
- *Radiation Research*

Student Mentoring
- Columbia University, resident in Radiation Oncology
- Albert Einstein School of Medicine, M.D. candidate

HALL, ERIC J., D.Phil., D.Sc., FACR, FRCR

Member
- Royal College of Radiology
- British Institute of Radiology
- American Board of Radiology, *Radiotherapeutic Written-Test Committee*
- American Society of Therapeutic Radiology and Oncology (ASTRO)

Radiation Research Society
American Radium Society
International Association of Radiation Research, *Pres.*
Columbia University, Herbert Irving Comprehensive Cancer Center, *Internal Advisory Committee/Executive Committee*
Columbia-Presbyterian Medical Center, Joint Radiation Safety Committee, *Chairman*; Radioactive Drug Research Committee, *Chairman*
National Council on Radiation Protection and Measurements, Committee 1, *Member*

Editorial Work

Intl Journal of Radiation Oncology Biology Physics, Senior Editor, Biology
International Journal of Brachytherapy

HANG, HAIYING, Ph.D.

Member

Radiation Research Society

HEI, TOM K., Ph.D.

Adjunct Faculty

Department of Radiological Health Science, Colorado State University, Fort Collins, Co., *Adjunct Professor*
Department of Ion Beam Bioengineering, Chinese Academy of Sciences, Hefei, China, *Adjunct Professor and Doctorate Student Mentor*
University of Hong Kong, *External Examiner*

Member

NIH Pathology C Study Section, *Chairman, Ad hoc review panel*
NCI Cancer Etiology Study Section, *Chairman, Ad hoc review panel*
NCI Division of Cancer Biology, *panel member*
EPA Expert Panel on Asbestos Toxicology
American Association for Cancer Research, *Annual Meeting Program Committee*
Department of Med. Faculty Recruitment Committee
Radiation Research Society
Environmental Mutagen Society
Oxygen Society

Students Mentoring

Doctoral Students of Environmental Heath Sciences, Columbia University, School of Public Health.
New York City high school science students for Intel Science project
Faculty Advisor for Exchange 4th year Chinese medical students from Fudan University

Reviewer

Proceedings of the National Academy of Sciences
Cancer Research
Carcinogenesis
Radiation Research
Environmental Health Perspective
International Journal of Radiation Biology
Cancer Letters
Book proposal for CRC
Book proposal for Kluwer Academic Publishers

Editorial Work

Advances in Space Sciences, section editor

LIEBERMAN, HOWARD B., Ph.D.

Member

Summer Research Program for NYC Secondary School Science Teachers, Columbia University, *Advisory Board*
Israel Cancer Research Foundation, *Scientific Advisory Board*
American Association for the Advancement of Science
American Society for Microbiology
Environmental Mutagen Society
Genetics Society of America
Radiation Research Society
Sigma Xi
Theobald Smith Society

Reviewer

Grants:
Basic and Preclinical Subcommittee C of the NCI Initial Review Group, *Member*
NIH Special Emphasis Panel, *Ad Hoc*
Joint Center for Radiation Therapy Foundation, Harvard Medical School, *Ad Hoc*
Israel Cancer Research Foundation, *Postdoctoral Fellowship Panel*

Manuscripts:
Intl Journal of Radiation Oncology, Biology and Physics
Mutation Research
Nucleic Acids Research
Oncogene
Radiation Research

MARINO, STEPHEN A., M.S.

Member

Columbia University Radiation Safety Committee
Radiation Research Society

MITCHELL, CATHERINE, Ph.D.

Member

Radiation Research Society

Reviewer

Radiation Research
Advances in Space Research

MITCHELL, STEPHEN, Ph.D.

Member

Radiation Research Society

Reviewer

Radiation Research

PONNAIYA, BRIAN, Ph.D.

Member
Radiation Research Society

Reviewer
International Journal of Radiation Biology
Radiation Research
Oncogene

Students Mentoring
Advisor for Ph.D. and M.Sc. candidates of Environmental Heath Sciences, Mailman School of Public Health, Columbia University

Reviewer
Cancer Research
Proceedings of the National Academy of Sciences

YIN, YUXIN, M.D., Ph.D.

Adjunct Faculty
Assistant Professor, Department of Environmental Health Sciences, Mailman School of Public Health, Columbia University,
Adjunct Professor, Xian JiaoTong University School of Medicine, Xian, China

Member
American Association for Cancer Research

ZHAO, YONGLIANG, Ph.D.

Member
Radiation Research Society
American Association for Cancer Research

Grants
RSNA Research Seed Grant
NIEHS Center Pilot Grant
NASA Project Grant ■

Publications

1. **Amundson SA** and Fornace AJ Jr. Complexity of stress signaling and responses, in *The Handbook of Cell Signaling* (Haley M, ed) pp. 179-83, Academic Press, San Diego, CA, 2003.
2. **Amundson SA** and Fornace AJ Jr. Microarray approaches for analysis of cell cycle regulatory genes, in *Cell Cycle Checkpoint Control Protocols* (**Lieberman HB**, ed) pp. 125-41, Humana Press, Totowa, NJ, 2004.
3. **Amundson SA** and Fornace AJ Jr. Microarray approaches for analysis of tumor suppressor gene function, in *Tumor Suppressor Genes: Methods and Protocols* (El-Deiry WS, ed) pp. 141-54, Humana Press, Totowa, NJ, 2003.
4. **Amundson SA** and Fornace AJ Jr. Monitoring human radiation exposure by gene expression profiling: Possibilities and pitfalls. *Health Physics* **85**:36-42, 2003.
5. **Amundson SA**, Bittner ML and Fornace AJ Jr. Functional genomics as a window on radiation stress signaling. *Oncogene* **22:**5828-33, 2003.
6. **Amundson SA**, Lee RA, Koch-Paiz CA, Bittner ML, Meltzer P, Trent JM and Fornace AJ Jr. Differential responses of stress genes to low dose-rate gamma-irradiation. *Molecular Cancer Research* **1**:445-52, 2003.
7. **Balajee AS** and Palitti F. Sensitivity of Werner syndrome cells to DNA damaging agents: insights into the biological functions of Werner protein. Invited Chapter in the book entitled *Molecular Mechanisms of Werner Syndrome*, pp. 1-16, Landes Biosciences, 2003
8. Bhat HK, **Calaf G**, **Hei TK**, Loya T and Vadgama JV. Critical role of oxidative stress in estrogen-induced carcinogenesis. *Proc Natl Acad Sci* (*USA)* **100**:3913-38, 2003.
9. **Bigelow AW**, **Randers-Pehrson G**, **Brenner DJ**. Proposed laser ion source for the Columbia University microbeam. *Nucl Instr and Meth in Phys Res B* **210**:65-9, 2003.
10. **Bigelow AW**, **Randers-Pehrson G**, Michel KA, **Brenner DJ** and Dymnikov AD. Sample Targeting during Single-Particle Single-Cell Irradiation AIP Conference Proceedings **680**:347-50, 2003.
11. **Brenner DJ** and **Hall EJ**. Mortality patterns in British and US radiologists: what can we really conclude? *Br J Radiol* **76**:1-2, 2003.
12. **Brenner DJ** and Sachs RK. Domestic radon risks may be dominated by bystander effects – but the risks are unlikely to be greater than we thought. *Health Phys* **85**:103-8, 2003.
13. **Brenner DJ**, Doll R, Dudley T, Goodhead DT, **Hall EJ**, Land CE, Little JB, Lubin JH, Preston DL, Preston RJ, Puskin JS, Ron E, Samet JM, Setlow RB and Zaider M. Cancer risks attributable to low doses of ionizing radiation: Assessing what we really know. *Proc Natl Acad Sci USA* **100**:13761-6, 2003.
14. **Brenner DJ**. Hypofractionation for prostate cancer radiotherapy – what are the issues? *Int J Radiat Oncol Biol Phys* **57**:912-4, 2003.
15. **Brenner DJ**. Revisiting nuclear power plant safety (author reply). *Science* **299**:201-3, 2003.
16. De Santis LP, **Balajee AS**, Garcia GL, Pepe G, Worboys AM and Palitti F. Inhibition of p53, p21 and Bax by pifithrin-alpha does not affect UV induced apoptotic response in CS-B cells. *DNA Repair (Amst)* 2891-900, 2003.
17. Filipic M and **Hei TK**. Mutagenicity of cadmium in mammalian cells: Implication of oxidative DNA damage. *Mut Res* **546**:81-91, 2004.
18. Fowler JF, Ritter MA, Chappell RJ and **Brenner DJ**.

What hypofractionated protocols should be tested for prostate cancer? *Int J Radiat Oncol Biol Phys* **56**:1093-104, 2003.

19. **Geard CR** and **Ponnaiya B**. Chromosomal changes and cell cycle checkpoints in Mammalian cells. *Methods Mol Biol* **241**:315-28, 2004.
20. **Hall EJ** and **Brenner DJ**. The weight of evidence does not support the suggestion that exposure to low doses of X rays increases longevity. *Radiology* **229**:18-9, 2003.
21. **Hall EJ** and **Hei TK**. Genomic instability and bystander effects induced by high LET radiation. *Oncogene* **22**: 7034-42, 2003.
22. **Hall EJ** and Wuu CS. Radiation-induced second cancers: The impact of 3D-CRT and IMRT. *Int J Radiation Oncology Biol Phys* **56**:83-8, 2003.
23. **Hall EJ**. Letter to the Editor, "Lessons we have learned from our children; cancer risks from diagnostic radiology." *Pediatr Radiol* 33:815-7, 2003.
24. **Hall EJ**. The Bystander Effect. *Health Physics* **85**:31-35, 2003.
25. Hande MP, Azizova TV, **Geard CR**, Burak LE, **Mitchell CR**, Khokhryakov VF, Vasilenko EK and **Brenner DJ**. Past exposure to densely-ionizing radiation leaves a unique permanent signature in the genome. *Amer J of Human Genetics* **72**:1162-70, 2003.
26. **Hang H** and Fox MH. Analysis of the mammalian cell cycle by flow cytometry. In *Cell Cycle Checkpoint Control Protocols* (**Lieberman HB**, ed), pp. 23-35, Humana Press, Totowa, NJ, 2004.
27. **Hei TK**, Xu An and **Zhao YL**. Genotoxic and carcinogenic mechanisms of mineral fibers: Role of reactive oxygen species. *Lung Injury and Disease* (in press 2004).
28. **Hopkins KM**, **Wang X**, Berlin A, **Hang H**, Thaker HM and **Lieberman HB**. Expression of mammalian paralogues of HRAD9 and Mrad9 checkpoint control genes in normal and cancerous testicular tissue. *Cancer Res.* **63**:5291-8, 2003.
29. Lenarczyk M, Ueno A, Vannais DB, Kraemer S, Kronenberg A, Roberts JC, Tatusumi K, **Hei TK** and Waldren CA. The pro-drug RibCys decreases the mutagenicity of high LET radiation in cultured mammalian cells. *Radiation Res* **159**:579-83, 2003.
30. **Lieberman HB** and **Hopkins KM**. Methods to induce cell cycle checkpoints. In *Cell Cycle Checkpoint Control Protocols* (**Lieberman HB**, ed) pp. 3-10, Humana Press, Totowa, NJ, 2004.
31. **Lieberman HB**. *Cell Cycle Checkpoint Control Protocols*. Edited by **Lieberman HB**, Humana Press, Totowa, NJ, 2004.
32. Roos-Mattjus P, **Hopkins KM**, Oestreich AJ, Vroman BT, Johnson KL, Naylor S, **Lieberman HB** and Karnitz LM. Phosphorylation of human Rad9 is required for genotoxin-activated checkpoint signaling. *J Biol Chem* **278**:24428-37, 2003.
33. Rossinow JK, **Balajee AS,** Gewanter RM, Ennis RD, Schiff PB, Katz AE and **Geard CR**. Effects of lycopene and vitamin E on gamma-irradiated prostate cancer cells. *Int J Radiat Oncol Biol Phys* **57**(2 Suppl):S 348-9, 2003.
34. Roy D, **Calaf G** and **Hei TK**. Allelic imbalance at 11p15.5-15.4 correlated with *c-Ha-ras* mutation during radiation-induced neoplastic transformation of human breast epithelial cells. *Int J Cancer* **103**:730-7, 2003.
35. Roy D, **Calaf G** and **Hei TK**. Role of Vitamin D receptor gene in radiation-induced neoplastic transformation of human breast epithelial cell. *Steroids* **68**:621-7, 2003.
36. Shen WH, **Yin Y**, Broussard SR, McCusker RH, Freund GG, Dantzer R and Kelley KW. Tumor necrosis factor a inhibits cyclin A expression and retinoblastoma hyperphosphorylation triggered by insulin-like growth factor-I induction of new E2F-1 synthesis. *J of Biological Chemistry* **279**:7438-46, 2004.
37. Shukla A, Gulumian M, **Hei TK**, Kamp D, Rahman Q, Aust A and Mossman B. Multiple roles of oxidants in the pathogenesis of asbestos induced diseases. *Free Radic Biol Med* **34**:1117-29, 2003.
38. Suzuki M, **Zhou H**, **Hei TK**, Tsuruoka C and Fujitaka K. Induction of a bystander chromosomal damage of He-ion microbeams in mammalian cells. *Biol Sci Space* **17**:251-3, 2003.
39. Van Hoffen A, **Balajee AS**, Van Zeeland AA and Mullenders LH. Nucleotide excision repair and its interplay with transcription. *Toxicology* **193**:79-90, 2003.
40. **Yin Y**, **Liu YX**, Jin YJ, **Hall EJ** and Barrett JC. PAC1 phosphatase is a transcription target of p53 in signaling apoptosis and growth suppression. *Nature* **422**:527-31, 2003.
41. **Yin Y**, **Zhu A**, **Hopkins KM**, Jin YJ, **Liu C** and **Lieberman HB**. Human RAD9 checkpoint control/pro-apoptotic protein can activate transcription of *p21*. *Proc Natl Acad Sci, accepted* 2004.
42. **Yin Y**. p53 kingdom, a new prospect for its control mechanism and apoptotic defense. *Cell Cycle* **2**:279-80, 2003.
43. **Zhao YL**, **Piao CQ** and **Hei TK**. Tumor suppressor function of Betaig-h3 gene in radiation carcinogenesis. *Adv Space Res* **31**:1575-82, 2003.
44. **Zhou H**, **Randers-Pehrson G**, **Geard CR**, **Brenner DJ**, **Hall EJ** and **Hei TK**. Interaction between radiation-induced adaptive response and bystander mutagenesis in mammalian cells. *Radiat Res* **160**:512-6, 2003.
45. **Zhou H**, **Calaf GM** and **Hei TK**. Malignant transformation of human bronchial epithelial cells with the tobacco-specific nitrosamine, 4-(methylnitrosamino)-1-(3-pyridyl)-1-butanone. *Int J Cancer* **106**:821-6, 2003.
46. **Zhou H**, **Randers-Pehrson G**, **Geard CR**, **Brenner D**, **Hall EJ** and **Hei TK**. Interaction between radiation induced adaptive response and bystander mutagenesis in mammalian cells. *Rad Research* **160**:512-6, 2003. ■